Ana Francisca Silva de Lima

Mestre em Biologia Celular e Molecular

Biophysical modulation of cell fate through chromatin remodelling

Dissertação para obtenção do Grau de Doutor em Bioengenharia

Orientador: Doutor Ricardo Neves, Investigador Auxiliar, Universidade de Coimbra

Co-orientador: Professor Doutor Tariq Enver, Professor Catedrático, University College of London

Co-orientador: Doutor Manuel Luís Magalhães Nunes da Ponte, Professor Catedrático, Faculdade de Ciências e Tecnologia da Universidade Nova de Lisboa

Júri:

Presidente:	Doutor José Paulo Barbosa Mota, Professor Catedrático da Faculdade de Ciências e Tecnologia da Universidade Nova de Lisboa
Arguentes:	Doutor Pedro Jorge Gomes Teodósio Castelo Branco, Professor Auxiliar do Centro de Investigação – CBMR da Universidade do Algarve
	Doutor Carlos Filipe Ribeiro Lemos Pereira, Investigador Auxiliar do Centro de Neurociências e Biologia Celular da Universidade de Coimbra
Vogais:	Doutor Ricardo Neves Pires das Neves, Investigador Auxiliar do Centro de Neurociências e Biologia Celular da Universidade de Coimbra
	Doutor José Eduardo Marques Bragança, , Professor Auxiliar do Centro de Investigação – CBMR da Universidade do Algarve
	Doutora Paula Maria Marques Leal Sanches Alves, Professora Associada Convidada da Faculdade de Ciências e Tecnologia da Universidade Nova de Lisboa

FACULDADE DE CIÊNCIAS E TECNOLOGIA
UNIVERSIDADE NOVA DE LISBOA

Dezembro de 2016

Ana Francisca Silva de Lima

Mestre em Biologia Celular e Molecular

Biophysical modulation of cell fate through chromatin remodelling

Dissertação para obtenção do Grau de Doutor em Bioengenharia

Orientador: Doutor Ricardo Neves, Investigador Auxiliar, Universidade de Coimbra

Co-orientador: Professor Doutor Tariq Enver, Professor Catedrático, University College of London

Co-orientador: Doutor Manuel Luís Magalhães Nunes da Ponte, Professor Catedrático, Faculdade de Ciências e Tecnologia da Universidade Nova de Lisboa

Júri:

Presidente:	Doutor José Paulo Barbosa Mota, Professor Catedrático da Faculdade de Ciências e Tecnologia da Universidade Nova de Lisboa
Arguentes:	Doutor Pedro Jorge Gomes Teodósio Castelo Branco, Professor Auxiliar do Centro de Investigação – CBMR da Universidade do Algarve
	Doutor Carlos Filipe Ribeiro Lemos Pereira, Investigador Auxiliar do Centro de Neurociências e Biologia Celular da Universidade de Coimbra
Vogais:	Doutor Ricardo Neves Pires das Neves, Investigador Auxiliar do Centro de Neurociências e Biologia Celular da Universidade de Coimbra
	Doutor José Eduardo Marques Bragança, , Professor Auxiliar do Centro de Investigação – CBMR da Universidade do Algarve
	Doutora Paula Maria Marques Leal Sanches Alves, Professora Associada Convidada da Faculdade de Ciências e Tecnologia da Universidade Nova de Lisboa

FACULDADE DE CIÊNCIAS E TECNOLOGIA
UNIVERSIDADE NOVA DE LISBOA

Dezembro de 2016

Biophysical modulation of cell fate through chromatin remodelling

This work was partially funded by the individual scholarship SFRH/BD/51942/2012 and the project PTDC/SAU-ENB/113696/2009, both from the Portuguese Foundation for Science and Technology (FCT).

Acknowledgments

Above all, my PhD was a challenging and wonderful trip. It would had been impossible to go through all the steps without the support of bright scientific minds, good people and a "blessed family" that were always around.

I would like to thank the MIT-Portugal Program and *Fundação para a Ciência e Tecnologia* for the funding given for this PhD thesis work. I would like to thank all the MIT-Portugal Program coordination and the Universities involved in the program, with special thanks to *Faculdade de Ciências e Tecnologia da Universidade Nova de Lisboa*. I am grateful for the opportunity to learn in different scenarios all over the country and the opportunity to be in contact with international experts. Additionally, I would like to thank, for the help in all critical moments, Professor Manuel Nunes da Ponte and Professor José Silva Lopes.

I would like to thank my supervisor, Professor Ricardo Neves for his influence in my scientific perception. Thank you for teaching me and encouraging me to be always critical and par my work to high scientific standards. I am grateful for the collaboration opportunities you gave me through our international partners.

I would also like to thank all the Stem cells and tissue engineering Unit members from Centre for Neuroscience and Cell Biology (University of Coimbra) who have made my daily laboratory work an enjoyable experience even during "dark" times. I would like to thank Professor Lino Ferreira for the support given towards the development of my work. My special thanks to Adrián Jiménez, Diana Santos, Emanuel Quartin, Hugo Azevedo, João Monteiro, João Santos, Josephine Blersch, Luis Estronca, Maria Helena, Michela Comune, Miguel Lino, Pedro Gouveia, Renato Cardoso, Susana Pereira, Susana Simões and Vitor Francisco. Couldn't go without thanking "the musketeers" Catarina Almeida, Inês Honório, Patrícia Pitrez, Sandra Pinto, Susana Rosa for the joyful moments in the lab and for their friendship.

I would like to thank our collaborators in *Centro de Histocompatibilidade do Centro* (Coimbra) and a special thanks to Dr. Artur Paiva and Susana Pedreiro.

I would like to thank our collaborators in *Centro Nacional de Biotecnología* (Madrid), Professor Francisco Iborra and Juan Colunga for the bioinformatics analysis and for the great scientific discussions.

I would also like to thank the Stem cells Lab members from the Cancer Institute (University College of London) that welcomed the "Portuguese alien" with kindness and wiliness to help me. I will always be grateful to all. I would like to thank Professor Tariq Enver, for the productive brainstorming and for the opportunity to develop part of my work in his group. My special thanks to Professor Rajeev Gupta, Professor Jason Wray, Professor John Brown and Virginia Turati. To the PhD students undergoing the same "crazy stress", thank you, Elitza Deltcheva and Sara Marelli. A very special thank you to Gill May that provided me crucial support in both the lab and personally in the final steps of my PhD, I will always be grateful and in debt to you. Thank you so much.

Thank you, Sandra Godinho and Filipa Santos for you friendship, kindness and having me in the first year of the PhD in Lisbon and Braga. Thank you Marta Gómez, for all the support and your friendship.

Thank you to Carina Bernardo, Cristiana Faria, Ana Guedes and Irina Simões. Thank you for the good times spend together, for the good vibes and friendship.

Dear Renata Gomes, I will never forget everything that you did for me. Thank you for everything you taught me in the lab. Thank you for your optimistic vision of life. Thank you for calming me down when the "microRNA vanished" and for teaching me the "head glove technique". Thank you to you, your husband and your family for the friendship and the extra rooms that accommodated me so many times. Above all, thank you for your friendship and humanity.

My family knows that they were crucial to my success during this period of my life and during all my life. Thank you, to Ana Silva and João Lima for transforming me into who I am today. Thank you, also for the encouragement, comfort and concern that you always had with me. Thank you, Joana Lima for all your support and for making me feel capable of doing anything. Thank you, Vitor Teixeira for understanding that the time spent in the lab is never the predicted one (usually 3x more right?!). Thank you, for supporting my devotion to science and to my PhD. Understanding me in my "cranky days" during the thesis writing process. Thank you all, for your love and support.

I believe that without all the people above, and others whom will always be in my mind and my heart, doing this PhD would had been an impossible task.

A sincere Thank you to all!

Resumo

O ambiente extracelular é um dos factores decisivos para determinar a actividade e função celulares. Dentro deste ambiente extracelular existem vários factores determinantes para a manutenção do equilíbrio celular e homeostasia. A alteração de osmolaridade do meio extracelular está associada a inúmeras funções celulares fisiológicas e patologias. Apesar das alterações osmóticas fazerem parte de estímulos observados no microambiente celular estas alterações também podem ser vistas como ferramentas de modulação do fenótipo e destino celulares.

Os mecanismos de resposta a alterações osmóticas são complexos e incluem mecanismos de sinalização, transporte de osmólitos, manutenção da estabilidade e degradação de proteínas e manutenção da integridade genómica da célula.

Este trabalho tem como principal objectivo, aprofundar o conhecimento dos mecanismos que permitam a utilização da modulação osmótica como uma ferramenta de modulação do fenótipo celular.

A estratégia de modulação osmótica desenvolvida neste trabalho mostrou-se capaz de influenciar o balanço iónico intracelular, a quantidade de adenosina trifosfato intracelular, o tamanho da célula e o seu metabolismo. Um dos efeitos mais interessantes está relacionado com a alteração da actividade transcripcional induzida pelo aumento de RNA polimerase II ligada a ácido desoxirribonucleico genómico. Este efeito tem como co-factores vários factores de transcrição dependentes de zinco.

A capacidade da modulação osmótica interferir com decisões celulares determinantes para o destino celular foi mostrada com dois exemplos de alteração da especialização celular, a reprogramação ou pluripotência induzida e a transdiferenciação. Nestes exemplos, a modulação osmótica pode ser uma mais-valia pela sua actividade multifactorial, com efeitos em sinalizadores intracelulares, na mitocôndria, na estrutura global da cromatina e no padrão epigenético das células, bem como por interferir em processos de *splicing* alternativo e no processo de transcrição geral.

Estas características tornam a modulação osmótica uma fonte de modulação biofísica relevante para controlo do fenótipo celular e em futuras aplicações terapêuticas.

Palavras-chave: Modulação hiposmótica, alteração da cromatina, fenótipo celular, metabolismo, transcrição e destino celular.

Abstract

The use of non-lethal stimuli as cell modulators is a growing research area. The use of such strategies enables the control of cell behaviour and phenotype using stimuli that occur within the normal cellular environment. By using these stimuli, is possible to take advantage of their controlled application in benefit of a targeted cell phenotype modification and interfere with fate determination.

Osmoregulatory mechanisms are constituted by diversified signalling mechanisms, which share the objective of maintenance of cell integrity and function when an extracellular osmolarity disturbance occurs. Cellular osmoregulation comprises the regulation of cell volume and osmolyte transport and also protein structure and turnover, and genomic integrity. These mechanisms are observed under distinct physiological and pathophysiological scenarios.

This work aims to contribute to a better understanding of the relevance of the environmental osmotic modulation on cell physiology and its potential relevance to cell behaviour and phenotype.

The hyposmotic modulation described in this work induced differences in the transcriptional process by an increased RNA polymerase II binding to the chromatin. This has been mediated by the intervention of specific transcription factors such as zinc finger proteins to attain a specific RNA polymerase II binding profile.

The hyposmotic modulation has the ability to interfere with cell fate determination processes such as reprogramming and transdifferentiation. The potential of interfering with such complex processes has to do with the broad effect of the hyposmotic modulation on cellular signalling molecules (like calcium and adenosine triphosphate), mitochondrial activity and morphology, chromatin structure, epigenetic landscape, alternative splicing events and transcriptional pattern.

The area of cellular therapies is growing exponentially and the basic knowledge on cellular behaviour and cellular response to osmotic changes as well as the development of new tools responsive to osmotic changes can have a crucial role for the development of future therapeutic applications.

Keywords: Hyposmotic modulation, chromatin remodelling, cell phenotype, metabolism, transcription and fate determination.

Table of contents

List of figures

List of tables

List of abbreviations and symbols

- Acetyl-CoA – acetyl coenzyme A
- AP – alkaline phosphatase
- AQP – aquaporin
- ATMP – advanced therapy medicinal product
- ATP – adenosine triphosphate
- ATP – adenosine triphosphate
- BM – bone marrow
- BMSC – bone marrow stem cell
- C – cytosine
- CD – cluster of differentiation
- cDNA – complementary DNA
- Chip – chromatin immunoprecipitation
- Chip-Seq – chromatin immunoprecipitation sequencing
- CHO – chinese hamster ovarian cell line
- CPDA-1 – citrate phosphate dextrose adenine solution
- CpG – cytosine guanine dinucleotide
- CSF – colony stimulating factor
- CTD – C-terminal domain
- CTP – cytidine triphosphate
- DAPI – 4',6-diamidino-2-phenylindole
- DHS – DNase I hypersensitive sites
- DMEM – Dulbecco's Modified Eagle Medium
- DNA – deoxyribonucleic acid
- DNase I – deoxyribonuclease I
- ECL – enhanced chemiluminescence substrates
- ECM – extracellular matrix
- EGFP – enhanced green fluorescent protein
- ENaC – epithelial sodium channels
- ER – oestrogen receptor
- ERK – extracellular signal-regulated kinases
- ESC – embryonic stem cell

- Ets – E-twenty six TF
- EU – ethynyl uridine
- EUTP – ethynyl uridine triphosphate
- FACS – flow assorted cell sorting
- FBS – foetal bovine serum
- FGF – fibroblast growth factor
- FLIP – fluorescence loss in photobleaching
- Flt-3 – fms-related tyrosine kinase 3 ligand
- FSC/FS – forward scatter
- G – guanine
- GTP – guanosine triphosphate
- GVHD – graft versus host disease
- HAFTL – Ha-ras-oncogene-transformed mouse cell line
- HeLa – human adenocarcinoma cell line
- hESC – human embryonic stem cell
- HG – high glucose
- hiFBS – heat inactivated foetal bovine serum
- HLA – human leukocyte antigen
- HSC – hematopoietic stem cell
- HSP – heat shock protein
- ICM – inner cell mass
- IPDB – immunoprecipitation dilution buffer
- IPEB – immunoprecipitation elution buffer
- iPSC – induced pluripotent stem cell
- IPWB – immunoprecipitation washing buffer
- JNK – Jun amino-terminal kinases
- KG – ketoglutarate
- Kg – kilogram
- KO-DMEM – knockOut Dulbecco's Modified Eagle Medium
- KO-SR – knockOut serum replacement
- LG – low glucose
- lncRNA – long-non-coding RNA
- MACS – magnetic assorted cell sorting
- MAP2K – mitogen-activated protein kinase kinase

- MAP3K – mitogen-activated protein kinase kinase kinase
- MAPK – mitogen-activated protein kinase
- MAPKAPK – MAPK activated protein kinases
- MEF – mouse embryonic fibroblasts
- MEF I – inactivated mouse embryonic fibroblasts
- mESC – mouse embryonic stem cell
- miRNA – micro RNA
- mL – millilitre
- mM – millimolar
- MNase – micrococcal nuclease
- MNC – mononuclear cell
- mOsm – milliosmole
- MSC – mesenchymal stem cell
- mtDNA – mitochondrial DNA
- NAD^+ – nicotinamide adenine dinucleotide oxidised
- NADH – nicotinamide adenine dinucleotide reduced
- ncRNA – non-coding RNA
- NDHF – normal dermal human fibroblast
- NFAT – nuclear factor of activated T-cells
- NG – no glucose
- NLB – nuclear lysis buffer
- NLS – nuclear localisation signal
- nM – nanomolar
- OREBP – osmotic response element binding protein
- OSKM – Oct4, Sox2, Klf-4, c-Myc cocktail
- PBF – physiological buffer with Ficoll
- PBS – phosphate buffer saline
- PCR – polymerase chain reaction
- PFA – paraformaldehyde
- PLZF – promyelocytic leukaemia TF
- PSC – pluripotent stem cell
- qRT-PCR – quantitative real time polymerase chain reaction
- RFP – red fluorescent protein
- RNA – ribonucleic acid

- RNA Pol II – RNA Polymerase II
- RNA Pol II PhosphoS – RNA Polymerase II phosphorylated in serine
- RNA-Seq – RNA sequencing
- RNS – reactive nitrogen species
- ROS – reactive oxygen species
- RPMI – Roswell Park Memorial Institute
- rRNA – ribosomal RNA
- RTK – receptor tyrosine kinase
- RVD – regulatory volume decrease
- RVI – regulatory volume decrease
- SAPK – stress-activated protein kinase
- SC – stem cell
- SCF – stem cell factor
- SD – standard deviation
- SDS-PAGE – sodium dodecyl sulfate-polyacrylamide gel electrophoresis
- SEM – standard error mean
- SFFV – spleen focus-forming virus
- sncRNA – small-non-coding RNA
- SOD – superoxide dismutase
- SSC/SS – side scatter
- TAD – transactivation domain
- TBS – tris-buffered saline
- TBST – tris-buffered saline with tween
- TF – transcription factor
- TonEBP – tonicity-responsive binding protein
- tRNA – transfer RNA
- UCB – umbilical cord blood
- VPA – valproic acid
- ZF – zinc finger
- ΔΨm – mitochondrial membrane potential
- μg – microgram
- μL – microliter
- μm – micrometer
- μM – micromolar

Chapter 1 : Introduction

1.1. Aim

Stress responses, in human cells, are not fully understood, these are complex and collaborative signalling systems that promote homoeostasis. Physiological levels of stress trigger differentiation and specification of cell fates. Transient hyposmolarity modulation strategies, tailored to the right levels, might constitute a biophysical tool to modulate cellular transcription, metabolism and ultimately cell phenotype and cell fate.

Hyposmotic stress is underexplored but has already been associated with several interesting features like nuclear architecture changes, changes in ribonucleic acid (RNA) genes expression, ionic changes and cytoskeletal modifications (Di Ciano-Oliveira et al., 2006; Finan and Guilak, 2010; Hoffmann et al., 2009; Koivusalo et al., 2009; Lang et al., 1998; De Nadal and Posas, 2015; Okada, 2004; Waldegger et al., 1998; Wehner et al., 2003; Zhao et al., 2016).

Osmolarity is fundamental to a normal embryonic development and extreme osmotic scenarios can be observed in numerous physiological and pathophysiological situations such as renal, articular environments and cancer (Baltz, 2001; Baltz and Tartia, 2009; Halterman et al., 2012; Pedersen et al., 2013; Sontheimer, 2009; Voutouri and Stylianopoulos, 2014; Waldegger et al., 1998).

This work aims to contribute to a better understanding of the relevance of the environmental osmotic modulation on cell physiology and its potential relevance to cell behaviour and phenotype. This can be systematised under the following topics:

- To understand the impact of the hyposmotic environment in cell morphology, viability, cell physiology parameters and metabolism (Chapter 3);
- To elucidate the effect of the hyposmotic environment on nuclear and chromatin structure, chromatin accessibility and the transcription process (Chapter 3);
- To understand the impact of the hyposmotic environment on umbilical cord blood stem cell potency and phenotype (Chapter 4);
- To explore the impact of the hyposmotic environment on the induced pluripotency reprogramming process (Chapter 4);

- To investigate the impact of the hyposmotic environment on the transdifferentiation process (Chapter 5);
- To examine the impact of the hyposmotic environment on mitochondrial function and the impact of metabolic fates on alternative splicing events (Chapter 5).

1.2. Thesis outline

This thesis is divided into seven chapters. The first chapter is a general introduction to subjects which will be explored within the chapters of results. The general introduction contains a description of general environmental stresses and their effect on cell behaviour, with a specific attention to osmotic challenges to the cellular environment. Followed by a summary of cell-based products for potential clinical applications, that can benefit from a more broad knowledge of specific environmental cues to condition the cell performance according to the final therapeutic use.

Materials and methods provide a description of the techniques used during the experimental procedures along this work.

Chapter 3 provides a description of the cellular modifications after application of different hyposmotic modulation schemes. More specifically, parameters like cell size, adenosine triphosphate (ATP) levels, cell membrane potential, reactive oxygen species and mitochondrial function and intracellular calcium levels were evaluated. Also a connection between the osmotic modulation and chromatin state and chromatin marks, RNA polymerase II (RNA Pol II) binding to chromatin, RNA Pol II fully engagement in transcription, transcription speed, RNA Pol II initiation, RNA Pol II in its free form, binding profile of transcription factors and global transcriptional profile were studied.

Chapter 4 provides evidence of the importance of the osmolarity control and the phenotypic impacts that it can have under phenotypic characteristics of umbilical cord blood (UCB) cells. Additionally, explores the potential of hyposmotic modulation within the reprogramming process.

Chapter 5 provides a group of broad results that elucidate some important aspects of the hyposmotic modulation relevance in cell fate decisions and mitochondrial morphology. In addition to the mitochondrial morphology data, the relevance of glucose availability to cell phenotype was also explored.

Chapter 6 is a general discussion and the conclusions which we can take from the work developed. It also explores possible avenues of research which can be pursued taking into account the data presented and future challenges which this research area might face.

Chapter 7 provides the references mentioned throughout this thesis.

1.3. Environmental stress cues that impact in cell behaviour

Cells are complex sensors which can perceive and respond to numerous extracellular signals. These extracellular signals can be grouped into different categories like extracellular matrix (ECM) interactions, intercellular interactions and soluble signalling factors (ions, nutrients, cytokines, growth factors). The soluble signalling factor category comprises environmental changes such as alterations in oxidative mechanisms, external pH, nutrient supply, temperature changes and osmotic imbalances. These environmental cues promote the activation of an integrated response that ultimately alters the cell's phenotypic expression and function as an adaption to the environmental change (Gasiorowski et al., 2013; Kshitiz et al., 2012; de Nadal et al., 2011). The cellular microenvironment is constituted by factors which directly affect the conditions around cells and have a direct or indirect effect on cell's biophysical and biochemical repertoires (Ozcelik et al., 2014).

The concept of homoeostasis was introduced by Walter Bradford Cannon in 1926 and intended to describe the mechanisms which control the physiological equilibrium within a living organism (Davies, 2016). This term also applies to the cellular environment and to mechanisms which allow cellular equilibrium with its surroundings. Although cellular homoeostasis is the usual cell state, all of its physiological attributes fluctuate within a normal range, the so-called homeostatic range (Figure 1.1).

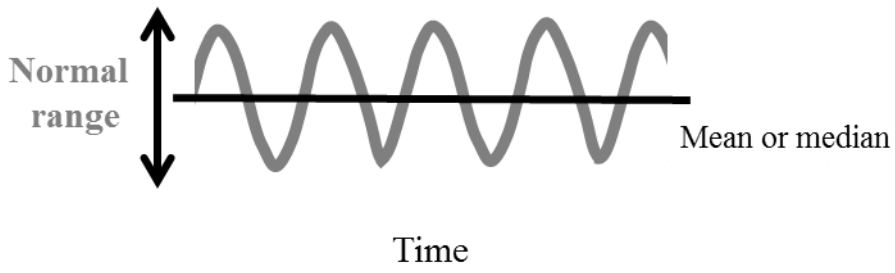

Figure 1.1 – Schematic illustration of the homoeostatic range concept. Figure adapted from Davies 2016.

On the other hand, stress is usually associated with a negative output, but the consequences of stress can be both harmful and beneficial depending on its intensity, duration and frequency. Exposure to a low dose of a chemical agent or environmental factor which is toxic at high doses can induce an adaptive advantage to the cell or organic system which is called hormesis (Davies, 2016). One of the most widely studied types of experimental hormesis is preconditioning ischemia, that occurs when an organ (the heart or brain, for example) is subjected to brief and mild ischemia. This type of exposure increases the

resistance of the cells to this type of stress and can eventually lead to the immortalisation of the cell (Mattson, 2008; Pong, 2004; Yellon and Downey, 2003). Therefore, ischemia is an example of a stress stimulus that exhibits a biphasic dose response, with brief periods being protective and prolonged periods resulting in irreversible cell damage or cell death. The cellular and molecular mechanisms underlying preconditioning ischemia hormesis may involve the activation of oxidative stress-induced cytoprotective signalling pathways involving kinase activation, changes in mitochondria, increased expression of antioxidant enzymes and protein chaperones (Juhaszova et al., 2004; Mattson, 2008).

Nevertheless, the transient exposure to some types of stress might promote a transient adaptation of cellular biochemical components, signalling molecules and transcription profile. These alterations do not promote a new or stronger phenotype, but instead an increased transient resilience to the stressor. This process has recently been suggested to be defined as adaptive homoeostasis (Figure 1.2) by Kelvin Davies (Davies, 2016). Examples of these adaptive responses are very small changes in oxygen, oxidants, temperature, acidity, alkalinity, salt content and others (Ceci et al., 2016; Demirovic and Rattan, 2013; Mattson, 2008; Zhang et al., 2015a). A specific example of these adaptations is the Keep1-Nrf2 (Kelch ECH-associated protein1; nuclear factor erythroid 2-related factor 2) system, where Nrf2 is usually bound to Keep1 in the cytoplasm. Nrf2 is usually found at low cytoplasmic levels because is targeted for proteasome degradation which prevents its nuclear translocation. In the presence of sub-toxic levels of various oxidants, Nrf2 undergoes phosphorylation, escapes proteolytic degradation and suffers nuclear translocation, where it binds and activates transient transcription of antioxidant response elements (Mattson, 2008; Zhang et al., 2015a).

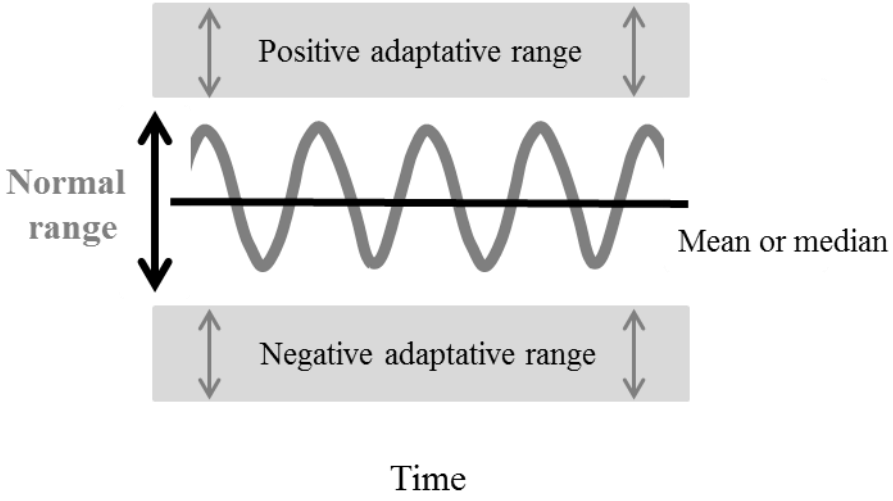

Figure 1.2 – Schematic illustration of the adaptive homoeostasis concept. Figure adapted from Davies 2016.

This adaptive plasticity of cells to extracellular changes and stressors might present an opportunity to modulate cell fate. In order to achieve this type of control one must understand how non-toxic and non-damaging stress responses exert their effect in cell behaviour and phenotype. For that a deep knowledge of stress-specific (at the transcription and metabolism level) and general (at organelle function level) responses is required.

1.3.1. Major types of environmental stress stimuli and cellular outputs

The continuous study of cellular stress response has shown that this response is a mixture of diverse molecular mechanisms. Different types of stresses can be grouped into mild, chronic or acute stresses. Classified has alterations in the optimal physical or biochemical conditions for cellular function and viability. The physical and biochemical factors of greatest relevance to eukaryotic cell function include nutrient availability, oxygenation, temperature, pH, and osmolarity (Ho, 2006; Kassahn et al., 2009; Kültz, 2005). In addition to these extracellular factors, intracellular parameters are also relevant to maintain cellular homoeostasis and can also activate stress-related pathways (Cláudio et al., 2013; Simmons et al., 2009). Intracellular conditions can promote activation of stress-related pathways such as the activation of the unfolded protein response during biosynthetic stress which leads to a coordinated inhibition of general protein translation. These biosynthetic stresses can also be induced by external factors which influence the intracellular compartments and its normal biosynthetic pathways (Cláudio et al., 2013; Pakos-Zebrucka et al., 2016; Simmons et al., 2009) .

The cellular stress response is a widely conserved mechanism of extreme relevance for physiological and pathophysiological conditions and it is characteristic of all the cells. This response is a generalised reaction which is triggered by macromolecule damage (lipids, proteins and deoxyribonucleic acid – DNA) and a major trigger for these damages is cellular redox imbalances. In parallel, environment disturbance can promote a series of stress-specific-induced alterations which are activated by cellular homoeostasis responses. In contrast to the transient nature of the cellular stress response, the cellular homeostatic response persists throughout exposure to the stressor or environmental change (Ho, 2006; Kassahn et al., 2009; Kültz, 2005).

Generically cellular signalling transduction pathways, like the stress response, are comprised of three major levels: a sensor which perceives environmental change; transducers to carry, amplify and integrate the signal; and an effector which promotes an adjustment of cellular function towards the correction of the environmental change and normal cell function (Kültz, 2005). The cellular stress response comprises

sensors which detect macromolecular changes within the cellular lipid membrane, DNA and proteins. These sensors will provide upstream signals to the cellular stress response signalling network and promote alterations in cellular growth, activation of macromolecule damage repair mechanisms (DNA repair mechanisms, heat shock protein response among others), protein homeostasis, cytoskeleton organisation, vesicular trafficking, modification of enzymatic activities, modulation of energy metabolism pathways and modulation of oxidative stress response (Jiang et al., 2011; Kassahn et al., 2009; Kültz, 2005; Muralidharan and Mandrekar, 2013; de Nadal et al., 2011; Simmons et al., 2009). In extreme situations where the activation of these pathways is not enough to repair the cell damage and the cellular tolerance limits are surpassed, induction of apoptosis follows. These stress pathways are in close communication with cellular homeostatic signalling networks which are activated by specific environmental changes. Central stress response elements are the chromatin rearrangements, transcriptional changes, posttranscriptional and posttranslational regulation processes (Finan and Guilak, 2010; Guo and Fang, 2014; Kültz, 2005; Malhas and Vaux, 2011; Martins et al., 2012; de Nadal et al., 2011).

All these generic elements within the cellular stress response and homeostatic response, above explored, are illustrated in Figure 1.3.

The ultimate stress response activation goal is to provide the cell with a repertoire of effector proteins, ribonucleic acids (RNAs) and messengers which will restore the normal cell function by induction of specific transcriptional targets. The more studied effectors within the cellular stress response are proteins, but the relevance of RNA molecules like long non-coding RNAs (lncRNAs) and microRNAs (miRNAs) have been more studied in recent years (Huang et al., 2011; Valadkhan and Valencia-Hipólito, 2016; Valgardsdottir et al., 2008).

Although the stress response involves a highly conserved set of protein (around 300), the specificity of this stress response is denoted by a low common percentage of genes, of approximately 30%, which are upregulated during exposure to different stress types as thermal stress, osmostress or oxidative stress (de Nadal et al., 2011).

The tolerance to environmental stress is highly dependent on the species and specific cell types and features such as increased tolerance to a specific stress after preconditioning with the same type of stress (stress-hardening) and increased tolerance to one type of stress after preconditioning with another (cross-tolerance) are commonly observed (Kültz, 2005; Mattson, 2008).

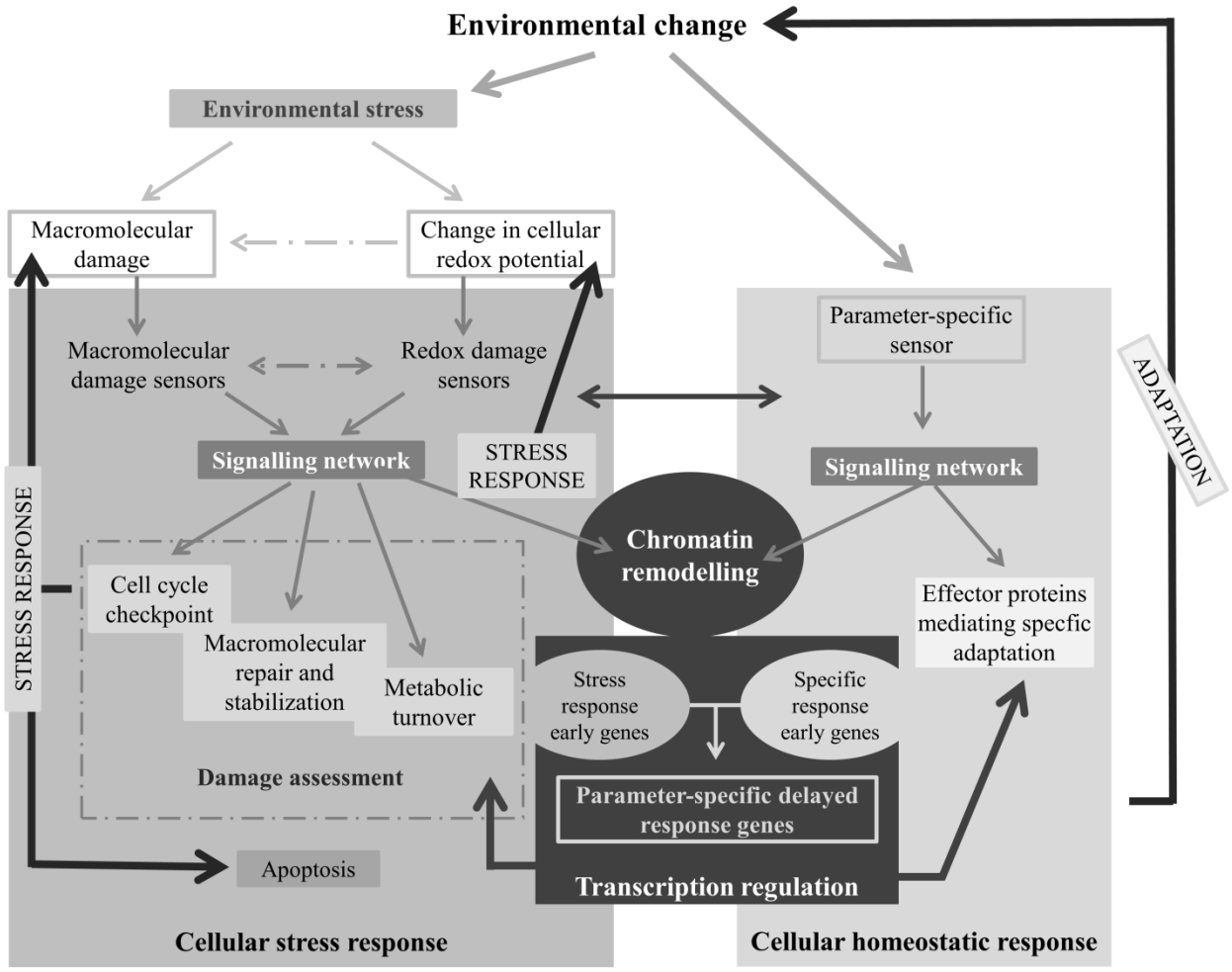

Figure 1.3 – Schematic illustration of important aspects of the cellular stress response and interactions with cellular homoeostasis response. Figure adapted from Kültz 2005.

Stress response mechanisms are also important players in normal development and homoeostasis. For example, impairments in the heat shock response prevent early development in mice (Xiao et al., 1999), and overexpression of the heat shock transcription factor (TF) in *Caenorhabditis Elegans* results in increased longevity (Garigan et al., 2002; Lund et al., 2002). Additionally, defects in systems related to stress responses contribute to human diseases such as cancer, diabetes (Dhillon et al., 2007; Oyadomari et al., 2002), Alzheimer's disease (Terro et al., 2002), Parkinson's disease (Yuzuru et al., 2000), and cardiovascular disease (Pockley, 2002) among others.

One types of stress that is less explored in human cells is the osmotic stress. The next subchapter will explore some specific features associated with the osmotic stress response.

1.3.2. The osmotic stress response

Control of cell size might seem a secondary task but it is highly relevant to several cellular functions. Cell size control is crucial for survival and it is not exclusively associated to environment tonicity but also with signalling which interferes with intracellular osmolarity changes as shown in Table 1.1.

Table 1.1 – Cell volume control mechanisms activated in isotonic environmental conditions. Physiological mechanisms involved in the activation of specific osmolyte transporters. Table adapted from Okada 2004.

Alteration in cell volume	Cellular function	Cell type	Transporters involved
Increase	Absorption	Enterocyte Renal tubular cell Hepatocyte	Na^+ organic solute symport
Increase	Insulin response	Hepatocyte	Na^+-H^+ exchanger Na^+-K^+-$2Cl^-$ cotransporter Na^+ pumps
Increase	Aldosterone response	Lymphocyte	Na^+-H^+ exchanger
Increase	Excitation	Nerve cells	Na^+ channels
Increase	Cell proliferation	S-phase entering cells	Nutrient transporter
Increase	Cell migration	Migratory cells	Na^+-H^+ exchanger K^+ channels Cl^- channels
Decrease	Secretion	Glandular epithelial cell	Cl^- channels
Decrease	Glucagon response	Hepatocyte	K^+ channels Cl^- channels
Decrease	Atrial natriuretic peptide response	Cardiac myocyte	Na^+-K^+-$2Cl^-$ cotransporter
Decrease	Erythrocyte maturation	Reticulocyte	K^+- Cl^- cotransporter

During embryonic development, the zygote maintains its specific diameter for an extended period implying mechanisms of active control over size specification and maintenance. Subsequently, as the embryo suffers successive cleavages into smaller cells, each embryonic stage possesses blastomeres which are maintained with characteristic dimensions (Baltz, 2001). Osmolarity during this developmental process is crucial for successful embryo development. Additionally, to control cell size the pre-implantation embryo uses a unique glycine-mediated osmoregulation mechanism within different osmotic

environments in mouse embryos; this is also likely to happen in human embryos (Baltz and Tartia, 2009). Osmolarity control is also fundamental in processes such as placental differentiation (Liu et al., 2009) oocyte metaphase II spindle formation (Mullen et al., 2004) gamete normal function (Pribenszky et al., 2010, 2012) and *in vitro* culture of mammalian embryos (Cagnone and Sirard, 2016).

On the other hand, some pathophysiological states can lead to a permanent osmotic disturbance either from the extracellular or intracellular environment, as shown in Table 1.2. Additionally, in pathologies such as solid tumours, there are physical constraints to normal diffusion processes and the different osmolarity within different regions of the solid tumour might play a role in cancer progression (Voutouri and Stylianopoulos, 2014).

Table 1.2 – Pathophysiological conditions that lead to an altered environment or intracellular osmolarity. Table adapted from Okada 2004.

Alteration in osmolarity	Pathophysiologic condition
Increased intracellular osmolarity	Ischemia/hypoxia Epilepsy Hepatic encephalopathy
Decreased plasma osmolarity	Congenital heart failure Hepatic cirrhosis Nephrosis Inappropriate ADH syndrome Myxoedema Hyponatremia (cancer)
Increased plasma osmolarity	Diarrhoea Excessive ethanol ingestion Diabetes *mellitus* Diabetes *insipidus* Uraemia Chronic renal failure

Cell volume maintenance mechanisms are very complex, are cell type dependent and still several pathways are not fully understood. Before exploring some of these mechanisms it is important to clarify some basic terms which are many times misinterpreted or misused in the literature. First of all, is important to note that osmolality, osmolarity and tonicity have distinct meanings. While the osmolality is a measure of total solute osmoles per kilogram (Kg) of solvent, taking into account the total solute concentrations (mOsm/Kg); osmolarity is a measure of total osmole per litre (L) of solute, taking into

account the total solute concentrations and is a temperature dependent measure (mOsm/L). On the other hand, tonicity considers just the solutes that cannot freely cross the semipermeable cell membrane like Na^+, K^+, Cl^-, HCO_3^- and glucose (Bersten and Soni, 2009; Rasouli, 2016; Verbalis, 2003). In this way, hyposmolality is always accompanied by hypotonicity but hyperosmolality might not be a synonym of hypertonicity. An example where hyperosmolality is not a synonym for hypertonicity is the excess of urea in plasma, a freely diffusing osmolyte, which induces plasma hyperosmolality without changing tonicity or water movement in the cell because it is evenly distributed between the extracellular and intracellular space (Rasouli, 2016; Verbalis, 2003).

Cells are in general highly permeable to water, this property is closely related to the cellular content of aquaporins (AQPs) and the type of AQPs present, which mediate the type of cellular response (and its intensity) to hyposmotic environments (Galizia et al., 2008; Hoffmann et al., 2009; Liu et al., 2006). In an isotonic environment the characteristic cell volume is maintained by the active extrusion of Na^+ throughout the Na^+-K^+ pump. This steady state for cell volume regulation is called "double-Donnan mechanism" or "pump and leak" mechanism and it is schematized in Figure 1.4

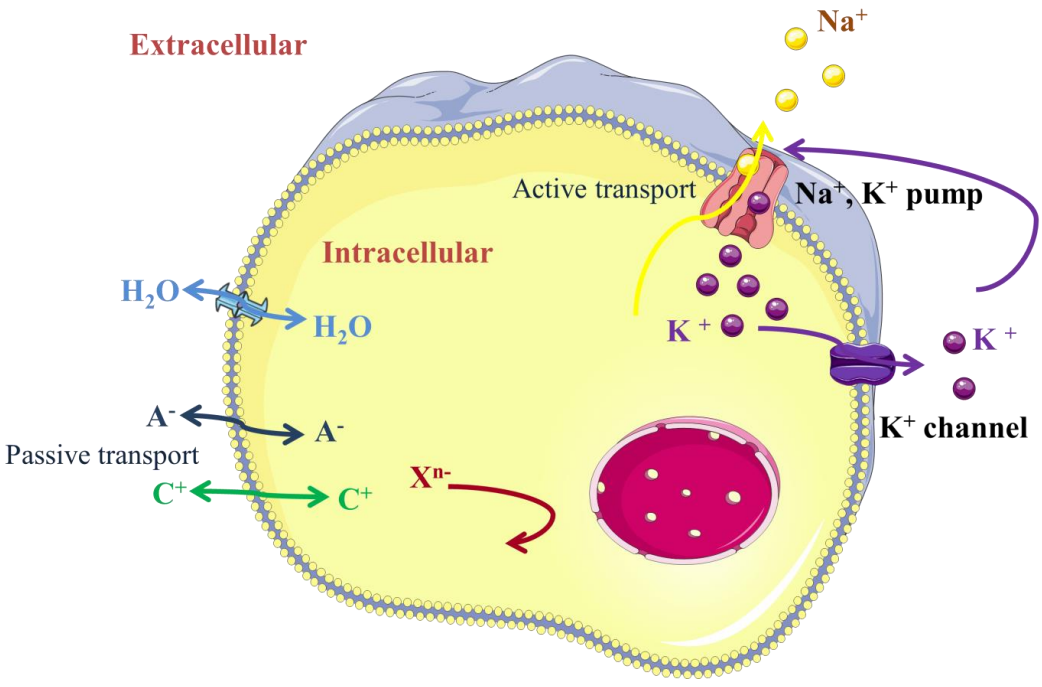

Figure 1.4 – Steady-state cell volume regulation under isotonic environment. This steady state cell volume regulation mechanism, called "double-Donnan mechanism" or "pump and leak", is observed in the great majority of mammalian cells. Figure adapted from Okada 2004.

When cells face an anisosmotic environment, a change in cell volume is observed as a response to the specific extracellular environment tonicity change. The cellular water content and cellular volume are determined by the extracellular concentration of osmotic active compounds and by the extracellular tonicity. The main players in the cell volume maintenance after a tonicity change in the cellular environment can be divided into inorganic osmolytes (mainly Na^+, Cl^- and K^+) and organic osmolytes (mainly taurine, betaine, sorbitol and others).

Therefore, when cells are placed in a hyposmotic environment they will osmotically swell, increasing the cell volume and water content. The cells in this situation will activate regulatory volume decrease (RVD) mechanisms to attempt to return to their normal volume (Figure 1.5) (Hoffmann et al., 2009; Lang et al., 1998; Okada, 2004; Pasantes-Morales et al., 2006; Wehner et al., 2003). During the RVD the cells release K^+, Cl^- and promote a water outflow to attain the original cell volume (Figure 1.7). In specific cell types, a Ca^{2+} influx is also observed during the RVD process (Hoffmann et al., 2009; Lang et al., 1998; Wehner et al., 2003). In a later response also organic osmolytes like taurine can be released from swollen cells (Figure 1.7) (Hoffmann et al., 2009; Lang et al., 1998; Wehner et al., 2003). If the tonicity stimulus is transient and cells are swollen in a hyposmotic environment and then placed into an isosmotic environment the cell will sense the environmental change, shrink and activate a regulatory volume increase (RVI) process. This will, in turn, promote a net gain of K^+, Cl^-, and intracellular water to promote an increase of cell volume to their normal volume (Figure 1.5 and Figure 1.7). As a late response, organic osmolytes like taurine, sorbitol and others can be captured by the shrunken cells (Figure 1.7).

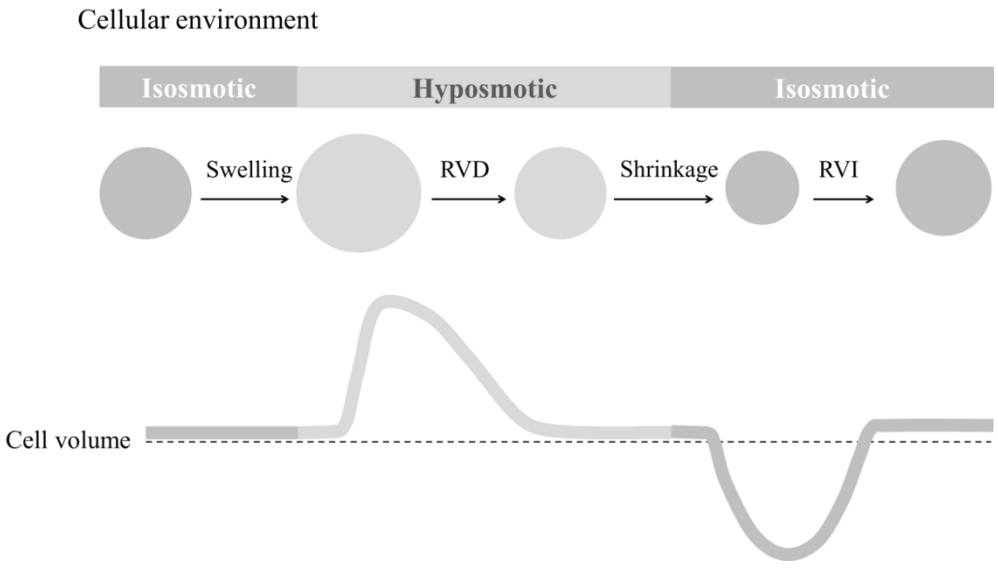

Figure 1.5 – Schematic representation of cell volume variations after presenting the cells transiently to a hyposmotic environment. RVD stands for regulatory volume decrease; RVI stands for regulatory volume increase. Figure adapted from Okada 2004.

Conversely, when cells are placed in a hypertonic environment they will suffer an osmotic shrinkage, and a consequent decrease in the cell volume and water content. The shrunken cells will behave in an opposite manner to the one described for the osmotically swollen cells. Shrunken cells will activate a RVI process and by a net gain of K^+, Cl^- and intracellular water they return to their approximate normal cell volume (Figure 1.6 and Figure 1.7) (Hoffmann et al., 2009; Lang et al., 1998; Okada, 2004; Pasantes-Morales et al., 2006; Wehner et al., 2003). The uptake of organic osmolytes like taurine, sorbitol and others can be seen as a late response of the shrunken cells (Figure 1.7) (Hoffmann et al., 2009; Lang et al., 1998; Okada, 2004; Pasantes-Morales et al., 2006; Wehner et al., 2003). If after transient exposure to a hypertonic environment the cells are placed into an isosmotic environment, the cells will be osmotically swollen and the RVD mechanism will be activated to restore the cell volume (Figure 1.6) as described above (Hoffmann et al., 2009; Koivusalo et al., 2009; Lang et al., 1998; Okada, 2004; Wehner et al., 2003).

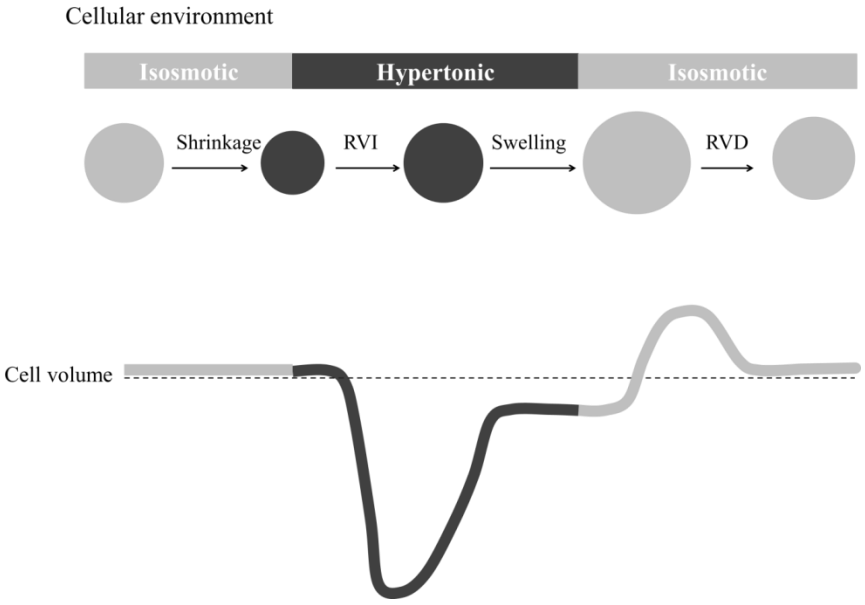

Figure 1.6 – Schematic representation of cell volume variations after presenting the cells transiently to a hypertonic environment. RVI stands for regulatory volume increase; RVD stands for regulatory volume decrease. Figure adapted from Okada 2004.

All the mechanisms behind the RVD and RVI processes are very complex and involve certain specific ionic channels and osmolyte transporters which are still undiscovered. Nevertheless, the knowledge in this field has been conquered over a long time and the information on the major players in the RVD and RVI is synthesised in Table 1.3.

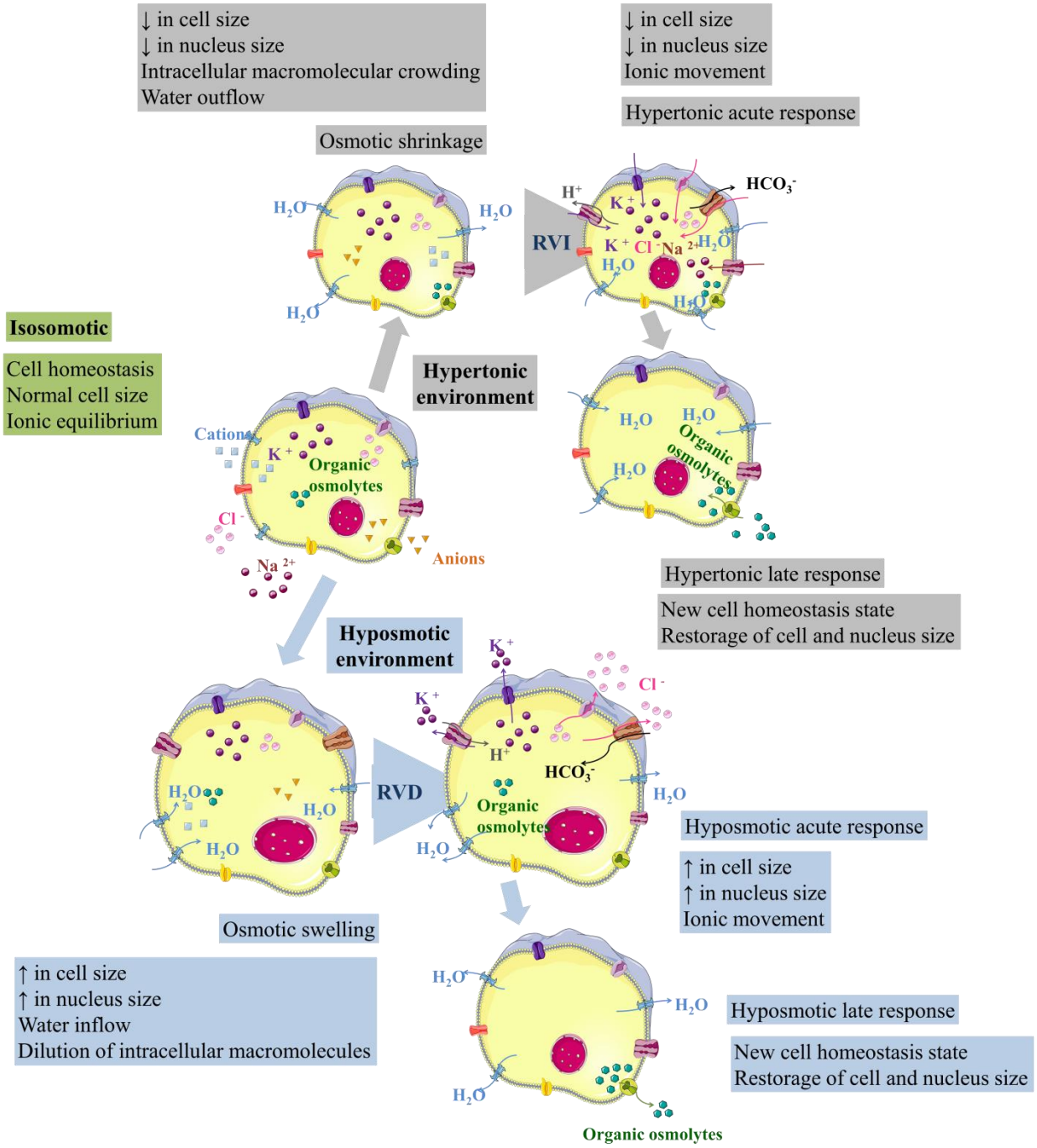

Figure 1.7 – Schematic illustration of cell volume variations after presenting the cells to anisosmotic environments and the main ions involved in cell volume regulatory mechanisms.

Table 1.3 – Summary of the main effectors of cell volume regulatory mechanisms. Table adapted from Koivusalo, Kapus, and Grinstein 2009.

Effector	Substrates (stoichiometry)	Regulators
Regulatory volume decrease		
K^+ channels	K^+	
Two pore domain K^+ channels (K_{2P} – e.g. TRAAK, TREK-1, TASK)		Arachidonic acid, leukotrienes, membrane stretch.
Large-conductance channels (BK_{Ca2+})		Leukotrienes, membrane stretch, Ca^{2+} concentration (μM).
Intermediate conductance channels (IK_{Ca2+})		Ca^{2+} concentration (nM).
Ca^{2+} activated channels of small conductance (SK_{Ca2+})		Ca^{2+} concentration (nM).
Voltage-gated K^+ channels (e.g. Kv1.3, Kv1.5, Kv4.2, Kv4.3, KCNQ1-4)		
Volume-regulated anion channels	Cl^-, HCO_3^-, organic osmolytes (?)	Fatty acids, cholesterol, Rho GTPase, reactive oxygen species, Ca^{2+}, kinases
K^+ - Cl^- co-transporters (isoforms 1-4)	K^+, Cl^-	Kinases
Taurine efflux	Taurine	Leukotrienes, lysophospholipids, reactive oxygen species, Ca^{2+}, kinases.
Transient receptor potential channels	Ca^{2+}	Membrane stretch.
Regulatory volume increase		
Na^+ /H^+ exchanger	Na^+ in exchange for H^+ (1:1)	Cholesterol, phosphatidylinositol bisphosphate, membrane deformation, kinases.
Anion exchangers	Cl^- in exchange for HCO_3^- (1:1)	
Na^+, K^+, Cl^- co-transporters (isoform 1,2)	Na^+, K^+, Cl^- (generally 1:1:2)	Kinases
Non-selective hyperosmolality-induced cation channels	Monovalent cations (mainly Na^+)	
Amiloride-sensitive, Gd^{3+} and flufenamate-insensitive		Phospholipase C, G-proteins.
Amiloride-insensitive, Gd^{3+} and flufenamate-sensitive		Ca^{2+} concentration (μM)
Amiloride-sensitive, Gd^{3+}-sensitive		
Transient receptor potential channels	Na^+	Membrane stretch.

Effector	Substrates (stoichiometry)	Regulators
Organic osmolytes		
Taurine: taurine transporter	Taurine, Na^+, Cl^- (1:3:1).	Osmotic response element, arachidonic acid.
Betaine: betaine/gamma-aminobutyric acid transporter (BGT1)	Betaine, Na^+, Cl^- (1:3:1).	Osmotic response element.
Inositol: sodium myoinositol transporter.	Inositol, Na^+ (1:2).	Osmotic response element.
Sorbitol: synthesised from glucose by aldose reductase.		Osmotic response element.
Glycerophosphocholine: synthesised from phosphocholine by phospholipase B.		Osmotic response element.

Ionic changes are also accompanied by changes in the cell membrane potential and mitochondrial function. In regard to the cell membrane potential, there are no comprehensive studies in different cell types, but the hyposmotic environment has been shown to promote stress evoked complex responses with both hyperpolarization and depolarization phases in rat's aortic endothelial cell layer (Marchenko and Sage, 2000). The maintenance of the cell membrane potential is highly related with the ionic balance between the intracellular and extracellular environment, as represented in Figure 1.8, and therefore an important function that is also altered in anisosmotic environments.

The ionic changes have the potential to impact all the organelles that function in a cytosolic milieu containing several cations and anions. The mitochondria are particularly interesting organelles as the inner mitochondrial membrane is impermeable to cytosolic ions and their flux and concentration in the mitochondrial matrix are controlled by specific channels and exchangers. Any imbalance in the ionic flux can affect the osmotic balance between cytosol and the mitochondrial matrix and promote the water movement between these compartments. The intracellular potassium concentration is considerably higher than other ions and therefore altered potassium fluxes can be a key mediator for mitochondrial matrix volume changes observed with depolarization, calcium overload and the opening of permeability transition pore. In addition to the mitochondrial swelling, osmotic imbalances will also affect the mitochondrial potential. Nevertheless, the experimental data on mitochondrial matrix swelling and mitochondrial potential changes are inconsistent. It has been suggested that a high membrane potential corresponds to the swollen state and that when the potential collapses the mitochondria contract (Garlid and Paucek, 2003; Kaasik et al., 2007). In contrast, several works based on fluorescence microscopy

studies suggest that mitochondria swell when they lose their membrane potential (Gao et al., 2001; Kaasik et al., 2007; Lyamzaev et al., 2004; Minamikawa et al., 1999), and others reported no volume change or a small change (Kaasik et al., 2007; Kahlert and Reiser, 2002; Poppe et al., 2001). Although some of the works did not establish a clear link between mitochondrial matrix swelling and mitochondrial potential additional findings demonstrate that the loss of mitochondrial membrane potential is associated with mitochondrial swelling promoted by a balanced influx of potassium (Kaasik et al., 2007; Safiulina et al., 2006).

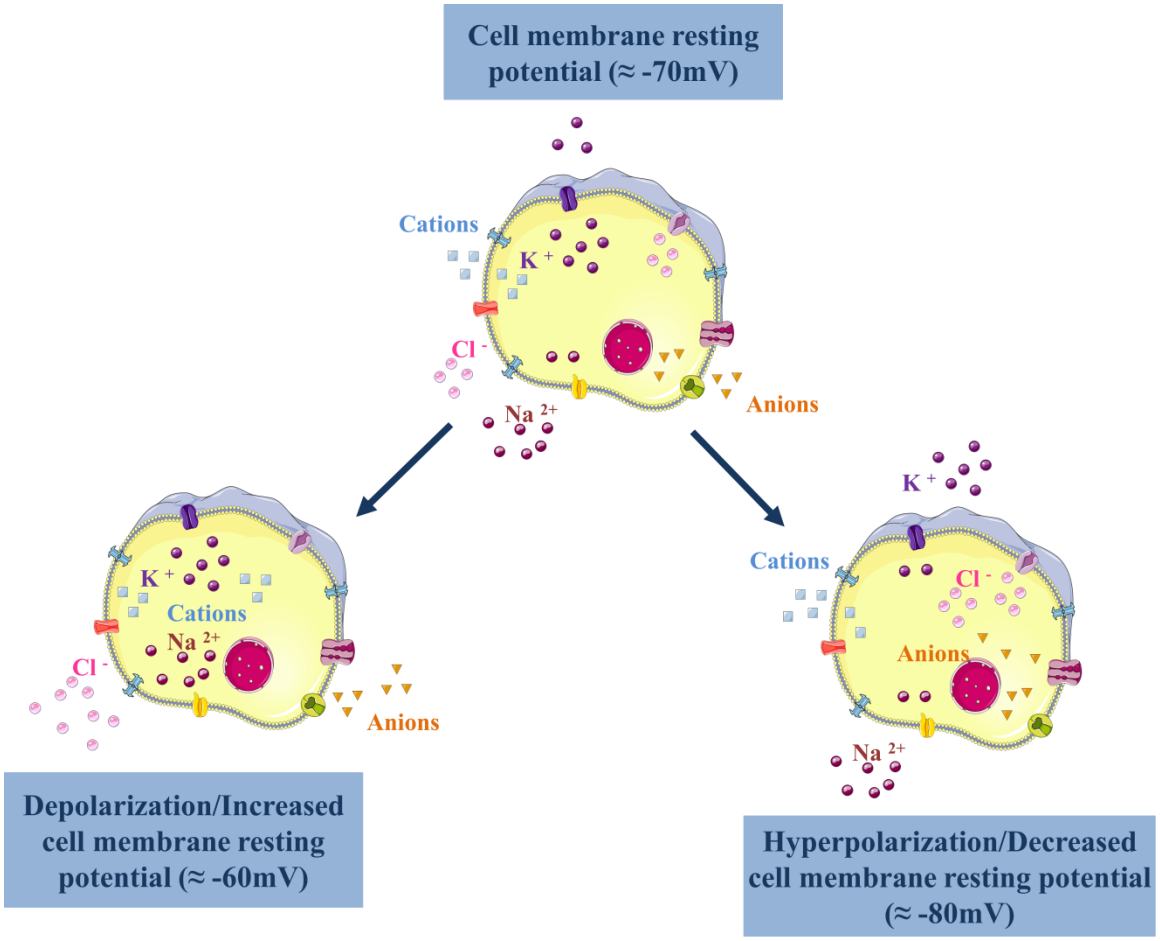

Figure 1.8 – Cell membrane potential changes associated with different ionic fluxes.

Although the cell volume regulatory response mechanisms have been well explored in the context of osmotic stress there are several alterations in signalling pathways, transcriptional profile, organelle function and other regulatory mechanisms that are common to various other types of stress. Therefore, the

next three subchapters explore the alterations in signalling cascades, transcriptional profile, nuclear shape and cellular metabolism in response to different stressors.

1.3.3. Signalling cascades

The cellular stress response leads to the activation of some common signalling pathways through mitogen-activated protein kinases (MAPK). Additional signalling can occur in a stress-specific manner, mainly by induction of specific TFs.

MAPK pathways exert major effects on cell physiology by orchestrating the gene transcription, protein biosynthesis, cell cycle control, apoptosis and differentiation processes (Ferreiro et al., 2010a; Gehart et al., 2010; Kyriakis and Avruch, 2012; de Nadal et al., 2011).

The three-layer phosphorylation cascade performed by different groups of kinases, the "core signalling modules" is a characteristic feature of MAPK signalling pathways. Within these modules, the MAPKs are phosphorylated and activated via simultaneous tyrosine and threonine phosphorylation within a Thr-X-Tyr motif within kinase subdomain VIII (Figure 1.9). This phosphorylation is catalysed by members of the dual-specificity MAPK kinases (MAP2Ks, also called MEKs or MKKs). The MAP2Ks are activated by serine/threonine phosphorylation, again within a conserved motif in kinase subdomain VIII (Figure 1.9). This phosphorylation is catalysed by a diverse group of protein kinase families referred to as MAPK kinase kinases (MAP3Ks) (Ferreiro et al., 2010a; Gehart et al., 2010; Kyriakis and Avruch, 2012; de Nadal et al., 2011).

Within this big MAPK family, there are at least four subfamilies which can be activated by environmental stressors: the extracellular signal-regulated kinases (ERK1/2); ERK5 (known also as BMK1 and MAPK7); Jun amino-terminal kinases (JNK1-3) and p38 kinases (p38α, β, γ and δ). Their main structural features are represented in Figure 1.9.

In summary, each group of these MAPKs is composed of a set of three evolutionarily conserved, sequentially acting kinases: a MAPK, a MAP2K, and a MAP3K as schematized (Figure 1.10). The MAP3Ks, which are serine/threonine kinases, are often activated through phosphorylation and/or as a result of their interaction with a small guanosine triphosphate (GTP)-binding protein of the Ras/Rho family in response to extracellular stimuli. The MAPK activity promotes the activation of the MAPK activated protein kinases (MAPKAPKs) as schematized to the conventional MAPK in Figure 1.10.

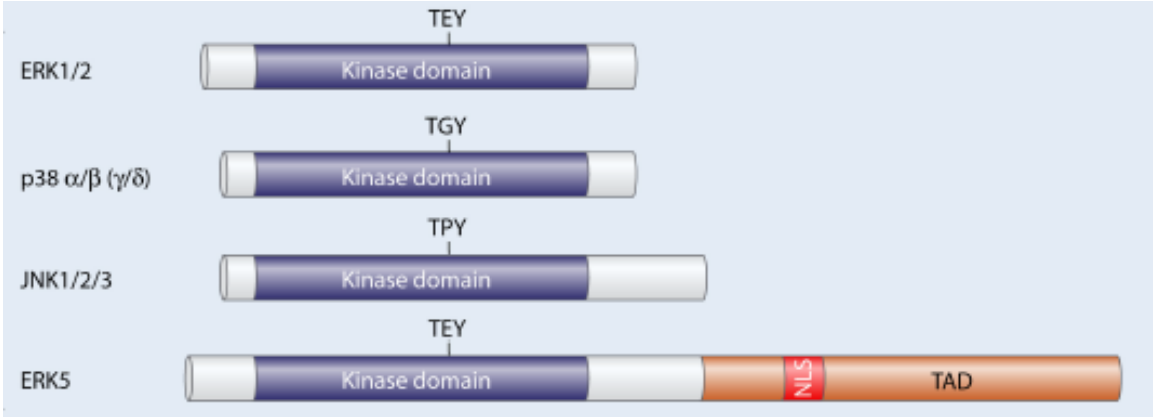

Figure 1.9 – Main structural domains of mitogen-activated protein kinases (MAPK) enzymes. All MAPKs contain a serine/threonine kinase domain flanked by N- and C-terminal regions with different sizes. Additional domains are also present in some MAPKs, including a transactivation domain (TAD) and a nuclear localisation sequence (NLS). Figure adapted from Cargnello and Roux, 2011.

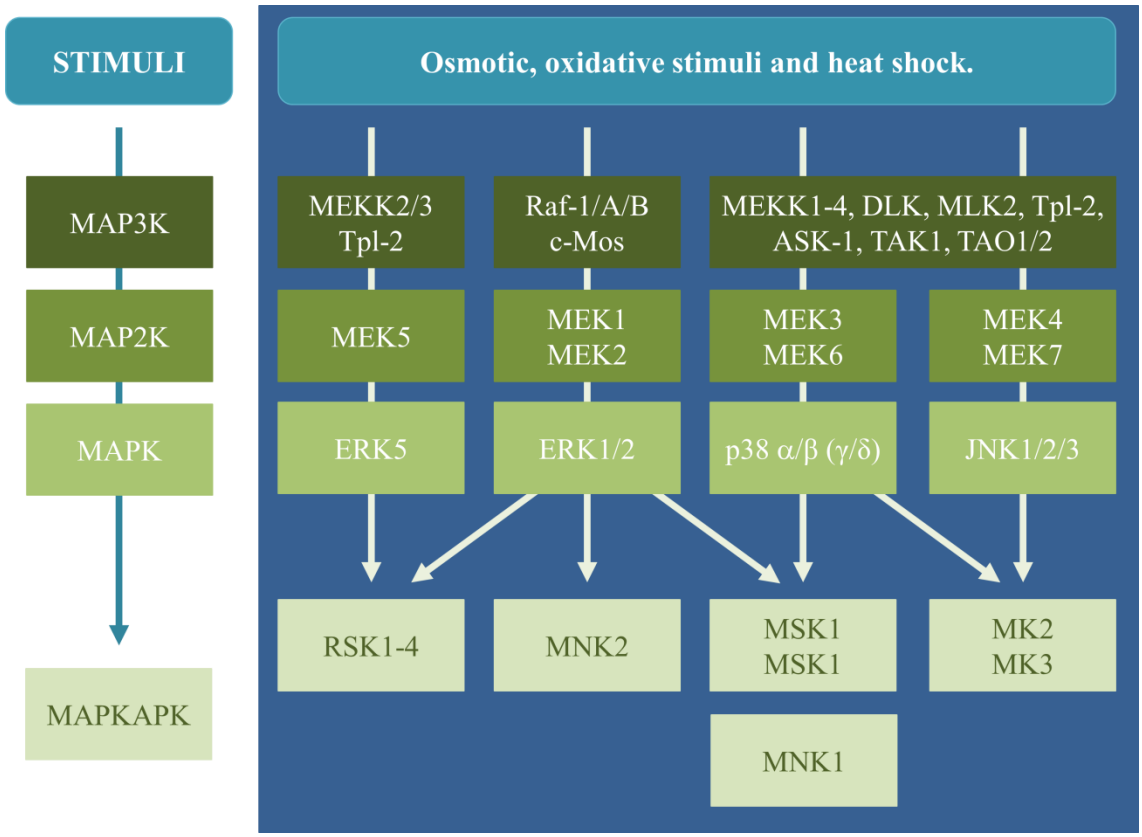

Figure 1.10 – Mitogen-activated protein kinase (MAPK) signalling cascades leading to activation of the MAPK activated protein kinases (MAPKAPKs). Cellular stresses can promote the activation of different MAPK pathways, which in turn phosphorylate and activate the five subgroups of MAPKAPKs, including RSK1-4, MSK1, MNK1-2 and MK2/3. MAP2K stands for MAPK kinases; MAP3K stands for MAPK kinase kinases. Figure adapted from Cargnello and Roux, 2011.

The molecular mechanism of ERK1/2 activation by receptor tyrosine kinase (RTK) involves Ras activation. Following ERK1/2 activation, these MAPKs translocate to the cell nuclei and phosphorylate TFs and downstream kinases (MAPKAPKs), which promotes cell cycle progression and proliferation (Cargnello and Roux, 2011; Kyriakis and Avruch, 2012; Zhou et al., 2016) via several mechanisms, including the induction of positive regulators of the cell cycle proliferation (Cargnello and Roux, 2011; Kyriakis and Avruch, 2012; Zhou et al., 2016).

ERK5 is ubiquitously expressed throughout all mammalian tissues and cell lines (Buschbeck and Ullrich, 2005; Gomez et al., 2016; Lee et al., 1995; Zou et al., 1995) and it is activated in response to several growth factors and oxidative and hyperosmotic stress (Diaz-Rodriguez and Pandiella, 2010; Gomez et al., 2016; Inesta-Vaquera et al., 2010; Kato et al., 2000). ERK5 has as main nuclear targets the TF Sap1, a member of the ternary complex factors; the three members of the myocyte enhancer factor-2 family of TFs (MEF2A, MEF2C, and MEF2D) which regulate cell differentiation in myocytes and neurons (Potthoff and Olson, 2007) and the promyelocytic leukaemia TF (PLZF) which acts as a tumour suppressor through activation of the CDK inhibitor p21 (Bernardi and Pandolfi, 2007) and act as a nodal point for stress-response in adult tissues (Kim et al., 2008).

The p38 MAPK and JNK MAPK are also designated as stress-activated protein kinases (SAPKs). JNKs and p38 are strongly activated by heat shock, ionizing radiation, oxidative stress, osmotic stress, DNA-damaging agents, cytokines, ultraviolet irradiation, protein synthesis inhibitors, endoplasmic reticulum stress, molecular damage and are slightly activated by mitogens (Cargnello and Roux, 2011; Chang and Karin, 2001; Cobb, 1999; Kyriakis and Avruch, 2012; Yang et al., 2013; Zhou et al., 2016). The MAP3Ks involved in JNK activation also activate the p38 MAPK pathways, and these two groups of MAPKs share some upstream regulators of MAP3Ks as represented in Figure 1.10 (Cargnello and Roux, 2011; Chang and Karin, 2001; Kyriakis and Avruch, 2012; Yang et al., 2013; Zhou et al., 2016).

The JNK family is composed by three isoforms; JNK1-3. Following activation, JNKs translocate to the nucleus and regulate gene expression through the phosphorylation of diverse TFs, such as activating TF 2 (ATF-2), nuclear factor of activated T-cells 1 (NF-ATc1), ETS TF (Elk-1), heat shock factor protein 1 (HSF-1), signal transducer and activator of transcription 3 (STAT3), c-Myc, Jun-b, c-Jun, tonicity-responsive binding protein (TonEBP), and p53. These regulatory mechanisms participate in the control of multiple cellular processes, such as c-Jun-dependent proliferation (Cargnello and Roux, 2011; Kyriakis and Avruch, 2012; de Nadal et al., 2011; Sabapathy et al., 2004; Zhou et al., 2016) .

The p38 MAPK family has four members, p38α/β/γ/δ. When the first p38 member (p38α) was identified in 1994, this kinase had shown to display significant homology to the product of the *Saccharomyces cerevisiae* HOG1 gene (Hohmann, 2002). The Hog1 MAPK that plays central roles in osmosignalling and adaptation during hypertonic stress in yeast. p38α MAPK is 50% identical to ERK2

(Cargnello and Roux, 2011; Cuadrado and Nebreda, 2010; Ferreiro et al., 2010a, 2010b; Kyriakis and Avruch, 2012; de Nadal et al., 2011; Sabapathy et al., 2004; Zhou et al., 2016). p38 MAPKs are activated via phosphorylation by MAP2Ks such as MKK3, MKK4, and MKK6 (Cargnello and Roux, 2011; Cuadrado and Nebreda, 2010; Ferreiro et al., 2010a, 2010b; Kyriakis and Avruch, 2012; de Nadal et al., 2011; Sabapathy et al., 2004; Zhou et al., 2016). Target substrate phosphorylation by p38 MAPKs regulates gene expression and the stability of specific targets, which affect processes such as cell cycle arrest, proliferation, autophagy, and apoptosis (Cargnello and Roux, 2011; Cuadrado and Nebreda, 2010). These players are schematized and organised by cellular function impact in Figure 1.11.

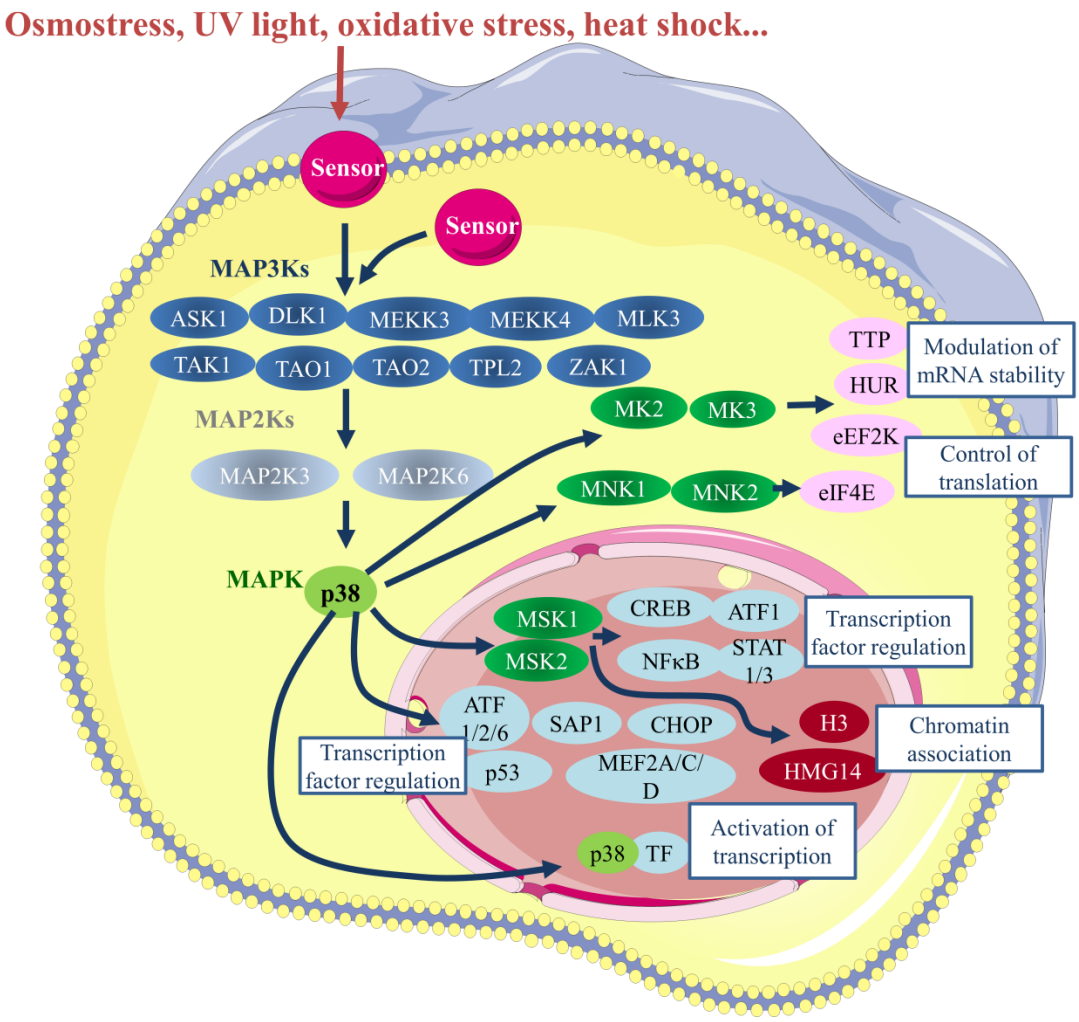

Figure 1.11 – Stress signalling by p38 MAPKs. Different environmental stresses, as well as other stimuli, such as growth factors and inflammatory cytokines, can activate the mammalian stress-activated protein kinase (SAPK) pathway. Downstream targets of p38 MAPKs include several kinases that are involved in the control of messenger RNA (mRNA) stability, the translational process, gene expression, regulators of chromatin remodelling and activation of transcription factors (TF in the figure). Binding of p38 MAPKs to stress-dependent *loci* allows the recruitment of RNA polymerase II and activation of transcription. Figure adapted from de Nadal et al., 2011.

From the different environmental stimuli, a decreased or increased osmolarity triggers the activation of ERK1/2, p38 MAPK, and JNK. Many reports demonstrate that the pattern of changes in MAPK activity during osmotic stress is dependent on cell type, culture conditions, and osmotic stress strength (Cargnello and Roux, 2011; Cuadrado and Nebreda, 2010; Ferreiro et al., 2010a, 2010b; Kyriakis and Avruch, 2012; de Nadal et al., 2011; Sabapathy et al., 2004; Zhou et al., 2016). Several studies have shown that during osmotic stress, MAPKs are relevant not only in long-term responses, such as cell proliferation, survival/cell death, and gene expression but also in immediate responses like the volume regulatory processes (RVD/RVI).

During hyposmotic stress, ERK1/2, p38 MAPK, and JNK are activated (Zhou et al., 2016). This activation is a rapid response in the great majority of the cases and appears to occur at a similar timeframe of RVD response activation. The pattern of the activation of the MAPK signalling cascade is dependent on cell type, showing that a cell-specific MAPK activation pattern might exist within the hyposmotic modulation. Hyposmotic stress-induced ERK1/2 activation is required for the RVD in human cervical cancer cells and rabbit corneal epithelial cells (Pan et al., 2007; Shen et al., 2001), while RVD after hypotonic swelling depends on p38 MAPK activation in renal epithelial A6 cells and perfused rat liver (Chiri et al., 2004; vom Dahl et al., 2001) and on JNK activation in rabbit corneal epithelial cells (Pan et al., 2007) as schematized, in a generic way, in Figure 1.12. The interdependence between MAPK activation and regulatory volume processes is not fully understood but some evidence shows that these pathways are closely related (Belsey et al., 2007; Crepel et al., 1998; vom Dahl et al., 2001; Du and Sorota, 2000; Franco et al., 2004; Shen et al., 2001).

Moreover, MAPKs are implicated in long-term hyposmotic stress responses and cellular functions like the transepithelial Na^+ reabsorption by renal epithelial cells (Figure 1.12). The long exposure to hyposmotic stress stimulates Na^+ entry through receptor tyrosine kinase JNK cascade-dependent translocation of epithelial sodium channels (ENaC) to the apical cell membrane (Taruno et al., 2007) which is supported by the p38 MAPK induction of ENaC mRNA expression (Niisato et al., 2007). Additional studies revealed that within the osmotic stress MAPKs are related with the activity of ionic channels, ATP release, production of cytokines (IL-8 and IL-1β) and to long-term adaptation to hyposmolarity through activation of cell survival and proliferation mechanisms (Cargnello and Roux, 2011; Cuadrado and Nebreda, 2010; Ferreiro et al., 2010a, 2010b; Kyriakis and Avruch, 2012; de Nadal et al., 2011; Sabapathy et al., 2004; Zhou et al., 2016).

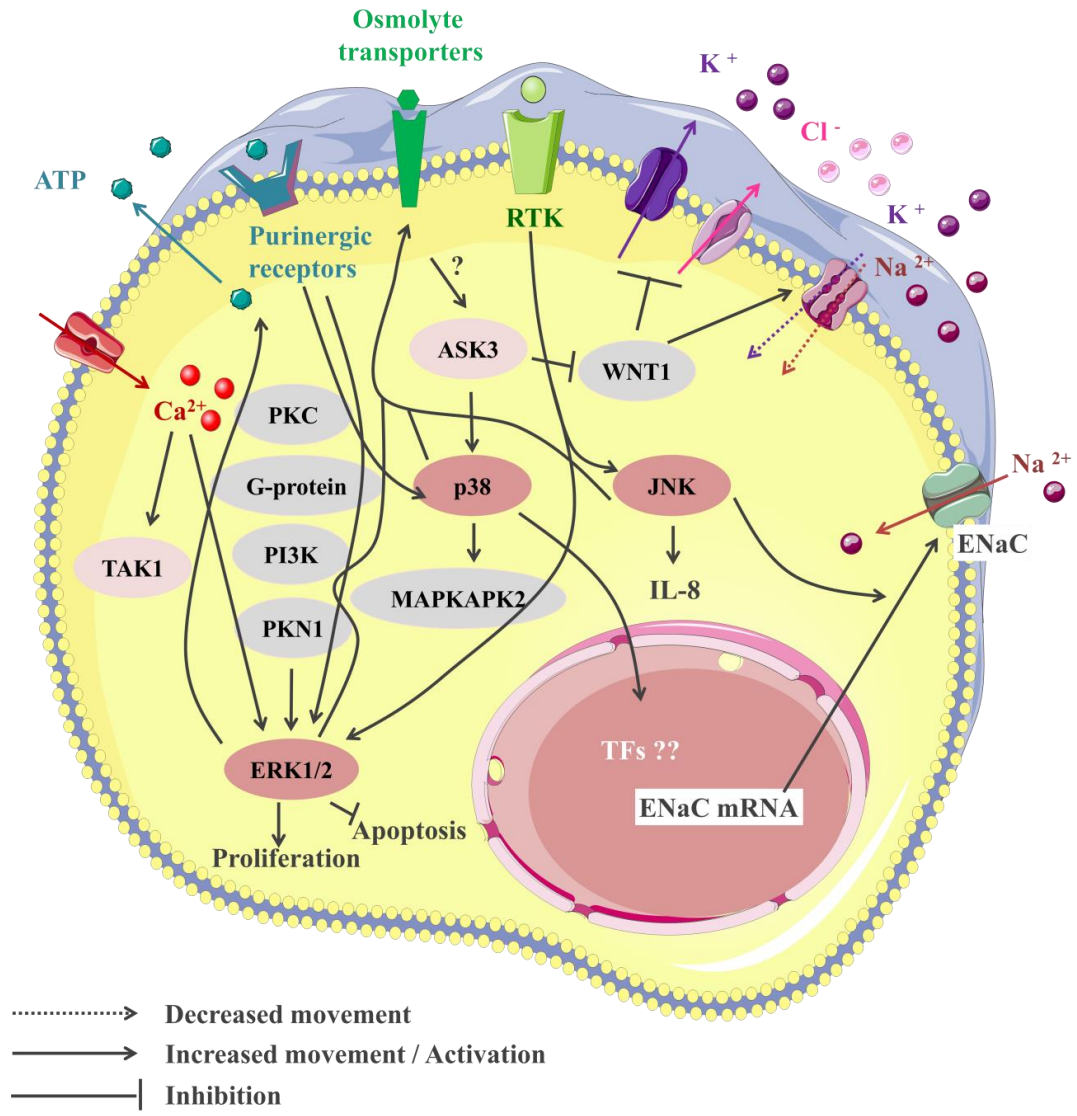

Figure 1.12 – MAPK signalling pathways under hyposmotic stress. Figure adapted from Zhou et al. 2016.

Also within a hypertonic environment, the cells activate the MAPK signalling pathway (Figure 1.13). As in the case of hyposmolarity, MAPK signalling is required for RVI changes at the level of ionic channels changes and osmolyte transport. When cells face persistent hypertonicity, MAPKs mediate signals which involve the regulation of TonEBP, also referred to as osmotic response element binding protein (OREBP) or nuclear factor of activated T-cells 5 (NFAT5), preparing the cells to adapt to stressful conditions. TonEBP is a member of the Rel family and, little is known about the mechanisms underlying TonEBP activation in response to hypertonicity. TonEBP is triggered by the joined action of p38 MAPK and the GTPase activity of Rac1 in human kidney cells (Dahl et al., 2001; Ko et al., 2002) and ATM

kinase also activates TonEBP in response to hypertonicity (Irarrazabal et al., 2004; Zhang et al., 2005). Moreover, TonEBP is responsible for the increase in the amount of several enzymes and chaperones like the heat-shock protein 70-2 (HSP70-2). The expression of HSP70 family proteins contributes to cell survival in high tonicity (Lee et al., 2005; Shim et al., 2002) and high osmolarity (Neuhofer et al., 1999) conditions.

The relevance of MAPK signalling in osmostress is summarised in Figure 1.12 and Figure 1.13.

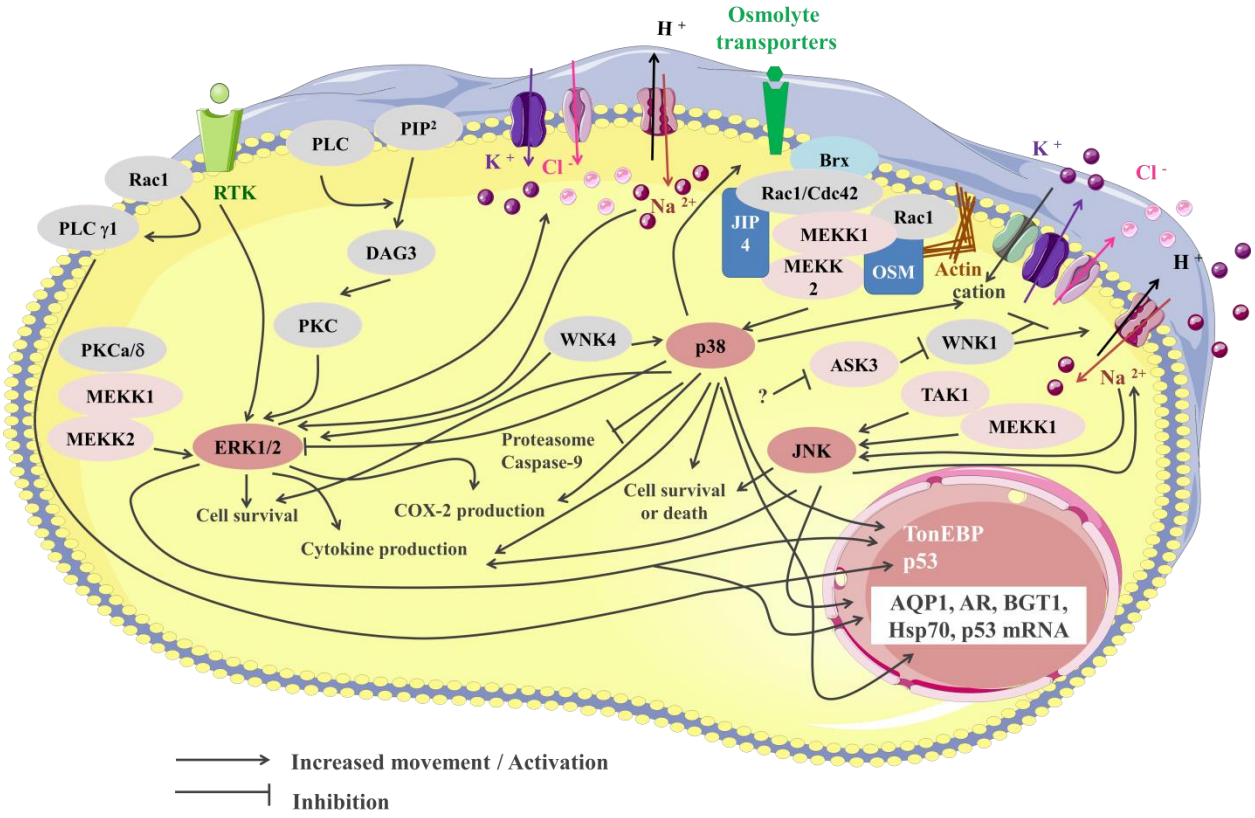

Figure 1.13 – MAPK signalling pathways under hypertonic stress. Figure adapted from Zhou et al. 2016.

The ultimate goal of the stress response is to alter the transcriptional profile of the cell and enable an adequate cell response to a specific stimulus. Therefore, the next subchapter will explore the transcriptional and nuclear changes that follow a stress response in more detail.

1.3.4. Transcriptional and nuclear structure changes

Transcriptional changes are a key element of cellular adaptation to stress. They provide the avenue for the establishment of new transcriptional networks and, therefore, an adapted repertoire of proteins and macromolecules, which enable the cell to react to disruption of homoeostasis (de Nadal et al., 2011).

Different TFs, summarised in Table 1.4, are activated in a stress-specific manner.

Table 1.4 – Summary of representative transcription factors which are activated in a stress-specific manner. Table adapted from Simmons et al., 2009.

Pathway	Sensor	Major transducers	Transcription factors	Activated gene promoters
Oxidative stress	Keap1	MAPK, ERK, PKC.	Nrf2, AP-1, NF-κB	HMOX1, NQO1, GST2A HSF-1
Heat shock response	Hsp90	CaMK2, CK2.	HSF-1	HSPA6
DNA damage	MDM2	ATM, JNK, Chk1, Chk2.	p53	CDKNIA, GADD45A, MDM2, BCL2, TP53I3
Hypoxia	VHL	p38 MAPK, PI3K.	HIF-1	VEGF, TF, EPO XBP-1,
Endoplasmic reticulum stress	BiP	IRE1α, S2P.	XBP-1, ATF6, ATF4	HSP90B1, HSPA5, DNAJB9
Hypertonic stress	Mucins? Glycocalyx components? ??	MAPK, ATM, PKA	TonEBP	AKR1B1, SLC6A12, SLC5A3
Hyposmotic stress	Mucins? Glycocalyx components? ??	MAPK DNA methylation? Direct structural influence?	TonEBP? SP1? Osmolyte sensitive transcription factors: ERG1?	ENaC? lncRNAs? miRNAs? ??
Inflammation	IkB	IKK	NF-κB	IL1α, TNFα

The commonly generic structured stress response signalling pathway with sensors, transducers and effectors, as mentioned earlier, allows cells to respond quickly and without delaying *de novo* gene transcription (Simmons et al., 2009).

The early key changes which occur in stress and other types of situations are not sensitive to protein synthesis inhibition and in a first impact involve alterations of the activity or degradation profile of components which are already inside the cell. One of the most common reversible, posttranslational

modifications is protein phosphorylation that is able to modulate the activity of numerous proteins. The transducer proteins which ultimately promote gene expression changes, the TFs, are often sensitive to the action of specific protein kinases and phosphatases (Cargnello and Roux, 2011; Kyriakis and Avruch, 2012; Zhou et al., 2016). Additional changes include organelle function alteration, macromolecule stability modulation, sequence-specific binding, and nuclear transport of numerous TFs and their regulators (Cyert, 2001; Gill, 2003; Markstein and Levine, 2002). Moreover the transcriptional programs are controlled by chromatin rearrangements, rearrangements of chromatin remodelling complexes and many posttranslational histone modifications (Berger, 2002; Fischle et al., 2003; Kültz, 2005; Zhang et al., 2015b).

Regarding posttranslational modifications, these are relevant modifications that can control the transcription process itself by the action of enzymes such as protein kinases. RNA Pol II is one fundamental form of RNA polymerases for gene expression and coordination of co-transcriptional processing (Jasnovidova and Stefl, 2013). The RNA Pol II form is not only responsible for transcription of protein-coding genes but also for several RNA genes like: small noncoding RNAs (sncRNAs), long non-coding RNAs (lncRNAs) and microRNAs (miRNAs). The other forms of RNA polymerase, RNA Pol I and III are responsible for the transcription of ribosomal RNA (rRNA), with the exception of 5S rRNA and production of transfer RNA (tRNA) and 5S rRNA, respectively (Weipoltshammer and Schofer, 2016). In contrast to the RNA Pol I and III, RNA Pol II contains within its larger subunit, the RPB1, a long and flexible C-terminal domain (CTD). The CTD can be subdivided into three structures: a flexible linker, a region of tandem repeats of the consensus sequence (Tyrosine, Serine, Proline, Threonine, Serine, Proline, Serine: $Y_1S_2P_3T_4S_5P_6S_7$) and a divergent C-terminal portion (Jasnovidova and Stefl, 2013).

This CTD is subjected to dynamic posttranslational modifications within the consensus sequence region and those modifications affect directly the transcriptional cycle progression. Phosphorylation is the most frequent modification of the consensus sequence region of the CTD. The phosphorylation of serine residues in the positions 5 and 7 of the consensus sequence region of the CTD is associated with transcription initiation and phosphorylation of serine residue in the position 2 of the CTD is associated with transcription elongation. Further posttranslational modifications within the consensus sequence region of the CTD can include glycosylation, methylation, ubiquitination, acetylation and sumoylation (Jasnovidova and Stefl, 2013).

Transcription is a highly complex and controlled process. In addition to posttranslational control of RNA Pol II function, a major regulator of transcription is chromatin structure, organisation and nuclear architecture (Iborra et al., 1996; Martins et al., 2012; Pombo and Dillon, 2015). The assembly of

transcription factories is considered to be crucial to ensure an efficient RNA production by increasing the temporal and spatial availability of transcription modulators (Weipoltshammer and Schofer, 2016). The spatial distribution of the transcriptional factories and the coordination with chromatin organisation and nuclear architecture is essential for coordinated gene expression. Additionally, this coordination might facilitate the spatial co-localisation of *cis*- and *trans*-acting transcription regulatory elements (Weipoltshammer and Schofer, 2016). For instance, distant *loci* from different chromosome territories which are co-regulated can be found in the same transcription factory by the formation of long-range loops such as the ones observed during some cellular differentiation processes (Park et al., 2014; Weipoltshammer and Schofer, 2016). The level of chromatin packaging in lightly compacted euchromatin areas or densely packed heterochromatin areas is usually associated with permissive or inhibitory signals to transcriptional events (Berger, 2002; Fischle et al., 2003; Pombo and Dillon, 2015; Schneider and Grosschedl, 2007; Zhang et al., 2015b). Usually, TFs cannot have access to the densely packed chromatin areas. Nevertheless, pioneer TFs present distinctive features which allow their binding to DNA target sites even in condensed chromatin areas including deoxyribonuclease I (DNase I) inaccessible chromatin sites (Cirillo et al., 2002; Zaret and Carroll, 2011; Zaret et al., 2016). These TFs also initiate nucleosomal remodelling by local histone modification and define the localisation of other TFs by cooperative recruitment. A representative list of pioneer factors is presented in Table 1.5.

Table 1.5 – Summary of representative pioneer transcription factors and their respective cellular functions. Table adapted from Iwafuchi-Doi and Zaret, 2014.

Pioneer transcription factor	Function
Forkhead box A (FoxA)	Development and metabolism.
Oct4	Self-renewal, stemness.
Sex-determining region Y-box 2 (Sox2)	Self-renewal, stemness.
Krüppel-like factor 4 (Klf4)	Self-renewal, stemness.
Achaete-Scute Family BHLH Transcription Factor 1 (Ascl1)	Development of specific neural lineages.
Paired Box 7 (Pax7)	Foetal development and cancer growth.
PU.1	Myeloid differentiation.
GATA Binding Protein 1 (GATA1)	Erythroid differentiation.
GATA Binding Protein 4 (GATA4)	Myocardial differentiation and function.
GATA Binding Protein 6 (GATA6)	Intestine, lung, and heart development.
CLOCK:BMAL1	Circadian rhythm.
p53	Cell cycle and apoptosis.

The chromatin state is determined by the DNA and histone modifications on the nucleosome particle, which include DNA methylation and histone acetylation, methylation, phosphorylation, ubiquitination and sumoylation (Martins et al., 2012). A very interesting feature related with DNA methylation has to do with the possible effect of hydration of the DNA molecules in the chromatin packaging process (Kaur et al., 2012). In the presence of water, chromatin reconstituted on methylated DNA is more compact due to the methyl group hydrophobicity that favours a stiffer DNA molecular conformation (A DNA) (Kaur et al., 2012). This effect is less noticeable when performing the same experiments with unmethylated DNA. These displacement water forces also play a role in the DNA interface with proteins like histone proteins, ligases and eventually the control over the access of TFs (Kaur et al., 2012). This hydration mechanism might be also playing a role in the regulation of CpG islands. These regions, are DNA sites in which the frequency of the cytosine (C) and guanine (G) nucleotide sequence is higher than other regions, they typically occur at or near the transcription start site of genes and regulate the transcriptional activity of those genes (Illingworth and Bird, 2009). The binding of TFs to these promoter regions is regulated by methylation of the CpG sequences. Also, the interaction of specific TFs and the DNA binding sequence is influenced by the presence of osmolytes and hydration of the DNA molecule. The early growth response protein 1 (EGR1), a zinc finger protein TF also known as Zif268, is subject of interactions with osmolytes which stabilise the conformational structure of the unbound EGR1 in detriment of the DNA-bound EGR1 conformational state (Mikles et al., 2015). On the other hand, PU.1 is a pioneer TF important for myeloid differentiation. It shows preferential hydration in sequence discrimination in a different way from what happens with other E-twenty six (Ets) TF family members such as Ets-1. Interestingly, PU.1 activity is critical to the development and function of macrophages and lymphocytes, which present osmotically variable environments, and hydration-dependent specificity of transcription binding may represent an important *in vivo* regulatory mechanism. A hypothesis which supports gene expression profiles of primary murine macrophages (Poon, 2012; Wang et al., 2014). The mechanism of regulation of binding affinity by DNA hydration for Ets-1 and PU.1 is schematized in Figure 1.14 and hypothesises the water dependence of PU.1 to identify its binding site and promotes the formation of high-affinity binding complexes between the TF and the DNA. This effect is no longer observed in the binding mechanism of Ets-1 to the DNA target sites (Poon, 2012; Wang et al., 2014).

These differences in preferential hydration give rise to a host of thermodynamic and kinetic features which qualitatively distinguish site recognition by these proteins and point to a mechanism by which the activity and specificity of Ets proteins may be differentially controlled through their osmotic environment *in vivo*.

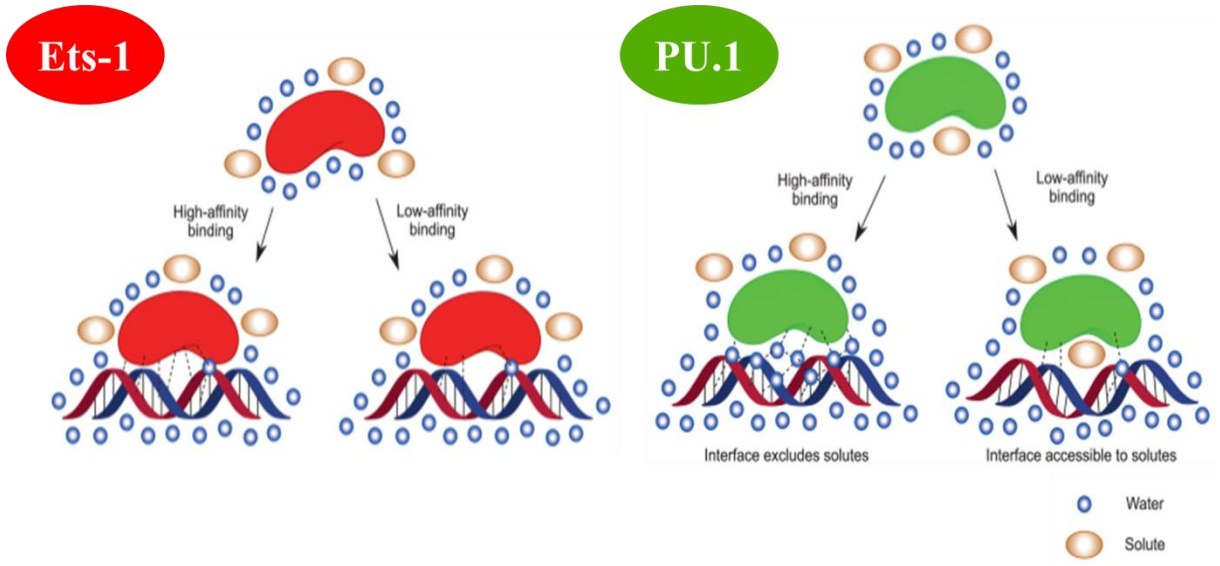

Figure 1.14 – Proposed mechanisms of DNA site recognition by the Ets domains of Ets-1 and PU.1. Figure adapted from Wang et al., 2014.

The binding of TFs to the DNA is also conditioned by the presence of specific histone modifications and histone variants (Swygert and Peterson, 2014; Tsompana and Buck, 2014; Zhang et al., 2015b). The most common histone modifications associated with transcription are summarised in Table 1.6. The state of these modifications can be also artificially controlled by several drugs and small molecules, such as valproic acid (VPA), that have an impact in the enzymatic machinery responsible for the histone modifications (Ehrensberger and Svejstrup, 2012; Huangfu et al., 2008; Mahmud et al., 2014; Swygert and Peterson, 2014). The action of VPA, as a general inhibitor of histone deacetylases, is clinically approved for mood stabilisation (Chateauvieux et al., 2010).

Table 1.6 – Summary of representative histone modifications associated with transcriptionally active or silent DNA regions.

Histone modifications	Gene location	Transcriptional state
H3K27 acetylation	Enhancers	Active
H3K4 trimethylation	Enhancers Gene promoter	
H3 tail acetylation (including H3K9 acetylation and H3K14 acetylation)	Gene promoter Body of the gene	
H4 tail acetylation (including H4K12 acetylation and H4K16 acetylation)	Gene promoter Body of the gene	
H2BK120 monoubiquitination	Body of the gene	
H3K36 trimethylation	Body of the gene	

Histone modifications	Gene location	Transcriptional state
H3K79 trimethylation	Body of the gene	
H3K27 trimethylation	Gene promoter Facultative heterochromatin	Inactive
H3K9 dimethylation	Constitutive heterochromatin	
H3K9 trimethylation	Pericentric heterochromatin Constitutive heterochromatin	
H2BK119 monoubiquitination	Facultative heterochromatin	

Stress alters several molecular players involved in the transcription process itself or at the epigenetic level and this impacts directly on the RNA repertoire produced during and after stress. Indeed, it was recently shown that permanent hyposmotic stress promotes the upregulation of specific lncRNAs that exert functions in rRNA gene silencing (Zhao et al., 2016). Also in yeast the osmotic modulation induces the production of lncRNAs (Valadkhan and Valencia-Hipólito, 2016). Moreover, heat shock promotes the transcription of non-coding RNAs (Satellite III) in pericentromeric heterochromatin (Valgardsdottir et al., 2008). The generation of lncRNAs has been described in stress situations induced by hypoxia, oxidative stress, DNA damage and heat shock, and many of these RNA molecules have also a role in the control of transcription and the epigenetic state of chromatin (Valadkhan and Valencia-Hipólito, 2016). Many lncRNAs are induced by hypoxia and have shown proximity to the previously identified hypoxia-inducible factors 1 and 2 (HIF-1/2) binding sites. One of these lncRNAs is the linc-ROR that is induced after hypoxic stimuli and is overexpressed in tumours but is also involved in reprogramming processes (Takahashi et al., 2014; Valadkhan and Valencia-Hipólito, 2016).

In addition to transcription modulation induced by direct stress signalling pathways, the impact on nuclear structure might enhance signalling along these pathways by providing a purely biophysical stress signal. The osmotic stress and mechanical stress are examples where this biophysical impact might play a role. Chromatin topology has a great influence on gene regulation, therefore biophysical distortion of the nucleus may alter gene expression by alteration of the nuclear organisation; nevertheless, direct experimental evidence for this is still lacking (Finan and Guilak, 2010; Irianto et al., 2013; Martins et al., 2012). Although several studies show the nuclear shape alterations which the cells suffer under osmotic stress and mechanical stresses (Finan and Guilak, 2010; Gasiorowski et al., 2013; Irianto et al., 2013; Martins et al., 2012; Stein et al., 1994), experimentally is very difficult to make a clear link between these

biophysical cues and the transcriptional changes. Nonetheless, a very interesting study has shown that the expression of chimeric histone H2B-GFP in forebrain principal neurones causes changes in chromatin architecture, such as the loss of peripheral heterochromatin, chromocenter declustering and changes in the texture of the nucleoplasm. These changes were explained due to the stearic impediment of highly-packed tertiary chromatin fibre folding in heterochromatin by the protruding GFP tags. These structural changes correlated with the relocation of alleles into the aberrant DNA *foci* and possibly explaining their downregulation and associated alterations in serotonin signalling and aberrant behaviour (Ito et al., 2014; Lopez-Atalaya and Barco, 2014; Medrano-Fernández and Barco, 2016).

The osmotic disturbance is a biophysical stressor. The entrance of water induces cell size variation and impacts on chromatin structure. Additionally, the potential role of direct osmolyte interaction with TFs and the hydration state of the DNA molecules might be another direct way by which osmotic stress can have a direct impact in cellular transcription. Osmolyte control has been implicated in several pathophysiological scenarios as it may regulate the activity of specific TFs with oncogenic potential such as EGR1 (breast, colon, lung and prostate cancer) (Mikles et al., 2015).

Additional common features of the different stress stimuli are the generation of oxidative stress, usually denominated like oxidative burst. These alterations provide critical second messengers upstream to the stress signalling network. Exposure of cells to ionising radiation or highly reactive chemicals, are examples of molecular events that directly increase the production of reactive species. Nevertheless, stresses like heat shock and osmotic shock are also related to a redox alteration but its molecular basis is poorly understood (Kültz, 2005). Nevertheless the ionic imbalance on mitochondria is a major player for redox and mitochondrial function changes (Guo et al., 2012; Jiang et al., 2011; Kültz, 2005; Solaini et al., 2010). For instance, elevation in Ca^{2+} levels causes a change in mitochondrial potential and leads to the production of superoxide ion radicals, which may result in a vicious oxidative cycle. Mitochondrial overload with Ca^{2+} is able to induce osmotic swelling and in extreme situations the rupture of the outer mitochondrial membrane (Garlid and Paucek, 2003; Guo et al., 2012; Kahlert and Reiser, 2002; Kaufman and Malhotra, 2014; Minamikawa et al., 1999).

These topics will be further explored within the next subchapter.

1.3.5. Cellular redox and metabolic changes

The redox cell state plays a central role in the stress response pathway which is shown by the high percentage (approximately 40%) of stress proteins which are related to the regulation of the intracellular redox state. The increase in cellular reactive oxygen species (ROS) and reactive nitrogen species (RNS) is observed in response to several stress stimuli and may represent a critical messenger within the stress signalling network (Dhawan, 2014; Jiang et al., 2011; Kültz, 2005). These ROS, in non-phagocytic cells, are mainly produced endogenously by the mitochondrial electron transport chain and RNS are generated by specific enzymes, such as the nitric oxide synthase. The main types of ROS and RNS produced within the cell are represented in Table 1.7.

Table 1.7 – Summary of different types of reactive oxygen species (ROS) and reactive nitrogen species (RNS) produced in the cell. Table adapted from Dhawan, 2014.

Reactive Oxygen Species (ROS)			
Radicals		Non-Radicals	
$O2^{\cdot -}$	Superoxide	H_2O_2	Hydrogen peroxide
$OH^{\cdot}$	Hydroxyl	$HOCl^{-}$	Hypochlorous acid
$RO^{2\cdot}$	Peroxyl	O_3	Ozone
$RO^{\cdot}$	Alkoxyl	$^1O_2$	Singlet oxygen
$HO2^{\cdot}$	Hydroperoxyl	$ONOO^{-}$	Peroxynitrite
Reactive Nitrogen Species (RNS)			
Radicals		Non-Radicals	
$NO^{\cdot}$	Nitric Oxide	$ONOO^{-}$	Peroxynitrite
$NO_2^{\cdot}$	Nitrogen dioxide	ROONO	Alkyl peroxynitrites
		N_2O_3	Dinitrogen trioxide
		N_2O_4	Dinitrogen tetroxide
		HNO_2	Nitrous acid
		$NO2^{+}$	Nitronium ion
		NO^{-}	Nitroxyl anion
		NO^{+}	Nitrosyl cation
		NO_2Cl	Nitryl chloride

The cell has a free radical scavenging system which includes compounds such as ascorbate, glutathione, thioredoxin and several antioxidant enzymes. The enzymes involved in the redox balance include superoxide dismutase (SOD – mitochondrial and extracellular), catalase, and peroxidases such as

peroxiredoxin among others. These compounds and proteins/enzymes are distributed in the cytosol, mitochondria, peroxisomes and plasma membrane. These players in redox balance are summarised in Table 1.8

Table 1.8 – Summary of the different types of enzymatic and non-enzymatic antioxidants involved in the cellular antioxidant defence system. Table adapted from Dhawan, 2014.

Cellular antioxidant defence system	
Enzymatic Scavenger	Non-enzymatic Scavenger
Thioredoxin	Vitamins C, E, A
Peroxiredoxins	Thiols
Glutaredoxin	β-Carotene
Glutathione peroxidase	Polyphenols
Reduced glutathione	NAC
Oxidised glutathione	Zinc, selenium
Glutathione reductase	Uric acid
Extracellular glutathione peroxidase	Lycopene
Catalase	Allyl sulfide
Peroxidase	Indoles
Superoxide dismutase (mitochondrial and extracellular)	Gallic acid
	Hesperitin
	Catechin
	Chrysin
	Glutathione
	Melatonin
	Bilirubin

Mitochondria are the most redox-active compartment of mammalian cells, accounting for more than 90% of electron transfer to O_2 as the terminal electron acceptor. Mitochondria use the potential energy available from the oxidation of various metabolic substrates such as pyruvate to produce ATP. The mitochondrial inner membrane contains five complexes with key functions in oxidative phosphorylation. From these complexes, three are redox-driven proton pumps: complex I (NADH-quinone oxidoreductase), complex III (coenzyme Q: cytochrome reductase), and complex IV (cytochrome oxidase). Complex II (succinate dehydrogenase) transfers electrons into the chain from succinate and complex V (ATP synthase) is a proton pump which uses the electrochemical proton gradient to drive ATP synthesis (Picard et al., 2013; Shaughnessy et al., 2015; Solaini et al., 2010).

Mitochondria are critical to normal cell function as key players in metabolic homoeostasis, apoptosis, control of cytosolic Ca^{2+} levels, lipid homoeostasis, steroid synthesis, innate immune response, and

metabolic cell signalling among other functions (Butow and Avadhani, 2004; Dai et al., 2014; Ito and Ito, 2016; Liu and Butow, 2006; Rizzuto et al., 2012). Therefore, it plays a central role in stress mediated responses not only by the energetics and ATP production but also through the generation of metabolites in the tricarboxylic acid cycle, as well as the mitochondrial–nuclear signalling that controls mitochondrial morphology, biogenesis, fission/fusion, mitophagy, apoptosis, and epigenetic regulation. Therefore, the importance and the extent of action of the mitochondria in normal or stressed environments are usually underestimated. Mitochondria provide key metabolites such as to β-nicotinamide adenine dinucleotide (NAD+), ATP, α-ketoglutarate (α-KG or 2-oxoglutarate, 2-OG), and acetyl coenzyme A (acetyl-CoA) that are required for numerous transcriptional and epigenetic regulatory processes like chromatin remodelling, histone modifications and nucleosome positioning (Shaughnessy et al., 2015).

Mitochondrial functions are also closely combined with cellular responses to damage in both mitochondrial DNA (mtDNA) and nuclear DNA. Given the significant generation of ROS during normal mitochondrial functions, base excision repair is a critical DNA repair mechanism that promotes mtDNA integrity. In addition, other mitochondrial quality control mechanisms such as fission, fusion, and mitophagy, are responsible for the protection of mitochondrial function and tolerance of mtDNA lesions (Shaughnessy et al., 2015).

As Ronai wrote in his article (Ronai, 1999), deciphering the mammalian stress response is a stressful task. The activated cellular responses are very complex and promote an integration of signals from the different organelles into the final cellular response or adaptation (Ronai, 1999). To further explore these networks and signalling mechanisms that culminate in a transcriptional change and establishment of a new repertoire of cellular proteins, non-coding RNAs and messenger molecules is essential to fully understand the cellular stress response. It is also very important to understand differences in the cellular response according to the type and magnitude of the stressor.

Quoting Gems and Partridge article, stress “which does not kill us make us stronger” (Gems and Partridge, 2008). In a cellular context, stressors can be used as a tool in a controlled manner and with a specific goal within a very specific context, enabling the modulation of specific cells towards a desired phenotypic change.

The understanding of the cellular biology and the complex interactions maintained with the microenvironment is fundamental to the development of new successful and innovative cellular therapy approaches that will be further explored in the next subchapter.

1.4. Cell-based therapeutic products for clinical application

The potential of cell-based clinical therapies to treat diseases, understand and model the molecular mechanisms behind pathologies and normal development of human tissues and organs is enormous. The number of publications in this area (Figure 1.15) and the increasing number of clinical trials (Figure 1.20) is a sign of its huge potential.

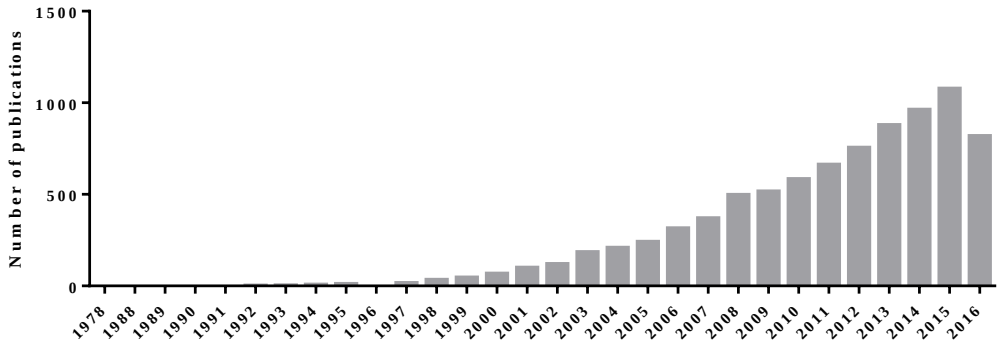

Figure 1.15 – Cell-based therapy related publications over time. Results for the search did on https://www.ncbi.nlm.nih.gov/pubmed/ with the keywords "cell-based therapies".

One main area of interest within cell-based therapies is the stem cell (SC) area. Although the knowledge generated across the years is very important, our understanding of the specific behaviour of SCs and their interactions with the surrounding environment or cell niche is still incomplete.

1.4.1. Evolution

Cell-based therapies are uniquely able to sense and respond to the surrounding environment and confer multifactorial effector functions *in vivo*. It is the most recent revolution within medicine towards a personalised medicine approach. Within cellular therapies, the cells can be considered as vehicles which can perform sophisticated functions that would not be achieved with conventional therapeutic alternatives (Dudek et al., 2014).

The field of haematology provided invaluable knowledge towards the field of SC biology and the description of hematopoietic stem cells (HSCs) by Dr. James Till and Dr. Ernest McCulloch (McCulloch

and Till, 1960) was a major advance in SC knowledge. Within the field of haematology and haematological diseases, SCs have been used as a therapeutic agent for more than 40 years. In 1968 Dr. Robert Good, performed the first successful allogeneic bone marrow (BM) transplantation from a matched sibling into an infant with haematological dysfunctions (Cooper, 2003). Since then several advances were achieved and the emergence of umbilical cord blood (UCB) cells as a complementary or alternative strategy to BM transplantation in specific cases was achieved. In 1988 the first UCB cells transplant was performed in a child with Fanconi anaemia in France (Coelho et al., 2016). UCB cells present very attractive characteristics to cellular therapies since these cells have some plasticity and are a naïve source of cells which present less mutagenic lesions than adult cells (Lee et al., 2010; McKenna and Brunstein, 2011; Park and Won, 2009; Roura et al., 2015).

In 1981 the SC field faced a major outbreak with the isolation of mouse embryonic stem cells (mESCs) by Dr. Martin Evans and Dr. Matthew Kaufman (Evans and Kaufman, 1981), Gail Martin (Martin, 1981). These scientists were able to isolate cells from the inner cell mass (ICM) of mouse blastocysts and maintain these cells *in vitro*. Nonetheless, the unequivocal proof of pluripotency for the mESCs was attained by the generation of mice entirely derived from these cells in 1993 by Nagy and colleagues (Nagy et al., 1993). Not far from this discovery, in 1998, Dr. James Thomson and Dr. John Gearhart described the isolation and culture methods for human embryonic stem cells (hESCs) isolated from blastocysts and primordial germ cells, respectively (Shamblott et al., 1998; Thomson et al., 1998). These discoveries allowed future studies of the biological networks controlling the fate and behaviour during cell commitment and self-renewal. Moreover, it unlocked the possibility of future regenerative medicine applications, disease modelling and toxicological studies. Nowadays, there are more than 120 lines of hESCs and several differentiation protocols are available to generate several cell types *in vitro* (Stojkovic et al., 2004).

The complexity and diversity of SCs discovered along the years generate the need to classify all these different cells. SCs have a self-renewal capacity that is responsible for the replacement of SCs and avoids exhaustion. This mechanism can be accomplished by symmetric cell division, when a stem cell gives rise to two daughter cells that maintain their stemness, or by asymmetrical cell division, when one stem cell originates a differentiated somatic cell and another SC (Mountford, 2008).

Although SCs are a vast and diversified group of cells, they all share the key features of self-renewal and differentiation potential (Bilic and Izpisua Belmonte, 2012; Krieger and Simons, 2015; Mountford, 2008; Tavakoli et al., 2009; Wagers and Christensen, 2002) (Figure 1.16).

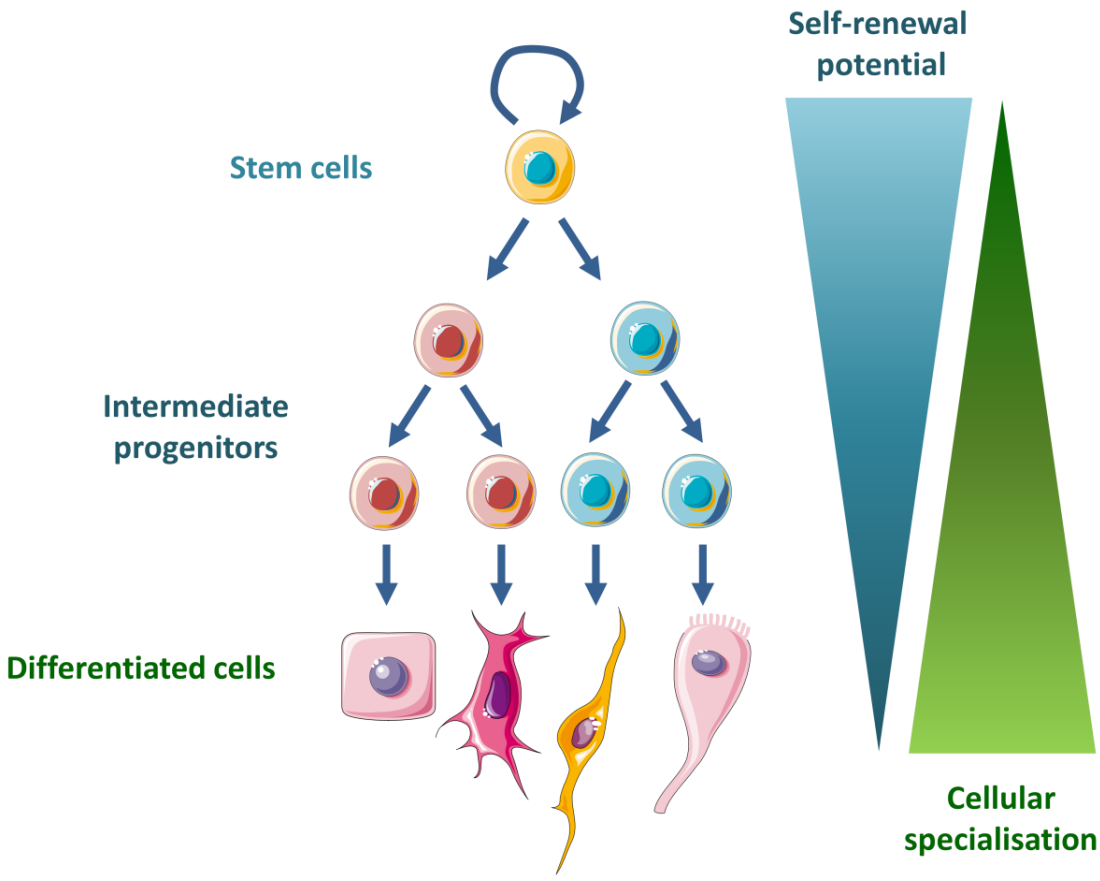

Figure 1.16 – Schematic representation of the self-renewal properties along cell differentiation process. Figure adapted from Krieger and Simons, 2015.

The stem cell behaviour is regulated by intrinsic and extrinsic signals in a complex network of interactions. The regulation of stemness involves environmental stimulus, transcriptional regulators, non-coding RNA regulators, posttranscriptional and posttranslational regulators, genetic and epigenetic control mechanisms that decide the fate of SCs (Gabut et al., 2011; Gan et al., 2007; Jaenisch, 2009; Jaenisch and Young, 2008; Li and He, 2012; Rosa and Ballarino, 2016) as represented in Figure 1.17.

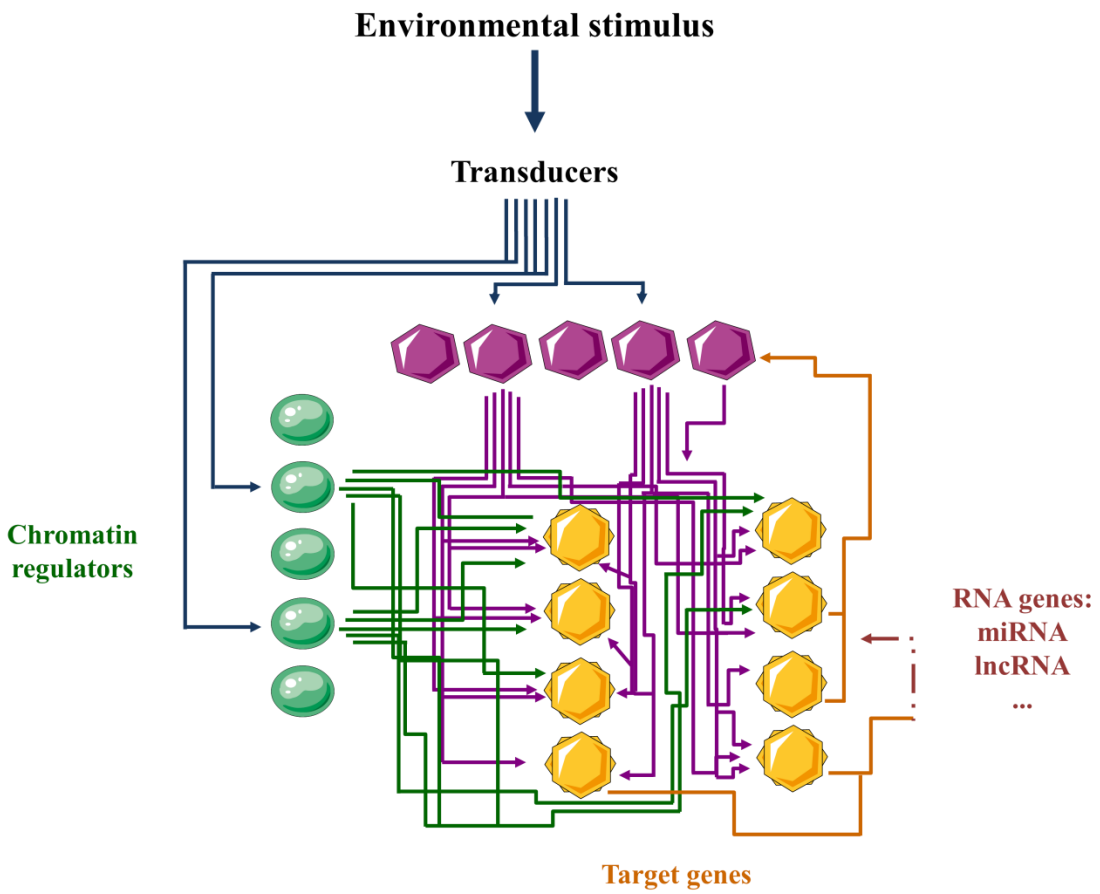

Figure 1.17 – Schematic representation of a transcriptional regulatory circuitry that regulates stem cells. Representation of possible connections between signal transduction pathways, transcription factors (purple hexagons), chromatin regulators (green circles), their target genes (orange "stars") including RNA genes that also regulate transcription. Figure adapted from Jaenisch and Young, 2008.

Generally, this vast group of cells can be grouped according to their potency or plasticity and further classified has embryonic versus non-embryonic adult stem cells (Brunt et al., 2012; Mountford, 2008; Serrano et al., 2013). Plasticity/potency is a concept that characterises the potential of differentiation of the stem or progenitor cells (Figure 1.16). From the normal embryonic development, after the formation of the zygote, the only totipotent cell able to generate all the adult somatic cells and the extraembryonic tissues, the cells will progressively turn into more committed and specialised fates. For example, the HSCs are multipotent SCs that have the ability to differentiate into progenitor cells from the blood lineage like common lymphoid progenitor, common myeloid progenitor that are more committed to their lineages and will be able to generate B-cells, T-cells, natural killer cells and erythrocytes, megakaryocytes, monocytes, neutrophils, eosinophils, basophils respectively (Bhatia, 2007; Fiedler and Brunner, 2012; Lim et al., 2013; Orkin and Zon, 2008).

Although, the cell fate was seen as a unidirectional pathway, the experiments of Dr. John Gurdon in 1958 showed that cell fate is not a static nor an irreversible state. These experiments proved that the transplantation of nuclei of intestinal epithelial cells from feeding tadpoles into enucleated eggs was able to give rise to normal and healthy tadpoles (Gurdon, 1962). This reversibility of the cell fate was recently challenged by the work of Dr. Shinya Yamanaka and colleagues (Takahashi et al., 2007). This team recently described a completely new concept of induction of pluripotency, attained by forced expression of embryonic related genes that reverts the somatic cell phenotype into induce pluripotency stem cells (iPSCs). This breakthrough changed the classical view of the cell fate and lineage commitment. In addition, the somatic nuclear transfer was also proven to be able to give rise to pluripotent cells (PSCs) as described by French and colleagues (French et al., 2008).

It has been also shown by several groups that by induction of specific TFs is possible to transdifferentiate a specific somatic cell into other different somatic cell (Chin, 2014; Eguizabal et al., 2013; Ladewig et al., 2013; Qin et al., 2016; Takahashi, 2012). This strategy has converted B cells into macrophages after ectopic expression of master TFs, CEBPα (Bussmann et al., 2009); pancreatic exocrine cells into insulin-producing β-cells (Koblas et al., 2016); and fibroblasts into neurons (Vadodaria et al., 2016), cardiac cells (Lee et al., 2015a), hepatocytes (Huang et al., 2014), and others. Apart from overexpression of master TFs, several other strategies to induce transdifferentiation have been used, such as delivery of proteins, miRNA, episomal-vectors, and small molecules (Eguizabal et al., 2013; Zhang et al., 2012).

All this knowledge provided a vast range of opportunities for different cellular therapies that are explored in more detail in the next subchapter.

1.4.2. Types of cell-based therapies

Cellular therapies can be classified according to the therapeutic indication, e.g. cardiovascular, neurological; to the type of cell source, autologous when the cells used for therapeutic purposes are taken and administered in the individual, or allogenic when the cells used are collected from a donor; and most commonly to the cell type (Mount et al., 2015). Using the most commonly used classification of cell therapies by cell-type eight categories can be defined as therapies using somatic cells, immortalized cells, *ex vivo* gene modified cells using viral vectors, *in vivo* gene modified cells using viral vectors, genome editing technologies, cell plasticity technologies, three-dimensional technologies and combinatory approaches as depicted in Figure 1.18.

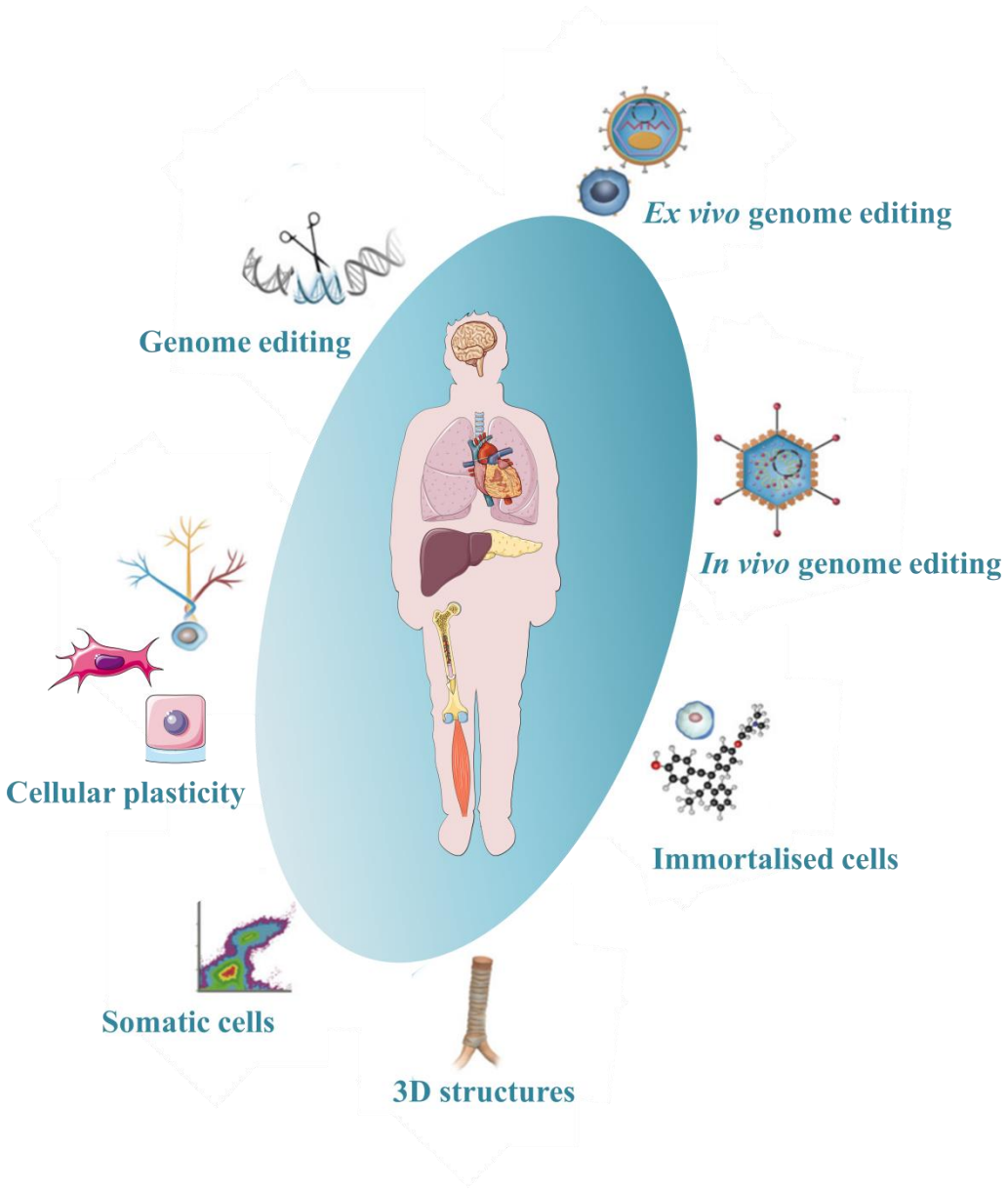

Figure 1.18 – Different types of cellular therapies. Figure adapted from Mount et al., 2015.

With the exception of HSC transplantation the great majority of the cellular therapies are experimental and under strict regulatory procedures. According to the European Medicines Agency's Committee for Advanced Therapies, cell-based therapies can be discriminated into a category of minimally manipulated cells for allogeneic use such as transplants or transfusions; and a second category of advanced therapy medicinal product (ATMP). These ATMP include medicinal products for human use such as gene therapy medicinal products, somatic cell therapy medicinal products and tissue engineered products (that contain engineered cells or tissues, and present properties for regeneration, repair or

replacement of a damaged tissue) (Hanna et al., 2016; Mount et al., 2015; Pearce et al., 2014; Sugawara et al., 2012; Whiting et al., 2015).

The recent data on immune cell-based therapy in the generation of engineered T-cell expressing anti-CD19 chimeric antigen receptor showing efficacy in B-cell leukaemia is one of the achievements of cellular therapy which resulted from over 20 years of clinical and research work (Mount et al., 2015). As this specific example shows, the development of novel cell-based therapy is intrinsically complex due to the need of understanding and controlling both the cell-based therapeutic itself and the interactions established with the microenvironment and with the host after administration.

Nevertheless, there are several ATMPs under development and already in the market. Eight years after the adoption of European Union regulation on ATMPs, only five have been granted with marketing authorisation in the European Union : one cell therapy, Provenge® with immune cells for advanced prostate cancer treatment (2013); one gene therapy, Glybera® to restore the lipoprotein lipase activity (2012); and three tissue engineer products, ChondroCelect® to articular cartilage repair with autologous cartilage cells expanded *ex vivo* expressing specific marker proteins (2009), MACI® for cartilage defects repair with matrix applied autologous cultured chondrocytes (2013), Holoclar® to restore burn-related eyesight of patients with severe corneal damage with *ex vivo* expanded autologous human corneal epithelial cells (2015). However, the marketing authorisations for MACI® and Provenge® were suspended and withdrawn, respectively (Hanna et al., 2016).

Additionally, within the gene editing category, the use of zinc finger nucleases to edit T-cells from HIV-infected subjects was the first indication that reached the clinical scenario (phase I ended) (Mount et al., 2015).

The development of bioengineering strategies might provide solutions to some of the disadvantages related to the use of cells as therapeutic agents. Healthcare is rapidly developing and a paradigm shift is being seen from replacement to regeneration by using concepts of tissue engineering and cellular therapies for tissue regeneration. Tissue engineering and cellular therapies, either on their own or in combination with therapeutic gene/drug delivery, have the potential to have a significant impact on the medical treatment of several conditions. The implementation of these therapeutic technologies requires a readily available source of cells for the generation of specific cells and tissues *ex vivo*, a profound knowledge of microenvironment relations and biocompatibility of the systems used (Hanna et al., 2016; Mount et al., 2015; Pearce et al., 2014; Sugawara et al., 2012; Whiting et al., 2015). Regarding the cell source, due to their unique regeneration capacity SCs are an attractive starting point for multiple biotechnological applications. As mentioned earlier, by definition they are self-renewing and have different differentiation abilities according to their plasticity and potency. Recent findings have shown

that SCs exist in most tissues and that tissue specificity may be more flexible than originally thought (Hanna et al., 2016; Mount et al., 2015; Pearce et al., 2014; Sugawara et al., 2012; Whiting et al., 2015). Despite the significant advances in the SC field knowledge and the high potential for producing novel SC-based products, there are currently no effective technologically relevant methodologies for *ex vivo* SC culture, or for reproducibly stimulating SCs to differentiate into functional fully differentiated cells.

Additionally, the adequate handling of fragile SC samples is essential for maintenance of their characteristics and phenotype, such as UCB samples. The lack of standardised collection, handling and storage methods specially developed to maintain the characteristics of UCB SCs can be a drawback to achieve the full therapeutic potential that UCB SCs offer (Hunt et al., 2003a, 2003b; Lee et al., 2010; McKenna and Brunstein, 2011; Park and Won, 2009; Roura et al., 2015). In addition, also the lack of an efficient *in vitro* technology for expansion of UCB SCs is preventing the application of this source of cells in therapeutic scenarios where a large amount of cells is required. Several studies show the potential of differentiation of these cells into the hematopoietic and endothelial lineages (Faivre et al., 2016; Jang et al., 2007). The control of the unique ability of UCB SCs to self-renew or differentiate is a key step in capturing the full therapeutic potential of this source of cells for regenerative medicine.

Although a great part of cellular therapies is experimental, the number of clinical trials to assess safety and efficacy for products using cells or cell editing technologies as therapies has suffered a dramatic increase throughout the last years (Figure 1.20) and fuels hope for future treatment of many incurable diseases. Within the next subchapter we will explore some of these undergoing clinical trials.

1.4.3. Clinical trials of cell-based therapies

Grand challenges for cell-based therapies include the extension of early successes to broader patient groups and to multiple types of disease while maximising both safety and efficacy. Making the transition to a clinical setting by proving safety and efficacy is crucial. The cell therapy clinical trials start in patients and have a seamless development path without the traditional formal separation between phase I (safety), phase II (efficacy detection), phase III (efficacy and safety confirmation) (Mount et al., 2015). For instance, Glybera® was approved in the European Union with clinical data from 27 patients studied in three small trials which could be described as combined phase I/II and phase II/III (Mount et al., 2015).

ATMPs hold great potential for restructuring the progression associated with numerous diseases such as Alzheimer’s disease, Parkinson’s disease, cancer, muscular dystrophy, macular degeneration among others. These therapies provide an option for curing or reversing diseases known as untreatable nowadays

or that are just controlled with symptomatic treatment (Hanna et al., 2016). The safety and efficacy are tested by clinical trials, and recent analysis showed that the majority of cellular therapies are in early stage of development focusing on demonstration of safety and early indication of efficacy, with a relatively low number of products reaching later clinical stages and marketing authorisation (Mount et al., 2015).

Almost half of the medicinal products in development were for somatic cell therapies (approximately 54%); the remainder were either tissue engineer products (approximately 23%), gene therapies (approximately 22%), or combined products (representing only approximately 1% of the products) as illustrated in Figure 1.19 (Hanna et al., 2016).

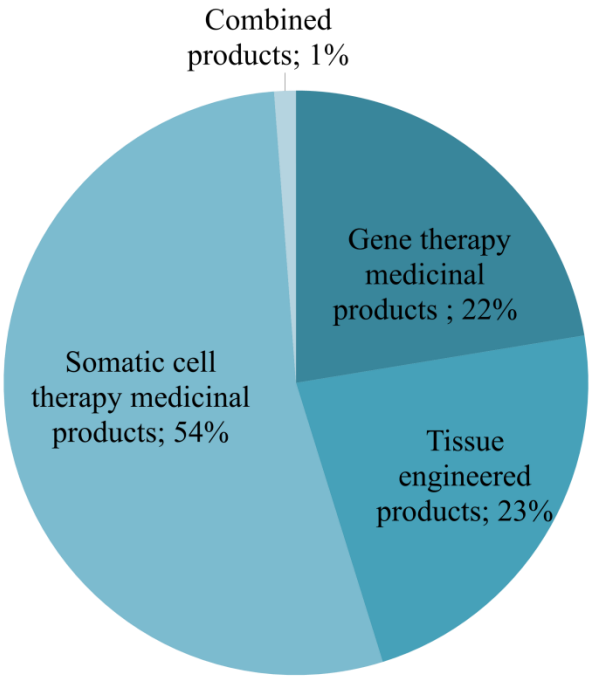

Figure 1.19 – Specific medicinal products within ATMPs. Figure adapted from Hanna et al., 2016.

Within somatic cell therapies, a huge variety of cells is available for therapeutic purposes and makes the choice of the adequate cell source a very difficult task. From naïve UCB cells, to the immunomodulatory mesenchymal stem cells (MSCs), to multiple progenitor cells and the "unlimited" source of iPSC- or hESC-derived cells (Abbasalizadeh and Baharvand, 2013; Hanna et al., 2016; McKenna and Brunstein, 2011; Mount et al., 2015; Pearce et al., 2014; Roura et al., 2015; Sugawara et al., 2012; Whiting et al., 2015; Ye et al., 2009, 2011). The main concerns with the clinical translation of cellular therapies have to do with tumourigenicity, biodistribution and risks resulting from the

implantation procedure (Hanna et al., 2016; Mount et al., 2015; Pearce et al., 2014; Sugawara et al., 2012; Whiting et al., 2015). All the cell sources present pros and cons regarding possible risks in medicinal use. Nonetheless, iPSCs technology provides the tools for a source of cells that are easily scalable and can be used in an autologous way. The main drawback is possible tumourigenicity, as in hESCs-related products side-effects. Nonetheless, the first human study with hESCs-derived oligodendrocyte progenitor cells for spinal injury treatment conducted by Geron in 2009 did not report the appearance of tumours in the few treated patients (Heslop et al., 2015). Additionally, the currently ongoing trial with hESC- and iPSC-derived retinal pigmented epithelial cells for macular degeneration treatment did not report either the appearance of tumours (Heslop et al., 2015). The "iPSC stock project" approved by the Japanese Health Ministry, headed by Shinya Yamanaka, intends to generate iPSC lines from several UCB banks around the world (De Lázaro et al., 2014). Surpassing the immunotolerance problem, the generation of 75 iPS cell lines from homozygous human leukocyte antigen (HLA) UCB donors would be enough to match 80% of the Japanese population without triggering an immune response, and if instead 150 iPS cell lines from characterized HLA UCB donors are generate would be enough to match 93% of the United Kingdom population (De Lázaro et al., 2014). The success of this iPS bank project, research in the field of SCs and the advent of new selection methods to eliminate pluripotent cells after differentiation might bring the huge potential of iPSC technology to the therapeutic use.

As mentioned above the number of clinical trials related with ATMPs suffered a marked increase over the past fifteen years as presented in Figure 1.20.

Although these therapies are being developed to target several different diseases, oncology remained the dominant therapeutic area, cardiovascular diseases represented the second biggest therapeutic area, and many other diseases are under clinical trials as represented in Table 1.9.

Figure 1.20 – Evolution of the number of ATMPs related clinical trials over time. Figure adapted from Hanna et al., 2016.

Table 1.9 – Representative examples of cell-based therapies related clinical trials.

Name of the clinical trial	Intervention
Human Craniomaxillofacial Allotransplantation	Bone marrow cell-based therapy and drug immunosuppression.
Cell Therapy by Autologous BMC for Large Bone Defect Repair	Biological: BMC2012 Device: beta-TCP Chronos® Synthes
Mesenchymal Stromal Cell Derivatives in the Treatment of Chronic Diabetic Foot Ulcers Type 1 and 2	Mesenchymal stromal cell derivatives + Fitostimoline
Personalized Cellular Vaccine for Recurrent Glioblastoma	Immunising the patients with personalised cellular vaccines including autologous tumour cells, antigen-pulsed dendritic cells and allogeneic peripheral blood mononuclear cells
Stem Cell Transplantation in Cirrhotic Patients	Mesenchymal stem cell transplantation

Name of the clinical trial	Intervention
Efficacy of Stem Cell Transplantation Compared to Rehabilitation Treatment of Patients With Cerebral Paralysis	Mesenchymal stem cells derived from umbilical cord injection
Multi-Center Study Safety of Adipose Derived Mesenchymal Stem Cells for the Treatment of Multiple Sclerosis	Autologous adipose-derived mesenchymal cells
Neoantigen-primed Dendritic Cells - Pre-activated T Cell Therapy for Refractory Non-small Cell Lung Cancer	Neoantigen-primed T cells
Safety Study of Autologous Umbilical Cord Blood Cells for Treatment of Hypoplastic Left Heart Syndrome	Injections of autologous umbilical cord blood
Safety and Efficacy of Allogenic Adoptive Cell Therapy for Immunodeficiency in Chronic HIV-1 Infected Patients	Allogeneic adoptive cell therapy
Dendritic Cell-based Immunotherapy for Advanced Solid Tumours of Children and Young Adults	Vaccination with autologous dendritic cells
Clinical Trial of Stem Cell-Based Tissue Engineered Laryngeal Implants	Stem cell-based tissue engineered partial laryngeal implants
Safety Study of a Dendritic Cell-based Cancer Vaccine in Melanoma	Dendritic cell-based cancer vaccination
Clinical study of autologous induced pluripotent stem cell-derived retinal pigment epithelium cell sheets for exudative age-related macular degeneration	Transplant of a cell sheet derived from induced pluripotent stem cell
The London Project to Cure Blindness clinical trial of a new treatment derived from embryonic stem cells for people with wet age-related macular degeneration	retinal pigment epithelium cells derived from embryonic stem cells

The area of cellular therapies is growing exponentially and the cure for several diseases might be closer. The academic research is one of the main sponsors for the technological advances in this area and the basic knowledge of cellular behaviour and cellular response to specific environmental changes as well as the development of new tools for cell fate control will be crucial for the success of cell-based therapeutic applications.

The classification of a cell therapy product or an ATMP makes reference to the “short or minimal manipulation” factor which denotes security worries related with the restrictions of having cells in artificial cell culture environments for long periods of time. As we have mentioned above in this chapter the adaptation of cells to artificial/stressful conditions is bad news for cell function and fate. The control of the cell culture environment in essential factors like: oxygen, sugar and osmotic levels over the time of manipulation of ATMPs, will certainly have a huge impact in the security and therapeutic efficacy of these products. This thesis makes important new contributions to this area.

Chapter 2 : Materials and methods

2.1. Materials

2.1.1. Cell culture

Throughout this work, several cell lines were used and maintained at 37ºC in humidified incubators with 5% CO_2 in specific growth culture conditions as described below.

A chronic myelogenous leukaemia cell line (K562 – ATCC® CCL-243™) was kept in Roswell Park Memorial Institute (RPMI) medium supplemented with 10% heat-inactivated foetal bovine serum (hiFBS) and 100units/mL of penicillin and 100µg/mL of streptomycin.

Normal dermal human fibroblasts (NDHFs – ATCC® PCS-201-010™) were maintained in Dulbecco's Modified Eagle Medium (DMEM) supplemented with 10% foetal bovine serum (FBS) and 100units/mL of penicillin and 100µg/mL of streptomycin.

A modified mouse neuroblastoma cell line (N2A pflare cell line – kindly donated by Professor Douglas L. Black) was maintained in DMEM supplemented with 10% FBS and 100units/mL of penicillin and 100µg/mL of streptomycin (Zheng et al., 2013).

The human adenocarcinoma cell line (HeLa – ATCC® CCL-2™) was maintained in DMEM supplemented with 10% FBS and 100units/mL of penicillin and 100µg/mL of streptomycin.

The human embryonic kidney cell line (293T – ATCC® CRL-3216™) was grown in RPMI supplemented with 10% FBS and 100units/mL of penicillin and 100µg/mL of streptomycin.

The induced pluripotent stem cells (iPSCs) used were kindly donated by Professor Ulrich Martin (Haase et al., 2009). These cells were cultured on top of a feeder cell layer. The feeder layer was prepared from mouse embryonic fibroblasts (MEFs – GlobalStem GSC-6001). Before inactivation, MEFs were expanded and grown in DMEM supplemented with 10% FBS and 100units/mL of penicillin and 100µg/mL of streptomycin. After 2 passages, the MEFs were inactivated with mitomycin C (8µg/ mL) for 2 hours at 37ºC (MEFsI). The iPSCs were cultured in KnockOut DMEM (KO-DMEM), 20% KnockOut serum replacement (KO-SR), 1mM glutamine, 0.1 mM β-mercaptoethanol, 4 ng/ml of fibroblast growth factor-basic (β-FGF), 1% of non-essential amino acids and 100units/mL of penicillin and 100µg/mL of streptomycin (iPS/hESC medium) (Amit et al., 2000).

The human embryonic stem (hESC) cell line H9 (WiCell, http://www.wicell.org/) was cultured in the same conditions as iPSCs (iPS/hESC medium).

Umbilical cord blood-derived cells were a culture in QBSF® 60 medium or StemSpan™ medium supplemented with 100ng/mL of stem cell factor (SCF), fms-related tyrosine kinase 3 ligand (Flt-3L) and 100units/mL of penicillin and 100µg/mL of streptomycin (hematopoietic stem cell medium).

An altered Ha-ras-oncogene-transformed mouse cell line (HAFTL-C10) stably expressing a CEBPαER was kindly donated by Professor Thomas Graf. It was maintained in RPMI without phenol red supplemented with 10% FBS (charcoal stripped), 100units/mL of penicillin and 100µg/mL of streptomycin, 50 µM β-mercaptoethanol (Bussmann et al., 2009). To induce transdifferentiation, these cells were presented to the same culture medium supplemented with 100 nM of β-estradiol, 10 ng/mL of interleukin-3 (IL-3) and colony stimulating factor-1 (CSF-1). Control cells were treated with 0.1% ethanol (solvent of β-estradiol).

The human adenocarcinoma cell line (HeLa – ATCC® CCL-2™) was modified with a lentiviral vector with an enhanced green fluorescent protein (EGFP) protein targeted to the mitochondrial matrix (kindly provided by Professor Rajeev Gupta) and selected for a stable clone. These cells will be designated by MitoGreen HeLa. This cell line was maintained in DMEM supplemented with 10% FBS and 100units/mL of penicillin and 100µg/mL of streptomycin.

A modified Chinese hamster ovarian (CHO-K1) cell line (Sugaya et al., 2000) that at 39ºC expresses an RNA Polymerase II-EGFP (RNA Pol II-EGFP) was maintained in DMEM/F12 supplemented with 10% FBS and 100units/mL of penicillin and 100µg/mL of streptomycin. Briefly, this cell line was originated from a mutant CHO-K1 cell line (Tsuji et al., 1990) with a temperature-sensitive mutation in the largest catalytic subunit of RNA pol II (tsTM4 cell clone). A human RNA Pol II wild-type subunit (hRPB1) was tagged with EGFP and expressed in the tsTM4 cell clone. This construct complemented the defect at the restrictive temperature and enabled the mutant cells to grow normally in contrast to what was observed in the parental cell line (Sugaya et al., 2000). Under culture conditions at 39ºC the RNA Pol II-EGFP is the main source of transcriptional elongation rather than the endogenous enzyme (Sugaya et al., 2000).

2.1.2. Reagents and solutions

The reagents, solutions/media, antibodies, primers and probes used in this study are listed below: Table 2.1, Table 2.2, Table 2.3,

Table 2.4 and Table 2.5.

Table 2.1 – List of reagents used for experiments. In addition to the reagent designation, the respective supplier and catalogue number are also shown in this table**.**

Product	Supplier	Catalogue number
1 Kb Plus DNA Ladder	Invitrogen	10787026
5-Ethynyl-UTP (EUTP) (aqueous solution)	Abcam	ab146744
Actinomycin D	Sigma	A9415
Adenosine 5′-triphosphate disodium salt hydrate	Sigma	A7699
AG® 501-X8 Mixed Bed Resin	BioRad	1436425
Agarose	Sigma	A9539
Amersham ECL Prime Western Blotting Detection Reagent	GE healthcare	RPN2232
Antifade mounting medium (Vectashield)	Vector Laboratories	H-1000
ATP Solution, Tris buffered	ThermoFisher	R1441
BayK	Sigma	B112
Blood bag	SURU	3031
Bovine serum albumin	Sigma	A4503
Bovine serum albumin fraction V	Sigma	85040C
Calcium chloride	BDH Analytical Chemicals	10070
Centrifuge tubes	Beckman Coulter	357002
Chloroform	Fisher Chemicals	C607SK-1
Click-iT® RNA Alexa Fluor® 488 Imaging Kit	Molecular Probes	C10329
Collagenase IV	Gibco	17104019
Colony stimulating factor-1 (CSF-1)	Peprotech	300-25
cOmplete™, Mini, EDTA-free Protease Inhibitor Cocktail	Roche	11836170001
CTP Solution, Tris buffered	ThermoFisher	R1451
DAPI	Sigma	D9542
DCFDA - Cellular Reactive Oxygen Species Detection Assay Kit	Abcam	ab113851
Deoxycholic acid	Sigma	D4297
DH5α competent cells	ThermoFisher	18265017
DiBAC4(3) (Bis-(1,3-Dibutylbarbituric Acid) Trimethine Oxonol)	Molecular Probes	B24570
Distilled water	Gibco	15230162
DL-Dithiothreitol solution	Sigma	43816
DMEM/F12	Gibco	11320-033
DNA Polymerase I, Large (Klenow)	NEB	M0210L

Product	Supplier	Catalogue number
Fragment		
DNase1	Roche	10104159001
Dulbecco's Modified Eagle Medium (DMEM) medium	Gibco	11965092
EDTA	Sigma	EDS
eFluor 514	eBiosciences	65-0859-70
EGTA	Invitrogen	E1219
Ethanol, Absolute	Fisher BioReagents™	BP2818500
Ficoll PM400 (Dry Powder)	GE healthcare life sciences	17-0300-10
Fms-related tyrosine kinase 3 ligand (Flt-3L)	Peprotech	300-19
Foetal bovine serum (FBS)	Gibco	10270106
Foetal Bovine Serum, charcoal stripped	Gibco	12676029
Formaldehyde solution (FA-36%)	Sigma	47608
G-agarose beads	Roche	0515952001
GFX PCR DNA and Gel Band Purification Kit	GE Healthcare	28-9034-70
Glutamine	Gibco	25030081
Glycerol	Sigma	G5516
Glycine	Sigma	G8898
Glycogen	Roche	901393
GTP Solution, Tris buffered	ThermoFisher	R1461
Heat inactivated foetal bovine serum	Gibco	10500064
HiSpeed Plasmid Midi Kit	Qiagen	12643
Hoechst 33258	Molecular Probes	H1398
Hoechst 33342	Molecular Probes	H3570
IGEPAL® CA-630	Sigma	I8896
Interleukin-3 (IL-3)	Peprotech	213-13
Isopropanol	Fisher Chemicals	A464-1
Klenow Fragment (3'→5' exo-)	NEB	M0212L
KnockOut Dulbecco's Modified Eagle Medium (KO-DMEM)	Gibco	10829018
KnockOut serum replacement (KO-SR)	Gibco	10828028
Leupeptin	Sigma	L8511
Lipofectamine 2000	Invitrogen	11668019
Lithium Chloride	Sigma	L4408
Luminescence viability assay	Promega	G7571
Lymphoprep	Axis-Shield	1114547
Magnesium chloride	Sigma	M2670
Magnetic beads CD133	Miltenyi	130-094-913
Magnetic beads CD34	Miltenyi	130-046-702
MES buffer	Novex	NP0002

Product	Supplier	Catalogue number
Micrococcal Nuclease	NEB	M0247S
Mitomycin C	Sigma	M4287
MitoProbe™ DiIC1(5) Assay Kit	Molecular Probes	M34151
MitoSOX™ Red Mitochondrial Superoxide Indicator	Molecular Probes	M36008
MOPS buffer	Novex	NP0001
MultiScribe™ Reverse Transcriptase	Invitrogen	4311235
Non-essential amino acids	Gibco	11140050
Nonidet™ P 40 Substitute	Sigma	74385
NuPAGE® LDS Sample Buffer (4X)	Novex	NP0007
Paraformaldehyde (PFA-16%)	Alfa Aesar	433689M
Pefablock SC	Sigma	76307
Penicillin-Streptomycin Solution	Gibco	15140130
Phenylmethylsulfonyl fluoride (PMFS)	Sigma	P7626
Phosphate buffered saline (PBS)	Gibco	10010015
PHOSS-RO ROCHE PhosSTOP™	Roche	04906837001
Phusion® High-Fidelity PCR Master Mix with HF Buffer	NEB	M0531S
Potassium acetate	Sigma	P1190
Potassium chloride	Sigma	P9541
Potassium phosphate dibasic	Sigma	P3786
Power SYBR Green PCR Master Mix	Applied Biosystems®	4368706
Proteinase K	Invitrogen	25530031
QBSF® 60	Quality Biological, Inc.	160-204-101
Qubit® dsDNA HS Assay Kit	Thermo Scientific	
Quick Ligation™ Kit	NEB	M2200L
RNaseA	MP Biomedicals	101076
Roswell Park Memorial Institute (RPMI) medium	Gibco	11875093
Roswell Park Memorial Institute (RPMI) medium without phenol red	Gibco	11835030
Saponin	Sigma	S-4521
SIGMAFAST™ BCIP®/NBT	Sigma	B5655
Sodium acetate	Sigma	S2889
Sodium bicarbonate	Sigma	S5761
Sodium butyrate	Sigma	B5887
Sodium chloride	Fisher Scientific	S271-500
Sodium dodecyl sulphate	Sigma	L3771
Sodium phosphate dibasic	Sigma	S7907
Spermidine	MP Biomedicals	0215206801
Spermine	MP Biomedicals	0215206905
Stem cell factor (SCF)	Peprotech	300-07

Product	Supplier	Catalogue number
StemSpan	Stem Cell Technologies	09650
Sucrose	Fisher Scientific	S5-500
SuperScript® II Reverse Transcriptase	Invitrogen	18064022
SYBR® Safe DNA Gel Stain	Invitrogen	S33102
T4 Polynucleotide Kinase	NEB	M0201L
TRI Reagent®	Sigma	T9424
Triton™ X-100	Sigma	T9284
Trizma® base	Sigma	T1503
Trizol®	Ambion	15596018
Trypan Blue Solution, 0.4%	Gibco	15250061
UltraPure™ 0.5M EDTA, pH 8.0	Invitrogen	15575020
UltraPure™ DNase/RNase-Free Distilled Water	Invitrogen	10977035
UltraPure™ Phenol:Chloroform:Isoamyl Alcohol	Invitrogen	15593031
Valproic acid	Sigma	P4543
Xfect Protein Transfection Reagent	Takara	631323
Xylene cyanol	Sigma	X4126
β-Estradiol BioReagent	Sigma	E2758
β-FGF	Peprotech	100-18B
β-mercaptoethanol	Sigma	M3148

Table 2.2 – Antibodies used for experiments. In addition to the antibody information, the technical application for what it was used; respective supplier and catalogue number are also shown in this table.

Specific target	Application	Catalogue number	Supplier
Normal rabbit IgG	Chip	12-370	Millipore
RNA polymerase II CTD repeat YSPTSPS	Chip	ab817	Abcam
RNA polymerase II CTD repeat YSPTSPS phosphoserine 2	Chip	ab5095	Abcam
RNA polymerase II CTD repeat YSPTSPS phosphoserine 2 (H5)	Chip/ Western Blot	ab24758	Abcam
RNA polymerase II CTD repeat YSPTSPS phosphoserine 5	Chip	ab5131	Abcam
APC anti-human CD117	Flow cytometry	550412	BD Biosciences
APC anti-human CD133	Flow cytometry	130-098-829	Miltenyi
APC anti-human CD90	Flow cytometry	559869	BD Biosciences

Specific target	Application	Catalogue number	Supplier
APC anti-mouse/human CD11b	Flow cytometry	101212	BioLegend
APC-H7 anti-human CD38	Flow cytometry	653314	BD Biosciences
FITC anti-human CD105	Flow cytometry	561443	BD Biosciences
FITC anti-human CD35	Flow cytometry	333404	BioLegend
PB anti-human HLA-DR	Flow cytometry	307633	BioLegend
PE anti-human CD123	Flow cytometry	130-098-894	Miltenyi
PE anti-human CD64	Flow cytometry	558592	BD Biosciences
PE anti-human myeloperoxidase	Flow cytometry	341642	BD Biosciences
PE/Cy7 anti-human CD13	Flow cytometry	301712	BioLegend
PE-CF594 anti-mouse CD19	Flow cytometry	562291	BD Horizon
PerCP/Cy5.5 anti-human CD34	Flow cytometry	347203	BD Biosciences
PO anti-human CD44	Flow cytometry	103020	BioLegend
PO anti-human CD45	Flow cytometry	MHCD4530	Thermofisher Scientific
Histone 4 lysine 16 acetylation	Immunofluorescence	ab109463	Abcam
β-tubulin	Western Blot	sc-9104	Santa Cruz Biotechnology

Table 2.3 – List of solutions used for experiments. In addition to the solution designation, the respective composition is also shown in this table.

Solution name	Components	Application
Immunoprecipitation dilution buffer (IPDB)	20mM Tris-HCl, pH8 2mM EDTA, pH8 150mM NaCl 1% Triton-X-100 0.01% SDS	Chip
IP Elution Buffer (IPEB)	0.1M NaHCO3 1% SDS	Chip
IP Wash Buffer 1 (IPWB1)	20mM Tris-HCl, pH8 50mM NaCl 2mM EDTA, pH8 1% Triton-X-100 0.1% SDS	Chip
IP Wash Buffer 2 (IPWB2)	10mM Tris-HCl, pH8 250mM LiCl 1mM EDTA, pH8 1% NP40 1% sodium deoxycholate	Chip
Nuclear lysis buffer (NLB)	50mM Tris-HCl, pH8 10mM EDTA, pH8	Chip

Solution name	Components	Application
	1% SDS	
Solution to pre-blocked protein G-agarose beads	10 mg/ml Fraction V BSA in IPDB	Chip
TE buffer	10mM Tris-HCl, pH8 1mM EDTA, pH8	Chip
TAE buffer	40 mM Tris-HCl, pH 7.6 20 mM acetic acid 1mM EDTA	DNA gel run
Buffer A+ Igepal-CA	15mM Tris-HCl, pH 8.0 15mM NaCl 60mM KCl 1mM EDTA, pH 8.0 0.5mM EGTA, pH 8.0 cOmplete™, Mini, EDTA-free Protease Inhibitor Cocktail Igepal-CA 0.1%	DNAse I / MNAse assays
Buffer A	15mM Tris-HCl, pH 8.0 15mM NaCl 60mM KCl 1mM EDTA, pH 8.0 0.5mM EGTA, pH 8.0 cOmplete™, Mini, EDTA-free Protease Inhibitor Cocktail	DNAse I assay
DNAse I stock solution	20mM Tris-HCl, pH 7.6 50mM NaCl 2mM MgCl2 2mM CaCl2 1mM dithioerythreitol 0.1 mg/mL Pefabloc SC 50% glycerol	DNAse I assay
DNaseI Digestion Buffer	6mM $CaCl_2$ 75mM NaCl 15mM Tris-HCl, pH 8.0 15mM NaCl 60mM KCl 1mM EDTA, pH 8.0 0.5mM EGTA, pH 8.0 cOmplete™, Mini, EDTA-free Protease Inhibitor Cocktail	DNAse I assay
Igepal-CA	2 grams AG501-X8 resin 40mL 10% IGEPAL solution	DNAse I assay
STOP buffer	50mM Tris-HCl, pH8.0 100mM NaCl 0.10% SDS 100mM EDTA, pH 8.0	DNAse I assay
PBB	PBS with 5% bovine serum albumin and 2% FBS	Immunolabeling

Solution name	Components	Application
Lysis dilution buffer	150mM NaCl 5mM EDTA	MNAse assay
Permeabilisation buffer 2	150mM sucrose 50mM Tris.HCl, pH 7.5 50mM NaCl 2mM $CaCl_2$	MNAse assay
TNESK (2x)	20mM Tris.HCl, pH 7.4 0.2M NaCl 2mM EDTA 2% SDS 0.2mg/mL proteinase K	MNAse assay
Physiological buffer with Ficoll (PBF)	100mM KAc 30mM KCl 10mM Na_2HPO_4 1mM $MgCl_2$ 1mM Na_2ATP 1mM DTT 0.2mM PMFS 10% Ficoll PM400	Transcription run on
PBF+saponin	PBF 250µg/mL saponin	Transcription run on
Run on cocktail	PBF 1,1mM ATP 100µM CTP/GTP 100µM EUTP 1.4mM $MgCl_2$	Transcription run on
β-estradiol	25mM in 100% ethanol	Transdifferentiation
Antibody dilution solution	TBS 5% skim powder milk	Western blot
Blocking solution	TBS 10% skim powder milk	Western blot
Laemmli buffer	2% SDS 10% glycerol 60mM Tris-HCl, pH6.8	Western blot
Transfer buffer	19.2mM glycine 2.5mM Tris 20% methanol	Western blot
Tris-buffered saline (TBS)	50 mM Tris-HCl, pH 7.5 150 mM NaCl	Western blot
Tris-buffered saline with Tween (TBST)	TBS 0.01% Tween 20	Western blot

Table 2.4 - Probes used for cell function assessment. In addition to the probe designation, the respective labelling output, concentration used and output measured are shown.

Probe	Method of labelling	Final concentration used	Output measure
SIGMAFAST™ BCIP®/NBT (5-bromo-4-chloro-3-indolyl phosphate/nitro blue tetrazolium)	Colorimetric	BCIP (0.15 mg/ml), NBT (0.30 mg/ml)	Alkaline phosphatase positive cells
Carboxy-DCFDA	Fluorescence	1μM	Reactive oxygen species
Click-iT® RNA Alexa Fluor® 488 Imaging Kit	Fluorescence		Transcription assessment, by incorporation of EU or EUTP
DiBAC4(3)	Fluorescence	1μM	Cell membrane potential
eFluor 514	Fluorescence	5μM	Intracellular free calcium
MitoProbe™ DiIC1(5)	Fluorescence	30nM	Mitochondrial membrane potential
MitoSOX™ Red	Fluorescence	5μM	Superoxide levels

Table 2.5 – List of primers used for PCR experiments. In addition to the target gene, the respective primers sequence and concentration used are shown in this table.

Target gene	Sense primer sequence	Anti-sense primer sequence	Final Concentration (μM)
β-Actin	5'-GATGTATGA AGGCTTTGGTC-3'	5'-TGTGCACTTT TATTGGTCTC-3'	10
ID2	5'-TCTGTGGCTA AATAAATGGC-3'	5'-CGATCATCCTT AGTTTTCCTTC-3'	10
NAB2	5'-GAGAGCACC TATCTTTCTTC-3'	5'-GTTCTCCAA CCTCTTGTTTC-3'	10
CEBP-A	5'-AAGGGTGTA TGTAGTAGTGG-3'	5'-AAAAAGAAGA GAAGGAAGCG-3'	10
CEBP-B	5'-ATCACTTAA AGATGTTCCTGC-3'	5'-TGTCTTCACT TTAATGCTCG-3'	10
CEBP-D	5'-ACAAAGTGTT TAGGTTGGAC-3'	5'-GTAAAGCTTC AGCCAGTATC-3'	10
FOS	5'-GAAGGGAA CGGAATAAGATG-3'	5'-CATCTTCAA GTTGATCTGTCTC-3'	10
FOSL2	5'-AGAAGTTC CGGGTAGATATG-3'	5'-GATAGGGAT TGGACATGGAG-3'	10
JUN	5'-CATGTTTGT TTGTTTGGGTG-3'	5'-ATGGATAAT GCAGCAAAGAG-3'	10
NFIL3	5'-AGCAGAAC CACGATAACC-3'	5'-ATGGTCTGC ATTTTTCTCAG-3'	10
PAX5	5'-CACAGTCC TACCCTATTGTC-3'	5'-CTTCCAGAAA ATTCACTCCC-3'	10
DNM3Tb	5'-GACTTCATG	5'-TATCATCCT	10

Target gene	Sense primer sequence	Anti-sense primer sequence	Final Concentration (µM)
	GAAGAAGTGAC-3’	GATACTCTGTGC-3’	
HDAC11	5’-CAAGCGAGT ATACATCATGG-3’	5’-CAGATATTCC TCATCTTCTGTG-3’	10
β2M	5’-GGGTTTCAT CCATCCGACATTG-3’	5’-TGGTTCAC ACGGCAGGCATAC-3’	10
Oct-4	5′-GACAACAATGAGAAC CTT CAG GAG A-3′	5′-CTGGCGCCGGTT ACAGAACCA-3′	10
Oct-4A	5’-CTTCTCGCC CCCTCCAGGT-3’	5’-AAATAGAA CCCCCAGGGTGAGC-3’	10
Oct-4B	5’-AGACTATTC CTTGGGGCCACAC-3’	5’-GGCTGAATA CCTTCCCAAATAGA-3’	10

2.2. Methods

2.2.1. DNA and RNA extraction

For ribonucleic acid (RNA) extraction, cells were lysed with Trizol® or TRI Reagent®; the purification of the RNA was done according to manufacturer’s protocol. RNA concentration was measured with Nanodrop2000 (Thermo Scientific).

For deoxyribonucleic acid (DNA) extraction, cells or suspensions were added to phenol:chloroform:isoamyl alcohol and well mixed. This mixture was then centrifuged, the aqueous phase was mixed with glycogen (20µg), sodium acetate (NaAc – 600mM, pH 5.2) and 1 mL of 100% ethanol was added. This mixture was precipitated at -20ºC overnight or at -80ºC for 1 hour. The samples were centrifuged at 16100g for 10 minutes at room temperature. The pellet was washed with 75% ethanol and air dried. The DNA was resuspended in ultrapure water and quantified with Nanodrop2000 (Thermo Scientific) or using Qubit® dsDNA HS Assay kit.

2.2.2. Production of cDNA

To prepare complementary DNA (cDNA) from total RNA, we used MultiScribe™ Reverse Transcriptase and Superscript III First-Strand Synthesis kit according to the manufacturer’s instructions (using random hexamers).

2.2.3. Immunolabeling

Immunofluorescent labelling was performed to characterise the expression of several markers and specific modifications of interest. A general immunodetection procedure was used throughout this thesis. The cells were fixed with 4% paraformaldehyde (PFA) at room temperature for 15 minutes, washed once with phosphate buffered saline (PBS) followed by a blocking step with PBB (Table 2.3) for 30 minutes at room temperature. Incubation was done with the primary antibody in PBB (dilution factor 1:100) at room temperature for 1 hour followed by three washes with PBS. Incubation with the secondary antibody in PBB (dilution factor 1:200) was done for one hour at room temperature. After the secondary antibody incubation, the cells were washed 3 times with PBS, refixed with 4% PFA for 5 minutes at room temperature. Where relevant, cells were stained with 4',6-diamidino-2-phenylindole (DAPI) or Hoechst (both at 200nM) and mounted with an antifade mounting medium.

2.2.4. Cellular stains

Cell staining with the probes presented in

Table 2.4 was done according to the manufacturer's instructions, and the concentration of each probe is also mentioned in this table. All the fluorescence probes labelling were performed in PBS to avoid non-specific interactions during the staining procedure.

When assessing alkaline phosphatase activity, an initial fixation step with 95% ethanol was added to the original protocol.

2.2.5. ATP measurements

The assessment of adenosine triphosphate (ATP) levels was done with the Luminescence viability assay (Table 2.1) according to the manufacturer's instruction, in a Synergy Mx Monochromator-Based Multi-Mode Microplate Reader (BioTek).

2.2.6. Quantitative real time polymerase chain reaction (qRT-PCR)

Gene expression profile for specific targets was evaluated in different cell types by qRT-PCR. An ABI PRISM 7500 System (Applied Biosystems) was used with Power SYBR Green PCR Master mix. Specific concentrations used for the different primers are shown in Table 2.5; specific reaction thermal profiles are shown in Table 2.6.

Table 2.6 – Reaction thermal profiles used for SYBR Green qRT-PCR reactions.

Master mix used	Reaction thermal profile	
Power SYBR Green PCR Master Mix	94ºC – 5 minutes	
	94ºC – 30 seconds	40 cycles
	60ºC – 30 seconds	
	72ºC – 33 seconds	

2.2.7. Western Blotting

The cells of interest were lysed directly into laemmli buffer and transferred immediately to an eppendorf on ice. After adding NuPage sample buffer (4x), the samples were warmed up to 90ºC for 10 minutes, sheared briefly with a 25G needle and straight away subjected to sodium dodecyl sulfate-polyacrylamide gel electrophoresis (SDS-PAGE) or stored at -20ºC.

Bis-Tris Protein gradient gels (4-12%) were used. The comb was removed, wells rinsed by pipetting up and down running buffer. Approximately 10µL of sample loaded per well. Gels were run in a MOPS/MES buffer (Table 2.1) at 200V for approximately 1 hour. The gel was assembled as manufacturer's instructions indicate. The gel run and gel transfer were done in the XCell SureLock® Mini-Cell and XCell II™ Blot Module (Invitrogen), respectively. The transfer was done in transfer buffer (Table 2.3) at 40V during 2 hours. The membrane was placed with the protein side up in a 50ml falcon tube and incubated for 1 hour in blocking solution (Table 2.3). Primary antibodies were diluted in antibody dilution solution (Table 2.3) and incubated with the membrane overnight at 4ºC. Secondary antibodies were diluted in antibody dilution solution (Table 2.3) and incubated with the membrane for 2 hours at room temperature. Following primary and secondary antibody incubations the membranes were washed three times for 15 minutes in TBST (Table 2.3). Membranes were incubated for 2 minutes with

enhanced chemiluminescence substrates (ECL – Table 2.1) and visualised on ImageQuant LAS 4000 (GE Healthcare Life Sciences).

2.2.8. Enzymatic digestions

For the deoxyribonuclease I (DNase I), one unit is defined as the enzyme activity that causes an increase in the absorbance of 0.001 per minute under assay conditions. On the hand, one gel unit of micrococcal nuclease (MNase) is defined as the amount of enzyme required to digest 1 µg of lambda genomic DNA in 15 minutes at 37°C, to the extent that the accumulation of low molecular DNA fragments (100-400 base pairs) disappears on a 1.2% agarose gel. A gel unit corresponds to 0.1 Kunitz units (being a Kunitz unit defined as the amount of enzyme required to release acid-soluble oligonucleotides that produce an absorbance increase of optic density 1.0 at 260 nm in 30 minutes at 37°C).

DNase I assay and MNase test were performed in K562 nuclei extracted with a lysis buffer (Buffer A+ Igepal-CA - Table 2.3). The nuclear release was confirmed by staining with diluted trypan blue (1:10 in PBS). For each digestion, $5x10^5$ nuclei were used.

In the case of DNAse, nuclei were resuspended in DNase digestion buffer (Table 2.3) for 3 minutes at 37ºC. Afterwards, the STOP buffer (Table 2.3) was added and incubated at 55ºC overnight. For the MNase digestion, the nuclei were resuspended in permeabilization buffer 2 (Table 2.3) and the amount of MNAse needed was added to each condition. The digestion was performed at 21ºC for 5 minutes and afterwards, the digested nuclei were resuspended in equal amounts of TNESK 2x and lysis dilution buffer (Table 2.3). This solution was incubated at 37ºC overnight.

Afterwards, ribonuclease A (RNase A) was added to the mixture and incubated for 30 minutes at 37ºC. The digests were purified for DNA content (as mentioned in the section for DNA and RNA extraction). DNA was quantified with Nanodrop2000 (Thermo Scientific) and 500ng of DNA were run in TAE buffer in a 1% agarose gel for 1hour at 80V. The gel was stained with SYBR® Safe DNA Gel Stain and visualised on ImageQuant LAS 4000 (GE Healthcare Life Sciences).

2.2.9. Cell imaging and cell cytometry

For cell imaging, a fluorescence microscope Axioivert 200M (Carl Zeiss), a confocal LSM 710 (Carl Zeiss) and a high content imaging platform IN Cell 2200 Analyzer (GE healthcare) were used. For analysis of the images from fluorescence and confocal microscopy, Image J and ZEN software were used.

For a specific analysis of mitochondrial morphology a specific plugin was used in Image J and references for this tool are described in Chapter 5. For IN Cell 2200 Analyzer image data analysis, the equipment software was used.

For cell cytometry, a BD FACSCalibur™ (Becton Dickinson Biosciences), BD FACSARIA III™ (Becton Dickinson Biosciences), BD FACSCanto II™ (Becton Dickinson Biosciences), GalliosTM (Beckman Coulter), BD FACSVerse™ (Becton Dickinson Biosciences) and BD Accuri™ C6 (Becton Dickinson Biosciences) flow cytometry machines were used. For analysis of the acquired data, Kaluza Analysis 1.5, and FlowJo™ software were used.

2.2.10. Osmotic cell modulation

The cells were exposed to different osmotic conditions for different times at 37°C with 5% CO2. The Table 2.7 describes each condition used.

Table 2.7 – Osmotic modulation cocktails used.

Medium used for the cocktail	Ratio of distilled water in the cocktail	Percentage of NaCl in the cocktail (%)	Time for stimuli
Growth culture media or PBS	1/4		From 15 minutes up to 24 hours
Growth culture media or PBS	1/3		
Growth culture media or PBS	1/2		
Growth culture media or PBS	3/4		
Growth culture media or PBS		1.8	

2.2.11. Transcription assessment

To assess transcription, Click-iT® RNA Alexa Fluor® 488 Imaging Kit (Molecular Probes) was used as per the manufacturer's protocol. Flow cytometry was used to assess the fluorescent signal (GalliosTM). Different time points for 5-Ethynyl Uridine (EU) incorporation were evaluated.

The number of active molecules of RNA polymerase II (RNA Pol II) was also measured after "run on" experiments using 5-Ethynyl-UTP (EUTP). Cells were permeabilised with the physiological buffer with Ficoll and saponin (PBF+ saponin) at 4ºC (Table 2.3) (Iborra et al., 1998, 2004; Pombo et al., 1999).

After five washes in PBF (in order to wash all the internal pools of nucleotides and other intracellular molecules that may interfere with the transcriptional process), cells were stimulated to transcribe at room temperature in the run on cocktail (Table 2.3) for 15, 30, 60, 90 and 120 min. Cells were then fixed with 4% PFA for 15 minutes at room temperature. The incorporation of EUTP was assessed with Click-iT® RNA Alexa Fluor® 488 Imaging Kit (Molecular Probes) according to manufacturer's protocol and using flow cytometry (GalliosTM).

The assessment of transcription dynamics was also done by a fluorescence loss in photobleaching (FLIP) performed in LSM 710 (Carl Zeiss) confocal microscope with the stage heated at 39ºC. For this experiment the CHO RNA Pol II-EGFP cell line was used after 4 days of culture at 39ºC to ensure the stable expression of the RNA Pol II-EGFP form. Cells expressing less RNA Pol II-EGFP in the cytoplasm were chosen to minimise any contribution of nuclear import to fluorescent recovery. A rectangle of half of each nucleus was selected where 100% laser power was applied, in order to bleach all the fluorescent molecules in these rectangles. This operation was repeated approximately every 5 seconds for a period of 900 seconds and the decay of the fluorescence in the unbleached half was analysed, as illustrated in Figure 2.1.

Fluorescence decay curves were analysed and the data were fitted to three populations with an exponential decay ($f = a \times \exp(-b \times x) + c \times \exp(d \times x) + g * \exp(-h \times x)$; R^2>0.99): one free form, one bound to DNA but not fully engaged, and another fully engaged in transcription. The half-life of RNA Pol II was calculated with the fully engaged slope (h) using the formula: $\frac{\ln 2}{Slope\ fully\ engaged\ form}$.

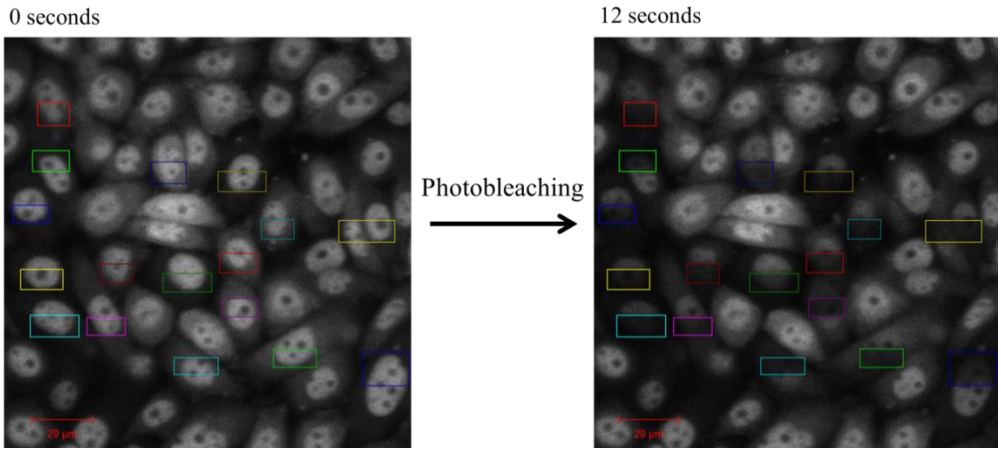

Figure 2.1 – Fluorescence loss in photobleaching (FLIP) experiment illustration. The layout of the FLIP experiment schematically represented before bleaching (0 seconds) and after 2 rounds of photobleaching (approximately 12 seconds) done in the LSM 710 (Carl Zeiss) confocal microscope (scale bar 20µm).

2.2.12. Chromatin Immunoprecipitation

A general overview of the chromatin immunoprecipitation (Chip) technique and possible outputs is represented in Figure 2.2.

K562 cells were cross-linked with 0.4% formaldehyde for 15 minutes at room temperature and with agitation in a glass bottle. To stop the cross-link, glycine (125mM) was added and incubated at room temperature for 10 minutes with agitation. The cell suspension was transferred to a 50mL falcon tube and centrifuged at 515g for 6 minutes at 4°C. The cell pellet was resuspended in 1.5 mL of ice-cold PBS containing 10mM of sodium butyrate, 50µg/mL of phenylmethylsulfonyl fluoride (PMFS) and 1µg/mL of leupeptin to inhibit protease activity and phoshpoSTOP to inhibit phosphatase activity (Table 2.1). The cell suspension was centrifuged at 400g for 5 minutes at 4°C and the cell pellets were frozen at -80°C ($5x10^7$ cells per pellet).

The K562 cell pellets were thawed on ice and resuspended in nuclear lysis buffer (NLB) (Table 2.3). This suspension was incubated on ice for 10 minutes and immunoprecipitation dilution buffer (IPDB) (Table 2.3) was added to obtain the optimal sodium dodecyl sulphate (SDS) concentration for sonication. Sample sonication was performed and optimised in a Bioruptor® Pico (Diagenode) to obtain DNA fragments sheared to approximately 150 to 500 base pairs (bp) as shown in Figure 2.3. After sonication, samples were centrifuged at 16100g for 10 minutes at 4°C. The supernatant was transferred to a new 15mL falcon and IPDB was added to dilute the amount of SDS to 0.2%.

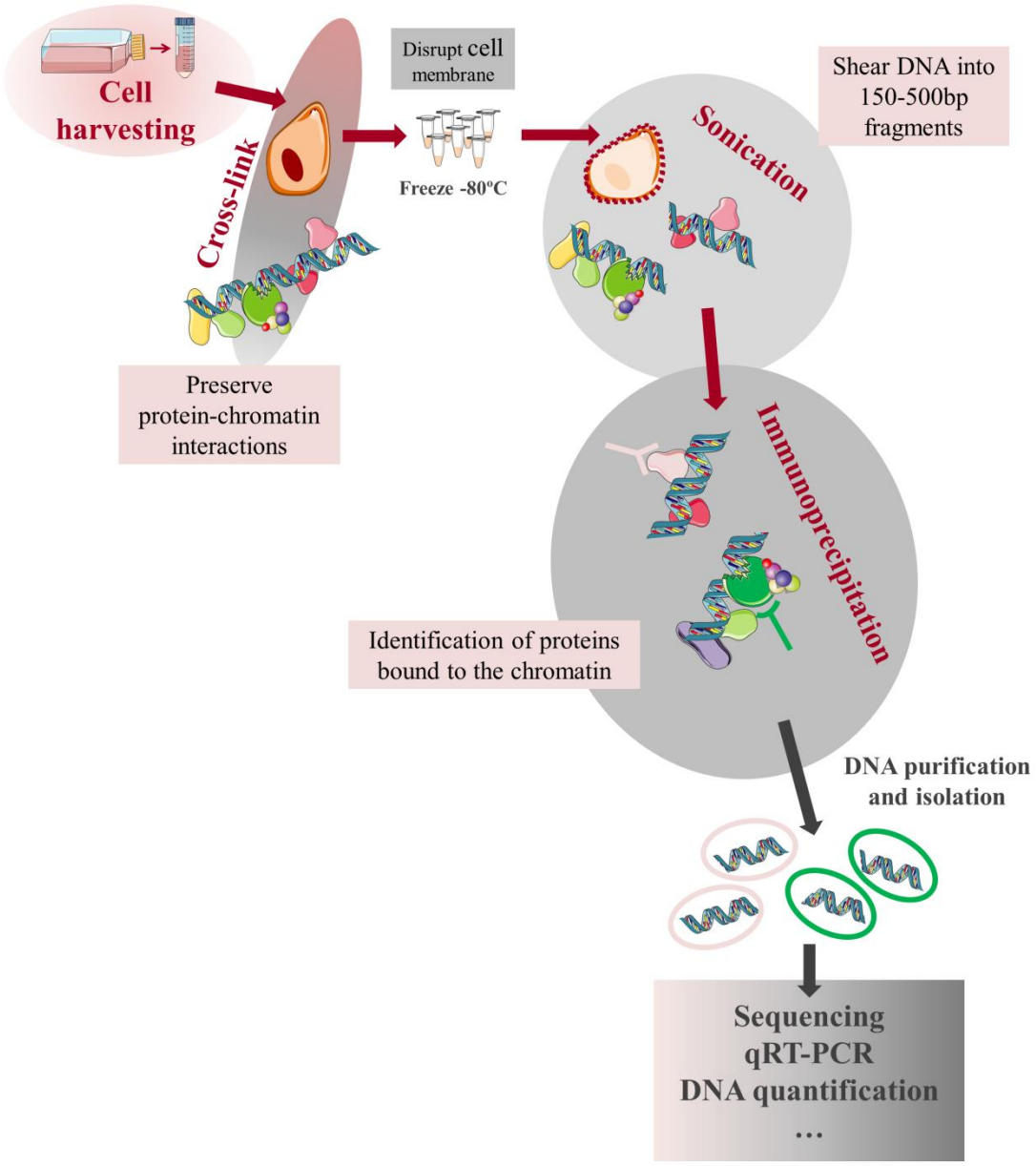

Figure 2.2 – Schematic representation of chromatin immunoprecipitation (Chip) experiments.

In order to pre-clear the chromatin, protein G-agarose beads were added to the chromatin and incubated on a rotary wheel for 3 hours at 4°C. This suspension was centrifuged at 500g for 5 minutes at 4°C and the supernatant recovered and incubated overnight with the antibodies of interest (≈10µg) on a rotary wheel at 4°C. After this incubation step, pre-blocked protein G-agarose beads (Table 2.3) were added to the suspension and incubated on a rotary wheel for 3 hours at 4°C. Several washing steps were

performed with immunoprecipitation washing buffer 1, 2 (IPWB1, IPWB2) and Tris-EDTA buffer (TE) and a final elution step with immunoprecipitation elution buffer (IPEB) (Table 2.3) was done to remove the chromatin bound to the antibodies. This DNA suspension was incubated with RNaseA (2µg) and sodium chloride (NaCl – 300mM) for 6 hours at 65°C. To degrade the remaining proteins the DNA suspension was incubated overnight with proteinase K (80µg) at 55°C.

To purify the recovered DNA, a phenol:chloroform:isoamyl alcohol extraction and ethanol precipitation were performed. The purified DNA was quantified using the Qubit® dsDNA HS Assay kit (Thermo Scientific) according to manufacturer's protocol.

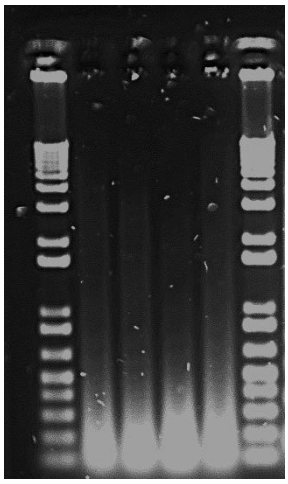

Figure 2.3 – Sonication profile of chromatin samples. Lane 1: 500ng of 1kb plus ladder; Lane 2 to lane 5: optimisation of chromatin sonication – 500ng of DNA samples (Lane 2: 500ng of PBS 0h sample chromatin; Lane 3: 500ng of hypo2+/PBS 0h sample chromatin; Lane 4: 500ng of PBS 1h sample chromatin; Lane 5: 500ng of hypo2+/PBS 1h sample chromatin); Lane 6: 500ng of 1kb plus ladder (lane ordered from left to right).

2.2.13. Chip-Sequencing library preparation and sequencing

Chromatin immunoprecipitation-Sequencing (Chip-Seq) libraries were prepared with New England Biolabs (NEB) reagents and NEB adapters and primers (Table 2.1) using manufacturer's protocol. In brief, this protocol included steps of DNA end-repair, the addition of dA tails, ligation of adapters, and amplification of the library and gel purification of the Chip-Seq libraries. For DNA Chip library gel extraction, after cutting the interesting DNA bands from the 2% agarose gel with a clean blade in a blue light transilluminator, the GFX PCR DNA and Gel Band Purification kit was used to purify the DNA according to manufacturer's protocol. Sequencing preparation was done according to NextSeq Illumina protocol.

2.2.14. Chip-Sequencing analysis

The reads were mapped to the mouse genome using Bowtie (Langmead et al., 2009). Peaks were detected against rabbit IgG control using MACS (Zhang et al., 2008). Peaks in different experiments were called as "new peaks" if the peaks had a fold enrichment greater than 15 (for RNA Pol II phosphorylated on Serine2) or 30, a p-value smaller than 10^{-9} and absence of peaks within 1 kb of that genomic location.

To further explore the data provided by the Chip-Seq we also used two bioinformatics tools to describe the involvement of transcription factor in the binding of RNA Pol II to the specific genomic areas. These tools were PASTAA, a tool from Max Planck Institute (http://trap.molgen.mpg.de/cgi-bin/pastaa.cgi), and TransFind (http://transfind.sys-bio.net/index.php/home.html).

2.2.15. Plasmid amplification

To transform DH5α competent cells with plasmid DNA, competent cells were thawed on ice and aliquoted into 30µL in a 1,5mL eppendorf tube. The DNA of interest was added to the cells (1µL-approximately 50 to 100ng) and incubated on ice for 30 minutes. The cells were heat shocked for 40 seconds at 42ºC and placed on ice during 2 minutes. For the recovery of the competent cells 450µL of Luria-Bertani (LB) medium was added to each tube and incubated at 37ºC for 1 hour. The cell suspension was then plated on an appropriate antibiotic selection agar plate and incubated overnight at 37ºC.

On next day, one colony was picked from each agar plate and grown in an LB maxiculture (150-200mL) with appropriate antibiotic selection incubated overnight at 37ºC with agitation (225rpm).

The DNA purification from bacterial maxiculture was done with QIAGEN HiSpeed Plasmid Midi kit according to manufacturer's protocol.

2.2.16. Lentiviral production

The viral packaging was performed in 293T with the appropriate amounts of transfection agent Lipofectamine 2000 and plasmids of interest. The lipofectamine was mixed with DMEM without serum and incubated at room temperature for 10 minutes. After incubation, the plasmids were added and maintained at room temperature for 30 minutes. Lastly, this mixture was added to a 70%-80% confluent

293T culture flask (T75 flask). The 293T medium was changed by fresh medium after 16 h of incubation (at 37ºC).

Three days after transfection, the 293T viral supernatants were collected into 50mL tubes and spun at 300g for 5 minutes to pellet the cellular debris. After centrifugation, the supernatants were filtered (0,4µm syringe filter) into centrifuge tubes and centrifuged at 19000g for 4 hours. The pellets were then resuspended in 200µL of PBS and stored in aliquots at -80ºC.

2.2.17. Cell reprogramming

The cell reprogramming protocol used was based on the report by Professor Juan Carlos Izpisúa Belmonte (Giorgetti et al., 2010) and is schematized in Figure 2.4 and Figure 2.5. The viral vector used is a polycistronic lentiviral vector containing c-Myc, Sox2, Oct4, Klf-4 cDNA kindly donated by Professor Axel Schambach (Warlich et al., 2011). One day after the last viral infection, the cells were plated on a feeder cell layer of MEFsI. For kinetic studies, colonies growth and reporter fluorescence were monitored by fluorescence microscopy (Axioivert 200M – Carl Zeiss). In experiments where was only evaluated the endpoint, alkaline phosphatase stain was done at day 17 (SIGMAFAST™ BCIP®/NBT).

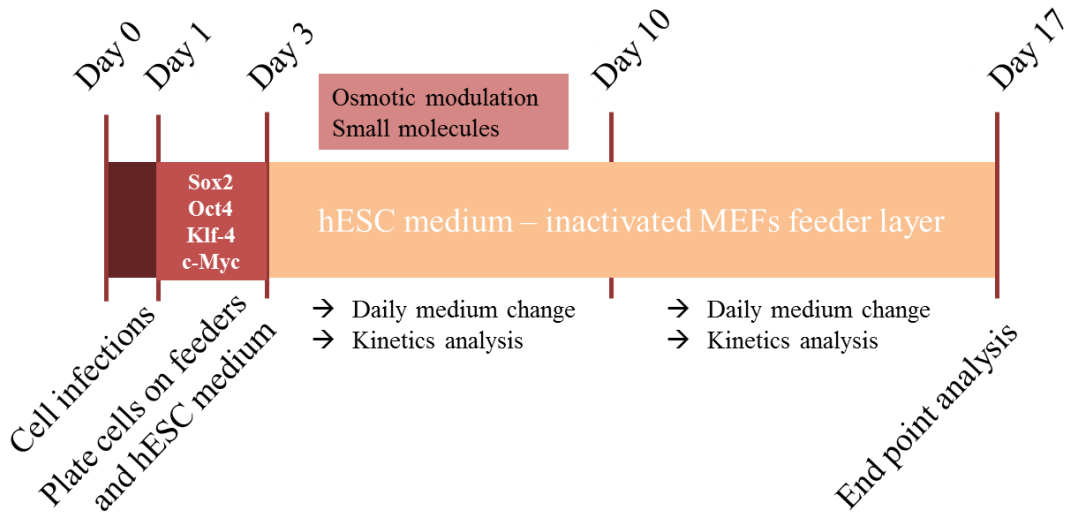

Figure 2.4 – Schematic representation for reprogramming experiments with umbilical cord blood cells. The osmotic modulation was done only during the first week with the cells in feeder layer. Depending on the type of experiment, fluorescence microscopy follow-up was done throughout the reprogramming period or an end point alkaline phosphatase staining was performed.

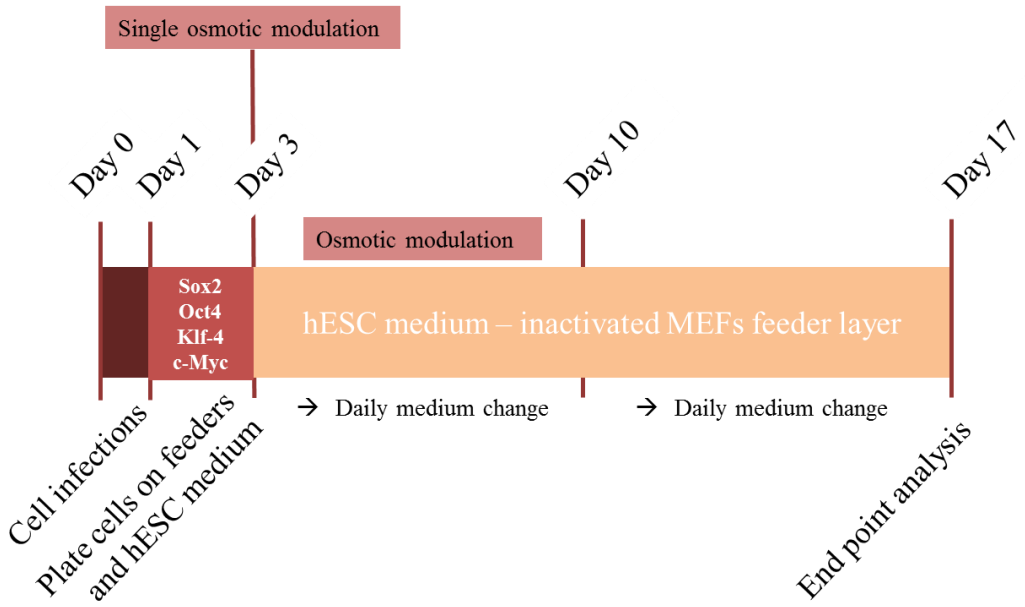

Figure 2.5 – Schematic representation for reprogramming experiments with normal dermal fibroblasts (NDHFs). The osmotic modulation was done once straight before seeding the NDHF in feeder cells or three modulations during the first week of reprogramming. At the end point, alkaline phosphatase staining was performed.

After some reprogramming experiments, the colonies were further expanded by colony mechanical picking (Figure 2.6). The picked colonies were placed in fresh medium and afterwards in a new MEFsI feeder layer.

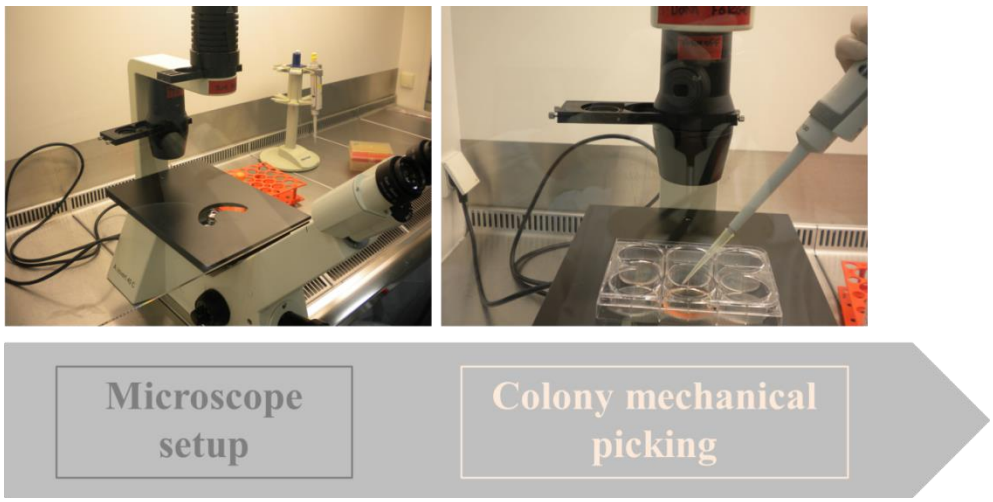

Figure 2.6 – Representation of the setup for colony mechanical picking.

2.2.18. Umbilical cord blood isolation and cell population sorting

Umbilical cord blood (UCB) was collected by the maternity units from *Hospital de Aveiro* and *Maternidade Daniel de Matos* according to standard collection procedure using a blood bag (SURU). The collected samples were stored at room temperature until processing the samples.

To isolate the specific cell populations within the UCB, flow cytometry cell sorting and magnetic assorted cell sorting techniques were used.

Firstly, the UCB was fractioned to isolate the mononuclear cells, using lymphoprep according to manufacturer's protocol. The magnetic assorted cell sorting was performed against CD34 and CD133 epitopes according to manufacturer's protocol. A schematic workflow representation is shown in Figure 2.7.

For fluorescence-activated cell sorting, a BD FACS Aria III was used in collaboration with *Centro de Histocompatibilidade do Centro* and the cells were collected in complete growth medium.

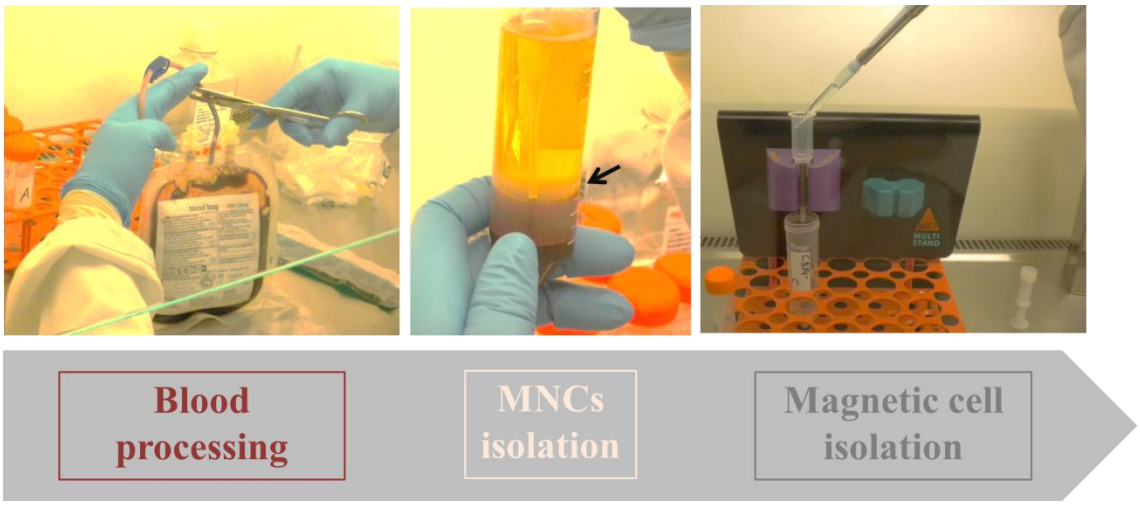

Figure 2.7 – Workflow for isolation of specific cell populations from the umbilical cord blood by magnetic activated cell sorting. The black arrow in the middle image denotes the layer of mononuclear cells (MNCs) after density gradient fractionation.

After the cell sorting, the cells were kept overnight in StemSpan supplemented with 100ng/mL of Flt3-L, SCF and 100units/mL of penicillin and 100µg/mL of streptomycin to recover.

2.2.19. Transdifferentiation process

The transdifferentiation protocol used was based on reports by Professor Thomas Graf group (Bussmann et al., 2009), whom kindly donated the HAFTL-C10 cell line. The protocol used is schematized in Figure 2.8. At the experimental endpoint, the cells were evaluated for CD11b and CD19 epitopes expression by flow cytometry (GalliosTM) and were also sampled for RNA purification.

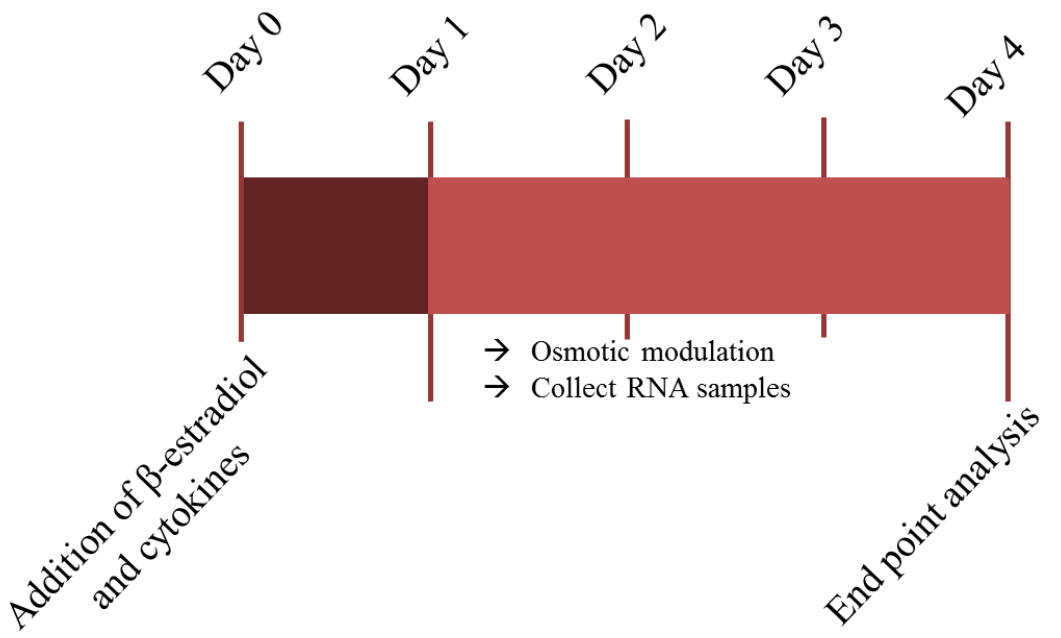

Figure 2.8 – Schematic representation for the transdifferentiation experiments with the HAFTL-C10 cell line. The osmotic modulation was done from day1 to day3 in different modulation schemes.

2.2.20. Statistical analysis

Two-tailed, two-sample Student's t-test, assuming unequal variances, was used to determine significance, unless stated otherwise. The number of independent repeats of each experiment (n) is indicated in the figures legends.

Chapter 3 : Impact of osmotic modulation on cell physiology

In this work, osmoregulation mechanisms have a central role in all the experiments. Although these mechanisms are highly conserved between different organisms, the degree of expression of its regulatory components is variable in different cell types (Finan and Guilak, 2010; Hoffmann et al., 2009; Kültz, 2001; Lang et al., 1998). Although cellular osmoregulation is constituted by diversified signalling mechanisms, there are a set of conserved adaptations with the objective to counterbalance extracellular osmolarity disturbances and maintain cell integrity and function. Cellular osmoregulation comprises the regulation of cell volume and osmolyte transport but also parameters like protein structure and turnover, and genomic integrity (Kültz, 2001; Lang et al., 1998). Additionally, it is also important to note that osmolarity changes in the extracellular environment (which are often seen as pathophysiological), are essential to several processes, like transepithelial transport, migration and cell division (Hoffmann and Pedersen, 2011; Hoffmann et al., 2009).

Herein, osmotic stress is seen as a tool which can be used to change downstream pathways and its direct physical impact can generate relevant outputs in the cellular state. Changes in cellular function imply alterations in the active transcriptional network that are correlated with the degree of chromatin compaction and its dynamic behaviour (Lavelle, 2014; Martins et al., 2012).

Therefore, this chapter is subdivided into three main topics: a) the effect of osmotic modulation on cellular characteristics and cellular metabolism; b) changes in chromatin and c) changes in transcription.

This thesis presents the hypothesis of using transient osmotic modulation as a safe tool to help in cell state or fate modulation protocols. In order to set-up, the most effective osmotic modulation levels for each cell type, long-term exposure experiments were performed to gain knowledge about specific toxicity thresholds.

3.1. Results and Discussion

3.1.1. Osmotic modulation effects on intracellular parameters and cellular metabolism

Animal cell membranes do not withstand significant hydrostatic pressure gradients. Water movement across the cell membrane is determined by osmotic gradients (Koivusalo et al., 2009; Lang et al., 1998; Wehner et al., 2003). Additionally, the animal cell membrane, with few exceptions, is highly permeable to water (Hoffmann et al., 2009; Koivusalo et al., 2009; Wehner et al., 2003). Therefore, by decreasing the extracellular osmolarity the entry of water into the intracellular compartment is favoured. The opposite effect is observed after increasing extracellular tonicity (Hoffmann and Pedersen, 2011; Hoffmann et al., 2009; Koivusalo et al., 2009; Wehner et al., 2003).

To understand the effects of extracellular osmolarity in cell behaviour we used several osmotic cocktail combinations and modulation schemes schematized in Table 3.1. From now on, the terminology presented in this table will be used to refer to the conditions used in each experimental setup.

The nomenclature used in Table 3.1 intends to simplify the distinction of experiments where the cells were in different osmolality conditions, induced in the presence of different components such as complete growth culture media or phosphate buffered saline (PBS). Therefore, it is important to clarify that, by using PBS (without magnesium and calcium) in the osmotic modulation cocktail mixture, only inorganic salts will be diluted by the addition of distilled water. On the other hand, by using a complete growth culture medium in the osmotic modulation cocktail mixture, not only inorganic salts will be present but other components of the complete growth medium will be diluted too. These components include amino acids, vitamins, glucose, serum and other organic osmolytes. The component concentration will be at lower levels within the extracellular space in hyposmotic media modulation experiments and consequently, influence some of the cell reaction components.

Table 3.1- Summary of the osmotic conditions used to modulate the cellular environment. The nomenclature presented in this table will be used to represent the conditions described (in the last column min stands for minutes). The complete growth medium osmolality was assumed to be within the isosmolar parameters (≈280mOsm/Kg) and the PBS osmolality was the average osmolality range provided by the supplier (280 - 315 mOsm/kg).

Name given to the experimental condition		Medium/ solution used	Distilled water in the total volume of the cocktail	NaCl % in the total volume of the cocktail	Type of stimuli
Hypo/M	Hyposmotic Media	Complete growth culture medium (≈280mOsm/Kg)	1/4 (≈210mOsm/Kg)		Permanent or transient (15 min) in the osmotic modulation cocktail during the experiment at 37ºC, 5% CO_2.
Hypo+/M			1/3 (≈187mOsm/Kg)		
Hypo2+/M			1/2 (140≈mOsm/Kg)		
Hypo3+/M			2/3 (93≈mOsm/Kg)		
Hypo4+/M			3/4 (≈70mOsm/Kg)		
Hyper/M	Hypertonic Media			1.8 (≈560mOsm/ Kg)*	
Hypo/PBS	Hyposmotic solutions	Phosphate-Buffered Saline (PBS) (≈297.5mOsm/Kg)	1/4 (≈223mOsm/Kg)		Permanent or transient (15 min) in the osmotic modulation cocktail during the experiment at 37ºC, 5% CO_2
Hypo+/PBS			1/3 (≈198mOsm/Kg)		
Hypo2+/PBS			1/2 (≈149mOsm/Kg)		
Hypo4+/PBS			3/4 (≈74mOsm/Kg)		
Hyper/PBS	Hypertonic solution			1.8 (≈600mOsm/ Kg)*	

The evaluation of the osmotic impact as an "isolated" modulation factor is a difficult task. The ideal scenario, in the scope of this study, would be to have control over the composition of the complete media formulations in order to discriminate between effects related with the osmotic regulatory response itself and/or effects induced by the presence of different levels of specific media components. This could be done to a certain point by performing the studies in osmotic cocktails containing PBS. Nevertheless, for long-term studies, cell viability can be compromised in certain cell types when using osmotic solutions containing PBS (such as umbilical cord blood-derived mononuclear cells – UCB-MNCs). Therefore, the use of osmotic cocktails made with complete growth medium or PBS was used throughout the study depending on the specific cell or technical restrictions. Additionally, several challenges are faced when using cells in suspension. One example is the need to centrifuge the samples after performing hyposmotic

transient stimuli. This step is essential to transfer the cells back to an isosmolar solution. This centrifugation step might introduce confounding variants related to alterations on cell membrane induced by hyposmolarity. Cell membrane fluidity alterations induced by hyposmolarity have been described but never correlated with the physical disturbance caused by centrifugation (Hoffmann et al., 2009). This change in cell membrane properties might leave the cell more vulnerable to deformation by centripetal force, and generate changes in cell size.

UCB-MNCs are sensitive cells and cannot be maintained in culture for long periods of time without losing stemness. Additionally, it is hard to control several variables associated with UCB collection, such as the elapsed time between collection and sample processing and the amount of UCB collected. Moreover, the *in vitro* culture of these cells is expensive due to the need of enriched media with cytokines. Due to these constraints, a leukaemia cell line (K562 cells - chronic myelogenous leukaemia) was chosen for some of the optimisation studies in this work. This cell line is easily cultured, and to some extent has similar physical features as UCB-MNCs, i.e. morphology, volume, cultured in suspension and share similar blood origin. As a starting point, cell behaviour was analysed in a broad range of osmotic conditions; cellular function and physiological parameters were evaluated. The work then proceeds towards using a more defined hyposmotic modulation strategy with sensitive cells of limited supply, like UCB-MNCs. In the studies with both cells types, there is an interest in understanding the impact of the extracellular hyposmotic constitution in different cellular behaviour patterns. Additionally, the behaviour observed in UCB-MNCs can be relevant to fields such as stem cell transplantation and cell differentiation.

The next two subchapters explore the impact of permanent and transient hyposmotic modulation on cell function by using distinct extracellular environments.

3.1.2. Permanent osmotic modulation effects

To evaluate the cellular impact of a permanent disturbance on the extracellular osmolarity environment, cells were exposed to different osmotic modulation cocktails and several cellular parameters were analysed. These parameters included: forward side scatter (FSC), as an indirect measure of cell size (Shapiro, 2003); adenosine triphosphate (ATP) levels, as a measure of cell viability; production of reactive oxygen species (ROS); cell membrane potential; mitochondrial membrane potential and intracellular free calcium levels.

3.1.2.1. Cell size and cell viability

The average cell FSC was evaluated at several time points by flow cytometry (BD FACSCalibur™). K562 cells were placed in complete growth medium (control cells), hypo+/M, hypo2+/M and hyper/M for approximately 20 hours (Figure 3.1).

In a global perspective, in Figure 3.1, it is clear that the cells in a hypertonic environment have a rapid decrease in cell size and this change cannot be counteracted by the cell to restore its initial size (namely by the activation of the regulatory volume increase mechanisms - RVI). On the other hand, the cells in a hyposmotic environment present a typical oscillatory behaviour in cell size that with time tends to go back to the initial size (by activation of regulatory volume decrease mechanisms – RVD).

In a more detailed study, K562 cells in the hyper/M have an abrupt and significant (p value < 0.05) decrease in cell size (Figure 3.2); these cells cannot counteract this effect over time (Figure 3.1 and Figure 3.2). This effect might be explained by the high concentration of NaCl in the extracellular medium that can increase the intracellular Cl^- concentration and consequently block the activation of RVI mechanisms (Lang et al., 1998).

In regards to the hyposmolar changes in the extracellular environment, cells in both types of hyposmotic media display an oscillatory cell size pattern over time. This behaviour was already observed in several cell types and it is known as RVD (Lang et al., 1998; Wehner et al., 2003). K562 cells in both hyposmolar media show a significant and prompt response. This significant difference (p value < 0.01) at 0.1 and 0.2 hours is an approximate increase of 35% in FSC comparing with the control (complete growth medium) (Figure 3.2). Straight after the increase in cell size, the cells present a significant (p value <0.05; p value < 0.01) oscillatory size behaviour during the first hours of treatment (Figure 3.2). After 20 hours these cells tend to display a similar size to the control cells by regaining a new stable state (Figure 3.1 and Figure 3.2). This behaviour is characteristic of the activation of the osmotic regulatory mechanisms (like RVD), where, after an initial increase in cell size and cell size oscillation, the cells restore their normal size (Hoffmann and Pedersen, 2011; Koivusalo et al., 2009; Wehner et al., 2003).

The kinetics of the oscillatory size behaviour is very similar between hypo+/M and hypo2+/M conditions (Figure 3.1 and Figure 3.2).

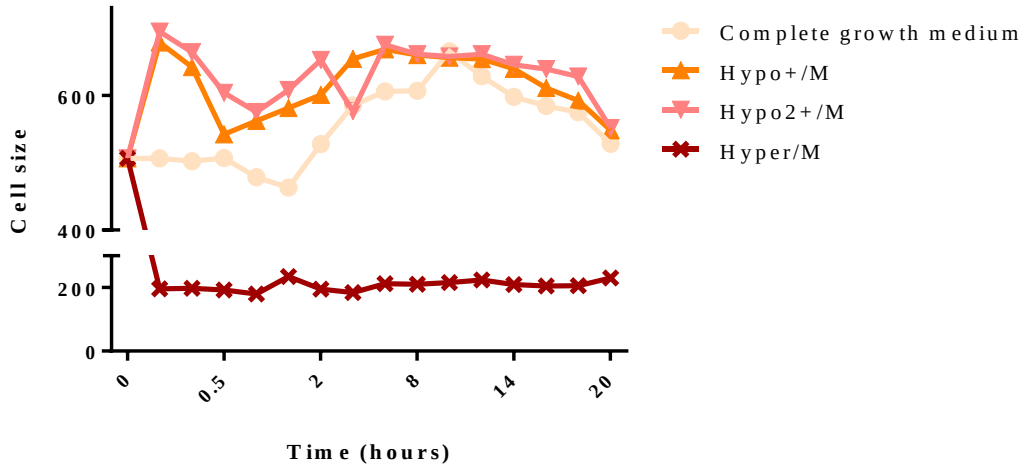

Figure 3.1 – Effect of constant osmotic modulation on cell size in K562 cells. Forward side scatter (FSC) mean value variation (as an indirect measure of cell size) over time (n=1) with different osmotic modulation protocols pointed out on the legend.

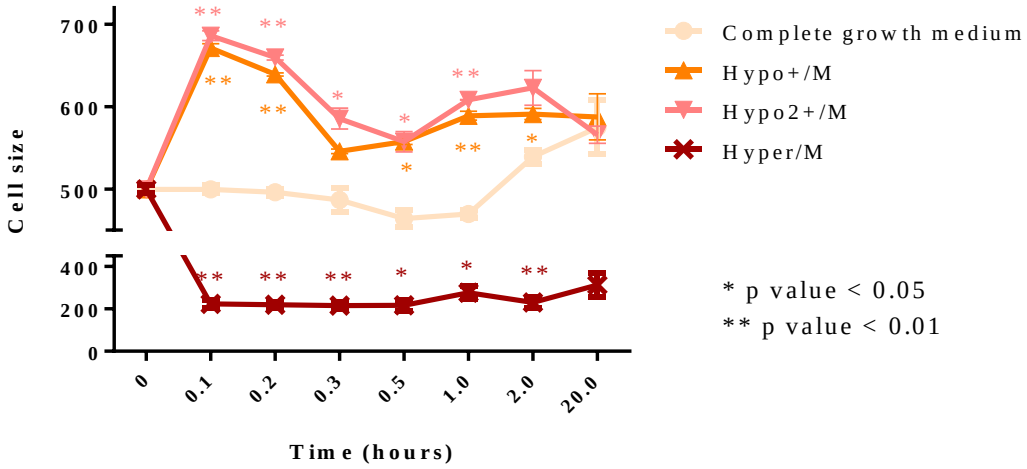

Figure 3.2 – Effect of constant osmotic modulation on cell size in K562 cells. Forward side scatter (FSC) mean value variation (± SEM) over time (as an indirect measure of cell size) (n=2). The different osmotic modulation protocols are described in the legend. These changes are statistically significant at the timepoints highlighted in the graph (p value < 0.05; p value < 0.01).

In addition to morphological changes, cell physiology is also challenged by extracellular environment osmolarity. The cellular responses are diverse, these depend on cell type and type of osmolarity stimuli (Hoffmann et al., 2009; Hohmann, 2015; Lang et al., 1998).

To evaluate cell viability, K562 cells were exposed to different osmotic environments and the total level of ATP was measured by a luminescence readout (CellTiter-Glo® Luminescent Cell Viability Assay).

Either by using hyposmotic media or hyposmotic solutions, in the conditions with lower osmolarity there was a marked decrease of total ATP level (Figure 3.3 and Figure 3.4). In condition hypo4+/M (Figure 3.3) there was a significant decrease (p value< 0.05; p value < 0.01) of the total ATP level.

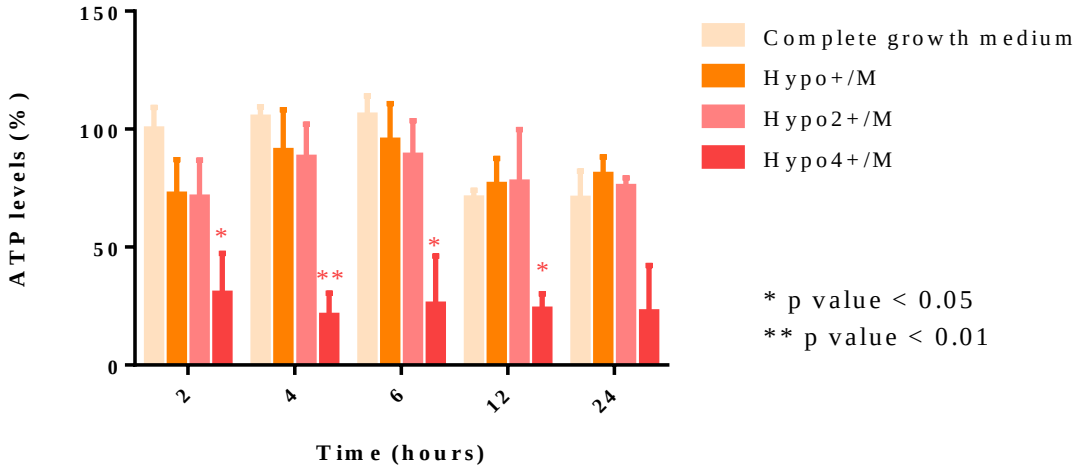

Figure 3.3 – Effect of constant osmotic modulation on total ATP levels in K562 cells. ATP level (normalised relative luminescence units) variation (±SEM) over time (n=3) with different osmotic modulation protocols shown in the legend. All values are normalised to the control at 2 hours (complete growth medium at 2h considered to be 100%). Changes are statistically significant at the timepoints highlighted in the graph (p value < 0.05; p value < 0.01).

The cells within other hyposmotic conditions (hypo+/M, hypo2+/M, hypo+/PBS and hypo2+/PBS) did not present significant changes from cells within the control group up to 24 hours (Figure 3.3 and Figure 3.4).

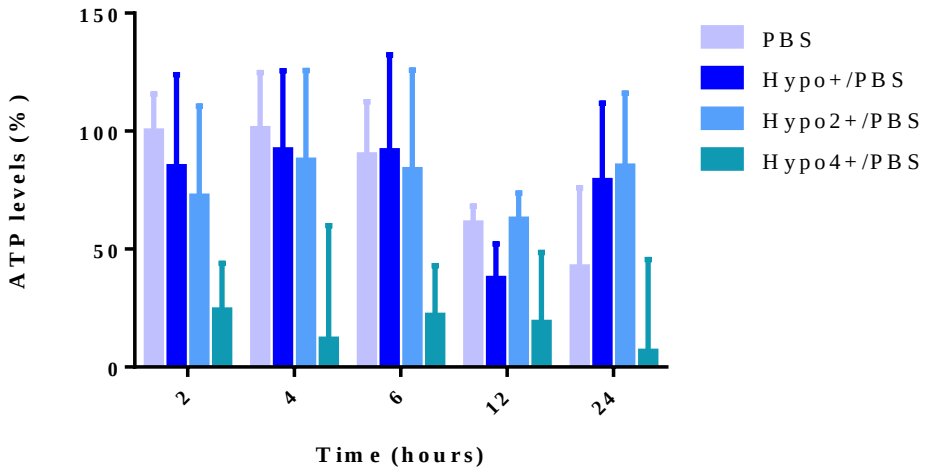

Figure 3.4 – Effect of constant osmotic modulation on total ATP levels in K562 cells. ATP level (normalised relative luminescence units) variation (±SEM) over time (n=3) with different osmotic modulation protocols show in the legend. All values are normalised to the control at 2 hours (PBS condition at 2h considered to be 100%).

An important point that should be particularly noted is the decrease of total ATP levels when K562 cells were incubated either with PBS or complete growth medium over time (Figure 3.5). This decrease becomes significantly different (p value < 0.05) between the two experimental conditions after 12 hours and 24 hours (Figure 3.5).

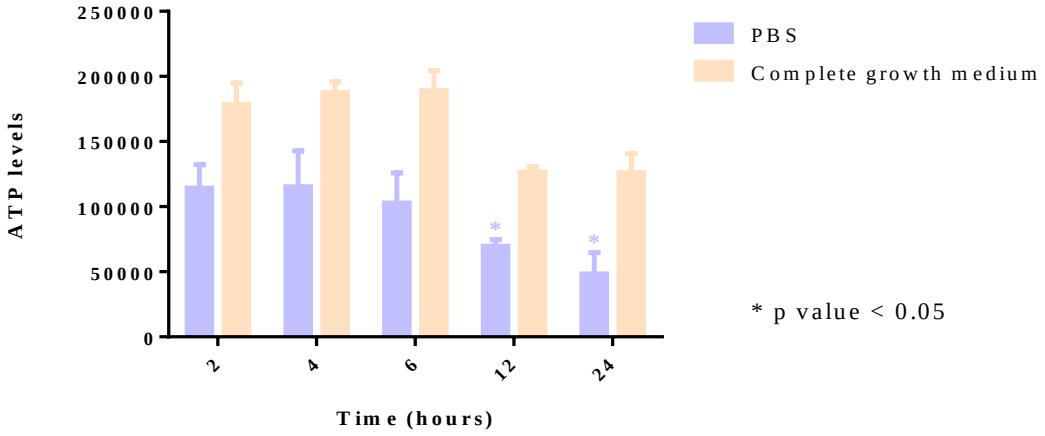

Figure 3.5 – Total ATP levels on control groups in K562 cells. Total ATP level (raw relative luminescence units) variation (±SEM) at different timepoints (n=3) with cells in complete growth medium and PBS. Changes that are statistically significant are highlighted in the graph (p value < 0.05).

The same type of effect, with regard to cell viability, was observed in UCB-MNCs (Figure 3.6). UCB-MNCs after 19h and 72h in hypo3+/M show a decrease in the ATP levels. Nevertheless, in this specific condition, there is variability associated with the ATP levels (Figure 3.6). Although this graph reflects only a single biological replicate, the high variability of condition hypo3+/M may reflect the mixed origin of this cell population (Figure 3.6).

Altogether, these results suggest that a permanent hyposmotic extracellular environment promotes a rapid increase in cell size, depending on the hyposmolarity range, the recovery to a normal cell size follows different patterns (Figure 3.1 and Figure 3.2). Additionally, cell viability was only affected by extreme hyposmotic conditions (hypo4+/M, hypo3+/M, hypo4+/PBS) (Figure 3.3, Figure 3.4 and Figure 3.6). Therefore, these extreme conditions can be classified as a non-physiological stimulus or toxic stress to either K562 cells or UCB-MNCs. On the other hand, the milder hyposmotic conditions (hypo/M, hypo+/M, hypo2+/M, hypo+/PBS, hypo2+/PBS) seem to have no relevant impact on cell viability either in K562 cells or UCB-MNCs (Figure 3.3, Figure 3.4 and Figure 3.6). Thus, these conditions were chosen to mimic physiological stimuli or sub-toxic stress on all other experiments throughout this thesis.

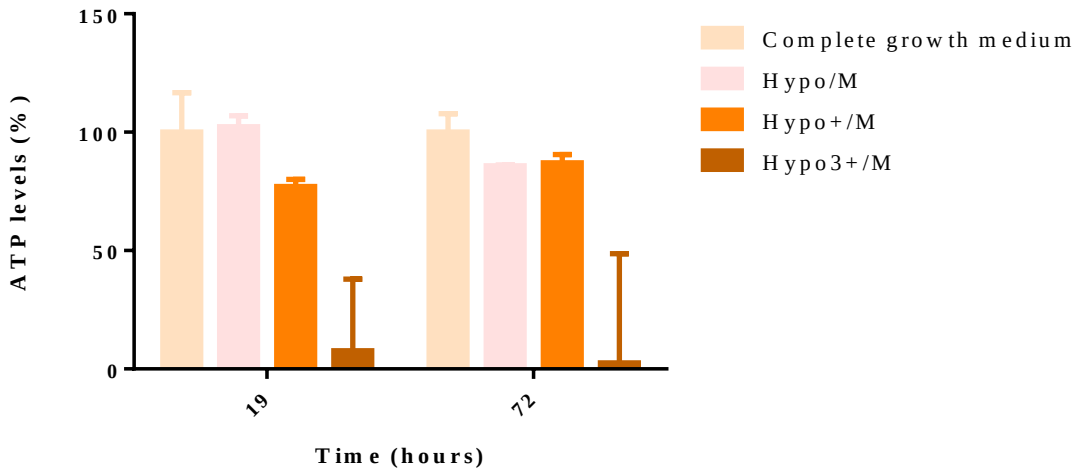

Figure 3.6 – Effect of constant osmotic modulation on total ATP levels in UCB-MNCs. Total ATP level (normalised relative luminescence units) variation (±SD) at different timepoints (n=1) with different osmotic modulation strategies pointed out on the legend.

3.1.2.2. Cellular physiology and metabolism

The analysis of the impact of osmotic insults on cellular behaviour has been the main focus of research in the field over the last decades. Cellular studies have focused essentially on studying how ionic currents are changed to counteract the effects of the initial osmotic stress and in signal transduction pathways that are activated after the osmotic stress (Hoffmann et al., 2009; Lang et al., 1998; Pasantes-Morales et al., 2006; Wehner et al., 2003). Some studies highlight a possible influence of metabolic changes as a key player in the osmotic response mechanisms. Nevertheless, the metabolic role in osmotic response mechanisms, and particularly the role of mitochondria, is a very underexplored field (Hohmann, 2015; Lang et al., 1998).

In this work, some cellular responses were systematised by using a diverse range of osmotic modulation schemes with the K562 cell line.

For this systematisation, cellular features like cell membrane potential, mitochondrial membrane potential ($\Delta\Psi m$), intracellular free calcium levels, and production of reactive oxygen species (ROS) were evaluated under hyposmotic modulation and control conditions. Changes in these parameters were assessed by measuring the fluorescence of different probes over time by flow cytometry (BD FACSVerse™).

The mechanism of RVD, besides other features, includes increased conductance in K^+, which can lead to a hyperpolarization of cell membrane potential (Hoffmann et al., 2009). The increase in K^+ conductance can promote the efflux of Cl^- and other osmolytes, the efflux pathways can be activated, contributing towards the restoration of basal cell membrane potential (Hoffmann et al., 2009).

To study the cell membrane potential, the slow-response potential-sensitive probe, DiBAC4(3), was chosen. This probe is excluded by mitochondria because of their overall negative charge, being, therefore, more accurate for plasma membrane potential assessment than other probes. When inside the cell, this probe binds proteins and membrane components and exhibits enhanced fluorescence characteristics. As the cell membrane inner leaflet becomes more negative (hyperpolarized), the anionic DiBAC4(3) leaves the cell and its fluorescent signal decreases. Conversely, as the cell membrane inner leaflet becomes more positive (depolarization), more DiBAC4(3) enters, and the DiBAC4(3) fluorescent signal gets more intense (Adams and Levin, 2014). Increases in the influx or efflux of this anionic dye correlate with an increase or decrease in the fluorescence signal that, in turn, reflects increase or reduction of cell membrane potential, respectively.

Regarding cell membrane potential assessment, K562 cells in complete growth medium, hypo+/M and hypo2+/M have a significant decay (p value < 0.0001) of the probe's fluorescent signal over time

(DiBAC4(3)) (Figure 3.7). This fluorescence decay should reflect a decrease in cell membrane potential, but no differences could be noticed between the control group and the osmotic modulatory conditions (Figure 3.7). Therefore, such effect might reflect a specific feature of the labelling with this probe and not due to any direct effect of osmolarity.

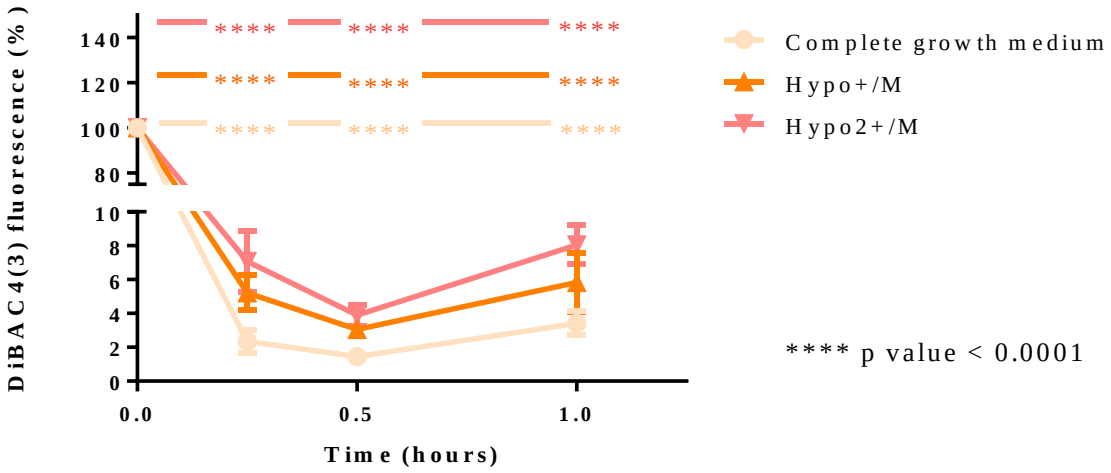

Figure 3.7 – Effect of constant osmotic modulation on cell membrane potential in K562 cells. Cell membrane polarisation (% of fluorescence signal normalised to 0h) differences (±SEM) over time (n=3) with different osmotic modulation strategies detailed in the legend. The statistical differences shown in the graph are a result of a comparison between timepoint 0h of each condition with the correspondent timepoints (p value < 0.0001). No statistically significant changes were observed between the osmotic conditions and the control (complete growth medium).

The labelling with the probe was done in PBS, as recommended by the manufacturer and might explain the instability of the probe when cells are placed back in growth medium and favour the efflux of the probe. This effect is not noticed when labelled cells are placed in PBS (Figure 3.8). Additionally, some unknown efflux mechanisms or quenching effects of the probe can also occur (Klapperstück et al., 2009; Wang et al., 2012).

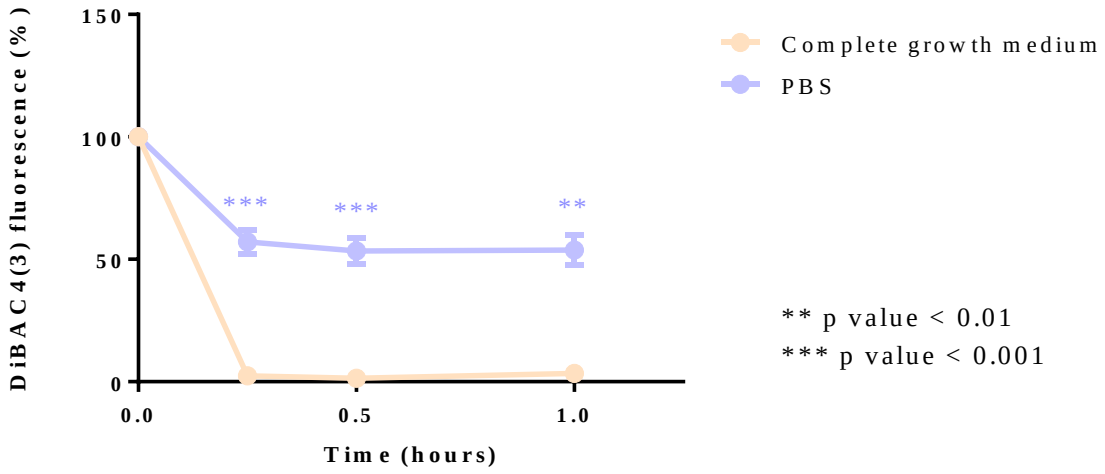

Figure 3.8 – Differences of environmental conditions on cell membrane potential in K562 cells. Cell membrane polarisation (% of fluorescence signal normalised to time 0h) differences (±SEM) over time (n≥3) with different conditions noted in the legend. The statistical differences are shown in the PBS condition (p value < 0.01; p value < 0.001) at all timepoints when compared to the complete growth medium condition.

When K562 cells are incubated in PBS there is a decrease of the DiBAC4(3) probe fluorescence signal (Figure 3.9). This decrease is less pronounced when compared to complete growth medium condition (Figure 3.8). The difference reflects a decrease in cell membrane potential or efflux of the probe in the complete growth medium condition. Interestingly, the conditions where cells are in hypo+/PBS or hypo2+/PBS, have a significant difference (p value < 0.05) in cell membrane potential over time when compared with the PBS control (Figure 3.9).

The major PBS components are sodium chloride and sodium phosphate dibasic (and to a lesser extent potassium phosphate monobasic). Therefore, by itself, PBS might activate pathways of ion influx/efflux, promoting a reduction in cell membrane potential over time. The differences in cell membrane potential, between the control and hypo+/PBS or hypo2+/PBS conditions, are significantly altered (p value < 0.05) at almost every time point (Figure 3.9). These differences are consistent with activation of systems involved in RVD mechanisms like Cl^- channels, anionic exchange channels and organic osmolyte channels (Hoffmann et al., 2009; Koivusalo et al., 2009; Lang et al., 1998). The activation of such channels might be an attempt to compensate for increased cellular volume by re-establishing an ionic/osmolyte equilibrium between the extracellular and intracellular environments. Consequently, the cell membrane potential changes can be counteracted by the entrance of anions. This suggests that PBS hyposmotic conditions may be more effective at producing transient changes in cell water content.

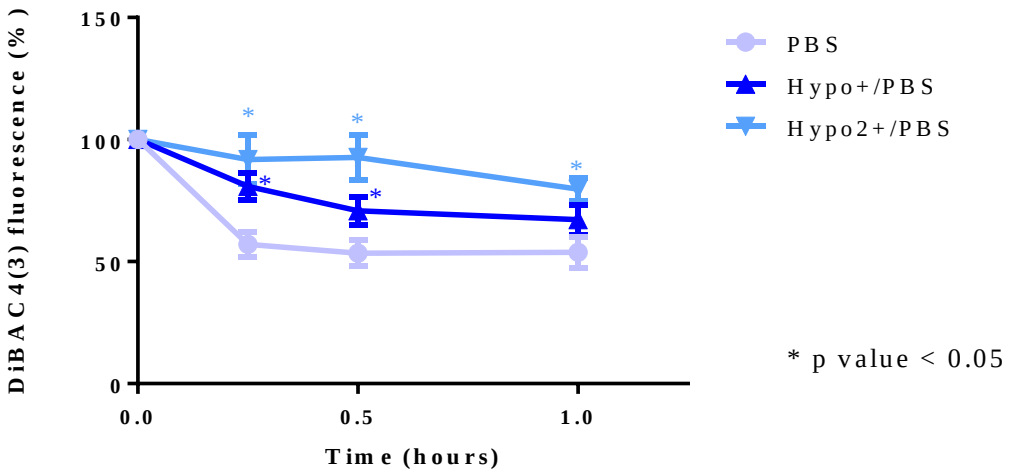

Figure 3.9 – Effect of constant osmotic modulation on cell membrane potential in K562 cells. Cell membrane polarisation (% of fluorescence signal normalised to time 0h) differences (±SEM) over time (n≥3) with different osmotic modulation strategies noted in the legend. The statistical differences are shown in the osmotic modulatory conditions (p value<0.05) at all timepoints when compared to the respective control (PBS).

Along with all the changes in the intracellular environment, another important player in the RVD mechanism in hypotonic induced swelling is the production of ROS, which can act as signalling molecules (Hoffmann et al., 2009; Lang et al., 1998).

In order to evaluate the production of ROS in the osmoregulation scenario, MitoSOX™ Red reagent was used to evaluate the production of superoxide radical within the mitochondria and DCFDA (2',7' – dichlorofluorescin diacetate) to evaluate the general production of ROS within the cell.

MitoSOX™ Red reagent is a probe which is rapidly and specifically oxidised by superoxide radical. After oxidation, it becomes highly fluorescent by binding to nucleic acids. When assessing the mitochondrial superoxide levels in K562 cells in PBS, hypo+/PBS or hypo2+/PBS an increase of MitoSOX™ Red intensity can be observed (Figure 3.10). After 1 hour, in all the conditions, there is an approximately 2 fold increase in MitoSOX™ Red fluorescence levels. The probe fluorescence change pattern over time is very interesting, it reaches a maximum intensity level at 30 minutes which may lead to speculation about the cell oxidative defence pathways and mitochondria that might be active and counteracting the initial increase of superoxide levels (Figure 3.10).

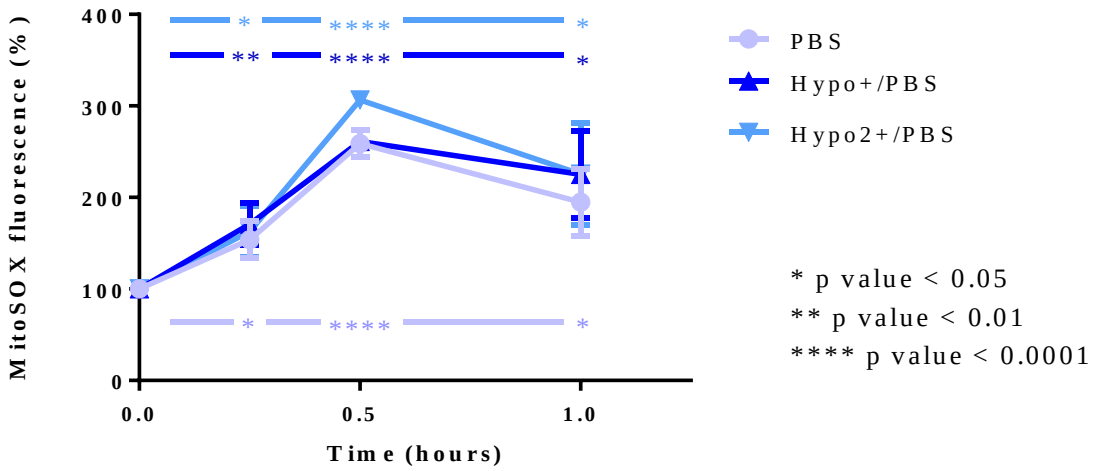

Figure 3.10 – Effect of constant osmotic modulation on mitochondrial superoxide levels in K562 cells. Mitochondrial superoxide (% of fluorescence signal normalised to time 0h) changes (±SEM) over time (n≥3). Different osmotic conditions were used as shown in the legend. The statistical differences shown in the graph are a result of a comparison between the timepoint 0h of each condition with the corresponding timepoints (p value< 0.05; p value < 0.01; p value < 0.0001). No statistically significant changes were observed between the osmotic conditions and the control (PBS).

In order to have a general overview of the cell's oxidative state, the DCFDA (2',7' – dichlorofluorescin diacetate) probe was used. This probe permeates cells, is deacetylated by cell esterases and loses its fluorescence. When oxidised by ROS, this probe gives rise to a highly fluorescent compound. When assessing the ROS levels in K562 cells in hypo+/PBS and hypo2+/PBS, a slight increase in ROS at 15 minutes can be noticed (Figure 3.11). Nevertheless, over time there is a slight decrease in the total ROS, but no differences between the control (PBS) and the osmotic modulatory conditions (Figure 3.11).

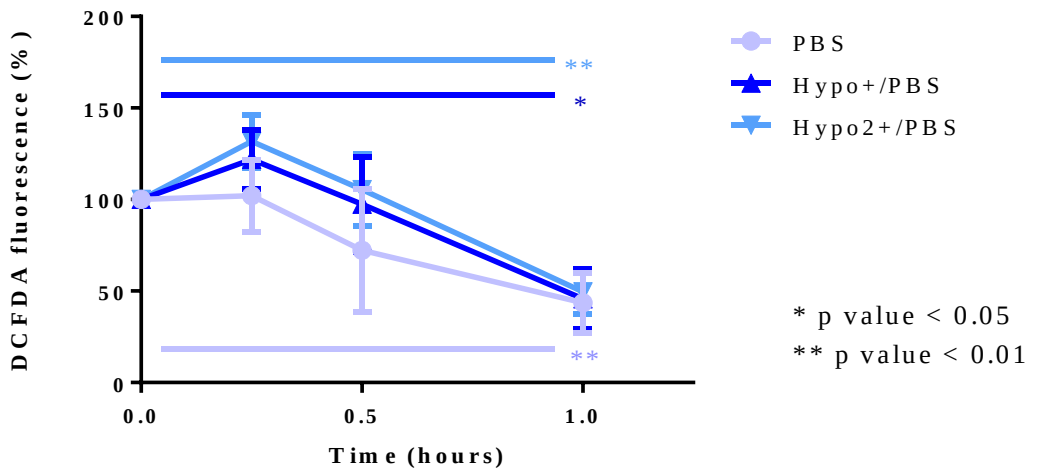

Figure 3.11 – Effect of constant osmotic modulation on ROS levels in K562 cells. Cellular ROS (% of fluorescence signal normalised to time 0h) levels (±SEM) over time (n≥3) with different osmotic modulation strategies shown in the legend. The statistical differences shown in the graph are a result of a comparison between the timepoint 0h of each condition with the corresponding timepoints (p value< 0.05; p value < 0.01). No statistically significant changes were observed between the osmotic conditions and the control (PBS).

Additionally, to understand the coupling between the cell's redox state and its metabolism, ΔΨm was evaluated using a $DiIC_1(5)$ probe. The metabolic changes induced by extracellular environment osmotic modulation are very underexplored (Hohmann, 2015; Lang et al., 1998).

Another factor related to mitochondrial function and ionic fluxes, which has become increasingly studied, is the mitochondrial ability to act as a buffering agent for intracellular calcium levels (Demaurex et al., 2009; Patergnani et al., 2011). The concentration and fluxes of calcium are also relevant for mitochondrial function (Jhun et al., 2016; Patergnani et al., 2011; Rizzuto et al., 2012). The hyposmotic stress has been described to increase intracellular calcium concentration in some cells types but in others, the intracellular calcium was not changed or was decreased after hyposmotic modulation (Hoffmann et al., 2009). Nevertheless, there are no studies that correlate mitochondrial function and intracellular calcium level oscillations. Therefore, it seemed very interesting to evaluate the intracellular concentration of free calcium in K562 cells. This ion might not only contribute to cellular volume regulation during osmotic shocks but also be correlated with alterations in cell metabolism and mitochondrial function.

In the evaluation of ΔΨm, the probe used, $DiIC_1(5)$, accumulates primarily in mitochondria with active membrane potentials, producing a bright fluorescence signal. The fluorescence intensity of this staining decreases with decreased ΔΨm. When K562 cells were placed in complete growth medium a

decrease in the initial fluorescent signal can be observed (Figure 3.12). This denotes a decrease in the ΔΨm. Nonetheless, no differences can be observed between the control (complete growth medium) and conditions where K562 cells were placed in hypo+/M and hypo2+/M (Figure 3.12).

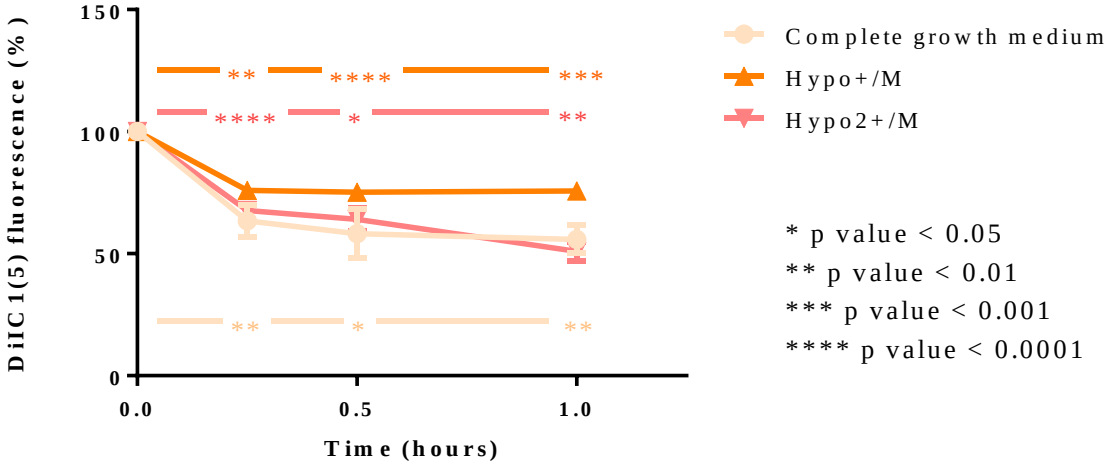

Figure 3.12 – Effect of constant osmotic modulation on mitochondrial membrane potential (ΔΨm) in K562 cells. Mitochondria membrane potential (% of fluorescence signal normalised to time 0h) differences (±SEM) over time (n=3) with different osmotic modulation strategies shown in the legend. The statistical differences shown in the graph are a result of a comparison between the timepoint 0h of each condition with corresponding timepoints (p value< 0.05; p value < 0.01; p value < 0.001; p value < 0.0001). No statistically significant changes were observed between the osmotic conditions and the control (complete growth medium).

On the other hand, when K562 cells are placed in PBS there is an increase in ΔΨm over time (Figure 3.13). When K562 are placed in hypo2+/PBS, there is a significant decrease of the ΔΨm (p value <0.05) in comparison with the control (PBS) (Figure 3.13). The decrease in ΔΨm within the hyposmotic solutions and the hyposmotic media related to the respective control condition may be indicative of less "efficient"/active mitochondria when cells face a hyposmotic extracellular environment in the absence of complete growth medium components.

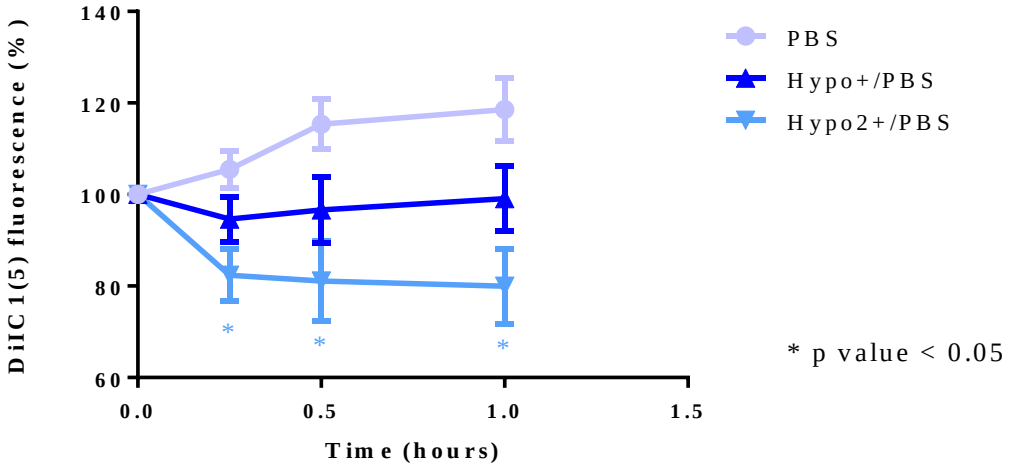

Figure 3.13 – Effect of constant osmotic modulation on mitochondrial membrane potential (ΔΨm) in K562 cells. Mitochondrial membrane potential (% of fluorescence signal normalised to time 0h) differences (±SEM) over time (n≥3) with different osmotic modulation methods shown in the legend. The strongest osmotic modulation (hypo2+/PBS), when compared with the control displays a significant decrease of the mitochondrial membrane potential over time (p value <0.05).

The trend of ΔΨm change described above is interlinked with changes observed in the levels of free intracellular calcium (Figure 3.14 and Figure 3.15). The calcium probe used, eFluor™ 514, is membrane-permeable and enables the monitoring of changes in free intracellular calcium concentrations. As to K562 cells, when placed in complete growth medium, a rapid and intense increase of the probe initial fluorescence signal is recorded (Figure 3.14). This increase in fluorescence signal indicates an increase in free intracellular calcium. When comparing the control group (complete growth medium) with cells in hypo+/M and hypo2+/M no differences are observed (Figure 3.14).

In contrast, when K562 cells are placed in hypo+/PBS or hypo2+/PBS there is a significant increase (p value < 0.05) of free intracellular calcium levels when compared with the control (PBS) (Figure 3.15).

The changes in ΔΨm and free intracellular calcium levels in both groups (Figure 3.12; Figure 3.14 and Figure 3.13; Figure 3.15) are both very interesting and intriguing.

In Figure 3.12, the decrease of ΔΨm is in the same range within all the conditions and in terms of free intracellular calcium also the same type of increase trend is observed in all conditions (Figure 3.14).

On the other hand, Figure 3.13 shows that when cells are in PBS there is an increase in ΔΨm; comparatively to control cells the hypo+/PBS and hypo2+/PBS conditions display a decreased ΔΨm. In

parallel, cells in hypo+/PBS and hypo2+/PBS present a marked increase in free intracellular calcium when compared with the control (PBS) (Figure 3.15).

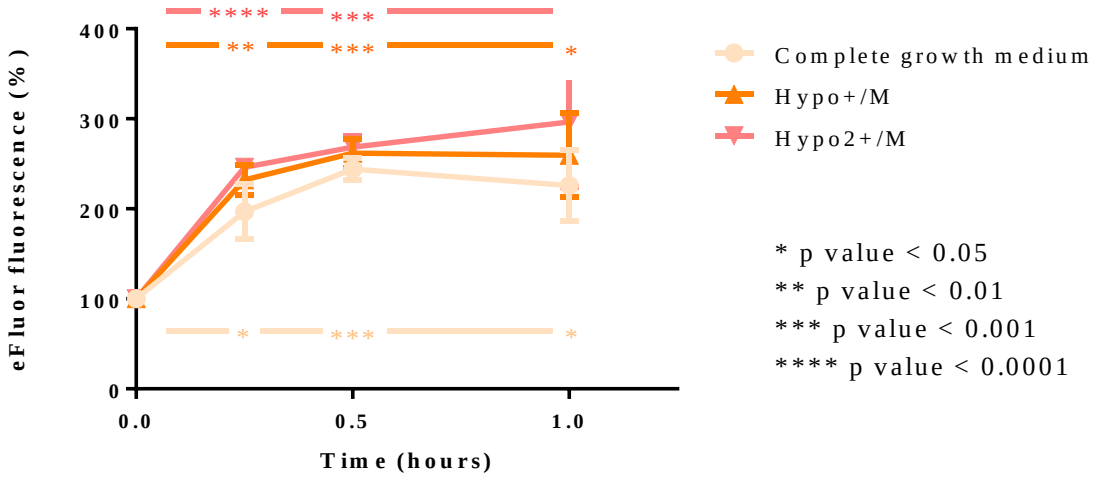

Figure 3.14 – Effect of constant osmotic modulation on intracellular free calcium levels in K562 cells. Intracellular free calcium level (% of fluorescence signal normalised to time 0h) changes (±SEM) over time (n=3) with different osmotic modulation methods shown in the legend. The statistical differences shown in the graph are a result from a comparison between timepoint 0h with its correspondent timepoints (p value< 0.05; p value < 0.01; p value < 0.001; p value < 0.0001). No statistically significant changes were observed between the osmotic conditions and the control (complete growth medium).

Moreover, if we analyse the increase pattern of free intracellular calcium, cells in PBS, hypo+/PBS and hypo2+/PBS have a slower increase over time. This trend is in part conditioned by the limited amounts of calcium within the intracellular reservoirs (like endoplasmic reticulum and mitochondria) because the extracellular environment is depleted of calcium.

These possible interconnections are very interesting, and in the literature, there are already some studies describing the mitochondria as an important coordinator of calcium homoeostasis and how calcium also impacts mitochondrial function (Jhun et al., 2016; Patergnani et al., 2011; Rizzuto et al., 2012). The role of mitochondria, specifically in buffering calcium, is unexplored in osmotic regulatory processes.

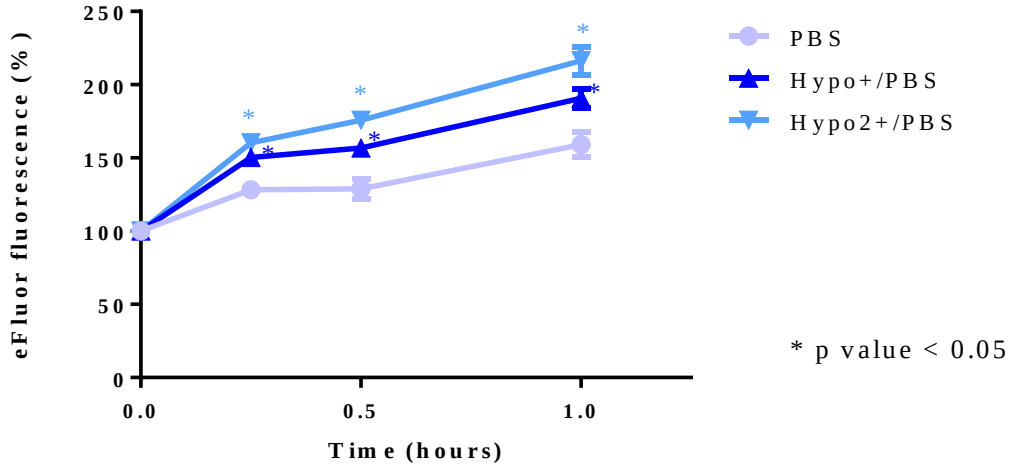

Figure 3.15 – Effect of constant osmotic modulation on intracellular free calcium levels in K562 cells. Intracellular free calcium level (% of fluorescence signal normalised to time 0h) changes (±SEM) over time (n≥3) with different osmotic modulation methods shown in the legend. The free intracellular calcium concentrations, indicated by the increase in fluorescence, is statistically increased in the osmotic modulatory conditions (p value<0.05), all timepoints are compared with the respective control (PBS).

Regarding this section is important to note that the evaluation of total production of ROS and mitochondrial superoxide was done only in PBS containing solutions since these were the conditions that in previous experiments had a greater impact on cell survival. Regarding the others cellular parameters evaluated, is important to note that the presence of media components is an important factor that modulates the cell response to hyposmolarity. Although we see clear changes when modulating cells in PBS hyposmotic cocktails, the effects observed are no longer present if the same stimuli are done in complete growth media. Therefore the presence of organic osmolytes and other media components in the extracellular environment might have a crucial role in cell response to hyposmolarity and somehow minimise the impact of hyposmotic effects in cellular function.

3.1.3. Transient osmotic modulation effects

Cellular response to osmolarity has been mainly studied in the context of permanent alterations of the osmotic environment and under stress (non-physiological) conditions (Andronic et al., 2015; Kim et al., 2000; Liu et al., 2009; Shen et al., 2001; Zhao et al., 2016). Transient modulation, using a hyposmotic extracellular environment, could be advantageous: does not influence cell viability but has a relevant

impact on cell behaviour in an acute manner. This transient modulation would also give the flexibility and precision of an adjustable experimental tool, able to manipulate or guide cell decision.

To evaluate the impact of transient changes in the extracellular osmolarity environment, cells were exposed to different osmotic modulation cocktails (Table 3.1) during fifteen minutes and placed back in normal complete growth culture media afterwards. Several cellular parameters were analysed: FSC (as an indirect measure of cell size); total ATP levels; intracellular and extracellular ATP levels and free intracellular calcium levels.

3.1.3.1. Cell size and cell viability

As for the previous studies on cell size, FSC was evaluated by flow cytometry (BD FACSCalibur™).

For cell size measurements, K652 cells were placed transiently in hypo+/M, centrifuged afterwards and resuspended in complete growth medium. In Figure 3.16 the time point 0.25 hours corresponds to the instant after transient modulation in hypo+/M but the cytometry reading was done already with the K562 cells in complete growth medium. The analysis of cell size was done during approximately 20 hours (Figure 3.16). When compared with the permanent osmotic modulation (Figure 3.2), the cell behaviour after transient osmotic modulation is very distinct (Figure 3.17).

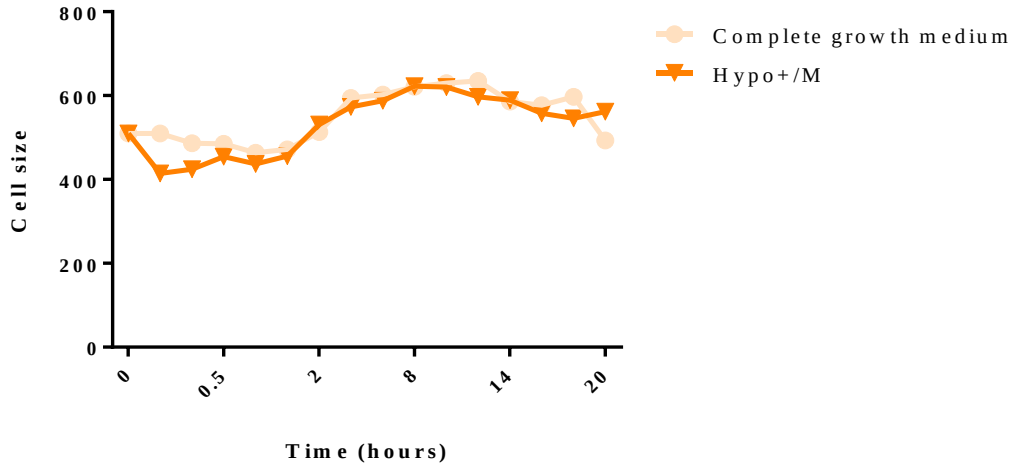

Figure 3.16 – Effect of transient osmotic modulation on cell size in K562 cells. Forward side scatter (FSC) mean value variation (as an indirect measure of cell size) over time (n=1) after exposing the cells to a transient osmotic modulation pointed out in the legend.

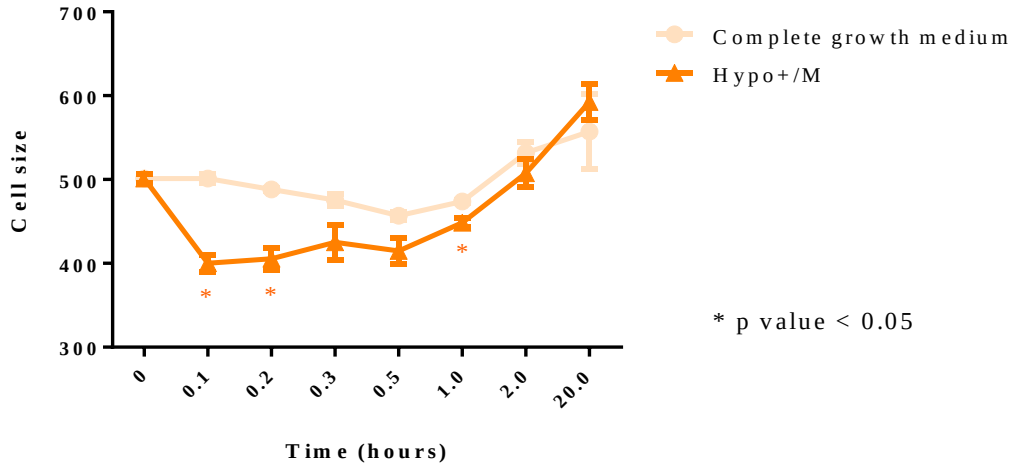

Figure 3.17 - Effect of transient osmotic modulation on cell size in K562 cells. Forward side scatter (FSC) mean value (as an indirect measure of cell size) variation (±SEM) over time (n=2) with transient osmotic modulation methods shown in the legend. Clearly the cells which were in a transient hyposmotic environment, display a decrease in cell size (p value < 0.05) at initial timepoints.

In the literature, the impact of transient hyposmolar environments and the correlation with fluctuations in cell size is mainly restricted to physiological examples; like in epithelial transport, where epithelial cells are constantly challenged to maintain their cellular volume (Lang et al., 1998; Okada, 2004). The differences in cell size observed between the permanent exposure and transient exposure to the hyposmotic environment might be related to technical constraints. After presenting the cells transiently to hypo+/M, cells are centrifuged and resuspended in complete growth medium (corresponding to time point 0.25 hours read at the flow cytometer - Figure 3.16 and Figure 3.17). The decrease in cell size noticed at this time point in the hypo+/M condition (Figure 3.17) might be an artificial effect due to centripetal forces. These forces may have a greater impact in cell morphology (after osmotic modulation) due to alterations in cell membrane induced by hyposmolarity, already reported in the literature (Pasantes-Morales et al., 2006; Wehner et al., 2003). Therefore, the fact that transient osmotic modulation induced a drop in cell size and non-oscillatory cell size behaviour (in contrast with previous observations) might be associated with these technical aspects.

To evaluate the impact of a transient osmotic modulation in cell viability, UCB-MNCs were exposed to different osmotic environments and the total ATP levels were assessed, as previously described (using CellTiter-Glo® Luminescent Cell Viability Assay). The transient osmotic modulation was done with hypo/PBS and hypo+/PBS, by exposing UCB-MNCs for 15 minutes to these hyposmotic solutions. The

cell viability assay was performed straight after osmotic modulation. After stimulation, no differences in total ATP levels were seen (Figure 3.18).

These results are in agreement with our previous results for permanent hyposmotic modulation (Figure 3.6). In the literature, ATP was also described as a possible participant in the osmotic answer. This molecule can be released from the cell and act in an autocrine/paracrine signalling pathway (Hoffmann et al., 2009; Lang et al., 1998; Pasantes-Morales et al., 2006; Wehner et al., 2003).

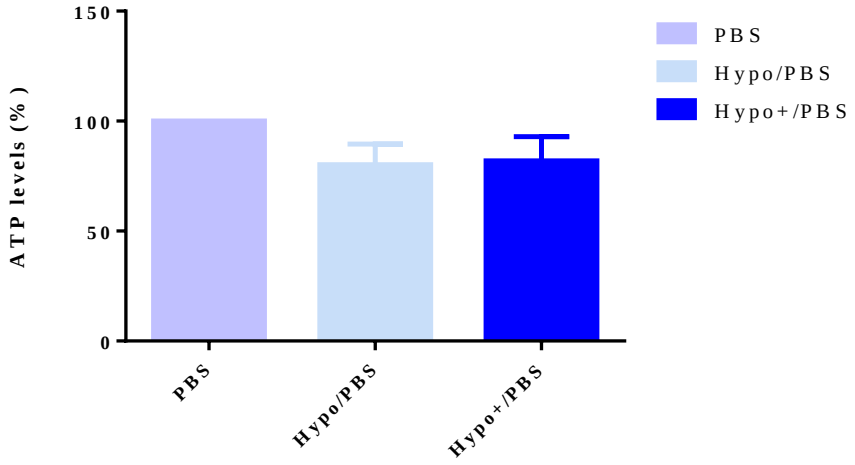

Figure 3.18 – Effect of transient osmotic modulation on total ATP in UCB-MNCs. Total ATP level (normalised relative luminescence units) variation (±SEM; n=3) straight after stimulation with different methods shown in the legend. No statistically significant differences were observed in ATP levels between all conditions.

The evidence for the importance of ATP as a signalling molecule in the osmotic environment change response guided this work towards a different path. Instead of measuring total ATP levels, next we attempted to acquire more accurate information about intracellular and extracellular ATP levels. After exposing the cells to hyposmotic media and hyposmotic solutions in a transient manner (15 minutes) the cell suspension was centrifuged into a fraction where the hyposmotic media and solutions did not contain cells (extracellular ATP level – Figure 3.19) and a fraction where the cells were pelletized (intracellular ATP level – Figure 3.20). The ATP measurement was done as previously described (using CellTiter-Glo® Luminescent Cell Viability Assay) straight after the transient osmotic modulation using the two different aliquots described before.

Within this experimental setup is clear that cells exposed to hypo4+/M and hypo4+/PBS have a significant increase (p value < 0.01; p value < 0.001 respectively) in extracellular ATP levels (Figure 3.19). Additionally, also with hypo2+/PBS, there is a slight increase in extracellular ATP (Figure 3.19).

These viability results (Figure 3.19) can also be due to some degree of cell bursting since osmolarity changes can impact cell viability as we have observed in the permanent hyposmotic modulation experiments (Figure 3.3 and Figure 3.4).

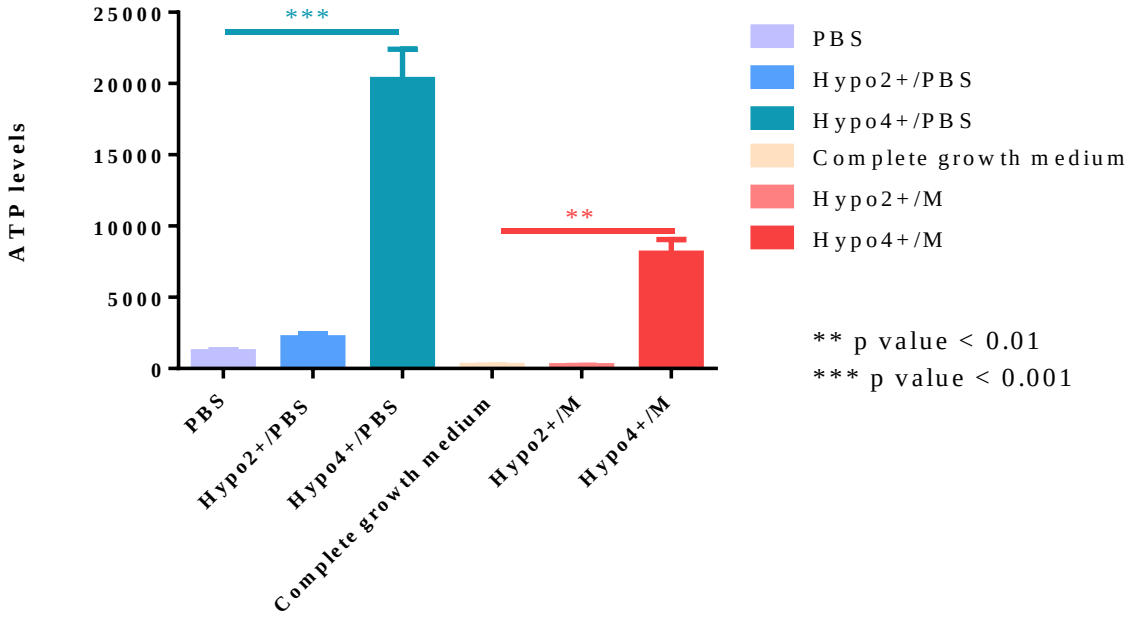

Figure 3.19 – Effect of transient osmotic modulation on extracellular ATP levels in K562 cells. ATP level (raw relative luminescence units) variation (±SEM) in extracellular medium right after of stimulation with different osmotic cocktails, shown in the legend (n=3). Statistically significant differences between controls (PBS/complete growth medium) and osmotic conditions are highlighted in the graph (p value < 0.01; p value < 0.001).

Interestingly, the increase in extracellular ATP levels after exposure to hypo2+/PBS (Figure 3.19) is correlated with a significant decrease (p value < 0.05) in intracellular ATP levels (Figure 3.20). This observation is in agreement with the extrusion hypothesis, where release of ATP from cells after hyposmotic modulation occurs.

Additionally, in parallel to the increase in extracellular ATP levels, after exposure to hypo4+/PBS (Figure 3.19), there is a significant decrease (p value < 0.0001) of intracellular ATP (Figure 3.20). Nonetheless, when exposing cells to hypo4+/M, although the increase of extracellular ATP levels is significant, there is no significant decrease of intracellular ATP (Figure 3.20).

When comparing the change in extracellular ATP levels, in hypo2+/PBS and hypo4+/PBS conditions the values are approximately 2.5 fold higher than in hypo2+/M and hypo4+/M (Figure 3.19). The underlying cause for this effect is unknown. But we speculate, that the presence of nutrients, serum and other organic osmolytes in the hyposmotic media, which are not present in the hyposmotic solutions

might support these differences by a metabolic effect. The components of osmotic media could enable the cells to metabolically compensate for stress and maintain the energy levels unchanged. Additionally, cells in hypo2+/M show a pronounced decrease in ΔΨm (Figure 3.12), thus these cells might start to use other pathways to compensate for the energy production.

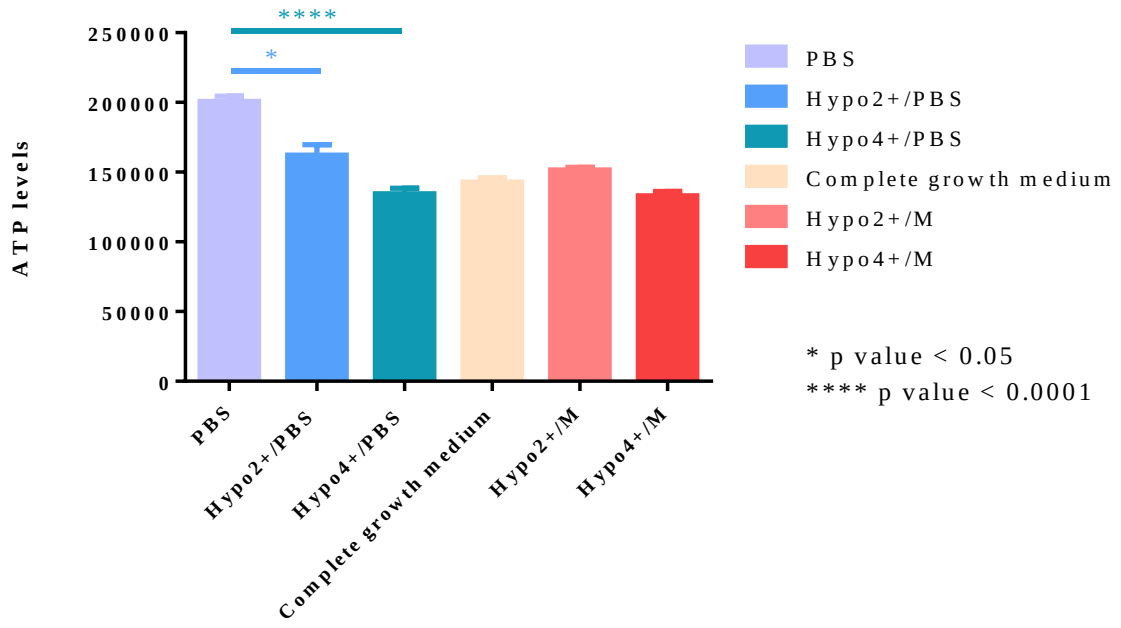

Figure 3.20 – Effect of transient osmotic modulation on intracellular ATP levels in K562 cells. ATP level (raw relative luminescence units) variation (±SEM) in the intracellular compartment right after stimulation with different osmotic cocktails, shown in the legend (n=3). Statistically significant differences between control (PBS/complete growth medium) and osmotic conditions are highlighted in the graph (p value < 0.05; p value < 0.0001).

The changes in ATP concentration and changes induced by the hyposmotic modulation made us think about the importance of the mitochondria and the metabolic pathways in this context. The previous results presented for mitochondrial membrane potential changes induced by hyposmolarity also show that the mitochondrial function is affected by this type of osmotic modulation. The mitochondrial function was more studied in this thesis because the correlation between mitochondrial morphology and activity is associated with important cell decisions, especially fate decisions (Hämäläinen, 2016; Prigione et al., 2015; Wanet et al., 2015).

The next subchapter explores changes in calcium levels that might also have a link with mitochondrial function.

3.1.3.2. Cellular physiology

As mentioned previously in this chapter, in this study one of the most striking and interesting effects of the hyposmotic extracellular environment is the possible relationship between free intracellular calcium levels and mitochondrial activity.

Mitochondria are multifunctional organelles that control several cellular processes. The mitochondrial uptake of calcium was shown to control intracellular calcium signalling, cellular metabolism, cell survival and other cell-specific functions (Jhun et al., 2016; Rizzuto et al., 2012). Physiological increases in cytosolic free calcium concentration are perceived in the mitochondrial matrix, and α-ketoglutarate, isocitrate, and pyruvate dehydrogenases are directly stimulated to boost mitochondrial metabolism together with other indirect effects (Jhun et al., 2016; Rizzuto et al., 2012). Mitochondria is one of the players that modulates calcium fluctuations within the cell and translates this into metabolic or apoptotic responses (Demaurex et al., 2009).

In this work, the impact of osmotic modulation in the cell mitochondrial function was one feature that got our attention during the development of the work. Therefore, the next step in this study was to evaluate the free intracellular calcium levels after transient exposure of K562 cells to hyposmotic media and hyposmotic solutions; then placed back into complete growth medium or PBS (Figure 3.21 and Figure 3.22), respectively.

When evaluating free intracellular calcium levels, in the presence of hyposmotic media there is a gradual and slow increase in the free intracellular calcium levels over time (Figure 3.21).

On the other hand, when hyposmotic solutions were used, as osmotic modulators, the increase in free intracellular calcium levels is sustained for less time and after 1 hour there are no differences between the cells exposed to hyposmotic solutions and the control group (Figure 3.22).

Once again, these differences in response to the osmotic stimulus might be related to the source of calcium which the cells are using in each specific situation. The K562 cells exposed to hyposmotic media have plenty of calcium in the extracellular environment during (and after) the osmotic stimuli (Figure 3.21). Therefore, the effect of the hyposmolar environment does not translate into an immediate increase in intracellular calcium. This is only seen in hypo2+/M, the most extreme condition. On the other hand, cells exposed to hyposmotic solutions do not have calcium in the extracellular environment during, or after the osmotic stimuli (Figure 3.22). Therefore in this last scenario, (Figure 3.22) cells have a limited

and finite amount of intracellular calcium stored inside the cell compartments which can be mobilised as a response to hyposmotic shock.

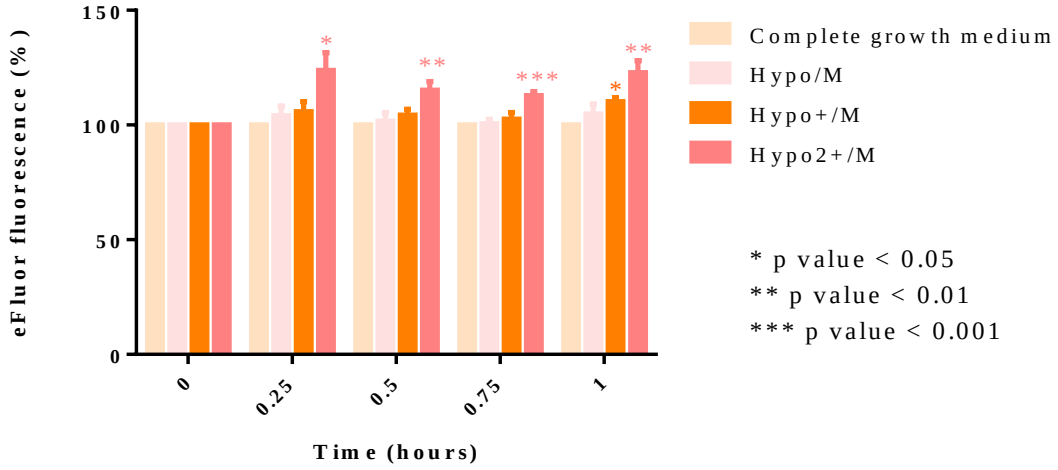

Figure 3.21 – Effect of transient osmotic modulation on intracellular free calcium levels in K562 cells. Intracellular free calcium level (% of fluorescence signal normalised to control) changes (±SEM) over time in K562 cells (n=4) after a transient modulation. The different osmotic modulation methods are presented in the legend. The free intracellular calcium concentrations, indicated by the increase in fluorescence signal, is a statistically significant increase in some osmotic modulatory conditions when compared with the respective control (complete growth medium) at the time points outlined in the graph (p value<0.05, p value < 0.01, p value < 0.001).

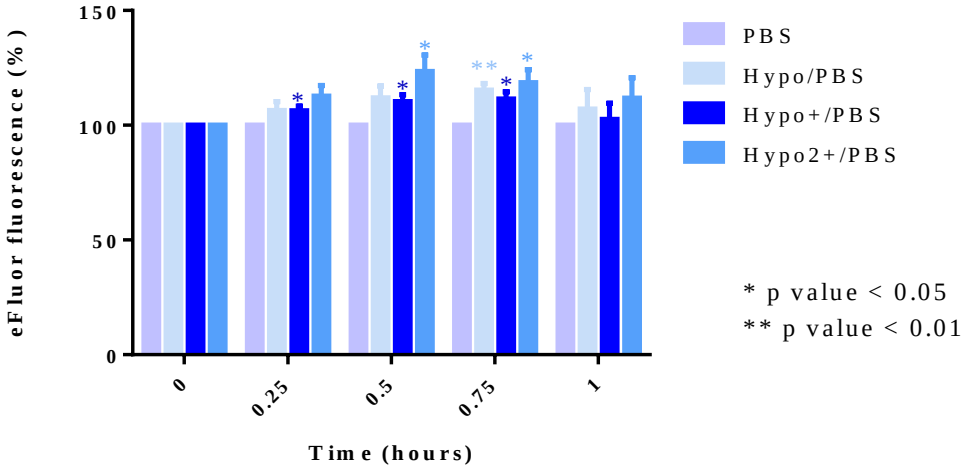

Figure 3.22 – Effect of transient osmotic modulation on intracellular free calcium levels in K562 cells. Intracellular free calcium level (% of fluorescence signal normalised to control) changes (±SEM) over time (n=4) after a transient modulation. The different osmotic modulation strategies used are presented in the legend. The intracellular free calcium concentrations, indicated by the increase in fluorescence signal, is a statistically significant increase in some osmotic modulatory conditions when compared with the respective control (complete growth medium) at the timepoints outlined in the graph (p value<0.05, p value < 0.01).

From the observations in this study, it would be important to evaluate other characteristics of the intracellular calcium levels fluctuations observed in response to hyposmotic modulation. For instance, the evaluation of intracellular calcium levels in the presence of different agonists and antagonists of specific calcium channels would be informative of what are the major players in the import of calcium from the extracellular environment. Also, the use of small molecules to inhibit calcium transport between the different intracellular stores would allow the assessment of the organelle-specific calcium contributions under osmotic modulation.

From the collection of data presented in this work, we can schematize in a simple way the toxicity effects of the hyposmotic modulations, either using a permanent or transient type of stimuli. The scheme presented in Figure 3.23 aims to simplify the terminology used to discriminate each group of osmotic modulation. In this way, the terminology used to discriminate these conditions can be easy and direct: hyposmotic solutions and media called as safe (hypo; hypo+; hypo2+) or toxic (hypo3+/M and hypo4+) applied in a transient or permanent way. In this schematic representation there are different thresholds for safe osmotic modulation using PBS or complete growth medium that are probably related with the presence of calcium and osmolytes in the medium that confer further robustness to the cells.

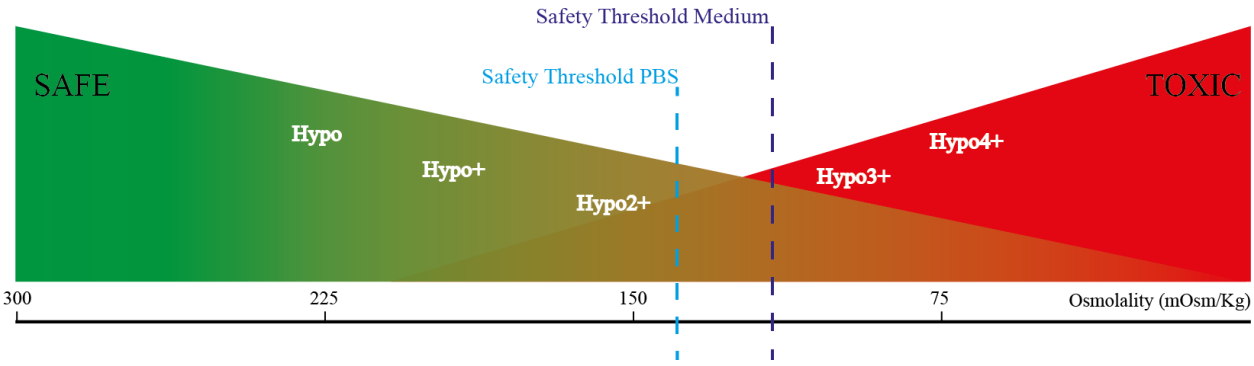

Figure 3.23 – Representative scheme of cell toxicity induced by osmotic modulation.

The calcium release induced by osmotic challenges has indirect and direct impacts in nuclear and chromatin structure (Finan and Guilak, 2010; Finan et al., 2011; Martins et al., 2012). This mechanism is associated with the water movement and the physical impact on the nuclear structure and consequently in chromatin structure (Finan and Guilak, 2010).

The importance of nuclear structure, lead us to explore this field and the next subchapter explores global and some specific chromatin changes induce by osmotic modulation.

3.1.4. Chromatin changes induced by osmotic modulation

A further outstanding effect of the osmolarity changes in the extracellular environment is the fast change on chromatin structure. This effect is already reported in the literature, but mostly in cells that usually have to face these osmotic challenges in their normal environment, as chondrocytes (Finan and Guilak, 2010; Okada, 2004).

The nuclear organisation is very complex, and some characteristics of this major organelle, like its stiffness, can be associated with processes of highest relevance for cell fate. These processes include cell differentiation, migration and even control of gene expression (Finan and Guilak, 2010; Martins et al., 2012).

Despite the major recent advances in several technological platforms that analyse chromatin state in a great detail (Mendenhall and Bernstein, 2008; Rando, 2007; Tsompana and Buck, 2014), the majority of experiments to assess the large-scale chromatin structure rely on microscopy techniques (Belmont, 2014). Here we have tried to complement this type of approach with enzymatic digestion and electrophoresis.

After a transient exposure of UCB-MNCs to different osmotic solutions, the differences in euchromatin and heterochromatin levels can be clearly observed by confocal microscopy (Figure 3.24 and Figure 3.25).

Heterochromatin can be perceived as the brighter fluorescence spots of DAPI (4',6-diamidino-2-phenylindole) staining present in the cell nucleus. These regions have high levels of chromatin compaction corresponding to inactive areas of transcription (Martins et al., 2012). In Figure 3.24, it is clear that the exposure to the hypertonic solution shows a great impact on heterochromatin spot density, intensity and abundance. These differences are also easy to be perceived in the respective 3D representation of the fluorescence intensity levels in Figure 3.25.

On the other hand, euchromatin can be perceived as the less intense and more homogeneous DAPI staining in the cell nucleus. These regions have low chromatin compaction, generally thought to be permissive to transcription (Martins et al., 2012). Looking at Figure 3.24, the exposure to hyposmotic solutions has a great impact on chromatin organisation. The cell nucleus becomes more homogeneous and presents less heterochromatic spots. These alterations are proportional to the decrease in osmolarity (hypo/PBS, hypo+/PBS, hypo2+/PBS, hypo4+/PBS) (Figure 3.24). These differences are also easily seen in the respective 3D representation of DAPI fluorescence intensity levels, Figure 3.25.

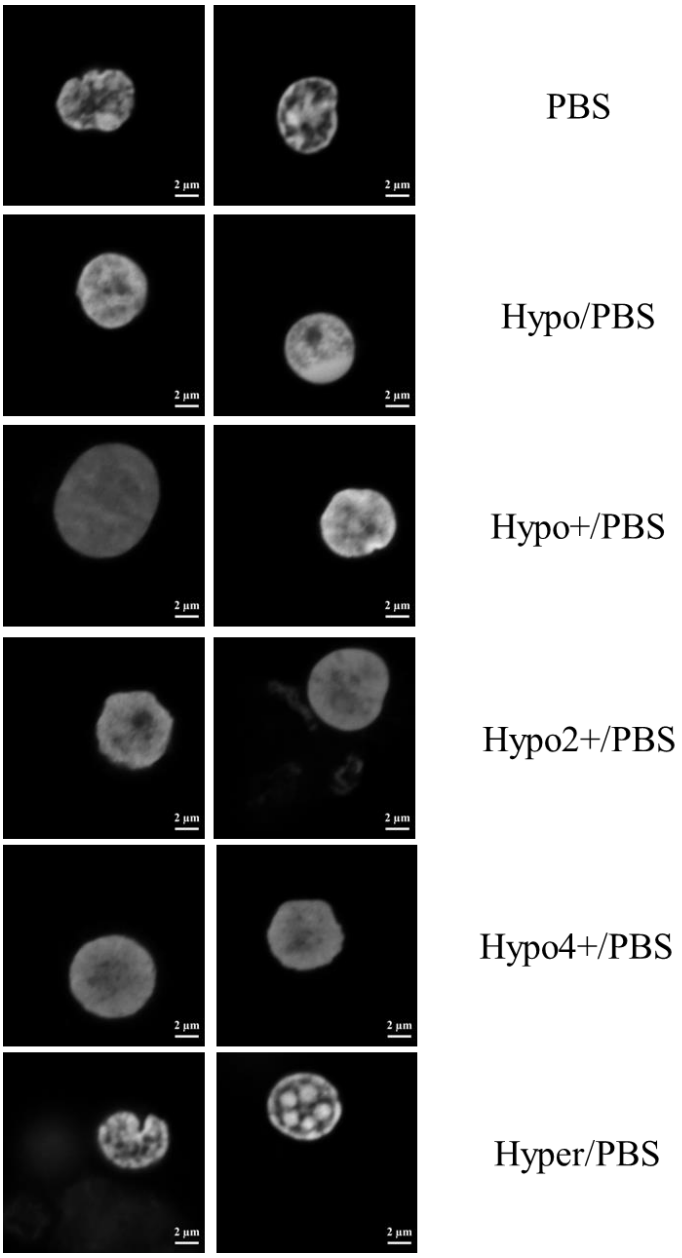

Figure 3.24 – Confocal imaging with DAPI stained UCB-MNCs, previously presented to different osmotic solutions. The cells were fixed and imaged straight after exposure to different osmotic modulation conditions, shown in the figure. Scale bar = 2µm.

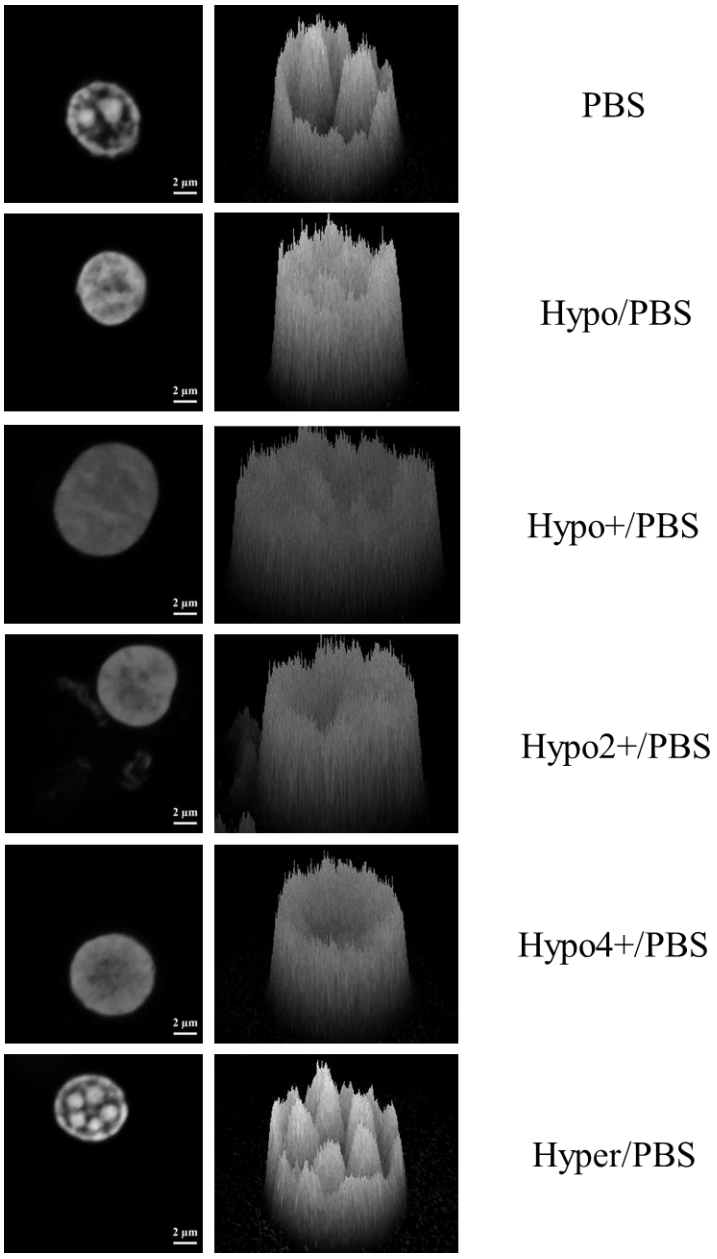

Figure 3.25 – Confocal imaging and respective 3D intensity plots of DAPI stained UCB-MNCs, previously presented to different osmotic solutions. The cells were fixed and imaged straight after exposure to different osmotic modulation conditions, shown in the figure. Also, their respective 3D intensity plots are presented. Scale bar = 2µm.

To gain knowledge regarding the temporal and sequential changes, cells were exposed transiently to different osmotic modulation cocktails and either fixed immediately after the osmotic stimuli, or placed in complete growth medium for 2 or 4 hours and fixed afterwards. In order to have a higher turnaround, but not to compromise on resolution (the magnification used was 20x), a high content imaging platform, IN

Cell Analyzer 2200 was used to image the cells. Within this platform due to technical restrictions, adherent cells were used to avoid autofocus problems. For practical reasons, an adenocarcinoma cell line (HeLa cells) was used.

On one hand, HeLa cells transiently placed in safe osmotic conditions (Figure 3.23) are represented in Figure 3.26 and Figure 3.28. On the other hand, HeLa cells transiently placed in toxic osmotic condition (Figure 3.23) are represented in Figure 3.27 and Figure 3.29.

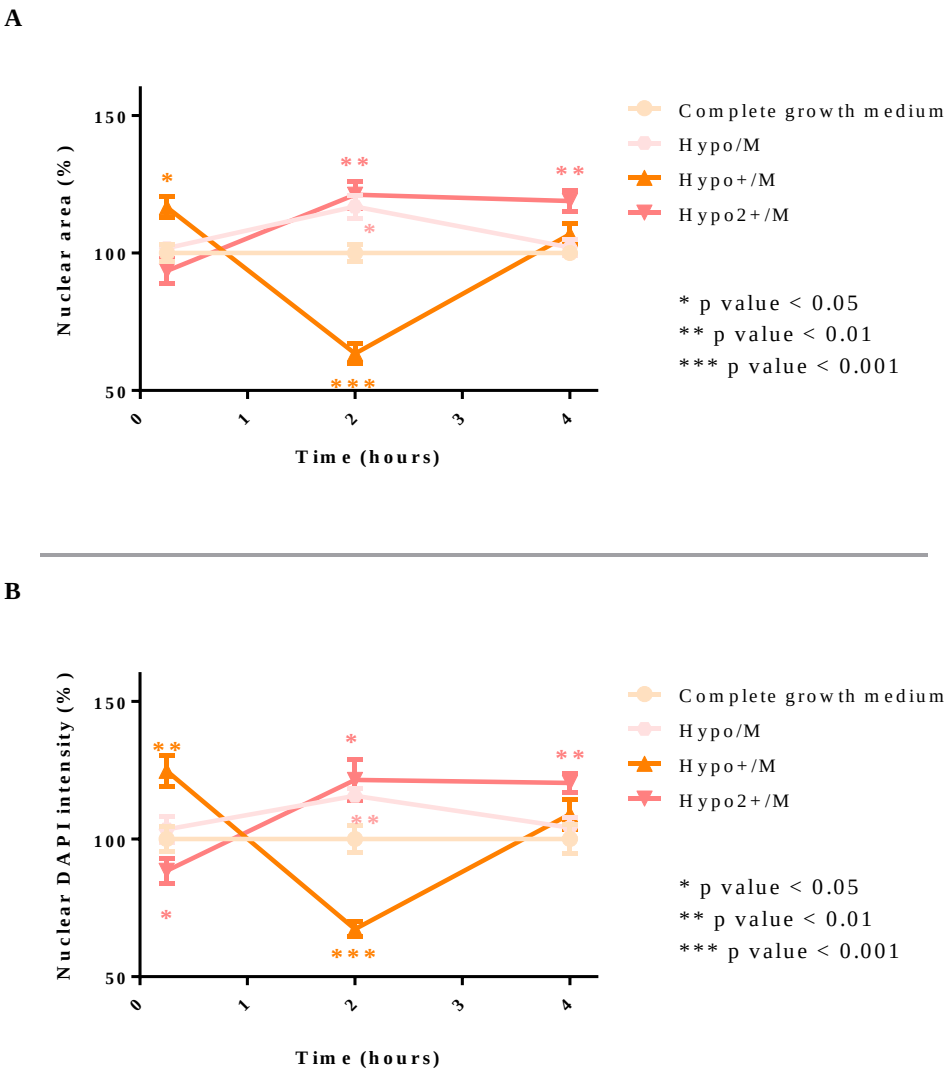

Figure 3.26 – Effect of transient hyposmotic "safe" modulation on cell nuclear parameters in HeLa cells. A) Nuclear area normalised to control (100%) over time; B) Nuclear DAPI intensity normalised to the control (100%) over time. Statistically significant differences in comparison with the control (complete growth medium) are

highlighted in the graph (p value < 0.05; p value < 0.01; p value < 0.001). The osmotic modulatory conditions used, are shown in each legend.

Similarly to what was observed previously in terms of K562 cell size (Figure 3.1 and Figure 3.2), there is also an oscillation in terms of nuclear area and nuclear DAPI labelling intensity in HeLa cells transiently exposed to different osmotic cocktails (Figure 3.26, Figure 3.27, Figure 3.28 and Figure 3.29).

The changes in HeLa nuclear area and nuclear DAPI labelling intensity are more significant (p value < 0.05; p value < 0.0; p value < 0.001; p value < 0.0001) under osmotic modulation in PBS-based conditions (Figure 3.28 and Figure 3.29) than in media based conditions (Figure 3.26 and Figure 3.27).

A

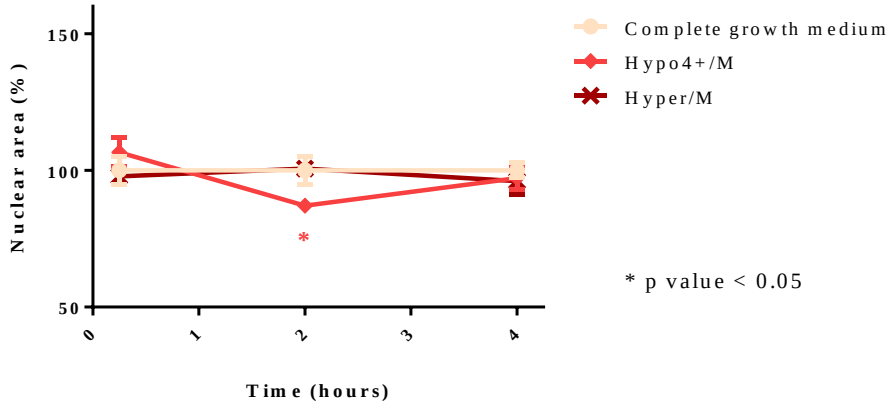

B

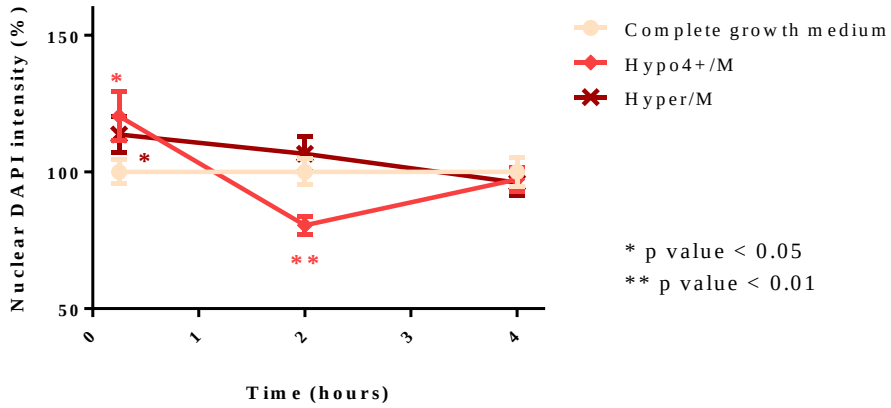

Figure 3.27 – Effect of transient osmotic "toxic" modulation on cell nuclear parameters in HeLa cells. A) Nuclear area normalised to control (100%) over time; B) Nuclear DAPI intensity normalised to control (100%) over time. Statistically significant differences in comparison with the control (complete growth medium) are highlighted in the graph (p value < 0.05; p value < 0.01). The osmotic modulatory conditions used are shown in each legend.

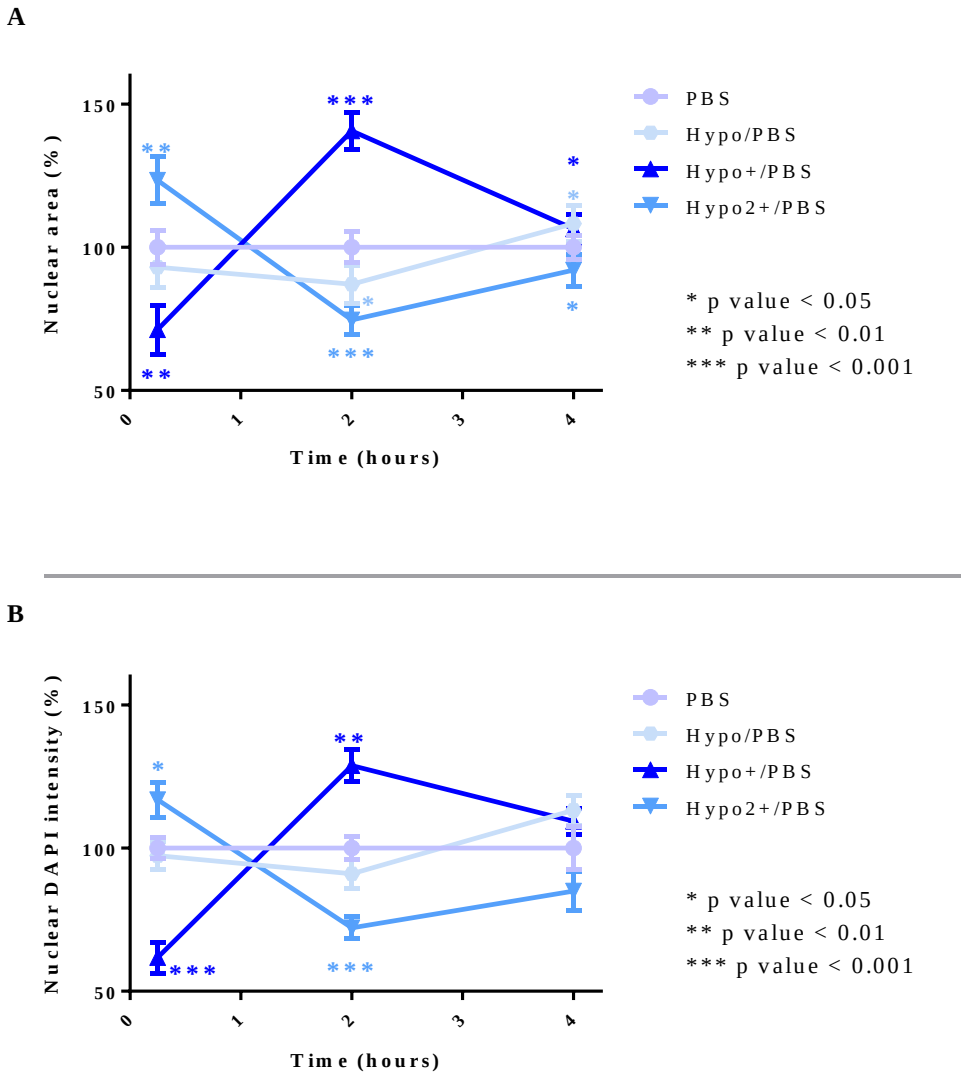

Figure 3.28 – Effect of transient hyposmotic "safe" modulation on cell nuclear parameters in HeLa cells. A) Nuclear area normalised to control (100%) over time; B) Nuclear DAPI intensity normalised to control (100%) over time. Statistically significant differences in comparison with the control (PBS) are highlighted in the graph (p value < 0.05; p value < 0.01; p value < 0.001). The osmotic modulatory conditions used are shown in each legend.

The oscillation in nuclear area and nuclear DAPI labelling intensity over time seems to follow the same pattern within the hyposmotic safe stimuli conditions (Figure 3.26 and Figure 3.28). On the other hand, when HeLa cells are transiently placed in toxic stimuli osmotic conditions (Figure 3.27 and Figure 3.29) this trend is just observed in conditions hypo4+/M and hypo4+/PBS. At 0.25 hours, although the

nuclear area is unchanged (hyper/M in Figure 3.27) or significantly decreased (hyper/PBS in Figure 3.29; p value < 0.01) under hypertonic conditions, the nuclear DAPI intensity is significantly increased (hyper/M – p value < 0.05, Figure 3.27; hyper/PBS – p value < 0.001, Figure 3.29). This increase in nuclear DAPI intensity is inversely proportional to the change in the nuclear area, which might reflect the compaction of chromatin.

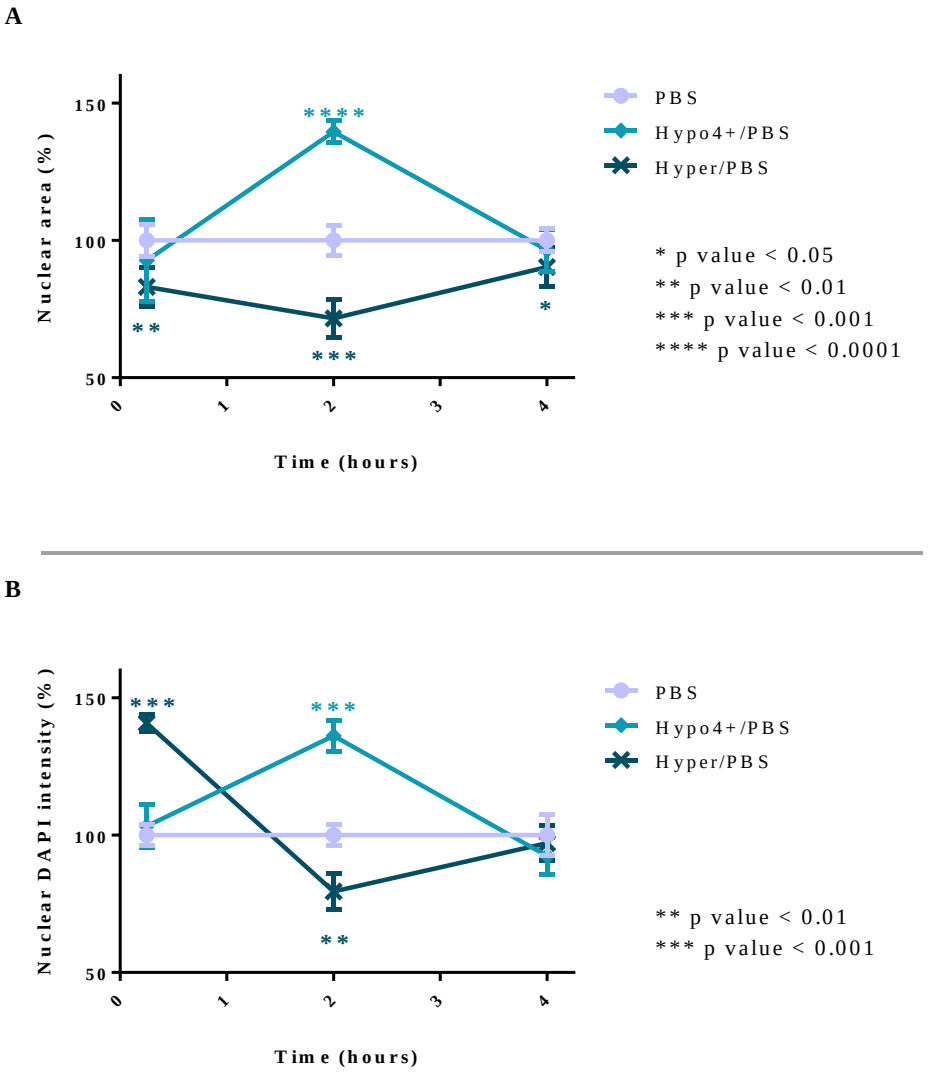

Figure 3.29 – Effect of transient osmotic "toxic" modulation on cell nuclear parameters in HeLa cells. A) Nuclear area normalised to control (100%) over time; B) Nuclear DAPI intensity normalised to control (100%) over time. Statistically significant differences in comparison with the control (PBS) are highlighted in the graph (p value < 0.05; p value < 0.01; p value < 0.001; p value < 0.0001). The osmotic modulatory conditions used are shown in each legend.

The ideal experimental setup would be a live imaging confocal platform able to record real-time changes in chromatin conformation, taking advantage of the image resolution capacity and temporal information. But at the time of this study was not possible to do this type of experiment.

It is also important to keep in mind that, K562 cells and HeLa cells, are very distinct, namely with regards to the cytoskeleton organisation and growth culture conditions. K562 cells grow in suspension, HeLa cells grow attached to culture plastic materials. Therefore, adaptation to altered extracellular environment osmolarity will have distinct responses. Both cell types will have different restraints to altered osmolarity and different osmoregulation mechanisms, as already shown for HeLa cells and other cell types (Hoffmann et al., 2009). Thus, comparisons between the two cell types must be done carefully.

The options to characterise the chromatin global physical state without using microscopy based techniques are limited. Nevertheless, there are some enzymatic methods which in an indirect manner allow the assessment of global chromatin changes (Cockerill, 2011; Ling and Waxman, 2013; Song and Crawford, 2013; Song et al., 2011; Tewari et al., 2012; Tsompana and Buck, 2014; Zaret, 2005).

In this study, the use of deoxyribonuclease I (DNase I) and micrococcal nuclease (MNase) to assess the global state of accessibility of chromatin was explored. DNase I liberates accessible chromatin by preferentially cutting within nucleosome-free genomic regions characterised as DNase I hypersensitive sites (DHSs) known to be enriched for promoters and enhancers (Rando, 2007; Tsompana and Buck, 2014). On the other hand, MNase preferentially digests linker deoxyribonucleic acids (DNA) and can indicate the frequency by which a DNA sequence is nucleosomal (Rando, 2007; Zaret, 2005), in an indirect manner, it can characterise chromatin accessibility; by the pattern of digestion which reflects the presence or absence of nucleosomes and other regulatory factors. The enzymatic digestion is usually followed by sequencing techniques to determine the specific genomic areas affected (Tsompana and Buck, 2014). Nonetheless, the specific DNA digestion pattern already gives an idea of the changes which are occurring and is usually performed as a preliminary assessment and to justify future sequencing assays.

In this thesis, for both enzymes used (DNAse I and MNase), the digestions were performed with isolated nuclei after transient hyposmotic modulation. The digestion products were purified for DNA content and posteriorly separated by electrophoresis (500ng of DNA), imaged and quantified by ImageJ. The analysis with ImageJ was done to extract a quantitative view of the data. This analysis was done by drawing a line through each gel lane and the grey value was evaluated in function of the distance from the beginning of each lane. These results are presented in a 2% agarose gel electrophoresis image in Figure 3.30 and Figure 3.33 for DNase I and MNAse, respectively. Additionally, the corresponding histograms,

obtained with the ImageJ quantification, are presented in Figure 3.31, Figure 3.32 and Figure 3.34, Figure 3.35 for DNase I and MNase, respectively.

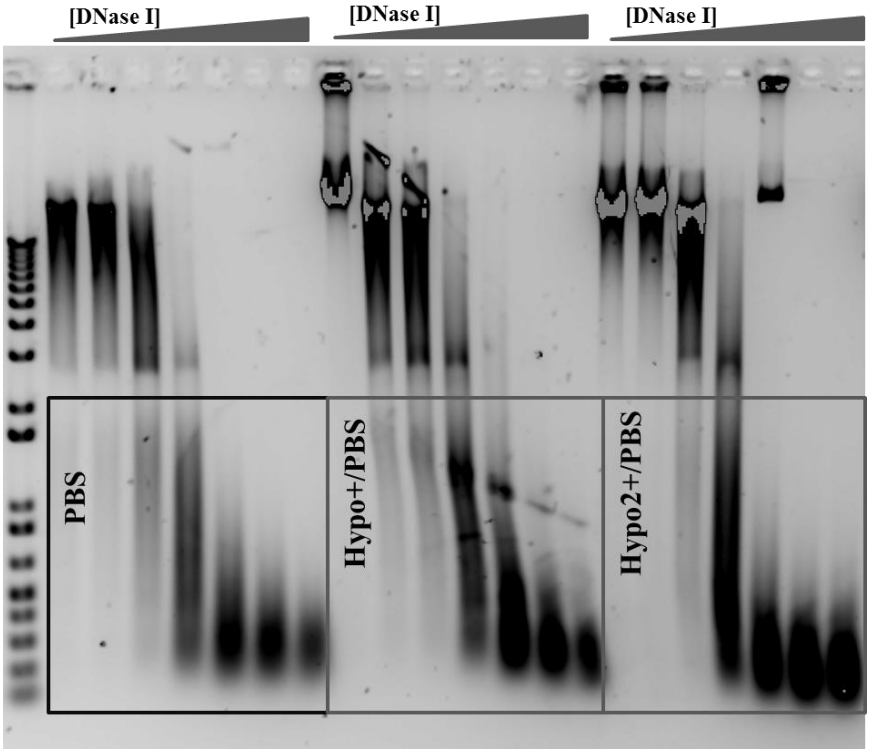

Figure 3.30 – DNA fragmentation pattern after digestion with DNase I using K562 cells. The digestion was performed with isolated nuclei from K562 cells which were transiently in different hyposmotic conditions and increasing DNase I concentrations (80; 120; 240; 480; 960; 1960; 2400 U/mL). The DNA loading in each lane was 500ng. The osmotic modulatory conditions used are shown in the figure.

The DNA fragmentation pattern of the samples subjected to transient osmotic modulation and digested with DNase I is shown in Figure 3.30. In a general way, there is a trend of smaller fragments with increasing amount of DNase I for cells in the conditions hypo+/PBS and hypo2+/PBS (Figure 3.30). This decrease in fragment size indicates more enzymatic activity which is indicative of more accessible DNA.

The quantification analysis, with ImageJ, of the digestions patterns with specific concentrations of DNase I are plotted in Figure 3.31 and Figure 3.32.

In Figure 3.31 nuclei exposed to hyposmotic solutions digested with lower amounts of DNase I (A – 120U/mL; B – 480U/mL) seems to favour to the same extent, the presence of DNA fragments distant from the beginning of the gel lane (smaller DNA fragments).

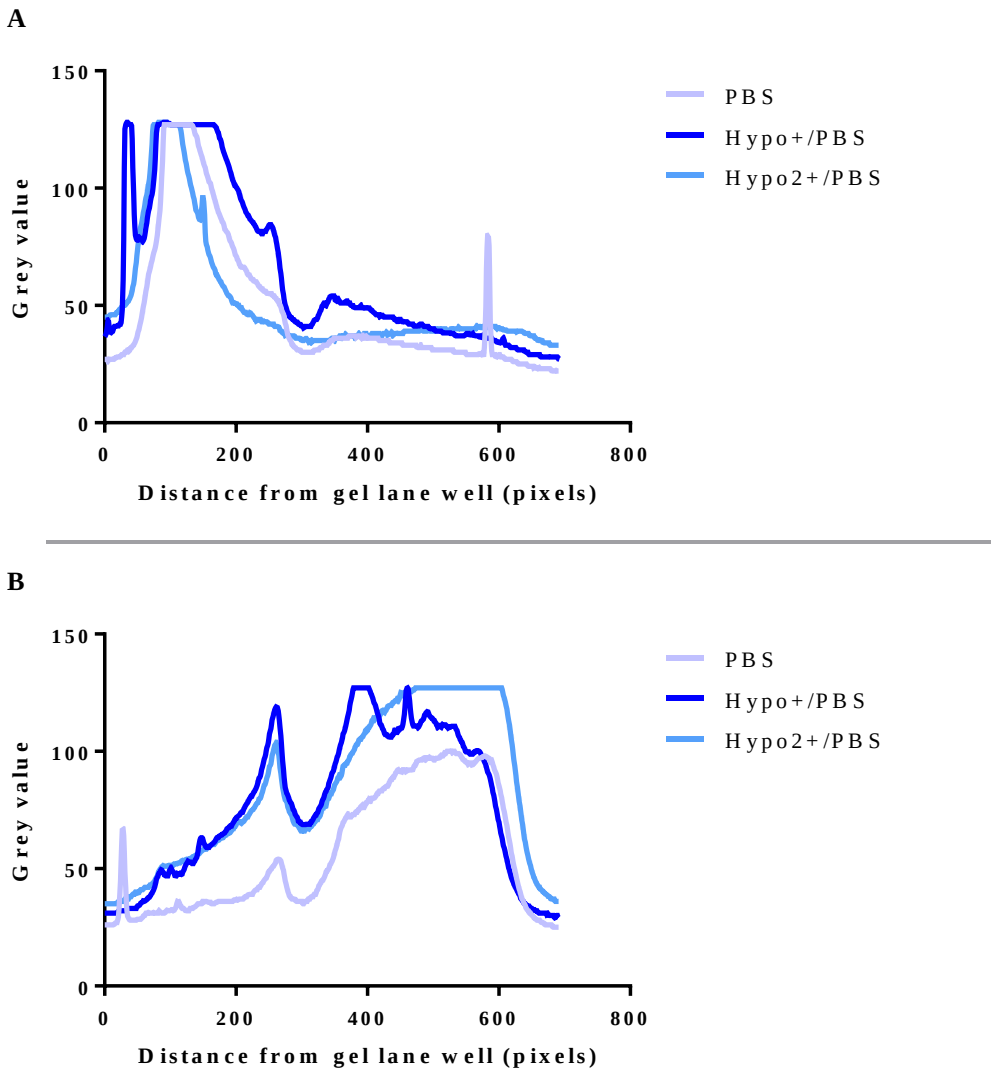

Figure 3.31 – Representative histogram of the DNA fragmentation pattern of DNase I digestion. The digestion pattern was analysed in Image J. A) Representation of the DNA fragmentation pattern digested with 120 U/mL of DNase I; B) Representation of the DNA fragmentation pattern digested with 480 U/mL of DNase I. The osmotic modulatory conditions used are shown in each legend.

In Figure 3.32 digested material exposed to hyposmotic solutions with higher amounts of DNase I (A – 960U/mL; B – 2400U/mL) appears, especially in the condition using 2400U/mL of DNase I, to be enriched with smaller DNA fragments. This quantitative analysis strengthens the trend observed in Figure 3.30. For further information regarding chromatin state, would be very interesting to do this type of study within specific genomic *loci*, for osmoregulation processes, as performed by others in different contexts (Kimura et al., 1983).

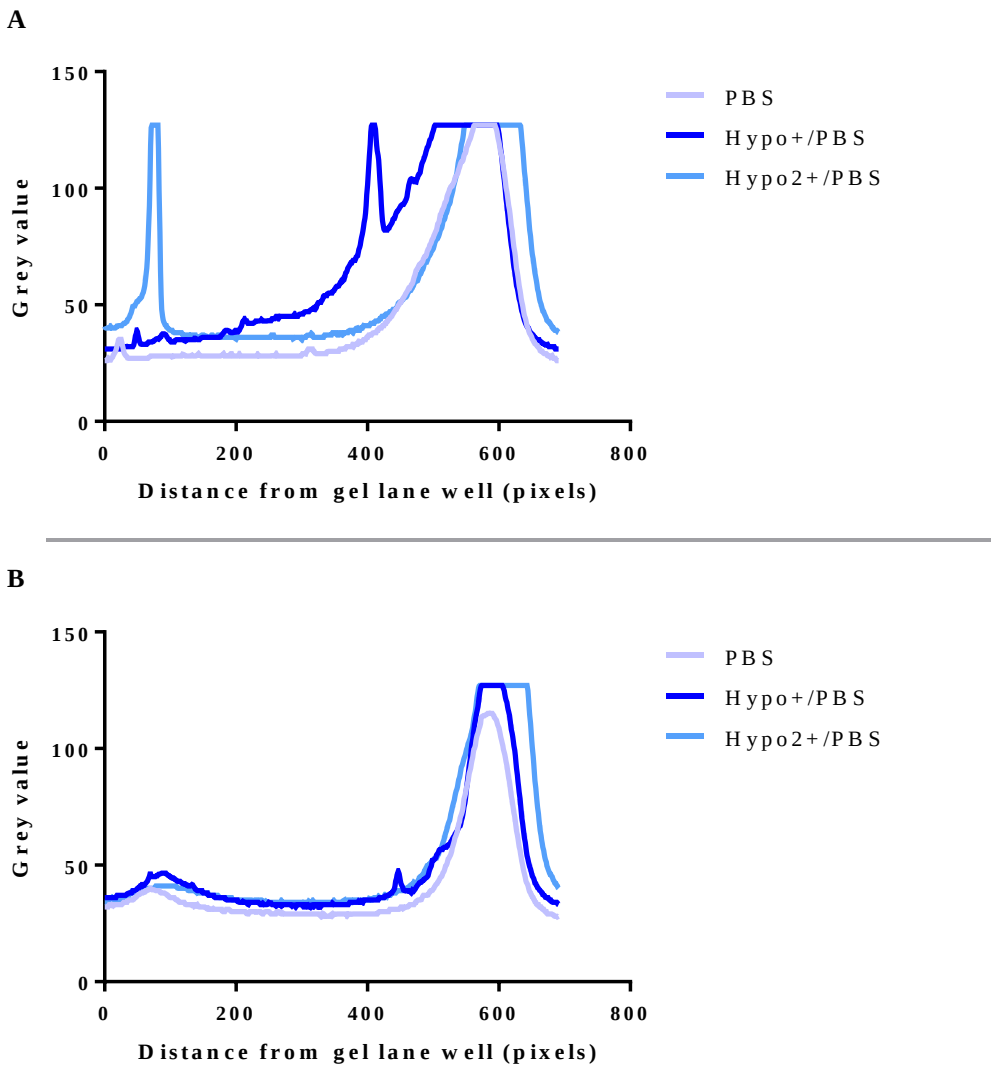

Figure 3.32 – Representative histogram of the DNA fragmentation pattern of DNase I digestion. The digestion pattern was analysed in Image J. A) Representation of the DNA fragmentation pattern digested with 960 U/mL of DNase I; B) Representation of the DNA fragmentation pattern digested with 2400 U/mL of DNase I. The osmotic modulatory conditions used are shown in each legend.

DNA distribution size of MNAse digested samples is presented in Figure 3.33 for the different hyposmotic settings. The general trend is an increase of lower order nucleosome structures (mononucleosomes) with increasing amount of MNase used in the conditions hypo+/PBS and hypo2+/PBS (Figure 3.33). This increase in lower order nucleosome structures should denote an increase in unprotected and accessible DNA.

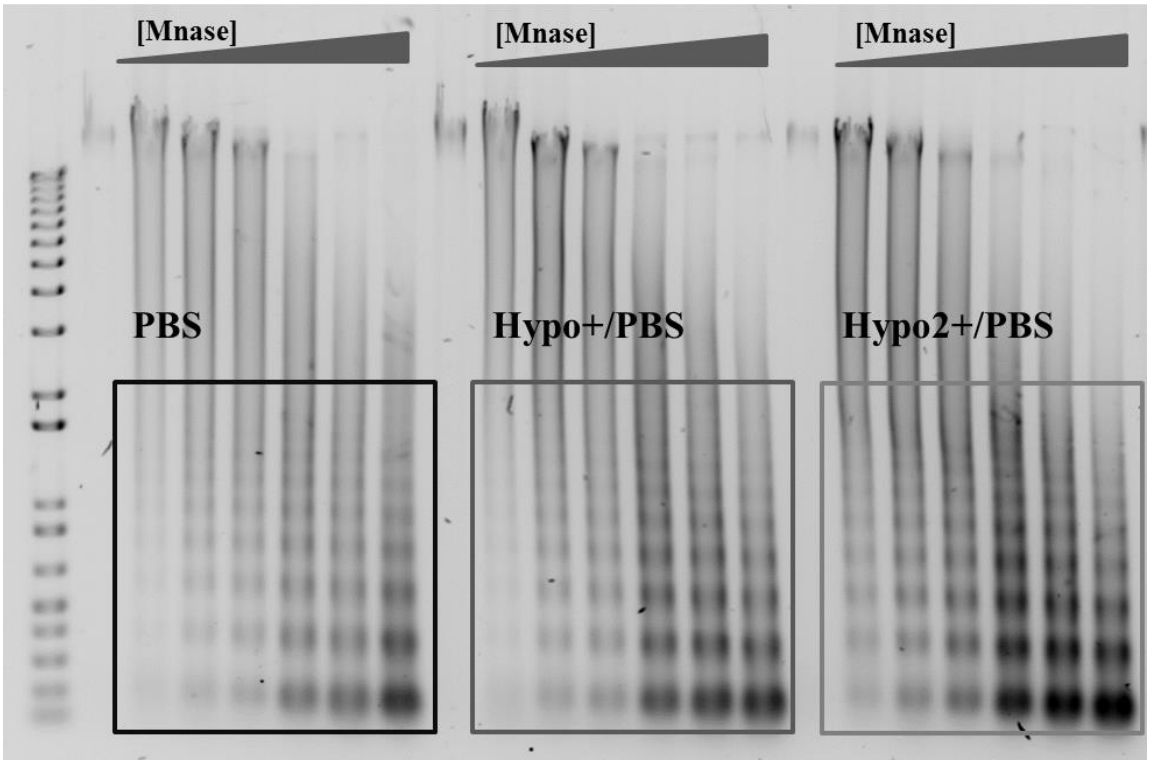

Figure 3.33 – DNA fragmentation pattern after MNase digestion using K562 cells. The digestion was performed with nuclei isolated from K562 cells that were transiently in different osmotic conditions and with increasing MNase concentrations (0; 12.5; 25; 50; 150; 250; 500 gel units). DNA loading in each lane was 500ng. The osmotic modulatory conditions used are shown in the figure.

For practical reasons, just digestions with some concentrations of MNAse were plotted for a more quantitative analysis with ImageJ in Figure 3.34 and Figure 3.35.

In Figure 3.34, with lower amounts of MNase (A – 25 gel units; B – 50 gel units), especially in the hypo2+/PBS condition, a broad fragment size distribution with a clear increase in lower order nucleosome structures (smaller DNA fragments bands) can be observed.

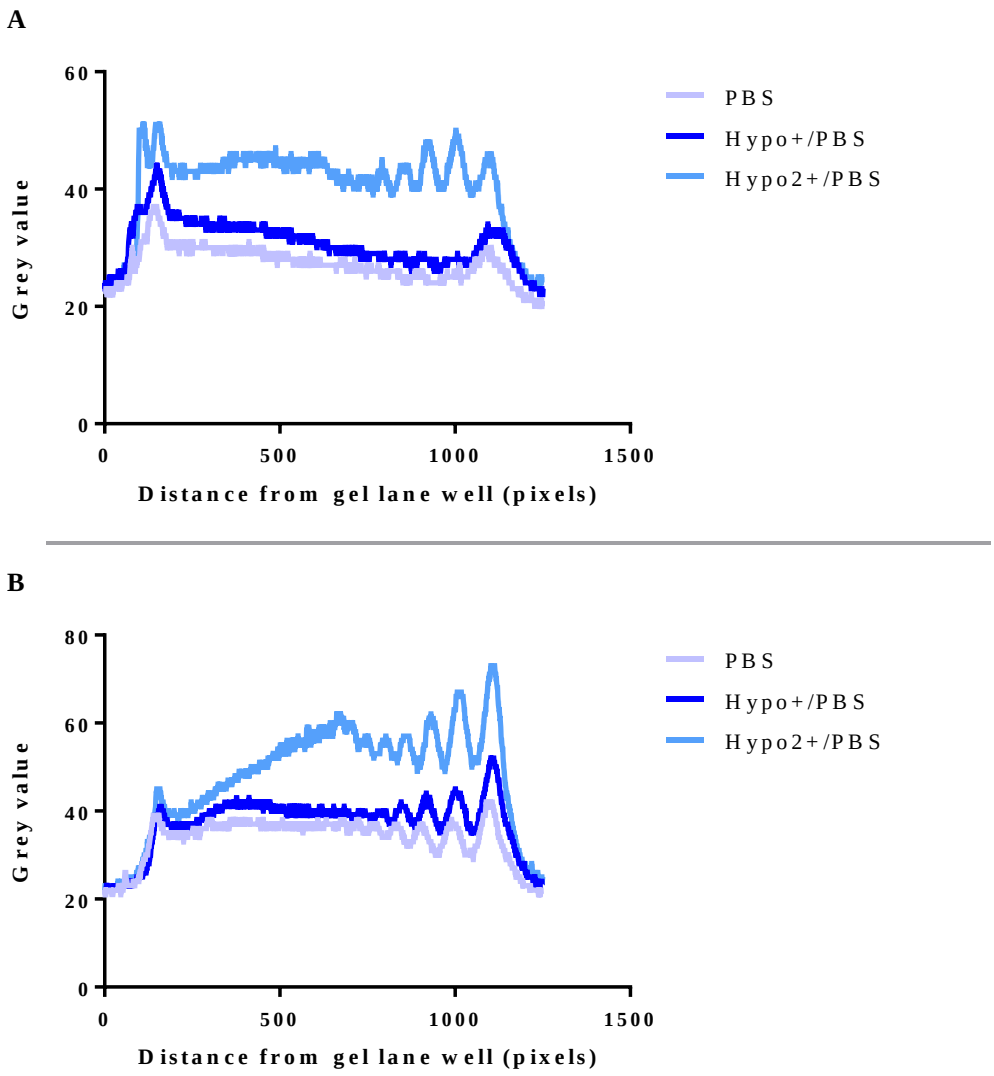

Figure 3.34 – Representative histogram of the DNA fragmentation pattern of MNase digestion. The digestion pattern was analysed in Image J. A) Representation of the DNA fragmentation pattern digested with 25 gel units of MNase; B) Representation of the DNA fragmentation pattern digested with 50 gel units of MNase. The osmotic modulatory conditions used are shown in each legend.

In Figure 3.35, cells exposed to hyposmotic solutions and digested with higher amounts of MNase (A – 150 gel units; B – 500 gel units) lead to distinct digestion patterns (Figure 3.35). Within the digestion with 150 gel units of MNase, there is a clear gradual increase in the amount of smaller DNA fragment bands from the control condition (PBS) to the hypo+/PBS condition and to the hypo2+/PBS condition (Figure 3.35). In the digestion with 500 gel units of MNase, the effect described for digestion with 150 gel units of MNase is lost and seems that a saturation point was reached (Figure 3.35).

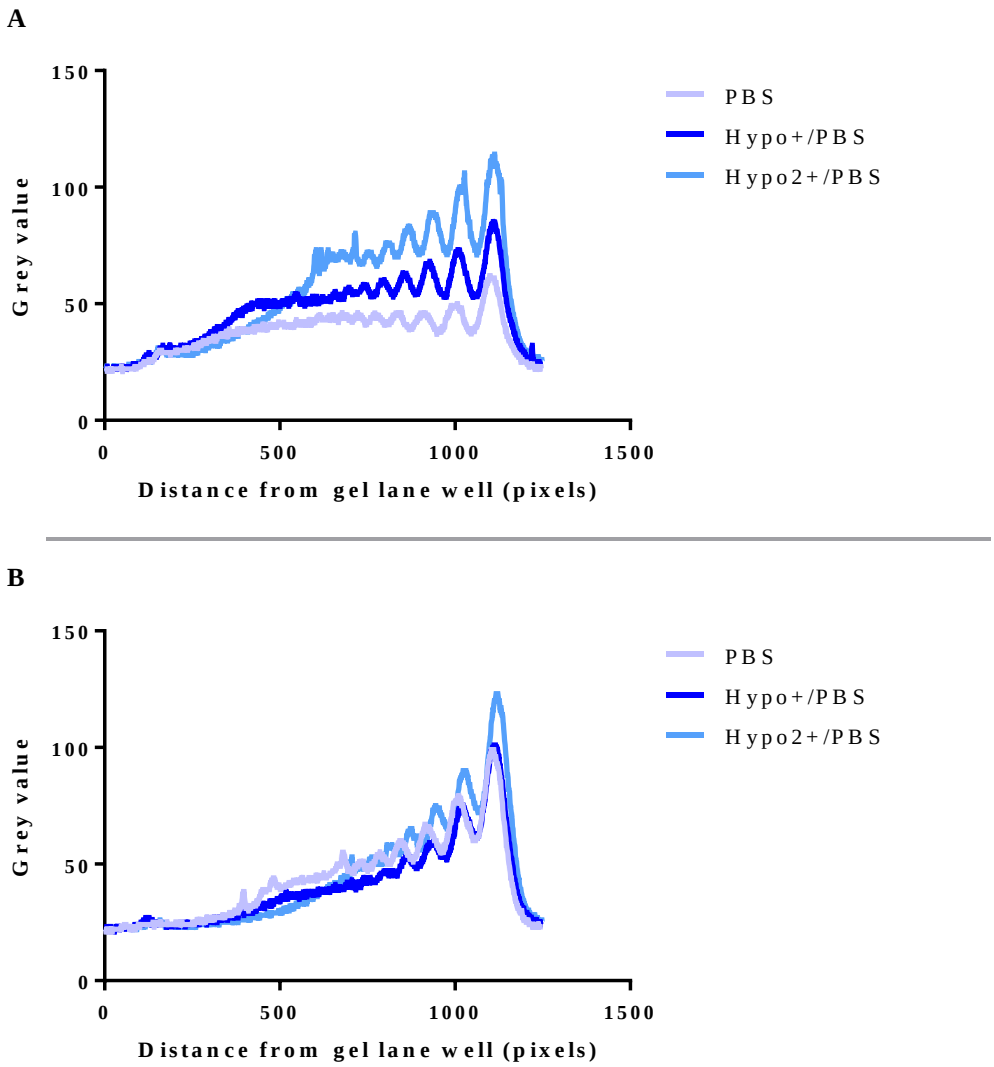

Figure 3.35 – Representative histogram of the DNA fragmentation pattern of MNase digestion. The digestion pattern was analysed in Image J. A) Representation of the DNA fragmentation pattern digested with 150 gel units of MNase; B) Representation of the DNA fragmentation pattern digested with 500 gel units of MNase. The osmotic modulatory conditions used are shown in each legend.

In addition, it would be very relevant to do this type of study where the osmotic related chromatin features could be mimicked in an artificial and permanent way (for example by overexpressing a gene, related with osmoregulation mechanisms, or presence of a drug) and perform the same type of digestion with MNase, as done by others in other contexts (Knoepfler et al., 2006; Liu et al., 2015b).

In addition to the global chromatin changes it is also interesting, but challenging, to find specific histone modifications that could be altered after a change in the extracellular environment osmolarity.

One of the histone modification marks known to be associated with loosening of chromatin and other features such as transcriptional activity is the histone 4 lysine 16 acetylation (H4K16ac) (Calo and Wysocka, 2013; Canals-Hamann et al., 2013; Shogren-Knaak, 2006).

The exposure to hyposmotic extracellular environments in our work was consistent with a chromatin loosening. On the other hand, the exposure to hypertonic extracellular environments was consistent with chromatin compaction.

H4K16ac prevalence, in UCB-MNCs, after transient exposure to hyposmotic extracellular environments shows an increase, in some hyposmolar conditions, and a decrease of H4K16ac labelling with a transient exposure to the hypertonic extracellular environment (Figure 3.36). This labelling show some instability within the different intensity levels of the hyposmolar conditions that might be coordinated with the fluctuations in cell size during RVD. Therefore at the same time point, different hyposmolar conditions show distinct levels of H4K16ac (Figure 3.36). Moreover, the expression of H4K16ac is highly variable (Figure 3.36) within the control cells (UCB-MNCs in PBS) and expression changes in a specific cell compartment within the UCB-MNCs might be difficult to evaluate at the population level.

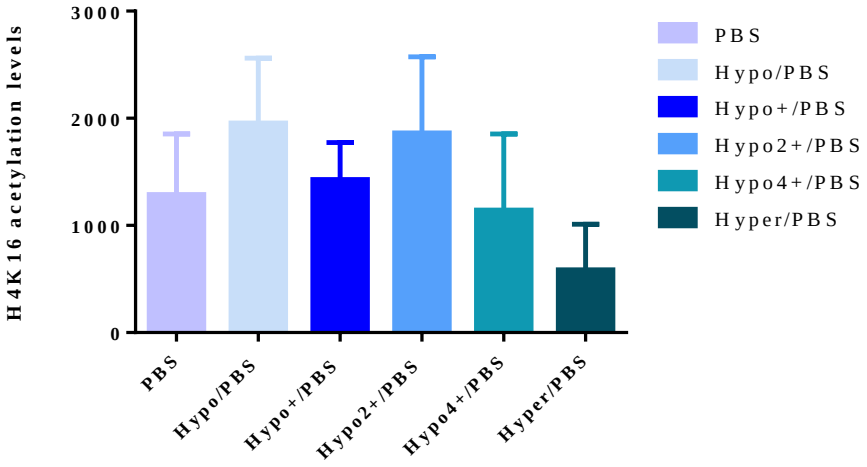

Figure 3.36 - Immunolabeling quantification of the fluorescence signal of H4K16 acetylation in UCB-MNCs presented to different osmolarity conditions. Straight after exposing UCB-MNCs to different osmotic modulations cocktails (n=2) the cells were fixed and the immunolabeling was performed and the mean intensity fluorescence (±SEM) evaluated with the high content imaging platform IN Cell Analyzer 2200. The osmotic modulatory conditions used are shown in each legend.

The high variability in the control cells can denote that this specific labelling in UCB-MNCs is variable and might not be easy to see significant changes. When the same type of experiment was

performed in HeLa cells, the differences in H4K16ac pattern are significantly decreased (p value < 0.01) after the transient stimulus and this pattern significantly increases (p value < 0.01) during the hours that follow the transient hyposmotic stimuli (Figure 3.37).

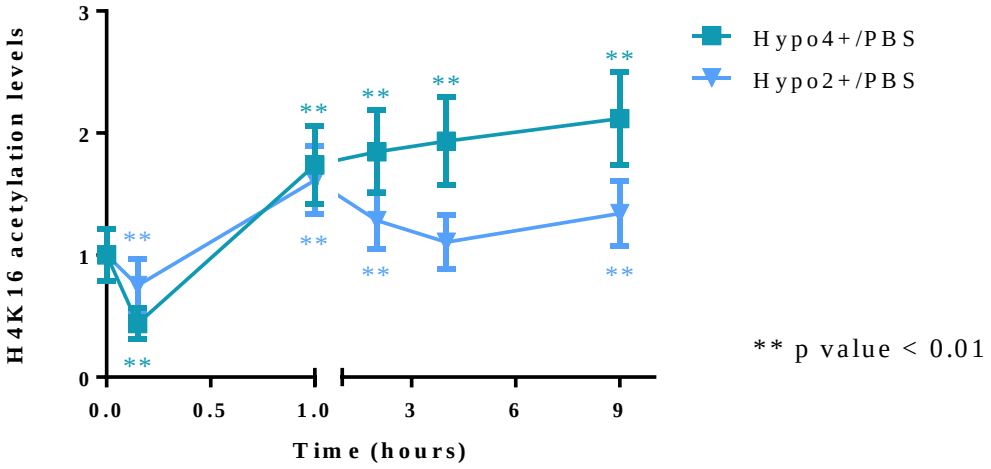

Figure 3.37 – Immunolabeling quantification of the fluorescence signal of H4K16 acetylation HeLa cells after a transient hyposmotic modulation. Straight after exposing HeLa cells to different osmotic modulations cocktails (n=3) the cells were fixed and the immunolabeling was performed. The mean intensity fluorescence (±SEM) normalised to the time point 0h was evaluated with the fluorescence microscope Axioivert 200M (Carl Zeiss). The osmotic modulatory conditions used are shown in each legend. Statistically, significant differences in comparison with the timepoint 0h are highlighted in the graph (p value < 0.01).

These alterations in the H4K16ac presence is nicely connected with chromatin structure studies previously presented. Moreover, these observations, opened within this study, the perspective of a possible impact of osmotic modulation on the transcriptional activity of the cell.

The next subchapter will be dedicated to the specific impact that osmotic modulation may have on transcriptional activity.

3.1.5. Transcriptional changes induced by osmotic modulation

There are a few reports in the literature connecting extracellular environment osmolarity changes to transcriptional changes (Huang et al., 2011; Liu et al., 2009; Zhao et al., 2016). From those reports, almost none is related to extracellular environment hyposmolarity or to transient osmotic modulation. A very recent report shows a key role of long non-coding ribonucleic acids (lnc-RNAs) in permanent hypotonic stress and its role in transcriptional repression of ribosomal RNA genes (Zhao et al., 2016).

To assess transcriptional activity, two different strategies were used: a traditional assay with incorporation and detection of 5-ethynyl uridine (EU) in newly synthesized RNA; and a "run on" approach where the internal pool of nucleotides is washed out from permeabilized cells and after that, a cocktail of nucleoside triphosphates (adenosine, cytidine, guanosine triphosphates - ATP, CTP, GTP and 5-ethynyl uridine triphosphate - EUTP), magnesium and other components (within the Physiological Buffer with Ficoll - PBF) are provided to the cells. As the newly RNA is synthesised, EUTP is incorporated and detected afterwards in newly synthesised RNA. Both techniques are adaptations of published protocols (Iborra et al., 1996, 2001, 2004; Jackson et al., 1998; Pombo et al., 1999) where the main difference is the use of click chemistry for detection of EU/EUTP in newly synthesised RNA instead of radiolabelling or immunolabeling techniques for detection of labelled RNA molecules.

The first approach, "the traditional one", showed a slower incorporation of EU in K562 cells permanently exposed to hypo2+/PBS when compared to the control condition (PBS) (Panel A of Figure 3.38 and Figure 3.39). By doing a linear regression to the different incorporation levels of EU over time is possible to achieve the slope of the correspondent equation and have values for the transcriptional rate (Johnston et al., 2012; das Neves et al., 2010). In this assay, the transcriptional rate for K562 cells permanently in hypo2+/PBS is approximately half of the transcriptional rate of K562 cells permanently in PBS (Panel A of Figure 3.38 and Figure 3.39). Additionally, the incorporation profile of EU suggests that after 1 hour the system starts to slow down (Panel A of Figure 3.40).

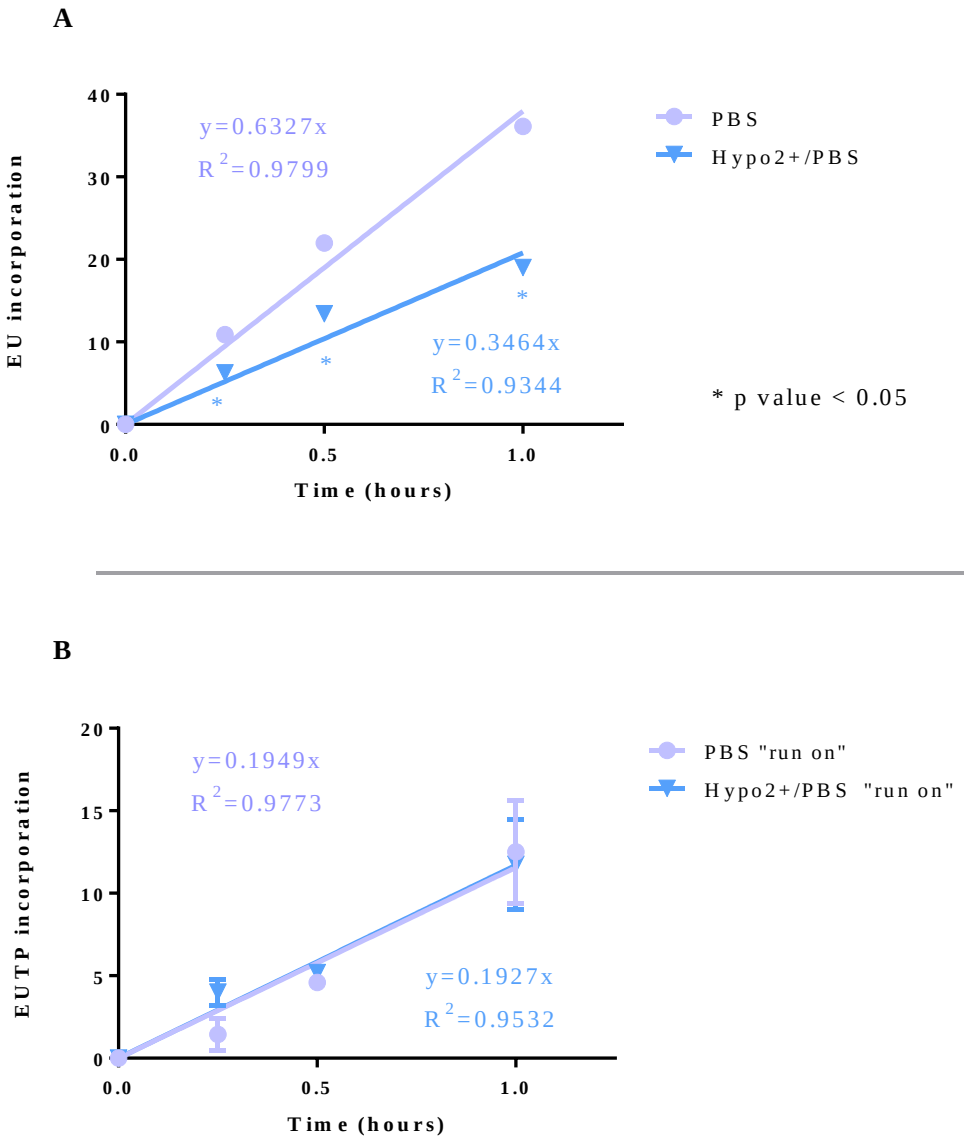

Figure 3.38 – Hyposmotic modulation effect on transcriptional activity over time in K562 cells. A) Effect of constant hyposmotic modulation on transcriptional activity assessed by EU incorporation (mean fluorescence intensity ±SEM; n=3); B) Effect of transient hyposmotic modulation ("run on") on transcriptional activity assessed by EUTP incorporation (mean fluorescence intensity ±SEM; n=3). A linear regression was done to each condition and respective equation and coefficient of determination are shown in each graph. The osmotic modulatory conditions used are shown in each legend.

This type of traditional transcriptional rate assay does not take into consideration the possible dilution of intracellular components. Within osmotic modulation, this might be a key aspect. Firstly, because with the entry or exit of water, the cellular components will be altered by osmotic response mechanism activation, but additionally in the first instants the cellular components will be diluted or concentrated,

respectively. The differences in cellular components concentrations may be critical to several cellular functions, such as ATP-dependent processes, as transcription is an example of (das Neves et al., 2010).

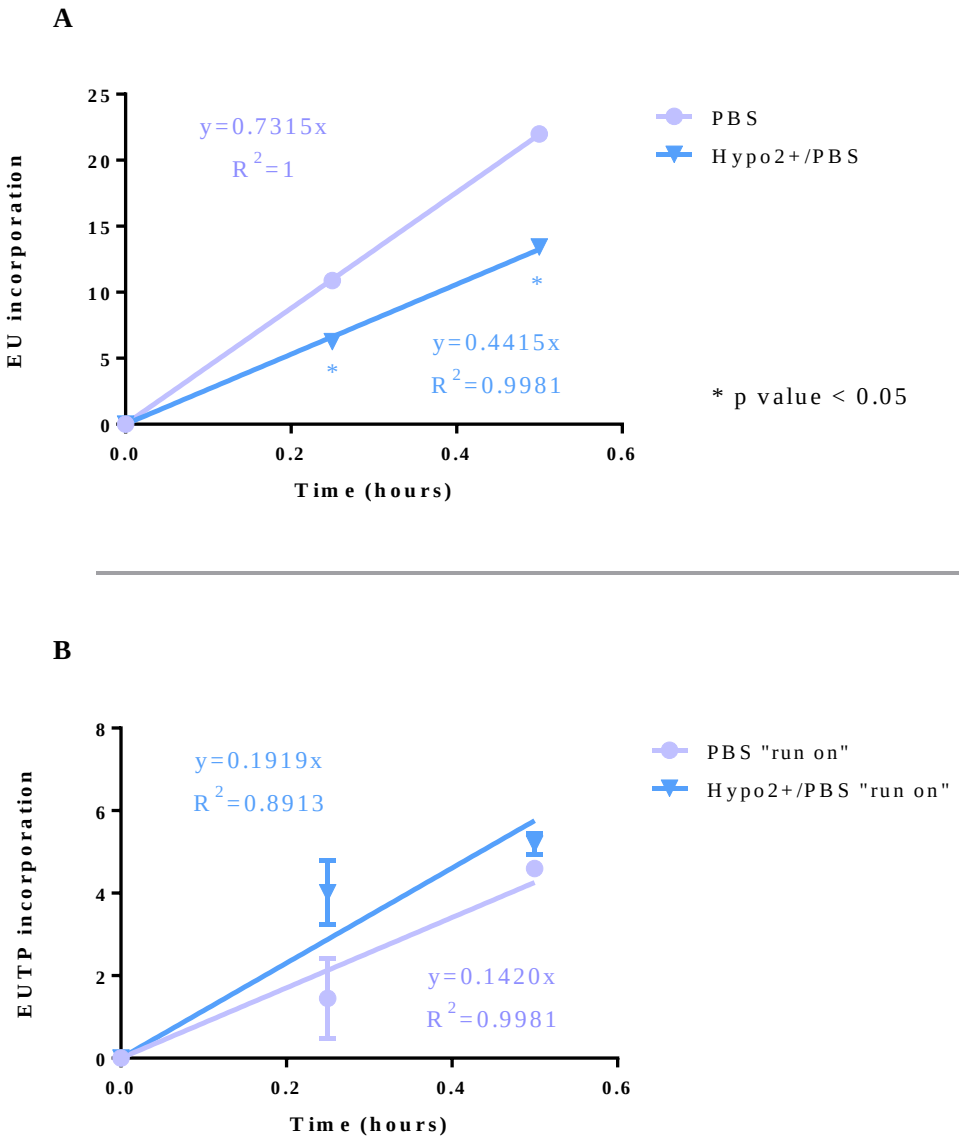

Figure 3.39 – Hyposmotic modulation effect on transcriptional activity over time in K562 cells. A) Effect of constant hyposmotic modulation on transcriptional activity assessed by EU incorporation (mean fluorescence intensity ±SEM; n=3); B) Effect of transient hyposmotic modulation ("run on") on transcriptional activity assessed by EUTP incorporation (mean fluorescence intensity ±SEM; n=3). A linear regression was done to each condition and respective equation and coefficient of determination are shown in each graph. The osmotic modulatory conditions used are shown in each legend.

The dilution of intracellular components and even extrusion of signalling molecules, as previously described for ATP, has to be closely monitored to understand the potential effects on cell behaviour. Cell ATP depletion has been correlated, for instance, with different transcriptional rate (das Neves et al., 2010), altered splicing (Guantes et al., 2015) and anisotropy of H2B histone (Talwar et al., 2013).

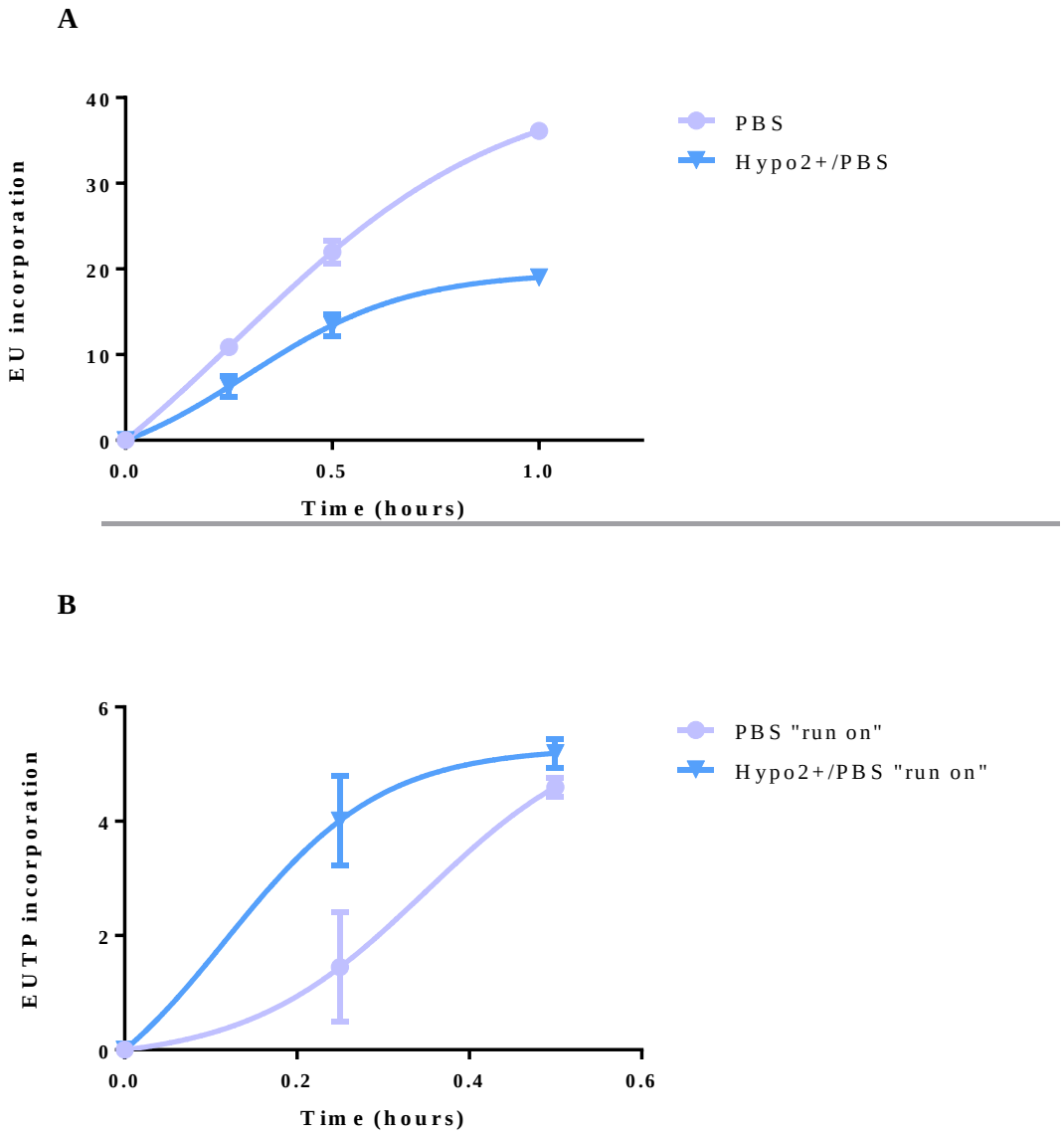

Figure 3.40 – Hyposmotic modulation effect on transcriptional activity over time in K562 cells. A) Effect of constant hyposmotic modulation on transcriptional activity assessed by EU incorporation; B) Effect of transient hyposmotic modulation on transcriptional activity assessed by EUTP incorporation ("run on"). A non-linear regression was done to each condition (n=3). The osmotic modulatory conditions used are shown in each legend.

To try to assess this possible dilution of intracellular components, transcription "run-on" was done with the second approach, where K562 cells were transiently placed in osmotic modulatory conditions or in PBS and then transferred to PBF (isosmolar) to perform the transcriptional assay. With this assay, it was possible to observe a quicker incorporation of EUTP during the first hour or 30 minutes in K562 cells transiently in hypo2+/PBS when compared to the control condition (PBS) (Panel B of Figure 3.38 and Figure 3.39). When a linear regression line was calculated for the different incorporation levels of EUTP over time, the transcriptional rate for cells in hypo2+/PBS is approximately 1.5 fold increased when compared to the control condition (PBS) during the first 30 minutes after the beginning of the assay (Figure 3.39). This effect seems to be lost with time (considering all the time points of the assay until 1 hour) as is shown in Figure 3.38. Additionally, the differences between EU and EUTP incorporation in the different experimental setups and hyposmotic cocktails is clear when doing a non-linear fit to both assays (Figure 3.40).

When using this second approach to assess transcriptional rate, the "run on" strategy, we did characterise many transient osmotic modulations and evaluated their incorporation levels of EUTP over time. The general trend observed is that K562 cells transiently exposed to hyposmotic solutions tend to have an increased level of incorporation of EUTP over time. K562 cells transiently exposed to the hypertonic solution show the opposite: a decreased level of incorporation of EUTP over time when compared to the control situation (Figure 3.41).

The levels of incorporation of EUTP in K562 cells transiently exposed to hypo+/PBS is four times increased when compared to the control after 0.25 hours. Also after 2 hours this same value is increased by approximately 37%. Although these values are not statistically significant they might reflect a relevant biological impact. To try to address these we will have in this subchapter some data of chromatin immunoprecipitation (Chip) and Chip-Sequencing (Chip-Seq) that will complement the information of this set of transcriptional data.

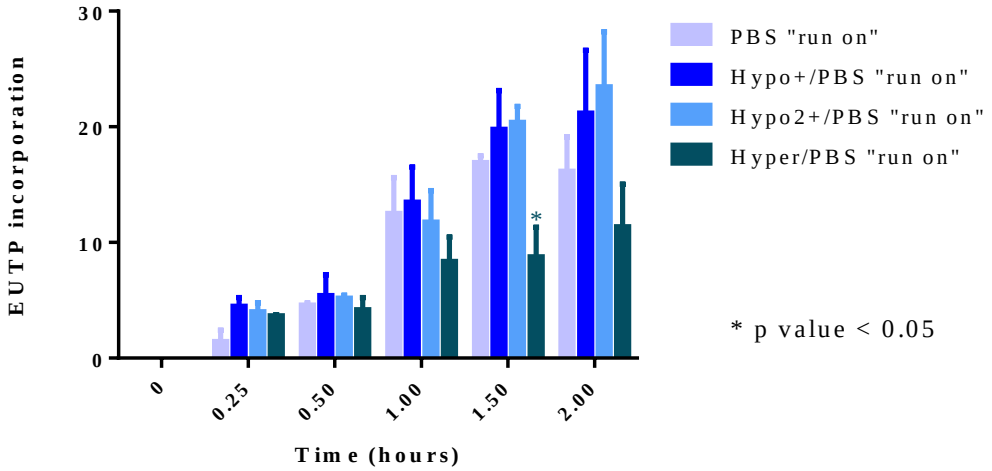

Figure 3.41 – Effect of transient osmotic modulation on transcriptional activity in K562 cells. Effect of transient osmotic modulations ("run on") on transcriptional activity assessed by EUTP incorporation (mean fluorescence intensity ±SEM; n=3). The osmotic modulatory conditions used are shown in the legend.

In addition to general transcription is important to understand if modifications that can alter the transcriptional behaviour of the cell, like the phosphorylation of serine 2 of the C-terminal domain (CTD) of the RNA polymerase II (RNA Pol II PhosphoS2) are changed (Hirose and Ohkuma, 2007; Jasnovidova and Stefl, 2013; Meinhart et al., 2005). This specific phosphorylation is associated with transcription elongation and would be interesting to explore if this modification can be favoured or inhibited by osmolarity (Hirose and Ohkuma, 2007; Jasnovidova and Stefl, 2013; Meinhart et al., 2005).

A western blot (WB) with K562 cells lysed right after a transient exposure to osmotic cocktails (0h) or allowed to recover from the hyposmotic modulations in complete growth medium during 1 hour (1h) (Figure 3.42 and Figure 3.43) was performed against RNA Pol II PhosphoS2. Straight after the osmotic stimulus (Panel A of Figure 3.42) a slight increase in Pol II Ser2P levels occurs in hypo+/PBS and hypo2+/PBS. On the other hand, after 1h (Panel B of Figure 3.42), K562 cells exposed transiently to hypo+/PBS present a slight increase in RNA Pol II PhosphoS2. An exemplification WB image can be observed in Figure 3.43 with the upper bands corresponding to RNA Pol II PhosphoS2 and the loading control used is β-tubulin (upper band from the double band).

The time gap where the assays were performed is critical and might be relevant to obtain data with lower temporal differences between sampling and also using a wider window of time points.

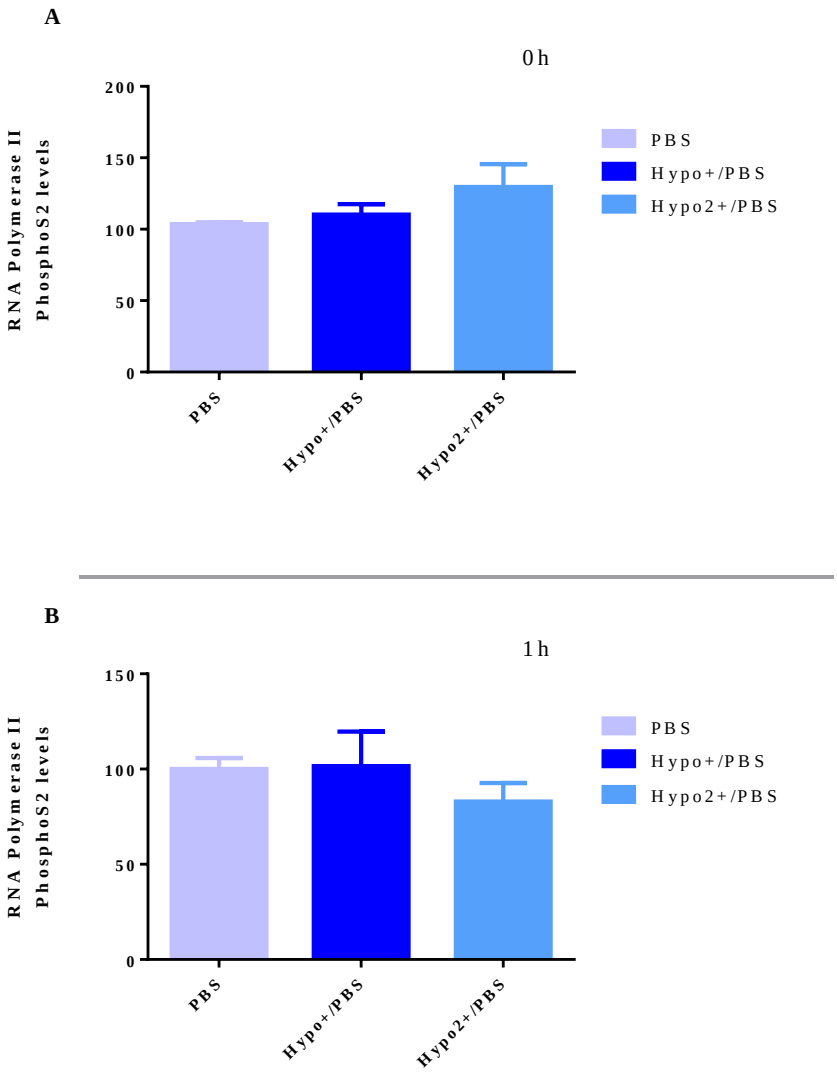

Figure 3.42 – Effect of hyposmotic modulation on transcriptional elongation. A) Evaluation of the transient osmotic modulation effect on transcriptional elongation (0h), by western blot quantification of RNA Pol II PhosphoS2 levels (±SEM; n=3); B) Evaluation of the transient osmotic modulation effect on transcriptional elongation (1h), by western blot quantification of RNA Pol II PhosphoS2 levels (±SEM; n=3).

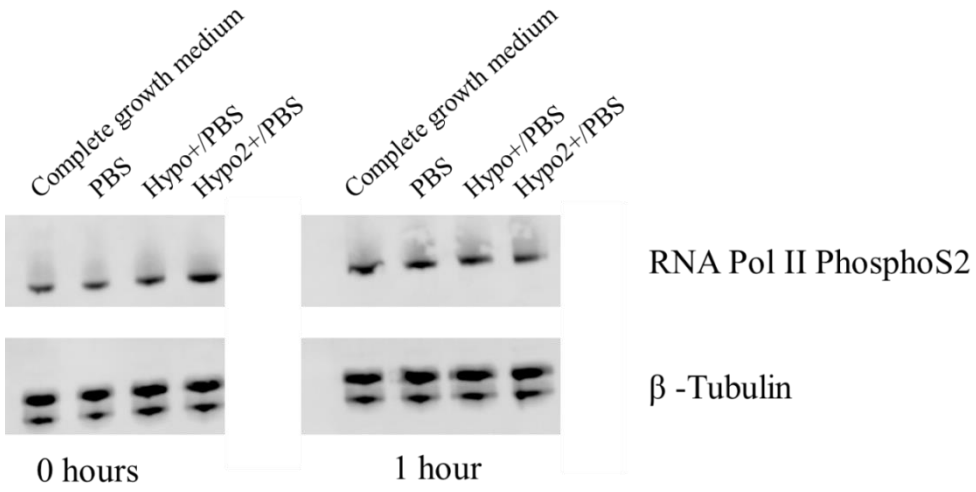

Figure 3.43 –Representative western blot image to detect the RNA Pol II PhosphoS2.

In addition to the results previously presented, a fluorescence loss in photobleaching (FLIP) assay was performed in the CHO RNA Pol II-enhanced green fluorescent protein (EGFP) temperature sensitive cell line. Briefly, at 39ºC this cell line expresses RNA Pol II – EGFP, for further details please see the Materials and methods section. For this experiment the CHO RNA Pol II-EGFP cell line was used after 4 days of culture at 39ºC to ensure the stable expression of the RNA Pol II-EGFP form. Rectangles of approximately half of each nucleus were selected and where 100% laser power was applied (please see Materials and methods section). This operation was repeated every ≈ 5 seconds for a period of 900 seconds and the decay of the fluorescence in the unbleached half nucleus was analysed. Fluorescence decay curves were analysed and the data were fitted to three RNA Pol II populations with an exponential decay ($f = a \times \exp(-b \times x) + c \times \exp(d \times x) + g * \exp(-h \times x)$; R^2>0.99): one free form (a), one bound to DNA but not fully engaged (c), and another fully engaged in transcription (g).

The hyposmolarity (hypo2+/PBS) promotes a significant decrease (p value <0.001) in the free form of RNA Pol II and a significant increase (p value < 0.05) in the initiating form of the polymerase (Figure 3.44).

Although the hyposmolarity (hypo2+/PBS) does not seem to have an impact in the percentage of RNA Pol II in transcriptional elongation (Figure 3.44) it does have a significant increase (p value < 0.01) in the half-life of RNA Pol II (Figure 3.45). The half-life of RNA Pol II was calculated with the fully engaged slope (h) using the formula: $\frac{\ln 2}{Slope\ fully\ engaged\ form}$. Assuming that a transcription unit in a CHO cell has the same length as a human gene (median length ∼14 kbp; Lander et al. 2001), and a polymerisation rate of 1.1–2.5 × 10^3 nucleotides/min (Jackson et al., 2000), a typical transcription unit

would be copied in 6–13 min (Kimura et al., 2002). In our experience, the average RNA Pol II half time in the isosmotic condition is approximately 16 minutes and this value is significantly increased (p value < 0.01) in the hyposmolarity condition (hypo2+/PBS) to 140 minutes (Figure 3.45). The control results are largely in agreement with other reports and discrepancies are perhaps related to different technical approaches used (Darzacq et al., 2007; Kimura et al., 2002).

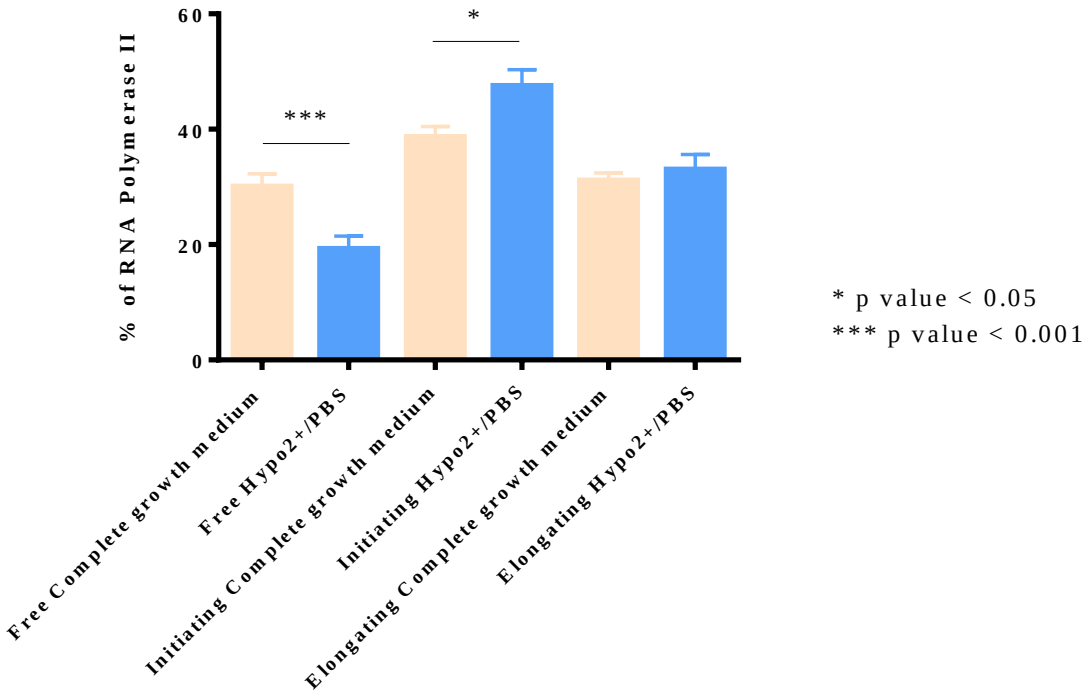

Figure 3.44 – Percentage of different RNA polymerase II forms within the transcription cycle in the CHO RNA Pol II-EGFP cell line. Fluorescence loss in photobleaching (FLIP) was performed in the LSM 710 (Carl Zeiss) confocal microscope with the stage heated at 39ºC with the CHO RNA Pol II-EGFP cell line. The EGFP intensity values in the unbleached area were evaluated with ImageJ and fitted to a three populations with an exponential decay (R^2>0.99). An isosmotic condition was used to determine the baseline values of each RNA polymerase II: free, initiating and fully engaged in transcriptional elongation (Complete growth medium). And compared with a hyposmotic condition where the same parameters were evaluated (hypo2+/PBS). The average values (n=3) of each RNA polymerase II form are presented (±SEM). Statistically significant differences in comparison with the timepoint 0h are highlighted in the graph (p value < 0.05; p value < 0.001).

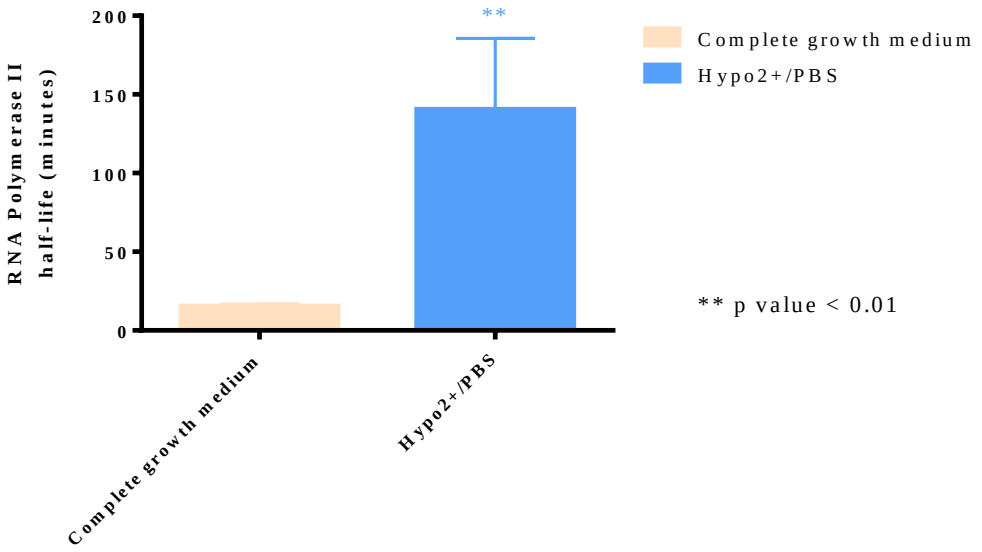

Figure 3.45 – RNA polymerase II half-life in the CHO RNA Pol II-EGFP cell line. Fluorescence loss in photobleaching (FLIP) was performed in the LSM 710 (Carl Zeiss) confocal microscope with the stage heated at 39ºC with the CHO RNA Pol II-EGFP cell line (n=3). The half-life was calculated with the fully engaged slope (d) using the formula: $\frac{\ln 2}{Slope\ fully\ engaged\ form}$ (±SEM). Statistically significant differences are highlighted in the graph (p value < 0.001).

To obtain additional accurate and precise data regarding RNA Pol II engagement in chromatin a Chip was performed against RNA Pol II and RNA Pol II PhosphoS5. The phosphorylation in serine 5 at the CTD of RNA Pol II is a characteristic alteration of transcription initiation (Hirose and Ohkuma, 2007; Jasnovidova and Stefl, 2013; Meinhart et al., 2005). K562 cells were transiently exposed to hypo2+/PBS and PBS, cross-linked and the chromatin was then sonicated. These steps were followed by an immunoprecipitation with the specific antibodies and afterwards, the pooled DNA was purified and quantified.

After performing the immunoprecipitation with K562 cells exposed transiently to hypo2+/PBS, the DNA recovered, normalised to initial amount of DNA for each condition (input control), is approximately five times higher in the case of RNA Pol II and approximately two times higher in the case of RNA Pol II PhosphoS5 than the normalised amount recovered from the respective immunoprecipitations in the control situation (PBS) (Figure 3.46 and Figure 3.47). This means that the amount of RNA Pol II and RNA Pol II PhosphoS5 bound to the chromatin of K562 cells exposed to hyposmotic extracellular conditions is increased and therefore the recovery yield of DNA is higher. These results are in agreement with the FLIP analyses described above.

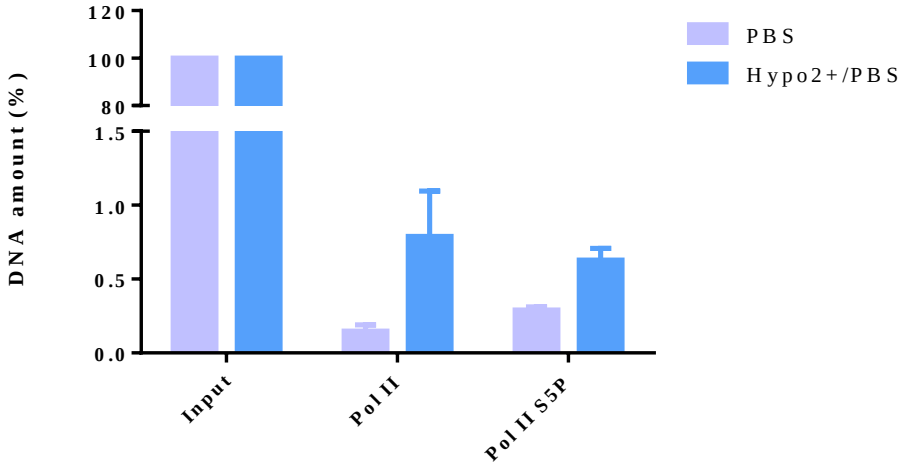

Figure 3.46 – Effect of transient osmotic modulation on DNA recovery after chromatin immunoprecipitation. The DNA recovered (normalised %) in each condition was normalised to the initial amount of DNA (±SEM; n=2) present within each control before immunoprecipitation (input). The hyposmotic modulatory condition used is shown in the legend.

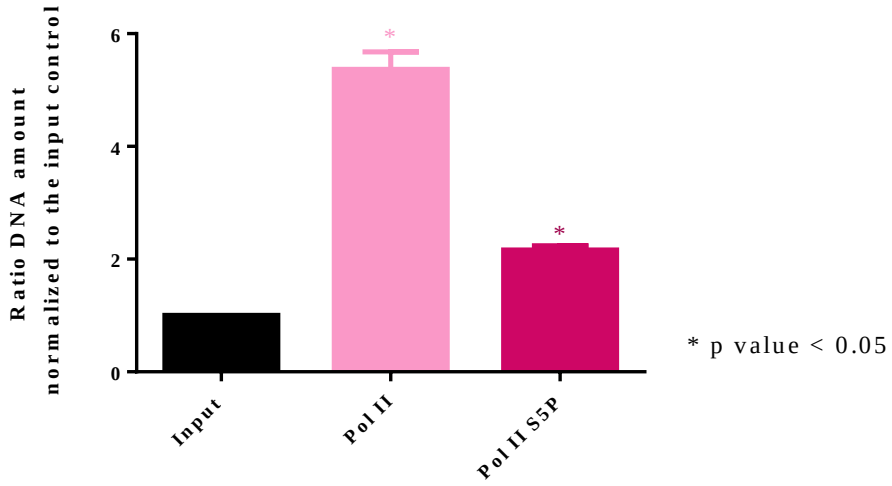

Figure 3.47 – Ratio of DNA amount recovered after chromatin immunoprecipitation. The ratio here presented is between the normalised DNA amounts (±SEM; n=2) recovered after Chip for the isosmotic sample versus the hyposmotic modulated sample $\left(\frac{\mathbf{PBS}}{\mathbf{hypo2+/PBS}}\right)$.

Nonetheless, the Chip protocol is an extensive and laborious protocol that can allow for many confounding variables in result interpretation. Within the DNA extraction and purification protocol by phenol/chloroform the error associated with sample manipulation is not significant, as can be observed in Figure 3.48. Where purifying the same amount of input DNA sample, in an independent manner does result in DNA quantification with a small range of error (Figure 3.48).

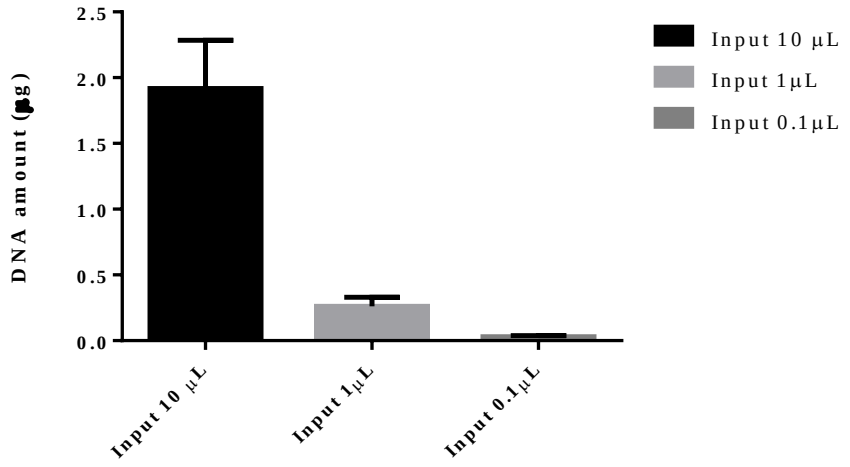

Figure 3.48 – DNA purification protocol reproducibility/robustness. DNA average amounts (±SEM; n=3).

Due to the extensive and laborious Chip protocol, and considering all the confounding variables which can be introduced in a DNA quantification output, a Chip-Sequencing (Chip-Seq) was performed to analyse in detail where total RNA Pol II and its phosphorylated forms, PhosphoS2 and PhosphoS5, are binding. Moreover, this Chip-Seq analysis can also help in the understanding of the binding pattern of the different forms of RNA Pol II, after transient exposure to hypo2+/PBS. We used a sample of K562 cells exposed transiently to the hyposmotic stimulus and we let another sample to recover in complete growth medium and analyse the same batch of cells after 1h of recovery.

The Chip-Seq data shows that the hyposmotic modulation has an impact on RNA Pol II binding to chromatin (Table 3.2). The detection of peaks in each condition shows that RNA Pol II PhosphoS5 has a high enrichment right after the hyposmotic modulation when compared to the control (Table 3.2). Moreover, after 1h of recovery from the transient hyposmotic stimulus, the chromatin is enriched for the RNA Pol II PhosphoS2 binding (Table 3.2).

Table 3.2 – Total number of Chip-Sequencing peaks detected after background noise subtraction. For the analysis of the Chip-Seq, the peak detection was done with MACS software using IgG immunoprecipitations as internal controls.

Condition	Pol II Total	Pol II PhosphoS5	Pol II PhosphoS2
PBS 0h	41906	31469	1897
PBS 1h	22196	27412	930
Hypo2+/PBS 0h	28064	45928	1370
Hypo2+/PBS 1h	28749	31631	2239

The most affected molecular functions, of the genes where the different RNA Pol II peaks were detected, were assessed with the Panther classification system (http://pantherdb.org/). The ontology for molecular function was not proportionally altered in the RNA Pol II Total (data not shown) but in Figure 3.49, Figure 3.50, Figure 3.51 and Figure 3.52 are the molecular function categories that are related to the closest genes where RNA Pol II PhosphoS5 and RNA Pol II PhosphoS2 peaks were detected, for the isosmotic and hyposmotic conditions, 1h after the transient hyposmotic stimulus (Figure 3.49; Figure 3.51 and Figure 3.50; Figure 3.52, respectively).

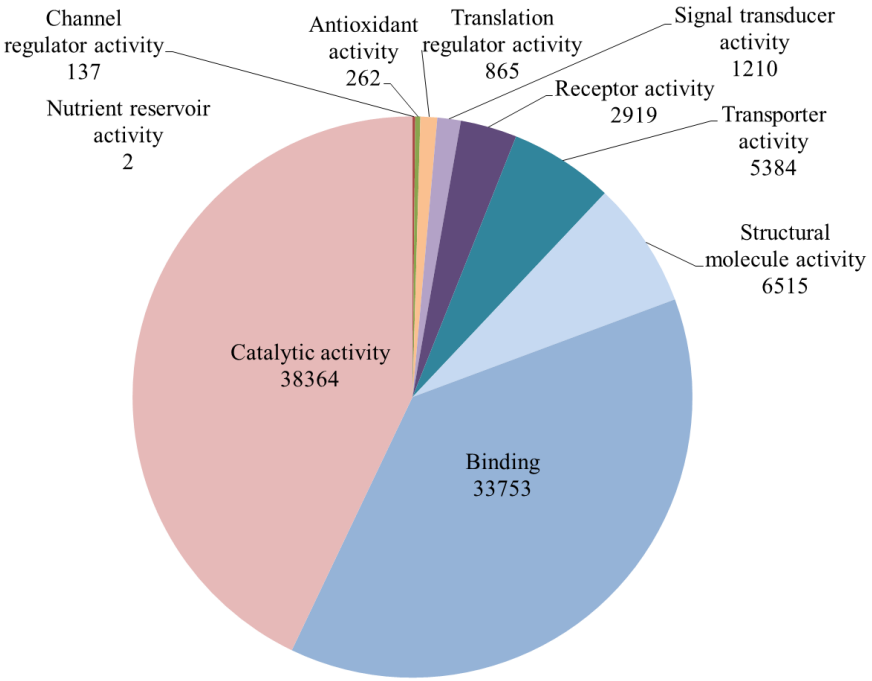

Figure 3.49 – Gene ontology analysis of the peaks detected within the condition PBS (1h) for RNA Pol II PhosphoS5. The chromatin immunoprecipitation was done 1h after the transient stimuli with PBS against the RNA Pol II PhosphoS5 modification. Analysis performed with the Panther classification system (http://pantherdb.org/).

The ontology category distribution is very general and the information analysis is not easy or clear. Nevertheless, within the RNA Pol II PhosphoS5 ontological categories, within the molecular functions evaluated it is noticeable an increase in the representation of the categories “receptor activity” and “signal transducer activity” in the hypo2+/PBS condition (Figure 3.50) when compared with the PBS control condition (Figure 3.49).

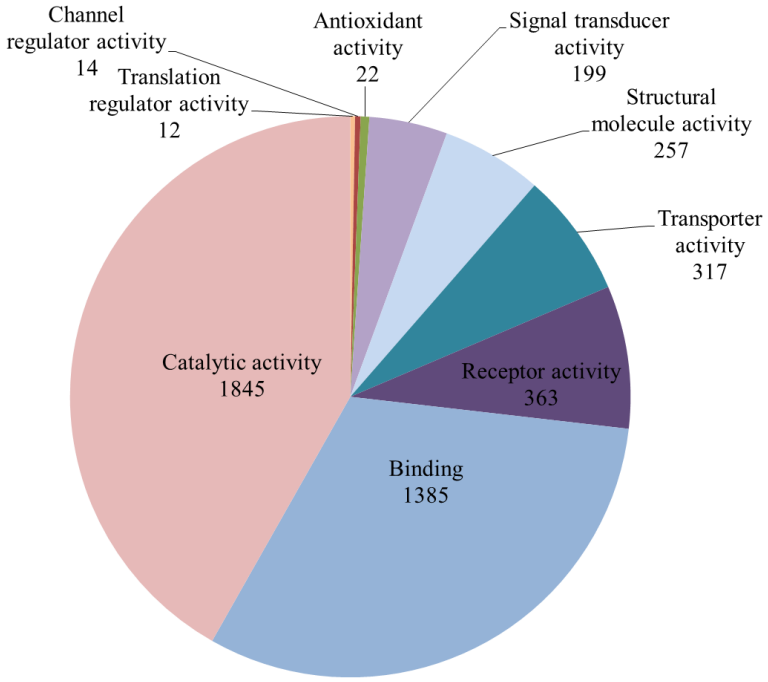

Figure 3.50 – Gene ontology analysis of the peaks detected within the condition hypo2+/PBS (1h) for RNA Pol II PhosphoS5. The chromatin immunoprecipitation was done 1h after the transient stimuli with PBS against the RNA Pol II PhosphoS5 modification. Analysis performed with the Panther classification system (http://pantherdb.org/).

On the other hand, within the RNA Pol II PhosphoS2 ontological categories, within the molecular functions evaluated there is an increase in the representation of the categories “receptor activity” and “signal transducer activity”, a slight increase in the “binding” category and a decrease in the “catalytic activity” category representation in the hypo2+/PBS condition (Figure 3.52) when compared with the PBS control condition (Figure 3.51).

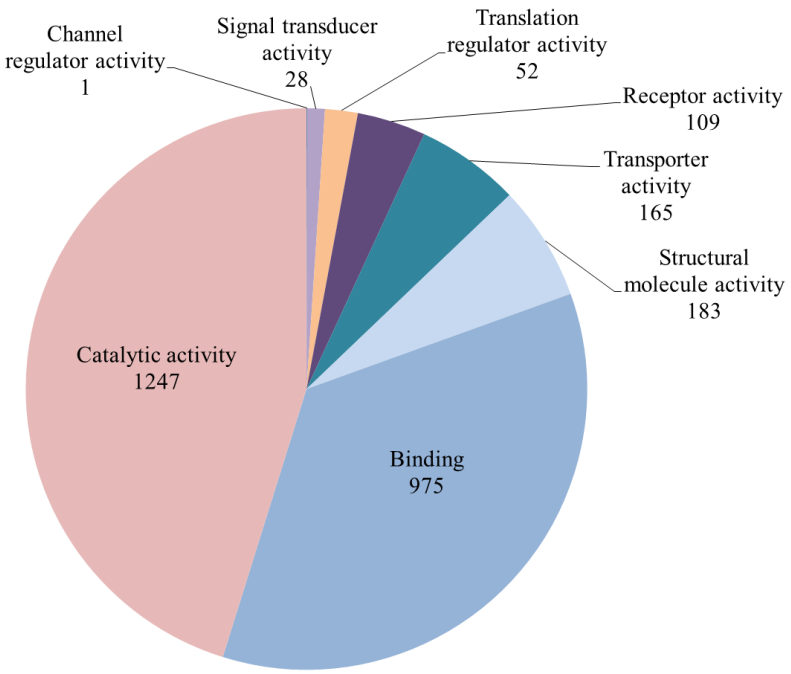

Figure 3.51 – Gene ontology analysis of the peaks detected within the condition PBS (1h) for RNA Pol II PhosphoS2. The chromatin immunoprecipitation was done 1h after the transient stimuli with PBS against the RNA Pol II PhosphoS2 modification. Analysis performed with the Panther classification system (http://pantherdb.org/).

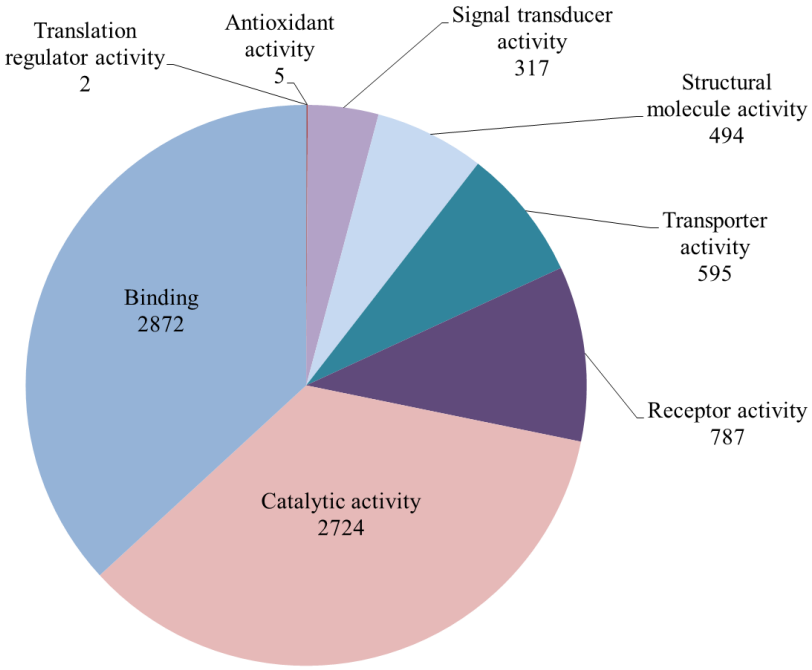

Figure 3.52 – Gene ontology analysis of the peaks detected within the condition hypo2+/PBS (1h) for RNA Pol II PhosphoS2. The chromatin immunoprecipitation was done 1h after the transient stimuli with PBS against the

RNA Pol II PhosphoS2 modification. Analysis performed with the Panther classification system (http://pantherdb.org/).

To further complement this analysis, we performed a very strict analysis to understand if the hyposmotic modulation was promoting just an enrichment of binding or if it was also promoting binding of RNA Pol II forms to new binding sites. For this analysis, we compared the peaks detected, in the samples PBS versus hypo2+/PBS both normalised to the IgG controls. Afterwards, we filtered them to have a fold enrichment higher than 30 or 15 (in the case of RNA Pol II PhosphoS2) and a p-value lower than $1x10^{-9}$. This analysis gave us a list of genes that were "new peaks" that were just present in the hypo2+/PBS condition and not in the correspondent control condition (PBS). This analysis showed that in general, the hyposmotic modulation promotes the binding of RNA Pol II to new sites of the genome. The number of "new peaks" detected with this analysis is presented in Table 3.3.

Table 3.3 – Total number of Chip-Sequencing "new peaks". These peaks are only present in the hypo2+/PBS condition when compared to the correspondent PBS condition.

RNA Pol II	0h	1h
Total	406	72
PhosphoS5	294	94
PhosphoS2	11	3

It is very difficult to understand the biological effect of these transcriptional changes in a very complex cellular transcriptional network. Nevertheless, the top 15 genes (when possible) in each list of "new peaks" is a mixture of genes with distinct functions and is presented in Table 3.4.

Table 3.4 – Top genes in Chip-Sequencing "new peaks" gene list. These peaks are only present in the hypo2+/PBS condition when compared to the correspondent PBS condition for the different chromatin immunoprecipitations performed (RNA Pol II Total, RNA Pol II PhosphoSer5 and RNA Pol II PhosphoSer2). The presented genes are in descendent fold enrichment and both name and generic function of the genes is given. The gene name and general function were obtained and adapted from the human gene database (http://www.genecards.org/).

Polymerase form and time point	Gene name	Function
Total Pol II 0h	Tyrosine 3-Monooxygenase/Tryptophan 5-Monooxygenase Activation Protein Zeta	Cell cycle checkpoints; p70S6K signalling; Poly(A) RNA binding; Kinase binding.

Polymerase form and time point	Gene name	Function
	SR-Related CTD Associated Factor 1	RNA binding; Protein domain specific binding; May function in mRNA splicing.
	Calponin 2	Actin binding and calmodulin binding.
	Histone Cluster 2, H2bc	Pseudogene.
	mir 4751	Unknown
	Matrix Remodelling Associated 7	Protein coding gene; Diseases associated include endometriosis of ovary.
	ADP-Ribosylation Factor-Like GTPase 6 Interacting Protein 6	Protein Coding gene; Diseases associated include cutis marmorata telangiectatica congenita.
	DNA Damage-Inducible Transcript 4	Cell growth, proliferation and survival; Responses to cellular energy levels and cellular stress, including responses to hypoxia and DNA damage; Regulates p53 -mediated apoptosis in response to DNA damage.
	ATPase Plasma Membrane Ca2+ Transporting 1	Intracellular calcium homoeostasis.
	Unc-13 Homolog D	Appears to play a role in vesicle maturation during exocytosis; Regulation of cytolytic granules secretion.
	Ribonuclease T2	Member of extracellular ribonucleases; Associated with human malignancies and chromosomal rearrangement.
	Cyclin-Dependent Kinase 19	Component of the mediator co-activator complex; Transcriptional activation by DNA binding transcription factors of genes transcribed by RNA polymerase II.
	Cytochrome B Reductase 1	Physiological role in dietary iron absorption.
	YY1 Transcription Factor	Zinc finger protein; Repression and activation of a diverse number of promoters; May direct histone deacetylases and histone acetyltransferases to a promoter in order to activate or repress transcription.
	Heterogeneous Nuclear Ribonucleoprotein F	Protein Coding gene; Involved in mRNA splicing; Nucleic acid binding and RNA binding.
Total Pol II 1h	Trans-2,3-Enoyl-CoA Reductase	Catalyses the final step, reducing trans-2,3-enoyl-CoA to saturated acyl-CoA.

Polymerase form and time point	Gene name	Function
	Unknown	Unknown
	Small Nucleolar RNA, C/D Box 3B-1	lncRNA; RNA transport and ribosome biogenesis.
	RNA, 7SL, Cytoplasmic 600, Pseudogene	Pseudogene; lncRNA.
	AT-Rich Interaction Domain 1A	Required for transcriptional activation of genes normally repressed by chromatin; Confers specificity to the SNF/SWI complex and may recruit the complex to its targets through either protein-DNA or protein-protein interactions.
	ADP-Ribosylation Factor-Like GTPase 6 Interacting Protein 6	Protein Coding gene; Diseases associated include cutis marmorata telangiectatica congenita.
	RNA, 7SK Small Nuclear Pseudogene 150	Binding to the CDK9/cyclin T complex (known as elongation factor P-TEFb); Negative regulation of P-TEFb transcription activation by phosphorylating the C-terminal domain of RNA polymerase II.
	Bromodomain Adjacent To Zinc Finger Domain 2A	Protein Coding gene; RNA binding; Lysine-acetylated histone binding.
	Myosin Light Chain 12A	Regulates smooth muscle and non-muscle cell contraction; May also be involved in DNA damage repair by sequestering the transcriptional regulator apoptosis-antagonizing transcription factor.
	Nuclear Paraspeckle Assembly Transcript 1	lncRNA; Retained in the nucleus where it forms the core structural component of the paraspeckle sub-organelle; May act as a transcriptional regulator of numerous genes, including some involved in cancer progression.
	Zinc Finger And BTB Domain Containing 7B	Zinc-finger-containing transcription factor; Key regulator of lineage commitment of immature T-cell precursors; Transcriptional repressor of type I collagen genes.
	Adenine Phosphoribosyltransferase	Purine/pyrimidine phosphoribosyltransferase family; Catalyses the formation of AMP and inorganic pyrophosphate from adenine and 5-phosphoribosyl-1-pyrophosphate;

Polymerase form and time point	Gene name	Function
		Produces adenine as a by-product of the polyamine biosynthesis pathway.
	FLJ13224	ncRNA
	Vomeronasal 1 Receptor 71 Pseudogene	Pseudogene; lncRNA.
	MicroRNA 7705	Unknown
Pol II PhosphoS5 0h	Solute Carrier Family 6 Member 8	Transport creatine into and out of cells.
	MicroRNA 3189	Unknown
	Inhibitor Of Growth Family Member 1	Tumour suppressor protein; Induction of cell growth arrest and apoptosis.
	RP1-309F20.3	RNA gene; ncRNA.
	Olfactory Receptor Family 4 Subfamily D Member 7 Pseudogene	G-protein-coupled receptors; Responsible for the recognition and G protein-mediated transduction of odorant signals.
	Ezrin	Protein-tyrosine kinase substrate in microvilli; Intermediate between the plasma membrane and the actin cytoskeleton; Cell surface structure adhesion, migration and organisation.
	ZEB2 Antisense RNA 1	lncRNA; May be involved in the regulation of zinc finger E-box binding homeobox 2 (ZEB2) expression, and may play a role in the progression of bladder cancer.
	Calponin 2	Actin binding and calmodulin binding.
	Prothymosin, Alpha	Protein coding gene; c-Myc transcriptional activation; Diseases associated include Hepatitis B and thymus cancer.
	Tyrosine 3-Monooxygenase/Tryptophan 5-Monooxygenase Activation Protein Zeta	Cell cycle checkpoints; p70S6K signalling; Poly(A) RNA binding; Kinase binding.
	DLGAP1 Antisense RNA 2	RNA gene; ncRNA.
	SR-Related CTD Associated Factor 1	RNA binding and protein domain specific binding: May function in mRNA splicing.
	AC011558.5	Uncategorized gene; Antisense RNA.
	Heterogeneous Nuclear Ribonucleoprotein A1	RNA-binding protein; Associate with mRNAs in the nucleus and influence mRNA processing, as well

Polymerase form and time point	Gene name	Function
		as other aspects of mRNA metabolism and transport; Regulation of alternative splicing.
	Matrix Remodelling Associated 7	Protein coding gene; Diseases associated include endometriosis of ovary.
Pol II PhosphoS5 1h	RP1-309F20.3	ncRNA
	Unknown	Unknown
	Small Nucleolar RNA, C/D Box 3B-1	lncRNA; RNA transport and ribosome biogenesis.
	Ubiquitin-Conjugating Enzyme E2 S	Formation of a thiol ester linkage with ubiquitin in an ubiquitin activating enzyme-dependent manner.
	RNA, 7SL, Cytoplasmic 472	Pseudogene; lncRNA.
	Histone Cluster 2, H2bd	Pseudogene.
	RNA, 7SK Small Nuclear Pseudogene 150	Binding to the CDK9/cyclin T complex (known as elongation factor P-TEFb); Negative regulation of P-TEFb transcription activation by phosphorylating the C-terminal domain of RNA polymerase II.
	Hyperpolarization Activated Cyclic Nucleotide Gated Potassium Channel 2	Protein coding gene; Protein binding and voltage-gated potassium channel activity; cAMP signalling; Diseases associated include sinoatrial node disease.
	MicroRNA 4738	Unknown
	AT-Rich Interaction Domain 1A	Required for transcriptional activation of genes normally repressed by chromatin; Confers specificity to the SNF/SWI complex and may recruit the complex to its targets through either protein-DNA or protein-protein interactions.
	Chromosome 19 Open Reading Frame 24	Protein Coding gene
	Oestrogen Related Receptor Alpha	Nuclear receptor that is closely related to the oestrogen receptor.; Site-specific transcription regulator Interaction with oestrogen and the transcription factor TFIIB by direct protein-protein contact.
	Sterol Regulatory Element Binding Transcription Factor 1	Involved in sterol biosynthesis.
	RP11-388M20.1	lncRNA.
	Small Nucleolar RNA, C/D Box 48	RNA gene; ncRNA.

Polymerase form and time point	Gene name	Function
Pol II PhosphoS2 0h	WAS Protein Family Member 1	Member of the Wiskott-Aldrich syndrome protein family; Critical role downstream of Rac, a Rho-family small GTPase; Regulation of the actin cytoskeleton required for membrane ruffling; Associates with an actin nucleation core Arp2/3 complex while enhancing actin polymerisation *in vitro*.
	Major Histocompatibility Complex, Class II, DR Alpha	A Central role in the immune system by presenting peptides derived from extracellular proteins.
	AC004893.10	Pseudogene; Antisense RNA class.
	PAQR9 Antisense RNA 1	RNA gene; ncRNA.
	Chromosome 3 Open Reading Frame 20	Protein Coding gene.
	Zinc Finger Protein 672	Protein Coding gene; Nucleic acid binding; May be involved in transcriptional regulation.
	Unknown	Unknown
	Small Cajal Body-Specific RNA 22	RNA gene; scaRNA.
	MAS Related GPR Family Member D	Protein coding gene; G-protein coupled receptor activity;.
	RP11-476B1.1	RNA gene; ncRNA.
	Isoamyl Acetate-Hydrolyzing Esterase 1 Homolog	Protein coding gene; Hydrolase activity, acting on ester bonds.
Pol II PhosphoS2 1h	Mitochondrial Translational Initiation Factor 3	Pseudogene; Antisense RNA.
	RP11-330O11.3	RNA Gene
	Glutaredoxin (Thioltransferase) Pseudogene 1	Pseudogene.

These data corroborates the theory that after a transient hyposmotic shock, cells have a distinct RNA Pol II binding profile and promote a change in the transcriptional network of the cell. Within the gene list presented above, there are numerous targets that will need further validation but that look very promising target genes associated with chromatin modifications, transcription control, calcium homoeostasis, potassium channels, kinases, several RNA genes (non-coding RNA, long-non-coding RNA, antisense RNA and others) and microRNAs (Table 3.4).

After this analysis of the gene pattern where RNA Pol II binds, with a significant difference after hyposmotic modulation, we wondered how the hyposmotic modulation impacts on transcription factor (TF) binding. It is generally accepted that for transcription to start there is the need for recognition of binding sites and recruitment of RNA Pol II by specific and general TFs. We used the Chip-Seq to evaluate the different capacity of recognition and binding of RNA Pol II under hyposmotic modulation. To make an analysis of the TFs that promote that specific RNA Pol II binding profile we used PASTAA, a tool from Max Planck Institute (http://trap.molgen.mpg.de/cgi-bin/pastaa.cgi). This tool enables the evaluation of the regulatory association between TFs in a set of genes (Roider et al., 2009). In our case we used the list of genes for which the Chip-Seq experiment could detect significant peaks for the different forms of RNA Pol II (initiating, elongating and total) after hyposmotic modulation and in isosmotic conditions. In this list of genes we interrogate what is their TF signature using PASTAA. We used the association scores computed in PASTAA (-log of the most significant hypergeometric p-value) as a readout of the binding/affinity probability of a TF to be involved in the regulation of a set of genes enriched in the Chip-Seq of RNA Pol II different forms.

There are a few examples in the literature of TF binding to DNA to be dependent on specific hydration of DNA sequences. One example is the pioneer factor PU.1. We decided to evaluate if in our Chip-Seq experiment there is an enrichment of PU.1-regulated genes in the hyposmotic modulation conditions. In theory, TFs that are affected by the levels of hydration of DNA will have their binding affinities influenced by the hyposmotic modulation and the obvious readout will be the presence of RNA Pol II in their gene regulatory network. As there is no extensive list of pioneer factors described in the literature we decided to test this hypothesis on the list available in Iwafuchi-Doi and Zaret, 2014. When the list of genes enriched in our Chip-Seq experiment of RNA Pol II Total, S5 and S2 phosphorylated forms were analysed in PASTAA we could only get scores for the pioneer TFs: PU.1, GATA4, GATA1, CLOCK:BMAL1 and p53, as presented in Figure 3.53; probably meaning that the other pioneer TFs are not expressed in K562 cells. Interestingly, although GATA4 shows up in the list of TFs involved in the regulation of the genes present in our Chip-Seq assay it was not possible to find it in the initiating (PhosphoS5) RNA Pol II Chip list. It shows up with very low scores in the PhosphoS2 and total RNA Pol II Chip-Seq data. This is in accordance with the fact that GATA4 promoter is hypermethylated in K562 cells (and in most acute myeloid leukaemias) and the levels of expression of GATA4 are low (Tao et al., 2015). This result is reassuring that our analyses are well done because if GATA4 levels are low in K562 and it is expectable that genes that are regulated by this pioneer TF are not enriched for RNA Pol II binding.

The most interesting results of these analyses are related to PU.1 and CLOCK:BMAL1 association scores (Figure 3.53). PU.1 has been shown to have specific needs of hydration in its binding sequences

(Poon, 2012; Wang et al., 2014). In the hyposmotic modulatory condition PU.1 shows a higher association score for total RNA Pol II immediately at time 0 hours which remains higher than the PBS condition at 1 hour. This is mainly due to the contribution of the elongating form of RNA Pol II and suggests that PU.1 is a co-factor for transcription in the body of genes that are more expressed in the hyposmotic condition. For comparison we looked for Ets1 (non-pioneer TF of the same family of PU.1) and we could not see the same behaviour as presented in Figure 3.54. For CLOCK:BMAL1 there is no description on hydration influencing binding affinities for this pioneer TF. What our results show is that it has a high association score with the hyposmotic condition particularly again for the elongation form of RNA Pol II (Figure 3.53).

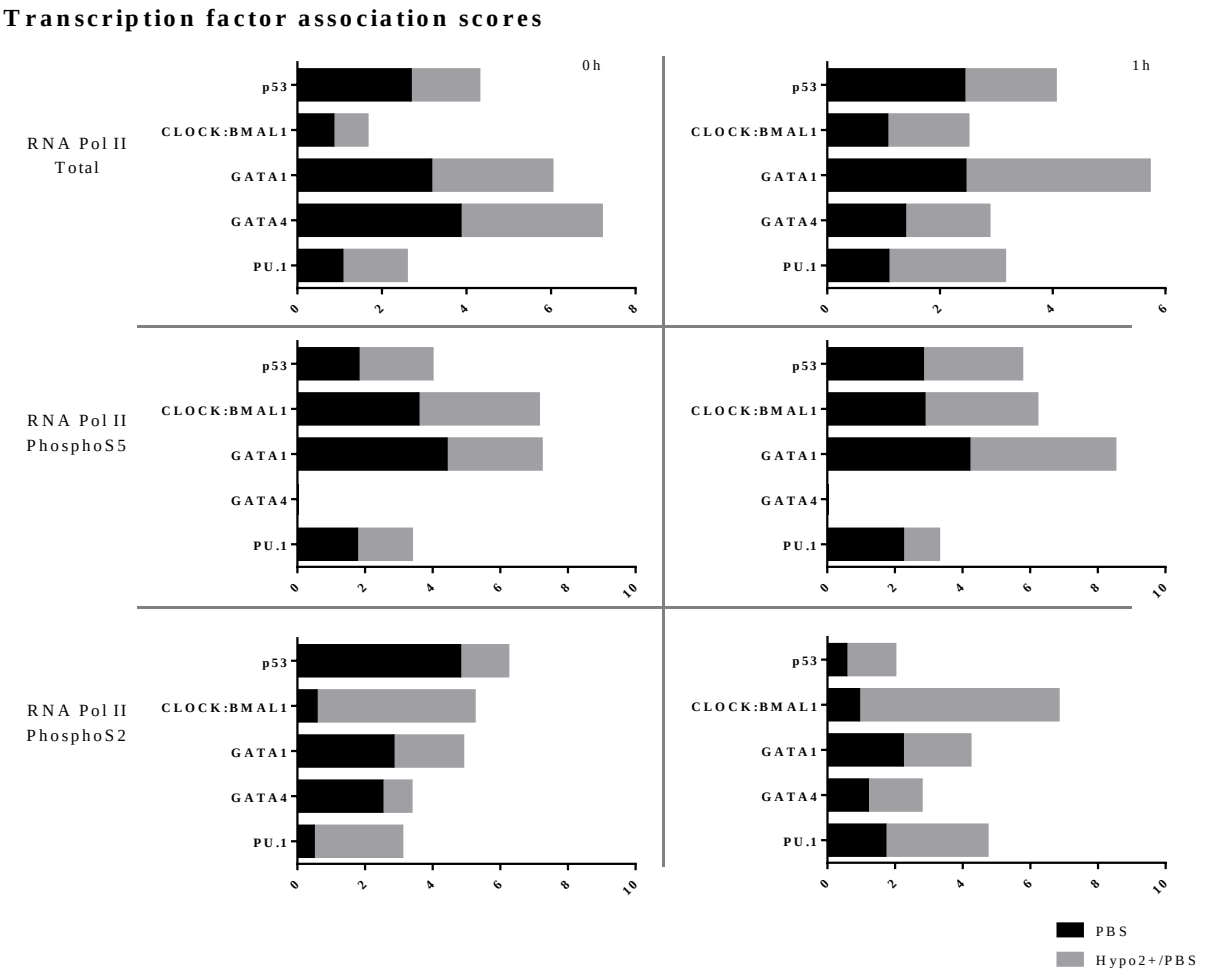

Figure 3.53 – Pioneer transcription factors association scores. Association scores computed with PASTAA (http://trap.molgen.mpg.de/cgi-bin/pastaa.cgi) as a readout of the binding/ affinity probability of a list of pioneer transcription factors to be involved in the regulation of a set of genes enriched in the Chip-Sequencing of RNA Pol II gene analysis lists.

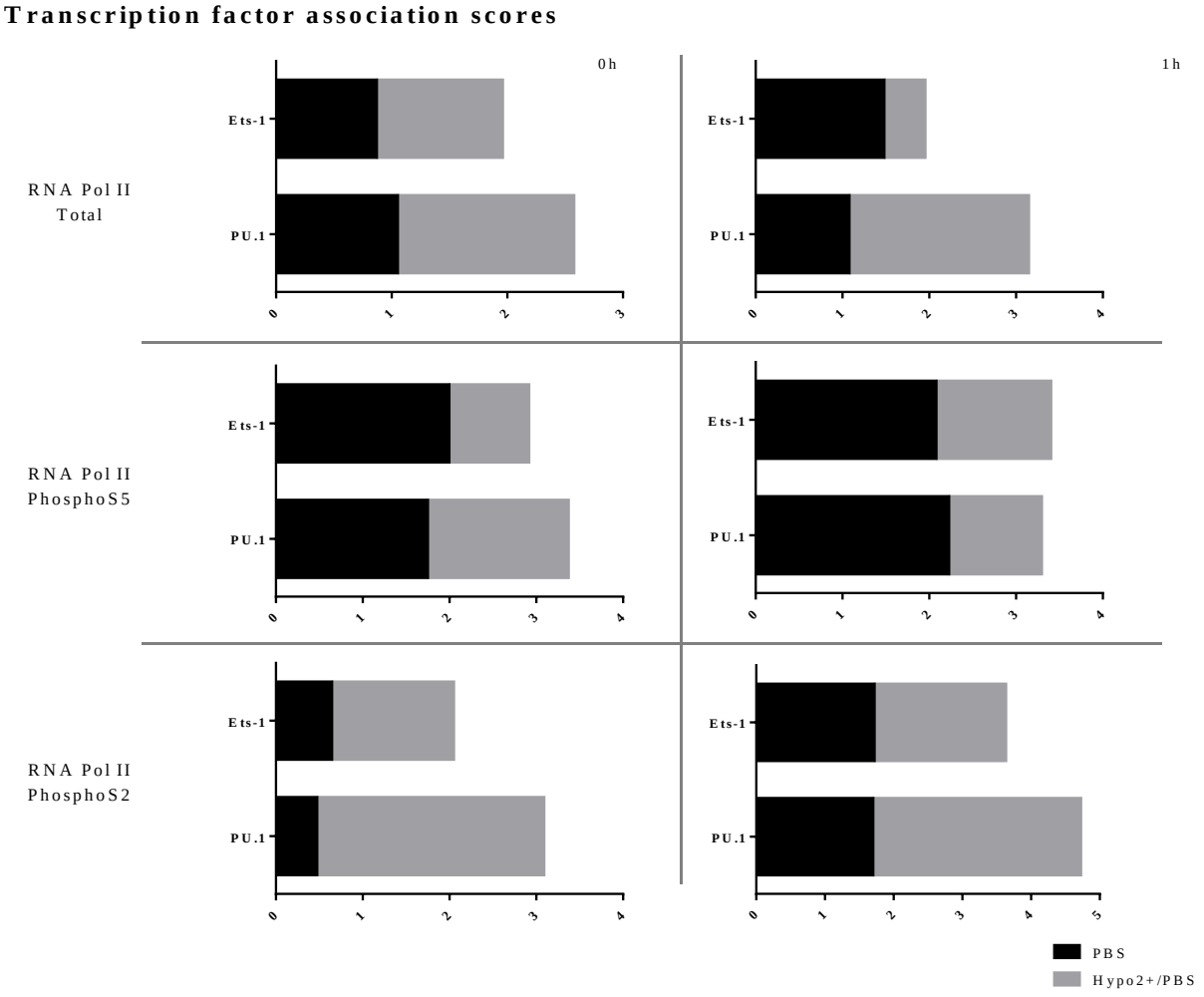

Figure 3.54 – Ets transcription factors association scores. Association scores computed with PASTAA (http://trap.molgen.mpg.de/cgi-bin/pastaa.cgi) as a readout of the binding/ affinity probability of PU.1 and Ets-1 to be involved in the regulation of a set of genes enriched in the Chip-Sequencing of RNA Pol II gene analysis lists.

We also wanted to validate our analyses looking at genes that are referenced in the literature as being affected by osmotic modulation. This was difficult to find specifically for hyposmotic conditions as most of the literature is available for hypertonic stress. We looked at the Human Osmotic Stress RT2 Profiler PCR Array from SABiosciences for a reference on validated TFs that are affected by this type of stress. This array profiles the expression of 84 key genes involved in the cellular response to changes in osmolarity and identifies the TFs: TonEBP, ATF4, DDIT3, EGR1, EGR3, FOS, JUN, PAX2, SNAI1, TP53 and ZFP36L1 as important regulators of the osmotic stress response. Based on this list we run our Chip-Seq data in PASTAA and looked for association scores of these TFs in hyposmotic or PBS conditions and the respective results are presented in Figure 3.55. The most interesting effects of the

hyposmotic condition were seen in the gene regulatory networks of TFs EGR1, EGR3 and FOS. EGR1 has been shown to be affected by osmolyte levels (Mikles et al., 2015).

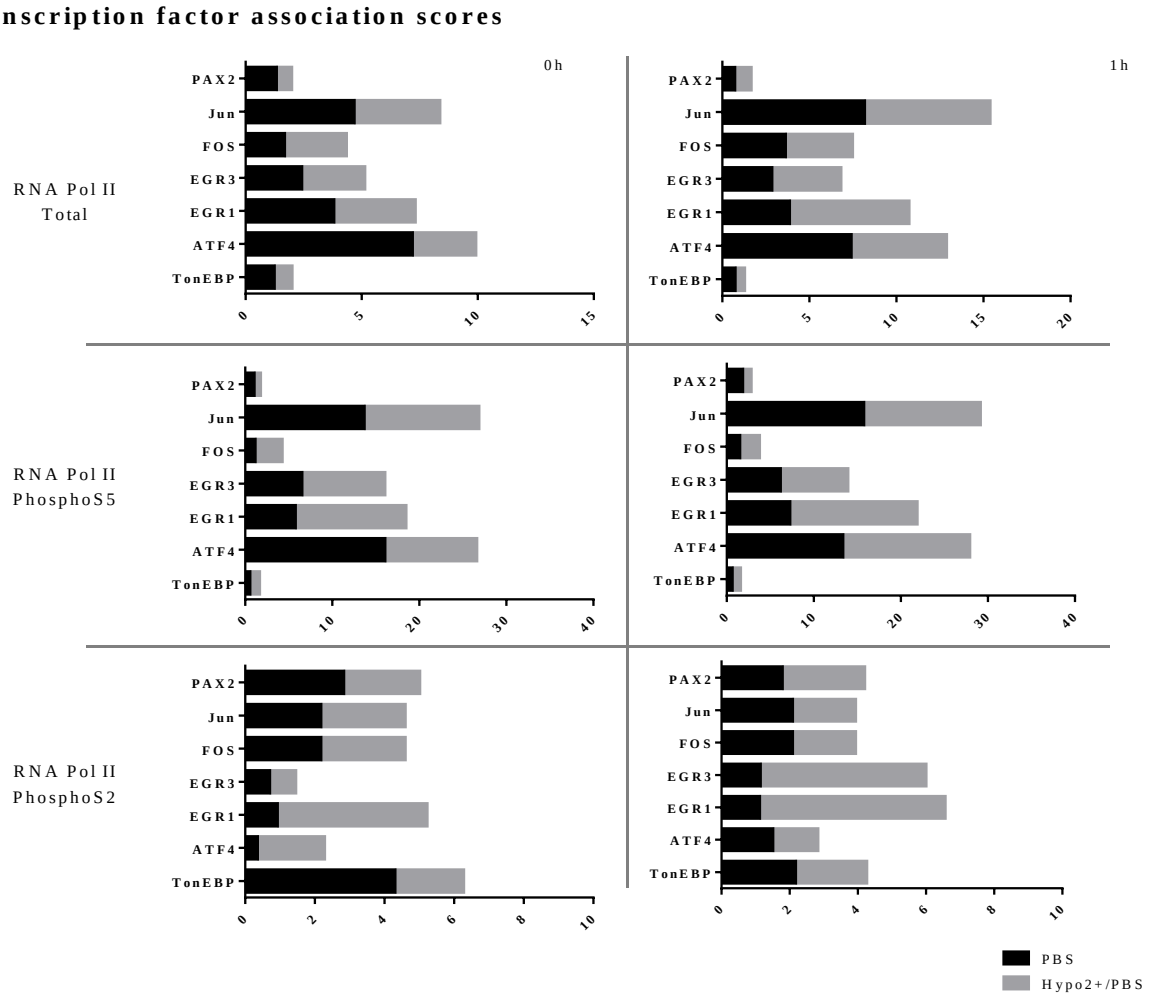

Figure 3.55 – Osmoregulatory transcription factors association scores. Association scores computed with PASTAA (http://trap.molgen.mpg.de/cgi-bin/pastaa.cgi) as a readout of the binding/ affinity probability of a list osmotic modulated transcription factors to be involved in the regulation of a set of genes enriched in the Chip-Sequencing of RNA Pol II gene analysis lists.

To understand if these TFs were the responsible for the new binding sites or the "new peaks" that are significantly enriched in the hyposmotic modulation condition, another tool called Classification of Human Transcription Factors and Mouse Orthologs (http://tfclass.bioinf.med.uni-goettingen.de/tfclass) was used. The results presented in Figure 3.56 resembles the information from the previous analysis with PASTAA, with a ranked prediction of TFs involved in the regulation of the submitted list of genes, and

additionally it gives details on the sequence and positional frequency matrix for each factor. Surprisingly, immediately after the hyposmotic stimulus (0h) eight out of the ten higher ranked TFs found to be associated with the "new peaks" Chip-Seq data of the initiating form of RNA Pol II belong to the superclass of "zinc-coordinating DNA-binding domains" as schematized in Figure 3.56.

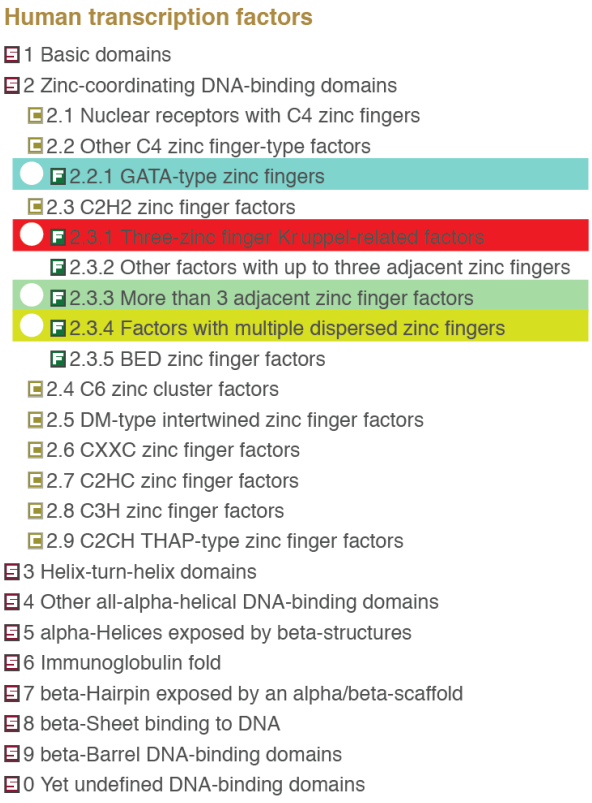

RNA Pol II S5P 0hour				
Rank	**Matrix**	**Transcription Factor**	**Association Score**	**P-Value**
1	CHCH_01	Chch	6.411	1.80E-05
2	SP1_Q2_01	Sp1 , Sp2	6.406	1.80E-05
3	ETF_Q6	N/A	6.397	1.80E-05
4	MZF1_01	Mzf-1	5.512	1.40E-04
5	EGR_Q6	Egr-1 , Egr-2	5.327	2.01E-04
6	SP1_Q4_01	Sp1 , Sp2	5.131	3.13E-04
7	GATA1_01	Gata-1	4.782	6.65E-04
8	WT1_Q6	N/A	4.427	1.36E-03
9	HIC1_03	Hic-1	4.39	1.50E-03
10	MUSCLE_INI_B	N/A	4.244	2.02E-03

RNA Pol II S5P 1hour				
Rank	**Matrix**	**Transcription Factor**	**Association Score**	**P-Value**
1	WT1_Q6	N/A	7.738	2.00E-06
2	ETF_Q6	N/A	6.806	4.00E-06
3	TFIII_Q6	Tfii-i	6.197	1.30E-05
4	MAZR_01	Mazr	6.113	1.40E-05
5	MAZ_Q6	Maz	6.067	2.10E-05
6	CACBINDING PROTEIN_Q6	N/A	5.401	8.90E-05
7	BRE_HAND	N/A	4.866	2.94E-04
8	MOVOB_01	Movo-b	4.866	2.94E-04
9	E2F1_Q3	E2f-1	4.476	6.69E-04
10	GC_01	N/A	4.444	7.38E-04

Figure 3.56 – Ranked prediction of transcription factors involved in the regulation of the "new peaks" gene list of Chip-Seq data for RNA Pol II PhosphoS5 at time-point 0h and 1h. Immediately after the hyposmotic stimulus (0h) eight out of the ten higher ranked transcription factors belong to the superclass of "zinc-coordinating DNA-binding domains". This analysis was done with PASTAA and classification of TFs was done at http://tfclass.bioinf.med.uni-goettingen.de/tfclass.

These results clearly show that this class of TFs can have some dependency on specific hydration/osmolyte conditions to exert their activity as already described for EGR1.

The analysis done with TransFind produces also a representation of the sequence of cytosine and guanine dinucleotides (CpGs) observed over expected ratio and the percentage of guanine and cytosine (%GC) content in the sequences of the gene list of the Chip-Seq analysis. This analysis showed that after hyposmotic modulation initiating RNA Pol II binds to CpG high regions immediately after the stimulus and 1h in medium recovery versus the PBS condition as shown in Figure 3.57, Figure 3.58, Figure 3.59,

Figure 3.60 and Figure 3.61. Some of these regions might fulfil the criteria for CpG islands and further evaluation of this possibility is needed.

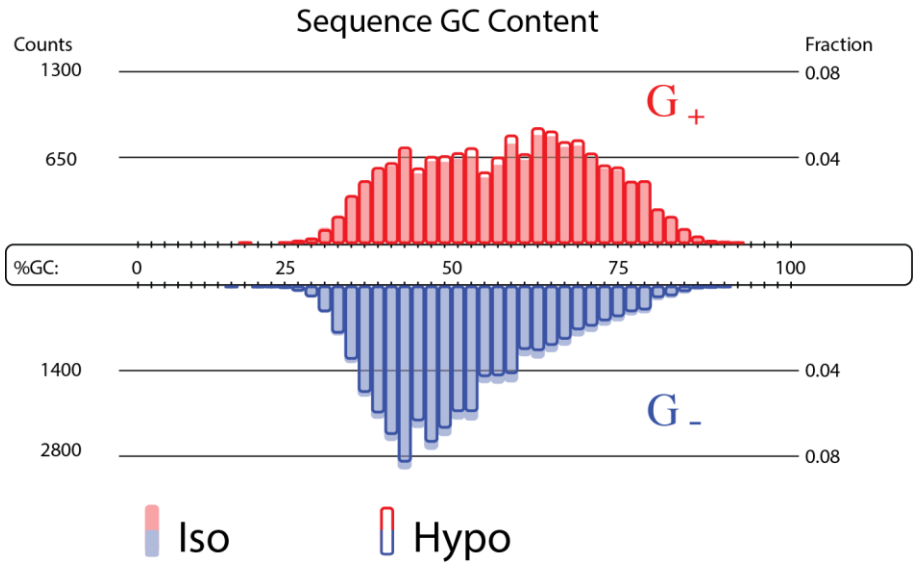

Figure 3.57 – Sequence of GC content in the sequences of the gene list for RNA Pol II PhosphoS5 at 0h. This analysis showed that after hyposmotic modulation (Hypo – hypo2+/PBS) initiating RNA Pol II (PhosphoS5) binds to CG high regions at time point 0h versus the PBS (Iso). This analysis was done with TransFind (http://transfind.sys-bio.net/index.php/home.html).

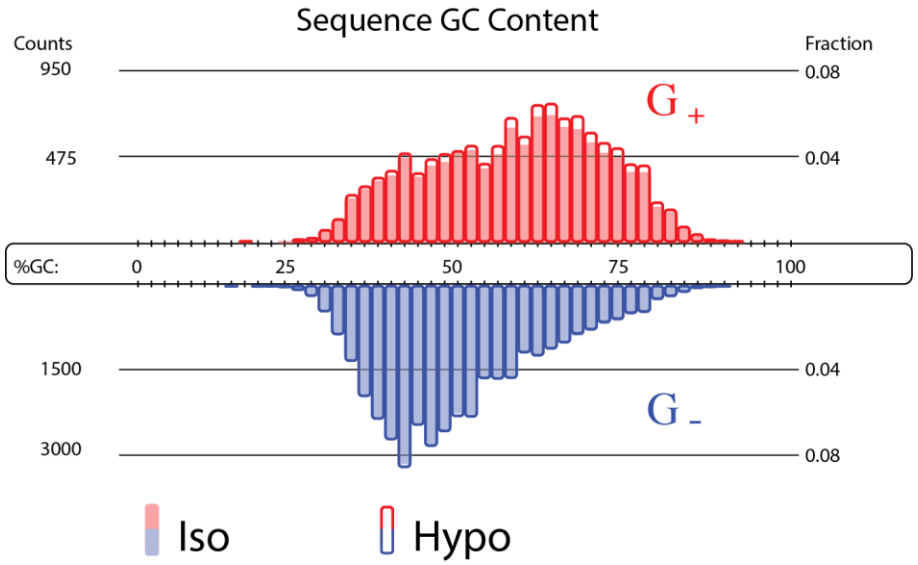

Figure 3.58 – Sequence of GC content in the sequences of the gene list for RNA Pol II PhosphoS5 at 1h. This analysis showed that after hyposmotic modulation (Hypo – hypo2+/PBS) initiating RNA Pol II (PhosphoS5) binds to CG high regions at time point 1h versus the PBS (Iso). This analysis was done with TransFind (http://transfind.sys-bio.net/index.php/home.htm).

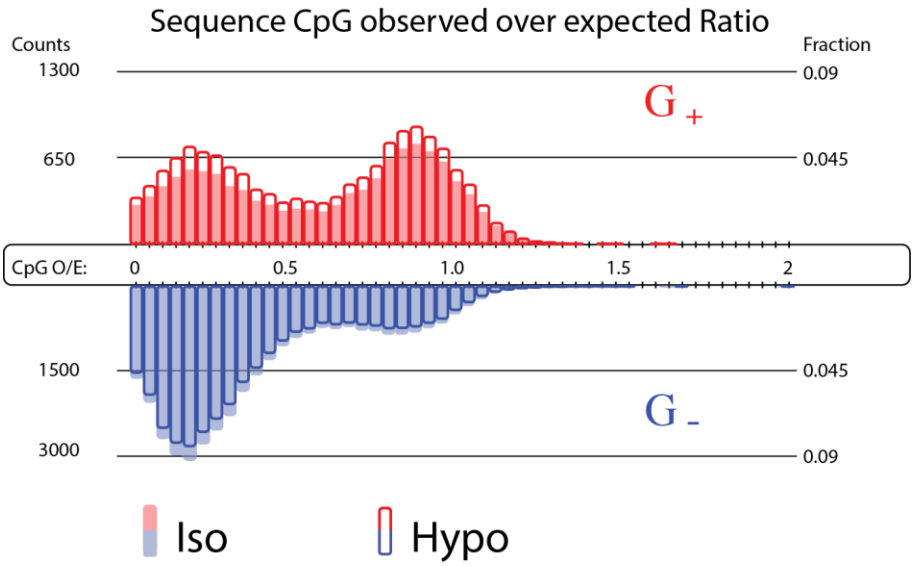

Figure 3.59 – Sequence of CpG observed/expected in the sequences of the gene list for RNA Pol II PhosphoS5 at 0h. This analysis showed that after hyposmotic modulation (Hypo – hypo2+/PBS) initiating RNA Pol II (PhosphoS5) has CpG higher ratio at time point 0h versus the PBS (Iso). This analysis was done with TransFind (http://transfind.sys-bio.net/index.php/home.html).

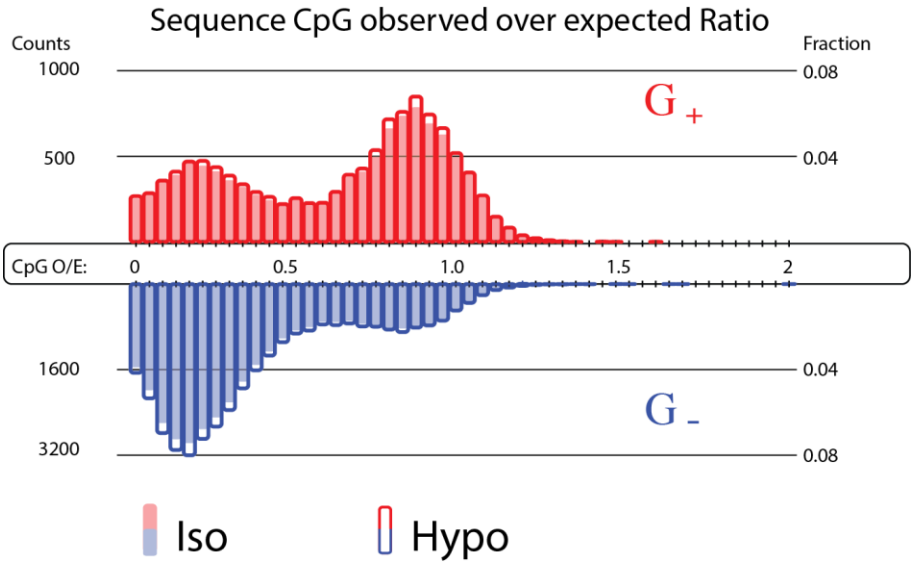

Figure 3.60 – Sequence of CpG observed/expected in the sequences of the gene list for RNA Pol II PhosphoS5 at 1h. This analysis showed that after hyposmotic modulation (Hypo – hypo2+/PBS) initiating RNA Pol II (PhosphoS5) has CpG higher ratio at time point 0h versus the PBS (Iso). This analysis was done with TransFind (http://transfind.sys-bio.net/index.php/home.html).

The ranked top five TFs with TransFind presented in Figure 3.61 at time point 1h bind to CpG enriched sequences. Within these areas we can find CpG islands, and this would be an interesting feature because these areas are usually associated with transcriptional inactivity that after a hyposmotic modulation would become accessible/active to new transcriptional events.

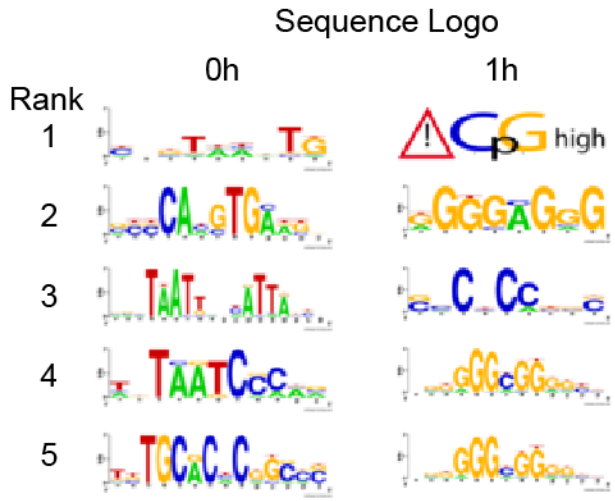

Figure 3.61 – Top 5 ranked prediction of transcription factors binding sequences of the "new peaks" gene list of Chip-Seq data for RNA Pol II PhosphoS5 at time-point 0h and 1h. Especially after 1h of recovery, the binding of the transcription factors is in CpG and GC enriched areas in cells exposed to hypo2+/PBS transiently. This analysis was done with TransFind (http://transfind.sys-bio.net/index.php/home.html).

3.2. Concluding observations

Within this chapter, it is clear that the type of hyposmotic modulation applied to cells has a distinct effect and in some extreme situations osmolarity changes can be harmful to the cells, but if optimised and used as a tool to change cellular behaviour, several cellular changes are observed.

In general, from our results, a hyposmotic environment promotes:

- Increased cell size, that activates a regulatory volume decrease mechanism;
- Similar or decreased ATP levels;
- Decreased cell membrane potential;

- Unchanged reactive oxygen species and mitochondrial superoxide levels;
- Decreased mitochondrial membrane potential;
- Increased intracellular calcium levels;
- Relaxed chromatin and increased H4K16 acetylation levels;
- Increased RNA polymerase II binding to chromatin;
- Increased RNA polymerase II fully engaged in transcription binding to chromatin;
- Decreased transcription speed;
- Increased RNA polymerase II initiation;
- Decreased RNA polymerase II in its free form;
- Altered binding profile of transcription factors;
- Changed transcriptional profile

Chapter 4 : Osmotic regulation in stem cell biotechnology and cellular products

The generation of stem cell-based products holds great potential for regenerative medicine. The biotechnology field is trying to provide solutions for major obstacles in stem cell-based technologies and to create tools for disease modelling (Abbasalizadeh and Baharvand, 2013; Avior et al., 2016; Jenkins and Farid, 2015; Wagers, 2012). One of the main challenges is to overcome the restricted stem cell (SC) number required for certain applications; the low number and availability of umbilical cord blood (UCB) SCs is an example. Although several expansion strategies have been developed the inefficiency of the processes has also been limiting; the generation of induced pluripotent stem cells (iPSCs) is an example (Brunt et al., 2012).

Transplantation using bone marrow stem cells (BMSC) has been the best and the most successful example of cell therapy. Vital knowledge has been attained, but unfortunately, there are still complications associated with BMSC usage which have not been resolved over the years. For example, one of such complications is graft versus host disease (GVHD), which can be life-threatening or have an impact on long-term survival. This condition is associated with allogenic transplantation, in which the differences between donor and recipient human leukocyte antigen (HLA) can cause donor cells to trigger an immune response against recipient's tissues and organs. UCB SCs have emerged as an alternative source of cells for BMSC that are immunologically naïve, and less susceptible to induce GVHD (Porada et al., 2016; Roura et al., 2015). The main disadvantage of UCB usage for cell transplantation is the limited cell number and slower reconstitution time for some specific lineages (Porada et al., 2016; Saudemont and Madrigal, 2016).

In 2012, the iPS Cell Stock project led by Shinya Yamanaka, from the Center for iPS Cell Research and Application (CiRA), was approved by the Japanese Health Ministry. This project aims to develop lines of iPSCs from thousands of samples of UCB in collaboration with eight Japanese cord-blood banks. It is widely accepted that UCB derived cells are a reliable source of cells for reprogramming since these cells have not accumulated genomic alterations as a result of ageing or disease, due to their immune naivety, and they are readily available in cryobanks (Roura et al., 2015; Ye et al., 2011). Shinya Yamanaka, plans to create until 2020, a standard array of 75 iPSC lines that are an adequate match to be tolerated by Japanese 80% of the population. If these goals are attained and clinical trials prove the safety

of these cells, the introduction of this pioneer biomedical technology into the medical field will be reached. This technology will have the potential to be used to treat many diseases (Cyranoski, 2012). In 2015, CiRA announced that they began to distribute iPSCs for use in regenerative medicine.

Solving problems related to UCB processing, cryopreservation and expansion could attenuate some problems related to bone marrow transplantation and be used in the treatment of blood malignancies and immune deficits. On the other hand, UCB cells, due to their unique characteristics, are a valuable source of cells for biomedical *in vitro* applications. These technologies, such as induced pluripotency technology, are a very important tool for disease modelling and drug toxicity assessment (Avior et al., 2016), and hopefully, in a near future might solve or alleviate many incurable diseases (Su et al., 2013b; Takahashi and Ohnuki, 2015; Takahashi and Yamanaka, 2016).

Environmental conditions have a great influence on cell behaviour and in this chapter we explore the importance of osmolarity in cell behaviour and its potential influence in techniques such as UCB collection, manipulation and generation of iPSCs.

4.1. Results and Discussion

4.1.1. Importance of osmolarity for Umbilical Cord Blood cells

The hematopoietic system is one of the most studied and the first source of SCs used for transplantation (Bianco, 2015; Porada et al., 2016; Sugimura, 2016). More recently, UCB was an alternative for some specific SC transplantation cases. But as a great part of knowledge gained regarding bone marrow hematopoietic stem cell transplantation, especially cryopreservation, has a significant empirical component, the know-how necessary to handle and store properly UCB samples still requires refinement. Refinement is also required in regards to osmotic changes which UCB samples undergo during collection, storage and cryopreservation (Hunt et al., 2003a; Nicoud et al., 2012). The influence of ionic concentration during these processes has not been studied in depth. Nevertheless, the importance of calcium as a signalling molecule has been described in several scenarios, and its role in chromatin loosening is described for T-cells (Lee et al., 2015b). Moreover, some studies show that certain osmolarity and temperature changes can condition colony forming capacity of UCB $CD34^+$ cells (Hunt et al., 2003a).

Calcium is affected during UCB collection, due to the presence of citrate in the anticoagulation solution (citrate phosphate dextrose adenine solution – CPDA-1), which chelates this ion (Park et al., 2016). There is no standardisation for the amount of blood collected and the collection of blood is not proportional to the amount of anticoagulant present in the collection bag.

In this study we decided to further explore the impact of CPDA-1 on the intracellular levels of calcium of UCB derived mononuclear cells (UCB-MNCs) as an ionic disturbance agent. Moreover, we aim to understand if the differences in CPDA-1 concentration can be a source of variability in the final cell quality and changes in phenotypic characteristics.

When UCB-MNCs are cultured in standard culture conditions in the presence of different amounts of CPDA-1 for 18 hours it is evident that the ionic balance is perturbed by the chelation of calcium (Figure 4.1). This result shows that this anticoagulant agent is able to change cell ionic physiology. With increasing concentrations of CPDA-1, there is a correspondent decrease in the intracellular free calcium concentration (Figure 4.1) suggesting that the extracellular imbalance of calcium has an impact in cellular homoeostasis and a possible impact in several cell functions and pathways regulated by calcium (Berridge et al., 2000; Thiel et al., 2012).

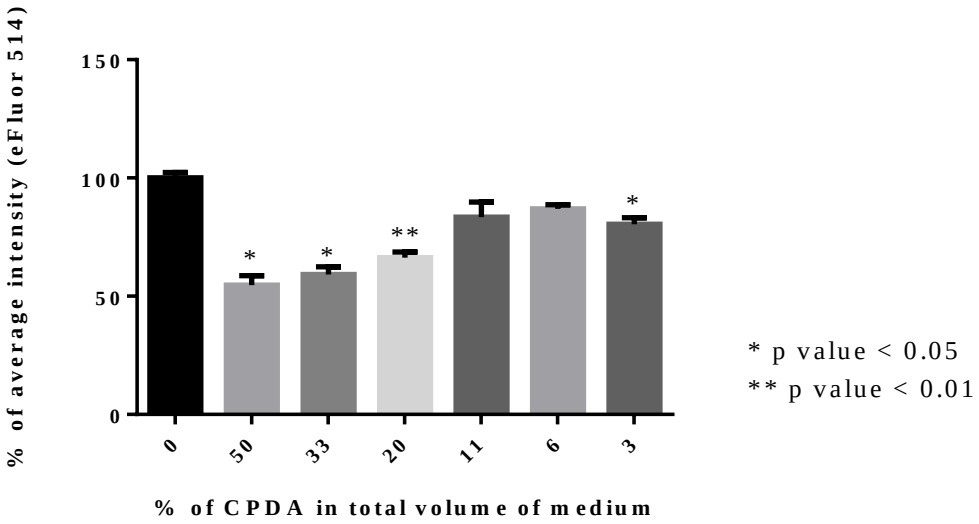

Figure 4.1 – CPDA-1 influence in intracellular calcium levels in UCB-MNCs. Intracellular free calcium levels were assessed with the eFluor514 probe by flow cytometry (BD FACSCalibur™) and the values of the average intensity (± SEM) were normalised to the control group (0) (n=2). The change is statistically significant when highlighted in the graph (p value < 0.05; p value < 0.01).

This result might suggest a possible effect of CPDA-1 in UCB-MNC physiology during and after collection, until cells are processed. Therefore, we tested this hypothesis by diluting one fresh UCB bag unit (immediately after collection) into several aliquots that were mixed with CPDA-1 in the proportion of 1:2 and 1:4 (UCB:CPDA-1) and incubated at room temperature for 48 hours. This period of time is considered as acceptable for transit from the maternity to the cryopreservation laboratories of the Portuguese Cryo-companies. Also, it is common to find collection bags with very low blood volume when compared to the volume of CPDA-1; so the proportions used in this study are realistic. After the incubation period, the UCB was fractioned into MNCs and these cells were cultured under standard conditions (hematopoietic stem cell medium, please see the Materials and methods section) for 4 days. The total number of MNCs was evaluated after the 48h incubation with CPDA-1 (Figure 4.2) and after the 4 days under standard culture conditions (Figure 4.3).

The CPDA-1 promotes a significant reduction (p value < 0.05; p value < 0.0001) in the number of total MNCs after 48h incubation with UCB as shown in Figure 4.2.

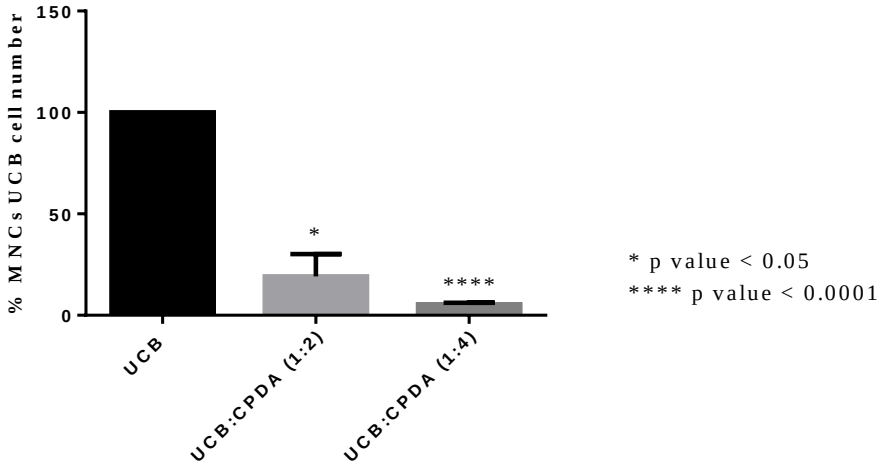

Figure 4.2 – CPDA-1 influence on the total UCB-MNCs number. The cell number was achieved by manual counting with a Neubauer chamber right after the 48h exposure of UCB-MNCs to CPDA-1. The average cell numbers presented (± SEM) were normalised to the control group (n=3). The change is statistically significant when highlighted in the graph (p value < 0.05; p value < 0.0001).

Nevertheless, when these MNCs are cultured at the same cell density ($1x10^6$ cells/mL) in standard culture conditions, the cells that were in contact with more CPDA-1 have a significant loss (p value < 0.05) of cell number after 4 days of culture (Figure 4.3). Although the cells that were in contact with less CPDA-1 (1:2) do not present any significant change in the MNCs survival profile (Figure 4.3) these cells present phenotypic changes as discussed below (Figure 4.4, Figure 4.5, Figure 4.6, Figure 4.7).

After 4 days of standard culture conditions a phenotypic analysis was done using the CD34 and CD133 markers (Figure 4.4), common markers to characterise hematopoietic stem cells (Bhatia, 2007; Garg et al., 2013; Lee et al., 2010; Radtke et al., 2015).

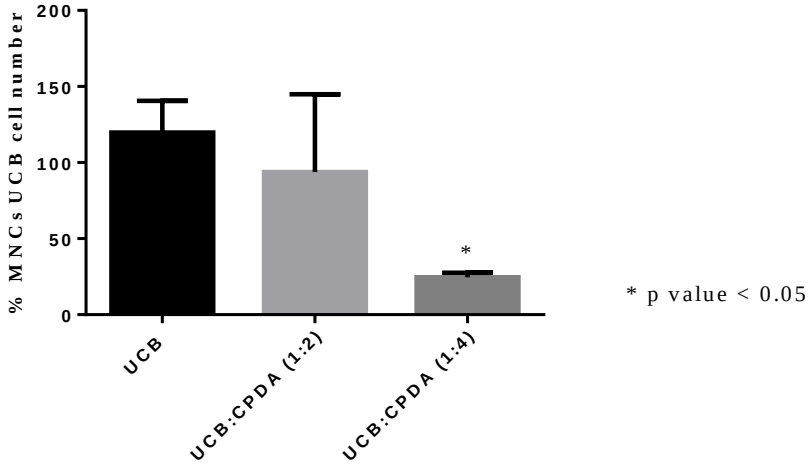

Figure 4.3 – CPDA-1 influence in total UCB-MNCs number. The cell number was achieved by manual counting with a Neubauer chamber right after the 4 days of standard UCB-MNCs culture. The average cell numbers presented (± SEM) were normalised to the control group (n=3). The change is statistically significant when highlighted in the graph (p value < 0.05).

The portion of cells expressing only the CD34 marker is not significantly altered in any of the conditions (Figure 4.5). In contrast, the contact with CPDA-1 interferes with the cell population expressing CD133 alone and both CD34 and CD133 as shown in the quantification profiles in Figure 4.6 and Figure 4.7.

The contact with CPDA-1 altered the percentage of cells expressing only CD133 and expressing CD34 and CD133 together as illustrated in Figure 4.4 and shown in Figure 4.6 and Figure 4.7. Therefore, the CPDA-1 induced ionic/osmotic imbalance might target a specific, more immature and sensitive target population within the UCB-MNC fraction.

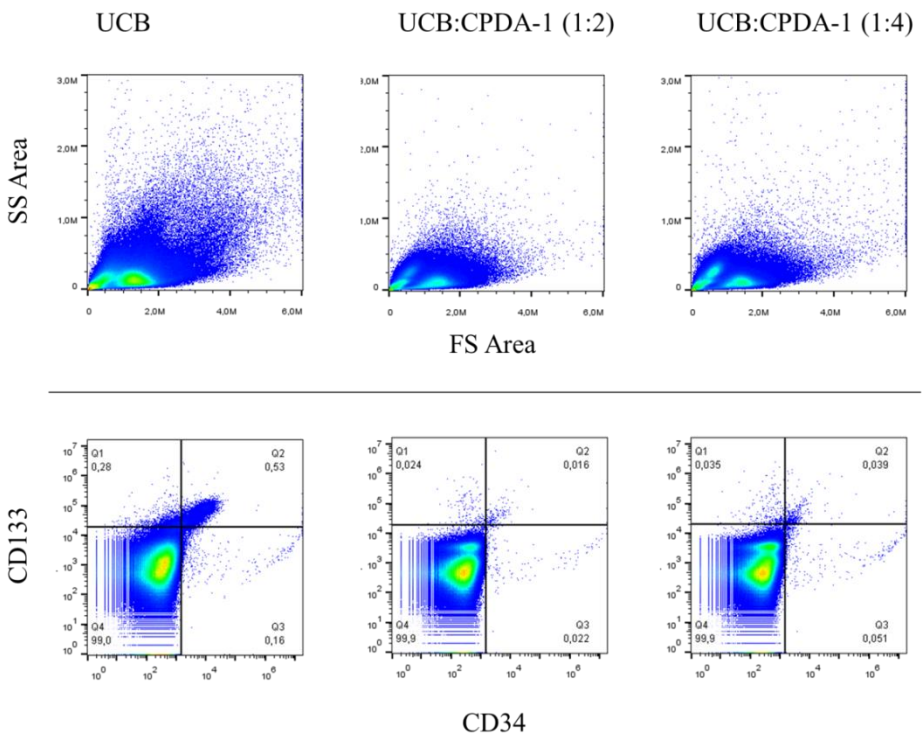

Figure 4.4 – CPDA-1 influence in the expression of CD34 and CD133 within UCB-MNCs. After 4 days of standard UCB-MNC culture, the evaluation of cell morphology, side scatter (SS) and forward side scatter (FS), expression of CD34 and CD133 markers was done by flow cytometry (BD Accuri™ C6). The treatment of the acquired data was done using the FlowJo™ cytometry analysis software. Although the images provided are from a single experiment, the same experiment was done at least two more times with similar results.

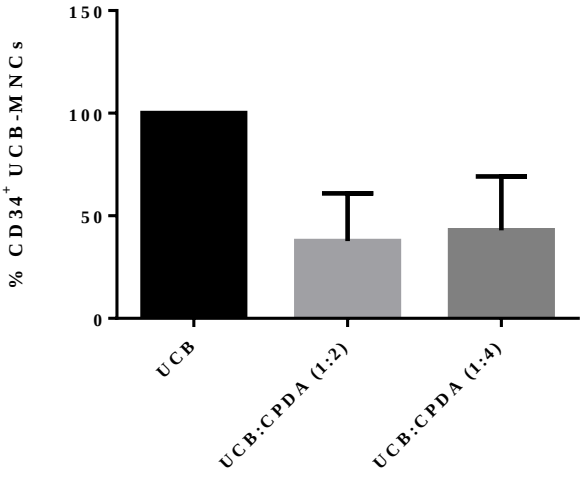

Figure 4.5 – CPDA-1 influence in the expression of CD34 within UCB-MNCs. After 4 days of standard UCB-MNC culture, the evaluation of expression of CD34 marker was done by flow cytometry (BD Accuri™ C6). The

percentage of UCB-MNCs expressing only CD34 was calculated, using FlowJo™ cytometry analysis software, and the average percentage of cells presented (± SEM) were normalised to the control group (n=3).

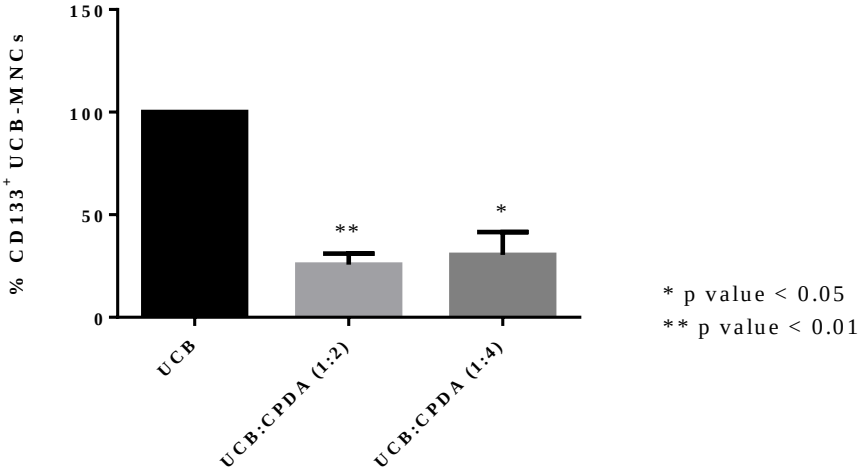

Figure 4.6 – CPDA-1 influence in the expression of CD133 within UCB-MNCs. After 4 days of standard UCB-MNC culture, the evaluation of expression of CD133 marker was done by flow cytometry (BD Accuri™ C6). The percentage of UCB-MNCs expressing only CD133 was calculated, using FlowJo™ cytometry analysis software, and the average percentage of cells presented (± SEM) were normalised to the control group (n=3). The change is statistically significant when highlighted in the graph (p value < 0.05; p value < 0.01).

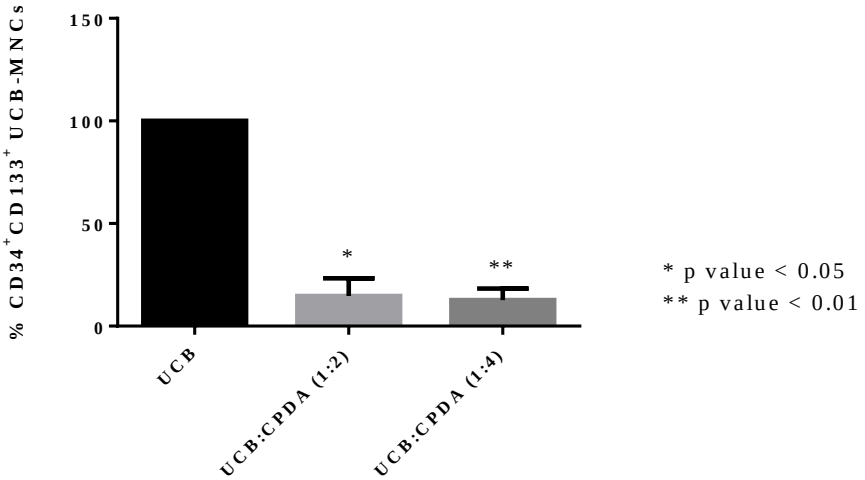

Figure 4.7 – CPDA-1 influence in the expression of CD34 and CD133 within UCB-MNCs. After 4 days of standard UCB-MNCs culture, the evaluation of expression of CD34 and CD133 markers was done by flow cytometry (BD Accuri™ C6). The percentage of UCB-MNCs expressing both CD34 and CD133 was calculated, using FlowJo™ cytometry analysis software, and the average percentage of cells presented (±SEM) were normalised to the control group (n=3). The change is statistically significant when highlighted in the graph (p value < 0.05; p value < 0.01).

These experiments show that the ionic imbalance induced by CPDA-1 has a great influence in the potential of the UCB cells and interferes with the fate commitment. Furthermore, CPDA-1 by itself has been shown to be hyperosmotic in the literature but it is still a commonly used compound in UCB collection and storage (Kurup et al., 2003; Picker et al., 2009). The lack of a specific designed collection strategy for UCB samples, using a fixed amount of CPDA-1 independently of the UCB volume might raise some concerns regarding the cell phenotype maintenance and metabolic stability of the cells (Broxmeyer, 2016; Hunt et al., 2003a; Kurup et al., 2003; Mancinelli et al., 2006; Park and Won, 2009; Roura et al., 2015; Thurman-Newell et al., 2015). Despite the UCB plasma buffering ability, the effect of CPDA-1 might compromise the phenotype and potency of UCB cells (Kurup et al., 2003; Lee et al., 2010; Thurman-Newell et al., 2015). Additional ionic imbalances can also be introduced by the freezing process itself (Hunt et al., 2003b), that will have an additive effect to possible deleterious effects previously induced by CPDA-1. Therefore, it is very important to develop strategies for collection and freezing of UCB having in consideration the maintenance of the ionic and osmotic balance to preserve UCB cell characteristics, namely their metabolic profile, potency and fate determination pathways.

The development of these strategies is crucial to embrace the full potential of this cell source and their practical applications (McKenna and Brunstein, 2011; Roura et al., 2015). One of these possible UCB applications is the reprogramming technology and will be discussed in the next subchapter.

4.1.2. Umbilical Cord Blood cells reprogramming

It is broadly accepted that UCB derived cells are a reliable source of cells for reprogramming, as mentioned previously in this chapter. Nevertheless, there are drawbacks associated with the use of these cells for generation of iPSCs and we will explore one of these in the next subchapter.

4.1.2.1. Variability in reprogramming efficiency of Umbilical Cord Blood cells

The reprogramming process is a mechanism that comprises alterations of phenotypic, genetic and epigenetic characteristics of differentiated cells in order to transform these into pluripotent cells. iPSCs can be maintained *in vitro* for several months without losing their properties, and resembling the embryonic SCs epigenetic pattern throughout the passages. Reprogramming is a stochastic and inefficient process (Krause et al., 2015; Welstead et al., 2008). Moreover, depending on the cell type used for this

process the efficiency can be highly variable approximately from 0.01% to 0.3% using different sources of cells (Feng et al., 2009; Takahashi, 2012). This might be related to the cell's epigenetic state and transcriptional network that needs to be rebooted to a new cell state.

UCB cell reprogramming has been shown to be variable and dependent on many factors. Such factors can have both technical and biological origins. Biological raw materials, such as UCB cells, have a high degree of complexity, sensitivity and plasticity associated with inherent variation of its source – human beings (Thurman-Newell et al., 2015). Additionally, some technical aspects like the use of specific viral vectors which leads to the expression of the reprogramming factors can introduce, among others, variability within the reprogramming process (Li et al., 2014).

The biological variability associated with UCB donors is illustrated by Figure 4.8 where the differences in reprogramming efficiency outputs between different UCB donors can be observed. In this figure both experimental plates were organised in parallel, i.e. they have the same order and were isolated, treated and infected at the same time with a polycistronic virus containing Sox2, Oct-4, Klf-4, c-Myc (Warlich et al., 2011). Although these samples were treated in the same way, in plate B, it was not possible to observe the generation of any alkaline phosphatase (AP) positive colonies. Contrariwise, in plate A, there are several conditions that lead to the generation of AP positive colonies. Donor variability has a role, but we believe that also the differences in UCB collection methods, the volume of blood collected, the time between collection and processing of the cells has an impact in the process. Unfortunately, many of these factors could not be controlled in this study.

We believe that the lack of standardisation of UCB collection might have a profound impact on the quality of UCB cells. Retrospective analyses from large cohort studies like the iPS cell stock project will certainly bring important insights into this matter. In this work, a standard blood collection bag (150 mL) with CPDA-1 (21 mL) was used. The amount of blood collected for our studies was highly variable and to some extent can be correlated with reprogramming efficiency as presented in Table 4.1. Nevertheless, the other variables, especially the time between collection and processing of samples might have a significant impact in cell phenotypic characteristics, like the amount of $CD34^+$ cells present in the UCB-MNC fraction, and functional characteristics, such as the ability to generate different blood lineages. In this study, it was not possible to establish a correlation between reprogramming efficiency and the time span between UCB collection and processing. The collection was done depending on the goodwill of varying medical staff that is sometimes overloaded with work in the maternity unit, therefore to register the time of collection was difficult and sometimes impossible due to complications during childbirth.

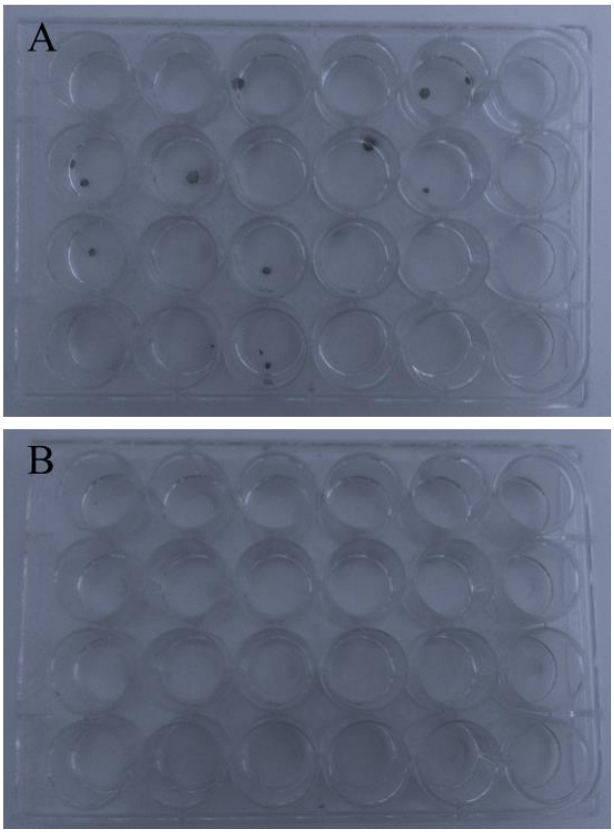

Figure 4.8 – Reprogramming variability in UCB cells from different donors. Alkaline phosphatase staining at day 17 of UCB cell reprogramming using the same methodology in both plates but using CD34+ cells from different donors (donor A and donor B, respectively).

Table 4.1 – Reprogramming variability in UCB cells.

Name of UCB unit	Sorting method	Volume of blood (mL)	Efficiency of reprogramming of control condition
A	FACS	150	0.17%
B	FACS	125	0.25%
C	FACS	85	0.18%
D	MACS	135	0.09%
E	MACS	90	0.02%

In addition to the UCB collection variability, the cell population within the MNC fraction and the $CD34^+$ population are highly heterogeneous (Hao et al., 1995).

As shown in Figure 4.9, by refining the UCB cell population used for reprogramming with CD34 labelling and lack of expression of CD15, a marker associated with neutrophilic lineage commitment (Kölbel et al., 2015), the reprogramming efficiency can be enhanced by a 2 fold increase. Therefore, the cells which still lack commitment to specific blood lineages and are more naïve are easier to reprogram.

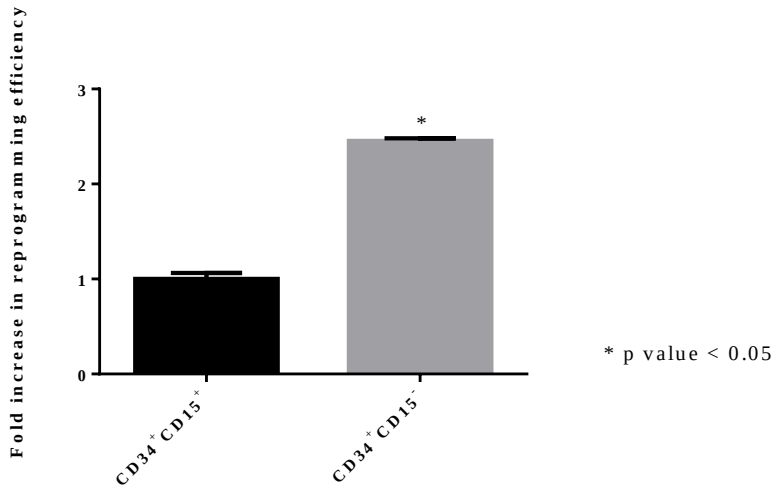

Figure 4.9 – Reprogramming efficiency within different UCB-MNC compartments. Reprogramming efficiency differences (± SEM) between UCB isolated cells $CD34^{+}CD15^{+}$ versus $CD34^{+}CD15^{-}$ (n=2). The fold increase in reprogramming efficiency is normalised to the $CD34^{+}CD15^{+}$ condition (considered to be equal to one). The change is statistically significant when highlighted in the graph (p value < 0.05).

We did not explore this feature with other lineage commitment markers but it would be an interesting study to perform. We proceeded by doing a UCB extensive characterisation to choose a simple and easy way to isolate a purer and immature population within the $CD34^{+}$ pool of cells. A morphological characterisation of the UCB cells is shown in Figure 4.10. In this figure, distinct cell populations with different cell sizes (forward scatter – FSC) and granularity (side scatter – SSC) can be identified: as granulocyte (≈ 48%), monocyte (≈ 7%) and lymphocyte (≈ 30%) cell groups. Within the lymphocytic compartment, there are approximately 0.7% of the cells that express the CD34 marker (Figure 4.10).

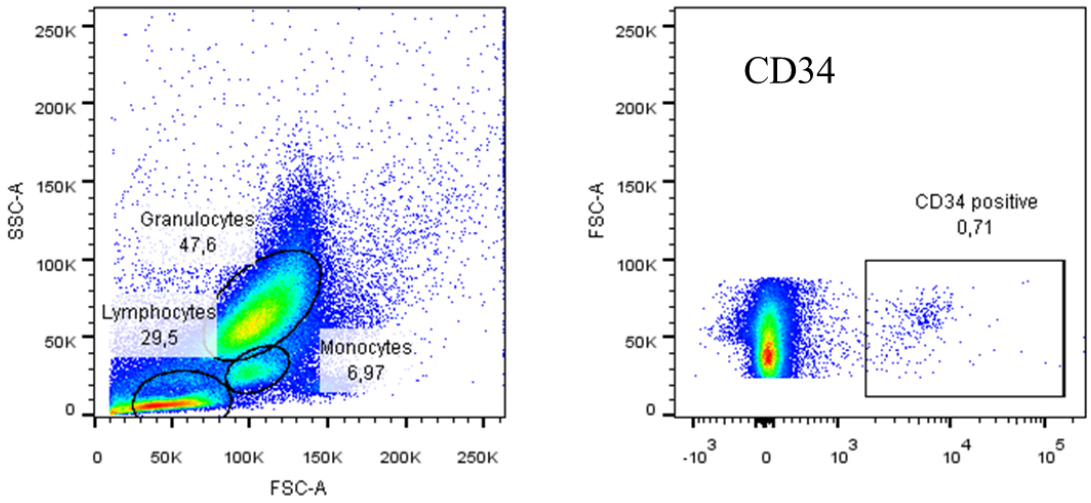

Figure 4.10 – UCB phenotypic characterisation. The evaluation of morphological parameters, side scatter (SSC) and forward side scatter (FSC), and expression of CD34 marker was done by flow cytometry (BD FACSCanto II™). The treatment of the acquired data was done using the FlowJo™ cytometry analysis software.

Within the $CD34^+$ UCB-lymphocyte population, we analysed the expression of several markers as presented in Figure 4.11 and Figure 4.12. This cell subset expresses CD133, CD117, CD44, HLA-DR and CD38. In a lower extent, these cells also present some expression of CD13 and a really low level of CD90 and CD123 (Figure 4.11).

Haematopoietic stem cell (HSCs) sources, like bone marrow and UCB, are usually constituted by a heterogeneous mixture of cellular populations. The more immature progenitors reside within the $CD34^+$ cell population compartment (Garg et al., 2013; Indumathi et al., 2013). To characterize the HSC compartment within the MNCs $CD34^+$ cells we used a matrix of markers that are usually expressed in hematopoietic cells like CD45 (all nucleated hematopoietic cells), CD117 (progenitor cells), CD13 (myeloid progenitors), CD38 (committed progenitors), CD133 (functional progenitor cells), CD44 (hematopoietic cells), HLA-DR (immunity development), CD90 (described in primitive cells), CD123 (subsets of hematopoietic progenitor cells) as described in the literature (Gori et al., 2012; Indumathi et al., 2013; Pessina et al., 2010; Radtke et al., 2015). Within the MNCs $CD34^+$ compartment we found the following phenotype (Figure 4.11): $CD45^+$, $CD133^{low/+}$, $CD177^{low/+}$, $CD44^+$, HLA-DR $^{low/+}$, CD38 $^{low/+}$, $CD13^{low}$, $CD90^{-/low}$, $CD123^{-/low}$.

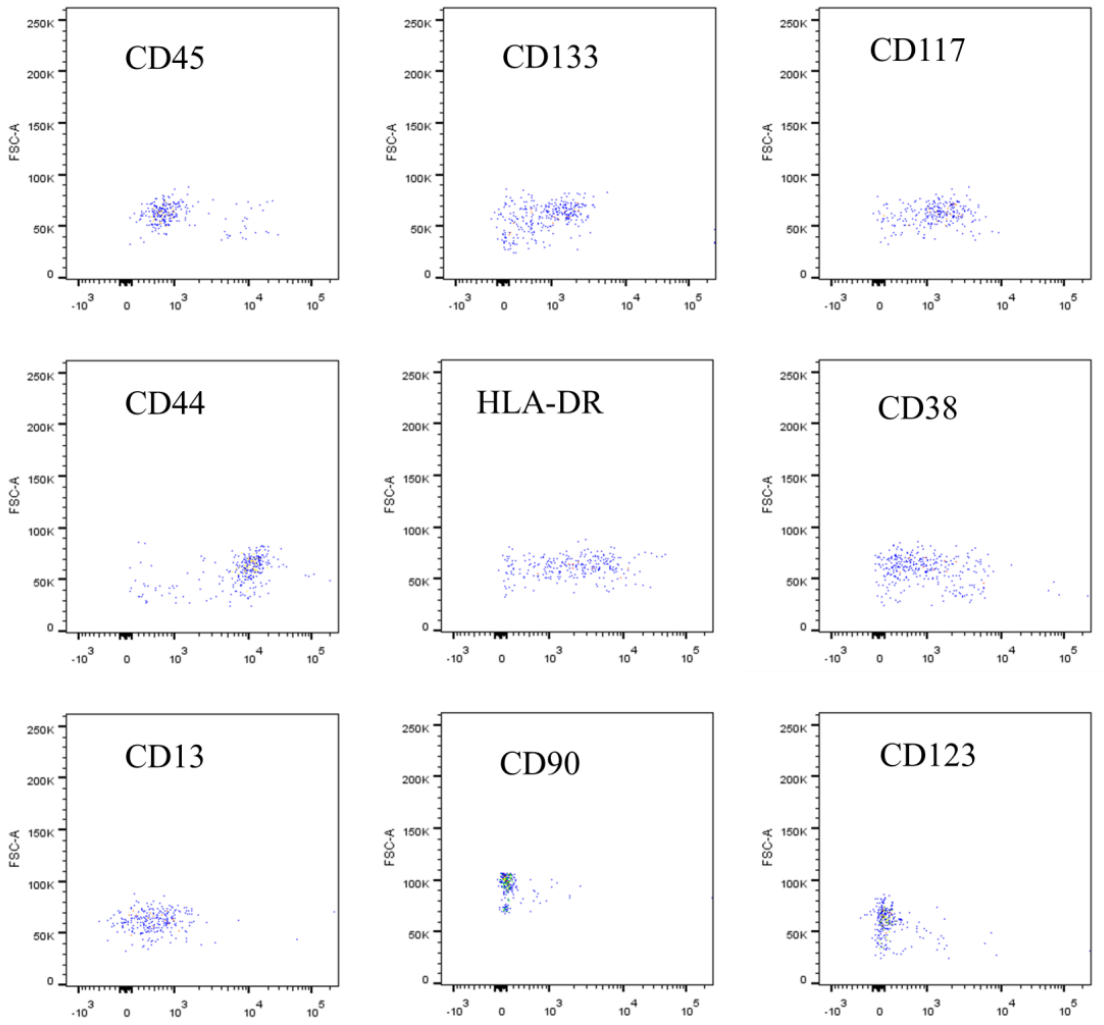

Figure 4.11 – UCB phenotypic characterisation. The evaluation of phenotypic parameters and expression of several markers within the $CD34^+$ cell population was done by flow cytometry (BD FACSCanto II™). The treatment of the acquired data was done using the FlowJo™ cytometry analysis software.

The cells within the MNCs $CD34^+$ compartment do not express CD105, CD35, myeloperoxidase (MPO) nor CD64 (Figure 4.12) as expected since these markers are associated with committed hematopoietic or endothelial phenotypes (Choi et al., 1998, 2012; Xu et al., 2012).

According to the literature and to our results, we chose the CD34 and CD133 markers for further experiments as a selection method for isolation of immature cells within the UCB-MNC compartment.

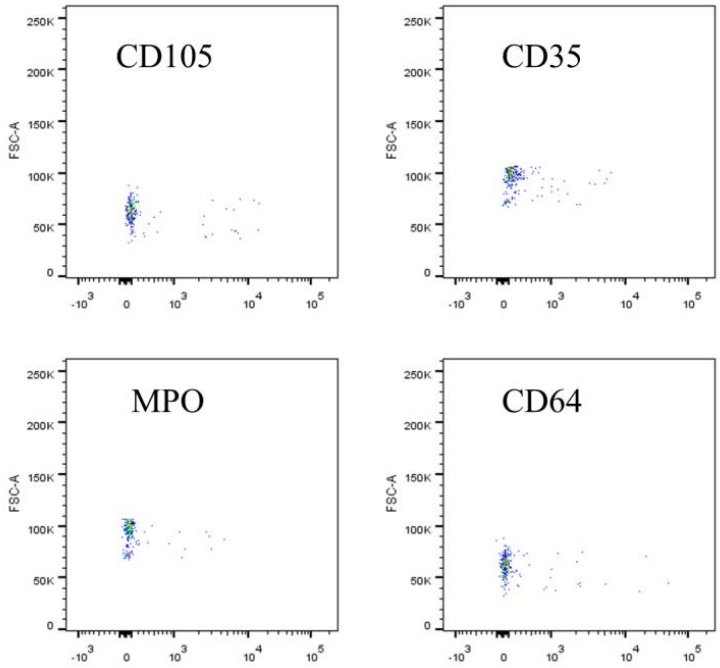

Figure 4.12 – UCB phenotypic characterisation. The evaluation of phenotypic parameters and expression of several markers within the $CD34^+$ cell population was done by flow cytometry (BD FACSCanto II™). The treatment of the acquired data was done using the FlowJo™ cytometry analysis software.

4.1.2.2. Osmotic influence in Umbilical Cord Blood cell reprogramming

We hypothesised that hyposmotic modulation could be used as a booster for reprogramming, particularly through the changes induced in chromatin structure. The major barriers to reprogramming are the epigenetic barriers that block or delay the establishment of new transcriptional programs (Brix et al., 2015; Delgado-Olguín and Recillas-Targa, 2011). Interestingly, some iPSCs display epigenetic marks characteristic from the mother cell (Anjamrooz, 2013; Delgado-Olguín and Recillas-Targa, 2011; Sebban and Buganim, 2016). Therefore, loosening the chromatin facilitates the access of the exogenous transcription factors (TFs) to the DNA and may promote the establishment of a new transcriptional network profile. This strategy of loosening the chromatin has been used through drugs and small molecules that modulate the activity of histone or DNA modifiers. These compounds can act on enzymes that regulate processes such as DNA methylation, histone acetylation and histone methylation and in an indirect way change the chromatin conformation and DNA accessibility (Feng et al., 2009; Su et al., 2013a; Wei et al., 2014).

In our point of view, a strategy to attain chromatin loosening by biophysical means would be unbiased and global. This strategy was already explored through the use of biomechanical cues given by different substrates but not with osmotic modulation (Downing et al., 2013). This could facilitate the access of TFs to the DNA, in a similar way to what happens to chromatin when histone and DNA modification drugs are used. Together with the presence of TFs and RNA Polymerase II (RNA Pol II) which are usually in stoichiometric excess within the cell, this could be used to improve processes of cell reprogramming or transdifferentiation.

Briefly, for UCB reprogramming, the MNC fraction was sorted for $CD34^+$ $CD133^+$ cells and infected with a polycistronic lentiviral vector containing the TF cocktail OSKM (Oct4, Sox2, Klf-4, c-Myc) (please see Materials and methods section for further details). The fluorescence-coded lentiviral vector used promotes a high expression of the OSKM factors but during reprogramming, these factors are rapidly silenced. This lentiviral vector was designed in parallel for murine and human applications and was shown to be able to transduce murine embryonic fibroblasts (MEFs) of an established and well-characterized Oct4-EGFP reporter mouse strain (OG2) and promote high expression of the fluorescent reporter protein (dTomato). The Oct4 driven expression of the EGFP was inversely correlated with the expression of the dTomato in this cell line. Therefore when differentiated cells acquire a pluripotent stem cell phenotype they lose the expression of dTomato. This loss of dTomato fluorescence is related with the retroviral promoter (spleen focus-forming virus U3 promoter – SFFV) used in the design of the viral vector. This promoter is highly efficient in driving expression in fibroblasts and other somatic cell types but is quickly silenced in cells undergoing epigenetic remodelling, like cells undergoing reprogramming processes (Warlich et al., 2011). Having these facts in mind, in this work, the complete reprogramming efficiency was calculated by counting the number of colonies that had already lost the expression of the lentiviral fluorescent reporter protein (dTomato) and at the same time displayed characteristic iPSC colony morphology. Additionally, colonies expressing the lentiviral fluorescent reporter protein (dTomato) were also evaluated over time and named as non-reprogrammed colonies. The modulation of the reprogramming process was done during the first week, detailed in Table 4.2, and the end point analysis was done at day 17.

In this work, apart from the hyposmotic modulation, some small molecules already described in the literature as reprogramming enhancers were used (Feng et al., 2009). These two small molecules were used as proxies for comparison of efficiencies of reprogramming between different strategies: (i) with respect to the impact on chromatin structure and (ii) to calcium modulation. We have chosen BayK (L-calcium channel agonist) a modulator of intracellular calcium levels as a proxy for the effect that the

osmotic modulation has on intracellular calcium and we have chosen valproic acid (VPA) a chromatin modification agent as a proxy for the physical effect that the osmotic modulation has on chromatin accessibility. On one hand, the precise effect of BayK on reprogramming efficiency boost is not clear, several publications claim different action mechanisms (Feng et al., 2009). On the other hand, VPA is a well-known histone deacetylase inhibitor that cannot by itself reprogram cells but promotes global transcriptional changes (Huangfu et al., 2008). In MEFs, VPA treatment induced upregulation of embryonic SC-specific genes and downregulation of lineage-specific genes (Huangfu et al., 2008). Therefore, VPA may support a predisposition towards pluripotency. Additionally, within the reprogramming context, the genome-wide acetylation induced by VPA allows the chromatin to relax, enhancing the binding of ectopically expressed reprogramming TFs (Huangfu et al., 2008). The osmotic modulation and small molecule treatments used in this work are presented in Table 4.2.

Table 4.2 – Modulation of UCB cells undergoing reprogramming.

Name condition	Scheme of osmotic modulation
Hypo2+/M after infection	Four hyposmotic shocks (15 minutes) during the first week of reprogramming.
Hypo2+/M before infection	One hyposmotic shock (15 minutes) before lentiviral infection plus four hyposmotic shocks during the first week of reprogramming.
Small molecules (VPA and BayK)	The drugs were always present in the culture medium during the first week of reprogramming.

The use of an L-calcium channel agonist (BayK) and a histone deacetylase inhibitor (VPA), promotes a significant increase (p value < 0.05; p value < 0.01) in the complete reprogramming efficiency of UCB $CD34^+$ $CD133^+$ cells (Figure 4.13). The reprogramming efficiency evaluation was done over time (Figure 4.14) and, in addition to counting the number of complete reprogrammed colonies, also colonies still expressing the lentiviral fluorescent reporter protein were assessed (Figure 4.15).

The hyposmotic modulation in this context (Table 4.2), using hESC media diluted with water, lead to a significant increase in complete reprogramming efficiency of UCB $CD34^+$ $CD133^+$ cells when the modulation started before the viral infection that induces the expression of pluripotency-related transcripts Figure 4.13.

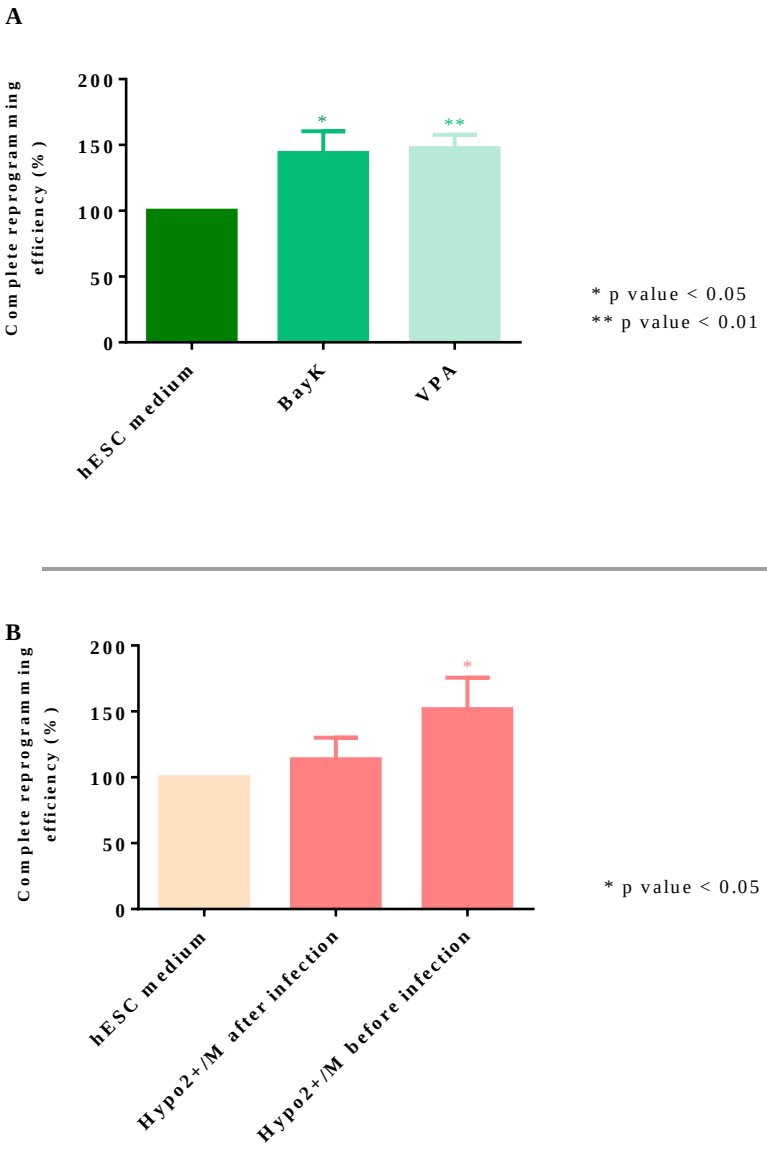

Figure 4.13 – Reprogramming efficiency with different modulation protocols in UCB CD34^{+}CD133^{+} cells. The reprogramming efficiency was assessed by counting the number of colonies that did not express the lentiviral fluorescent reporter protein (complete reprogramming efficiency) and displayed characteristic iPSC colony morphology at day 17. The control condition was considered to be 100% and the other conditions were normalised to this. In panel A, the effect of small drugs on UCB cell reprogramming is shown (±SEM; n=3). In panel B, the results of hyposmotic modulation on UCB cell reprogramming are shown (±SEM; n=3). These changes are statistically significant when highlighted in the graphs (p value < 0.05; p value < 0.01).

The hyposmotic modulation started before the lentiviral infection, which can be associated with a major drawback in regards to the number of viral inserts. Since the hyposmotic modulation alters the chromatin state and affects processes like endocytosis, the integration of viral inserts might be easier, as described for retroviruses in the literature (Lee and Peng, 2009). The hyposmotic environment was shown by others to be a promising tool that induces endocytosis and enhances retroviral transduction efficiency (Lee and Peng, 2009). Therefore, this type of osmotic modulation can lead to an increase in the reprogramming efficiency that might not be only related to the hyposmotic modulation itself but also with different levels of viral integration and expression of the reprogramming TFs.

Although the final reprogramming efficiency is the most important output to assess the potential use of this type of modulation to improve reprogramming protocols, it is very interesting and informative to study the kinetics of the process. During reprogramming, both colonies with and without expression of the lentiviral fluorescent reporter protein were monitored at day 10, 14 and 17. Within the small molecules group, the kinetic profile of reprogrammed colonies (Figure 4.14) is distinct between BayK and VPA. Although both conditions lead to the generation of approximately the same amount of colonies, with BayK the complete reprogrammed colonies emerge earlier (Figure 4.14). With regard to the hyposmotic modulation strategy, the kinetics of complete reprogramming follow a similar profile in both conditions (Figure 4.14).

With regard to the existence of colonies that express the lentiviral fluorescent reporter protein, there are some interesting features worthy of mention. The use of VPA significantly increases (p value < 0.05) the number of colonies expressing the lentiviral fluorescent reporter protein at day 10 and day 14 (Figure 4.15). This might be related to the inhibition of the histone modification machinery which might influence the silencing of the transgene. Additionally, when using the hyposmotic modulation strategies, the number of colonies expressing the lentiviral fluorescent reporter protein was very similar to the control situation (Figure 4.15). Although highly variable, at day 17 the condition with hyposmotic modulation after the infection shows an increase in the number of colonies expressing the lentiviral fluorescent reporter protein (Figure 4.15). Maybe this increase means that some colonies will reprogram in this condition at later time-points.

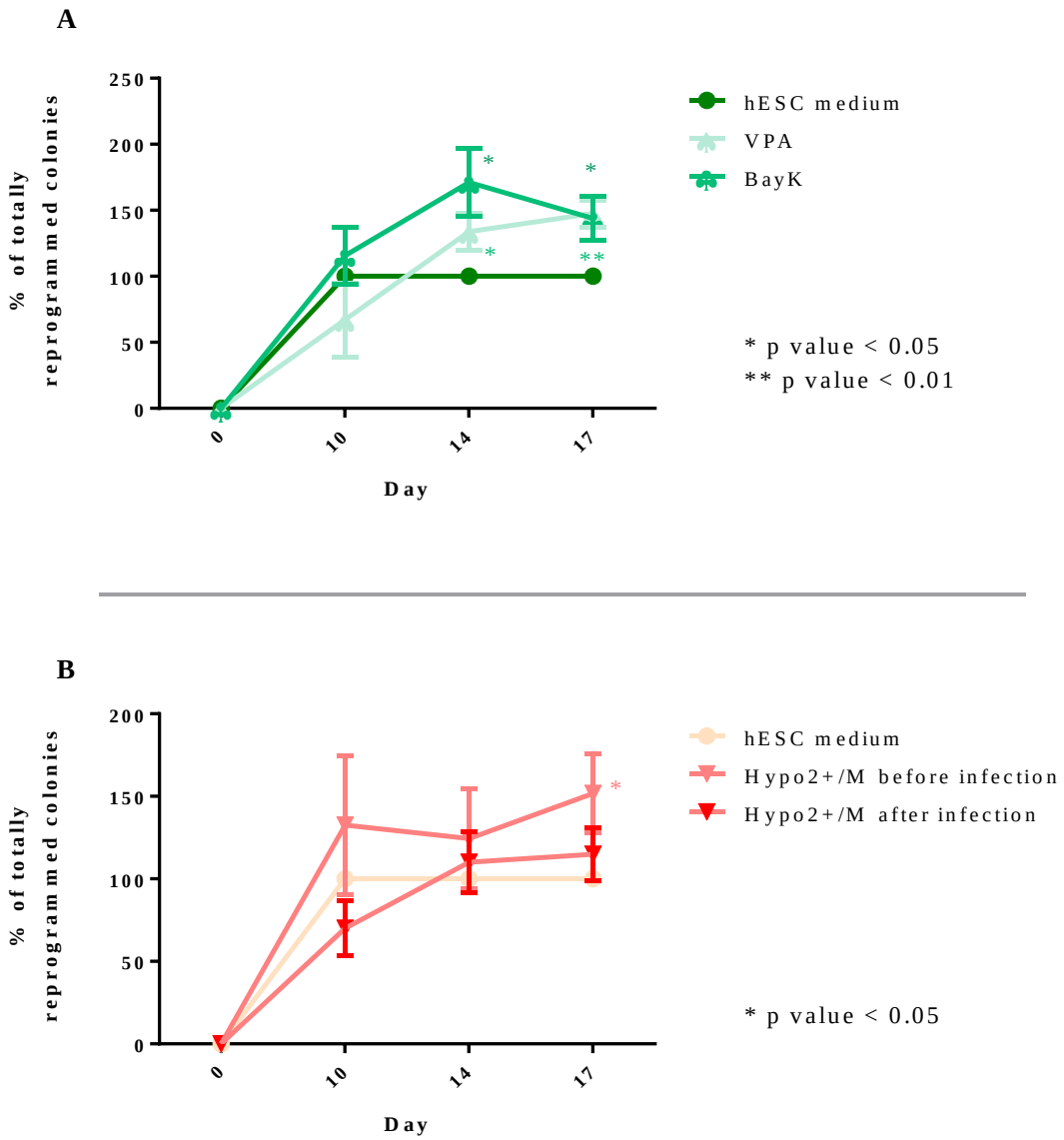

Figure 4.14 – Reprogramming kinetics with different modulation protocols in UCB CD34^{+}CD133^{+} cells. The reprogramming kinetics was assessed by counting the number of colonies that did not express the lentiviral fluorescent reporter protein (complete reprogramming) and display characteristic iPSC colony morphology at days 10, 14 and 17. The control condition was considered to be 100% and the other conditions were normalised to this value. In panel A, the effect of small drugs on UCB cell reprogramming over time is shown (±SEM; n=3). In panel B, the results of hyposmotic modulation on UCB cell reprogramming over time are shown (±SEM; n=3). These changes are statistically significant at the time points highlighted in the graphs (p value < 0.05; p value < 0.01).

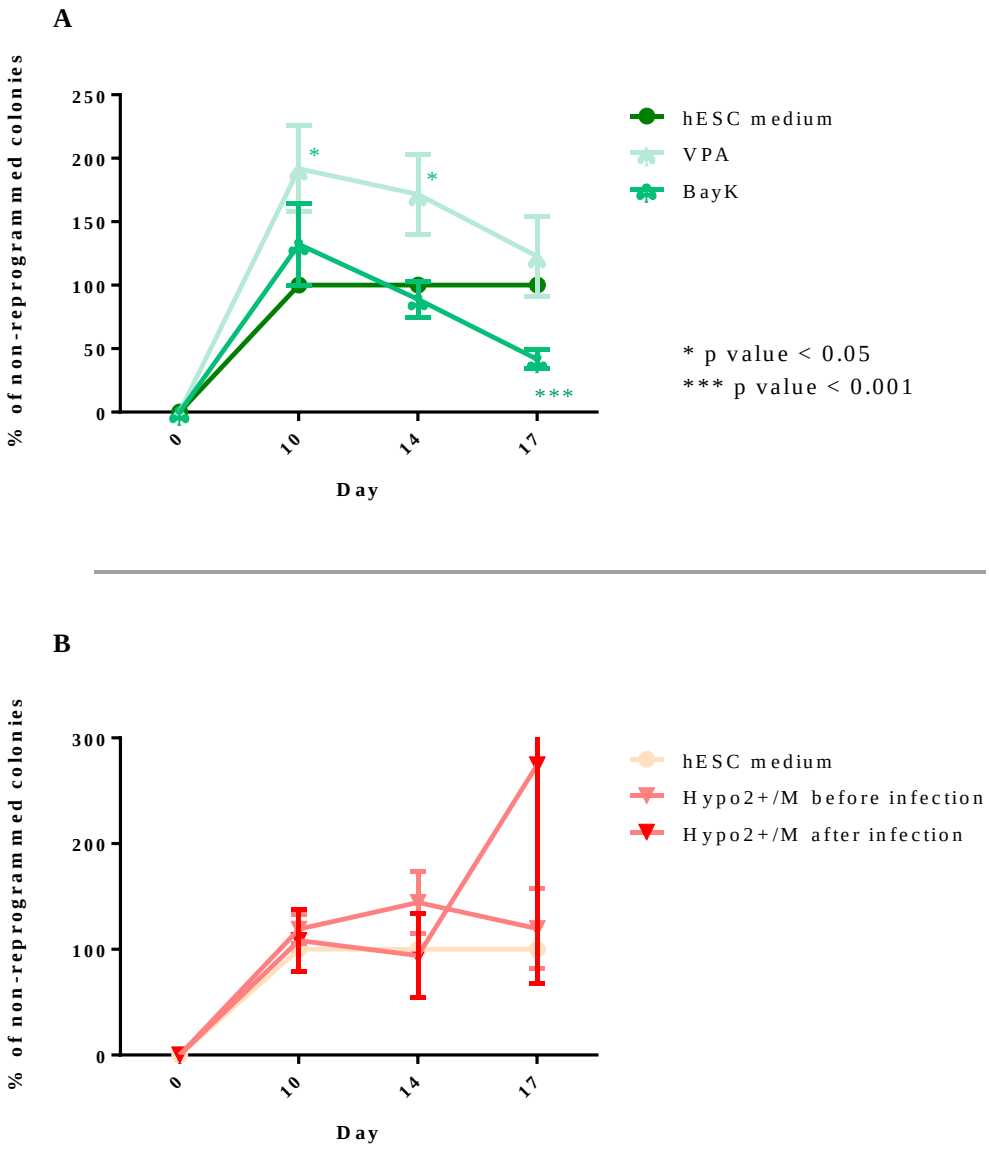

Figure 4.15 – Kinetics of non-reprogrammed colonies with different modulation protocols in UCB CD34^{+}CD133^{+} cells. The "non-reprogramming" kinetics was assessed by counting the number of colonies that did express the lentiviral fluorescent reporter protein (non-reprogrammed colonies) at days 10, 14 and 17. The control condition was considered to be 100% and the other conditions were normalised to this value. In panel A, the effect of small drugs on UCB cell "non-reprogramming" over time is shown (±SEM; n=3). In panel B, the results of hyposmotic modulation on UCB cell "non-reprogramming" over time is shown (±SEM; n=3). These changes are statistically significant at the time points highlighted in the graphs (p value < 0.05; p value < 0.001).

Nevertheless, the goal of this study was to obtain a hyposmotic modulation protocol which could in the same time frame, when compared with small molecules or other reprogramming boosters, have an impact on reprogramming efficiency.

Therefore, we decided to evaluate a new range of hyposmotic cocktails, containing PBS, and different modulation schemes. We did either a transient hyposmotic modulation or three transient hyposmotic modulations during the first week of reprogramming (Figure 4.16 A and B, respectively). Once again, the MNC fraction was sorted for $CD34^+$ $CD133^+$ cells and infected with a polycistronic lentiviral vector containing the TF cocktail OSKM.

Using both hyposmotic modulation strategies we couldn't see a significant impact in the reprogramming processes (Figure 4.16). Nevertheless, when performing the transient hyposmotic modulation three times during the first week of reprogramming there is an increasing trend from the condition hypo/PBS to hypo+/PBS (Figure 4.16). We believe that these results are also influenced by the variability of the cell state after UCB collection and storage. Although the biological number of replicates is two, we tried to perform the experiments in more samples but in some cases, we could not obtain any iPSC colonies after the reprogramming protocol. This variability problem will be reduced later in this chapter by using a cell line as a starting point for the reprogramming protocol.

The studies reported in this thesis with respect to the reprogramming experiments are based on the paper of Warlich et al. (2011) where the viral vector system that allows the visualisation and monitoring of the emergence of iPSCs are well described and validated. In order to be more confident that what we obtained in this work were really reprogrammed cells that could be cultured indefinitely without losing their properties, we decided to expand some of the iPSC colonies obtained from different UCB donors using the hyposmotic reprogramming protocol. Then we characterised the iPSCs phenotypically to see if they have the typical iPSCs markers.

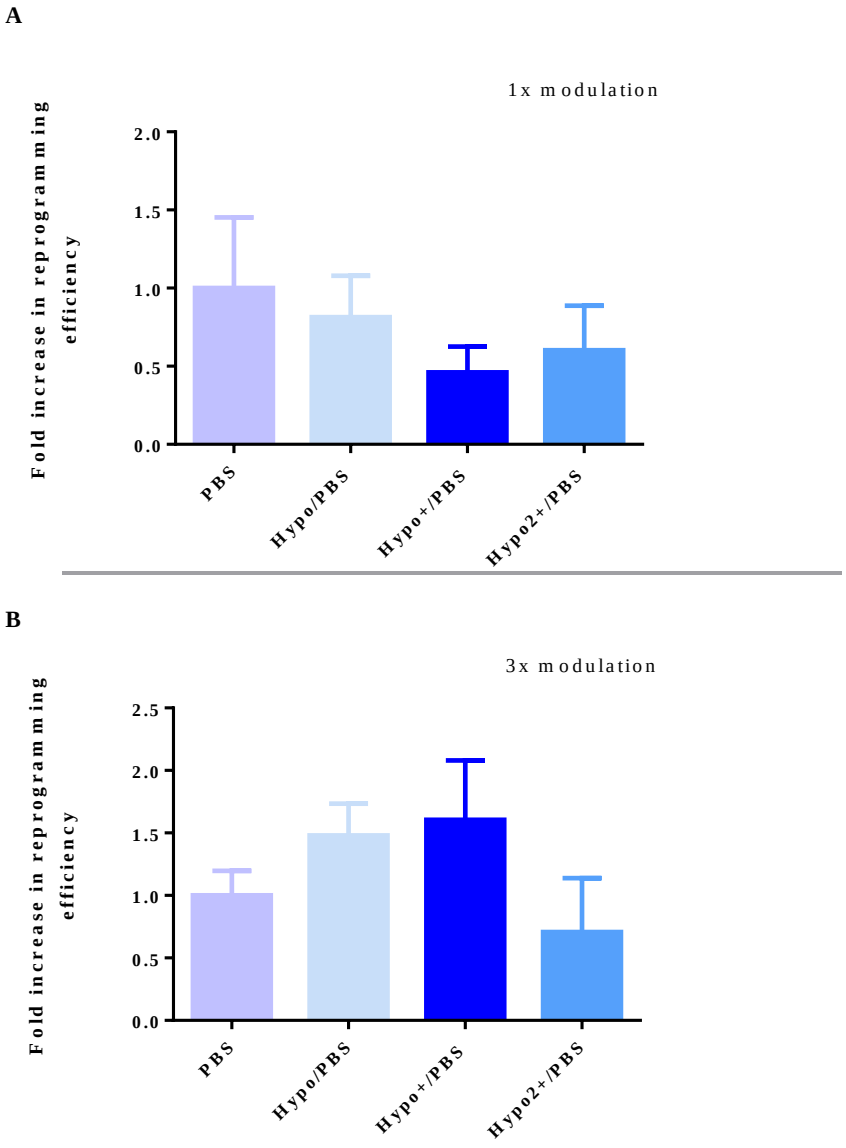

Figure 4.16 – Reprogramming efficiency with different hyposmotic modulation protocols in UCB CD34$^+$CD133$^+$ cells. The reprogramming efficiency was assessed by alkaline phosphatase staining of the cells in reprogramming at day 17. The control condition was considered to be 1 and the other conditions were normalised to this value. In panel A, the effect of a single hyposmotic modulation on UCB cell reprogramming is shown (±SEM; n=2). In panel B, the results of three hyposmotic shocks on UCB cell reprogramming is shown (±SEM; n=2).

The next subchapter is devoted to the phenotypic characterisation of UCB cells derived iPSCs and characterisation of an hESC line.

4.1.2.2.1. Characterisation of the derived induced pluripotent stem cells

After reprogramming, some colonies were mechanically picked and expanded for ten passages and treated enzymatically with collagenase IV afterwards. The cells showed typical features of iPSCs and strong expression of the pluripotency-related TFs Oct4, Sox-2 (Figure 4.17 and Figure 4.18) and Nanog (Figure 4.19).

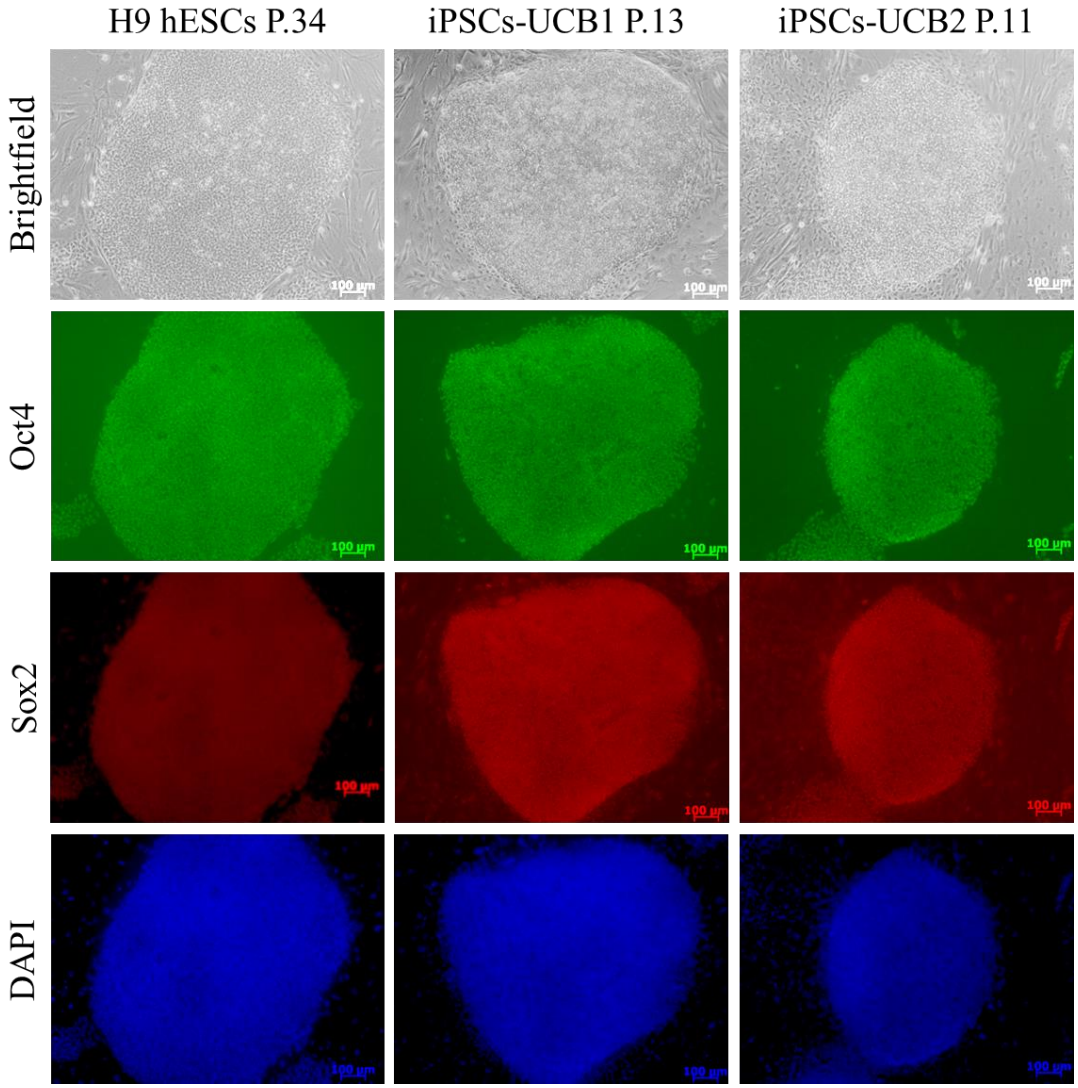

Figure 4.17 – Phenotypic characterisation of UCB derived iPSCs. Immunolabeling assessment of pluripotency-related markers expression (Sox2 and Oct4) in an hESC line (H9 hESCs passage 34) and in two different iPSC lines derived in our lab from two UCB donors (iPSCs-UCB1; iPSCs-UCB2 passages 13 and 11). The images were acquired with an Axioivert 200M microscope, scale bar 100μm.

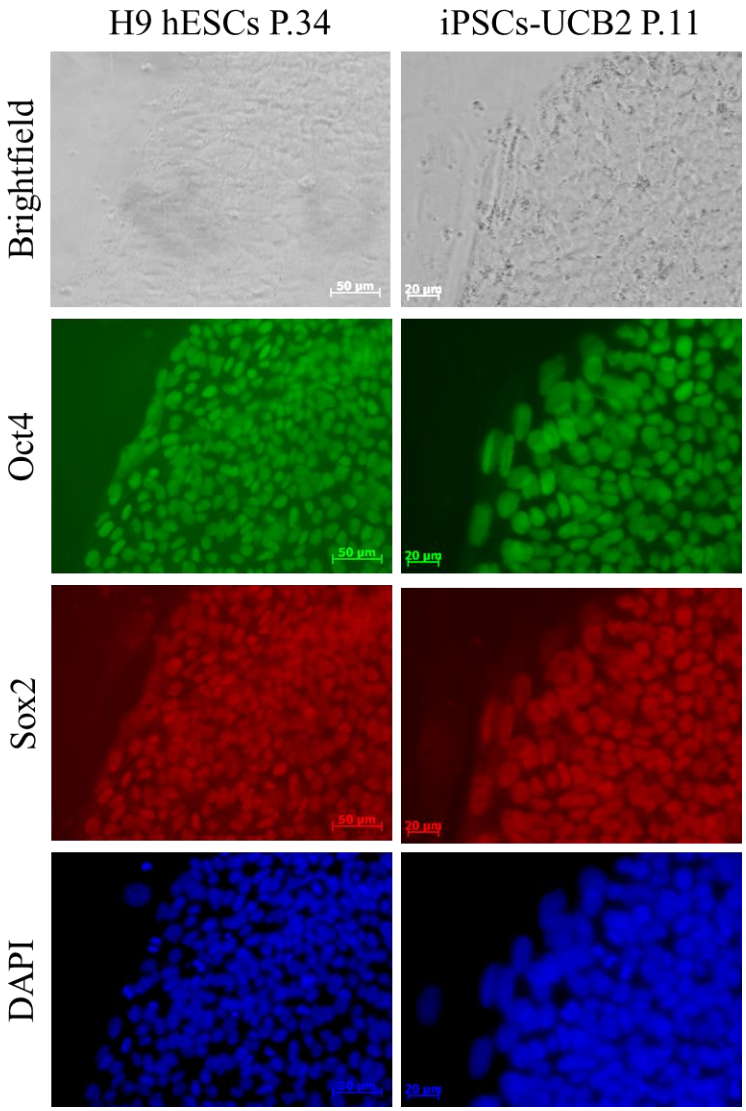

Figure 4.18 – Phenotypic characterisation of UCB derived iPSCs. Immunolabeling assessment of pluripotency-related markers expression (Sox2 and Oct4) in a hESC line (H9 hESCs passage 34) and one iPSC lines derived in our lab from UCB cells (iPSCs-UCB2 passage 11). The images were acquired with an Axioivert 200M microscope, (H9 hESC P.34 – scale bar 50µm; iPSCs-UCB2 P.11 – scale bar 20µm).

It is important to note that no transgene expression was present in these colonies as the fluorescent reporter protein is no longer expressed. Additionally, Nanog expression (Figure 4.19) is important to characterise the activation of the pluripotency-related transcriptional network since this TF was not included in the lentiviral vector used for the reprogramming process. Therefore, Nanog expression is not sustained by the lentiviral insert, so the iPSCs were at this point expressing pluripotent-related transcripts in an independent manner from the lentiviral vector.

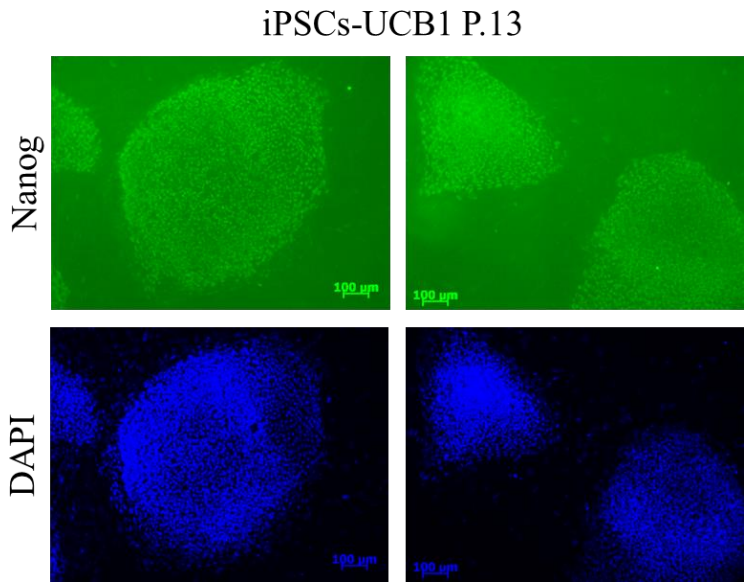

Figure 4.19 - Phenotypic characterisation of UCB derived iPSCs. Immunolabeling assessment of pluripotency-related marker expression (Nanog) in an iPSC line derived in our lab from UCB cells (iPSCs-UCB1 passage 13). Scale bar 100µm.

This characterisation is far from the full phenotypic and functional characterisation that usually is made to validate new iPSCs lines, including the ability to generate teratomas and contribution to germ line by the generation of chimaeras (for non-human iPSCs). Nevertheless, the objective here was to determine if these cells were able to express pluripotency-related markers in a similar fashion to what is seen in hESCs, independently from the viral vector we used.

As mentioned in the previous subchapter, the variability associated with UCB donor was a major drawback to assess the potential of the hyposmotic modulation protocol in terms of reprogramming efficiency. Although the tendencies were clear, statistical significance was difficult to be obtained in such a variable biological resource. Therefore, the next subchapter explores the use of a stable human fibroblast cell line for reprogramming studies.

4.1.3. Osmotic influence in fibroblast reprogramming

Normal dermal human fibroblasts (NDHFs) were subjected to several hyposmotic conditions during the reprogramming.

To assess the reprogramming efficiency a staining against AP at day 17 of the reprogramming process was done. In this case, as the colonies could not be counted manually, the IN Cell 2200 Analyzer was used to assess and calculate the positive AP staining area for each condition.

Cells were transiently modulated with a range of hyposmotic modulation cocktails, one or three times during the first week of reprogramming (Figure 4.20 A and B, respectively). When cells were transiently exposed to hyposmotic solutions once during the first week a significant increase (p value < 0.05; p value < 0.01) in the total AP positive staining was observed (Figure 4.20). This increase shows an inverse proportion to hyposmolarity (Figure 4.20). On the other hand, when the cells were transiently exposed to hyposmotic solutions three times during the first week there are no differences in the total AP positive staining when compared to the control (Figure 4.20). It seems that fibroblasts are more responsive to the hyposmotic modulation because a single modulation with the hyposmotic cocktails promotes an increase in reprogramming efficiency and three modulations seem to have no effect on the reprogramming efficiency (Figure 4.20). On the other hand in UCB cells, the scenario is the opposite and the condition where one stimulus was done in hypo+/PBS seems to have no impact in reprogramming efficiency when compared to three stimuli (Figure 4.16). Nevertheless, the UCB cells seem to reach a stress threshold imposed by the hyposmotic modulation because stimulating three times the cells in hypo2+/PBS has a deleterious effect in the process (Figure 4.16).

Although these results appear to be contradictory between them, it is important to consider specific important cellular features of these two cell types. During the reprogramming process, UCB cells are slightly attached to the feeder cell layer and, in general, they resemble the behaviour of cells which grow in suspension. Therefore, the compliance of both cell types, UCB cells (suspension cells) and NDHFs (attached cells), to hyposmotic modulation will be distinct because the cells will have osmotic regulatory systems and cellular structures (like the cytoskeleton, nucleus and cytoplasm) with different degrees of susceptibility to the same environment osmolarity challenges (Hunt et al., 2003a, 2003b). One of these restraints will be the different cytoskeleton structure and components that these cells have (Ragoonanan et al., 2013). Consequently, different modulation schemes and hyposmolarity range have different reprogramming outputs in these two cell sources (Figure 4.16 and Figure 4.20).

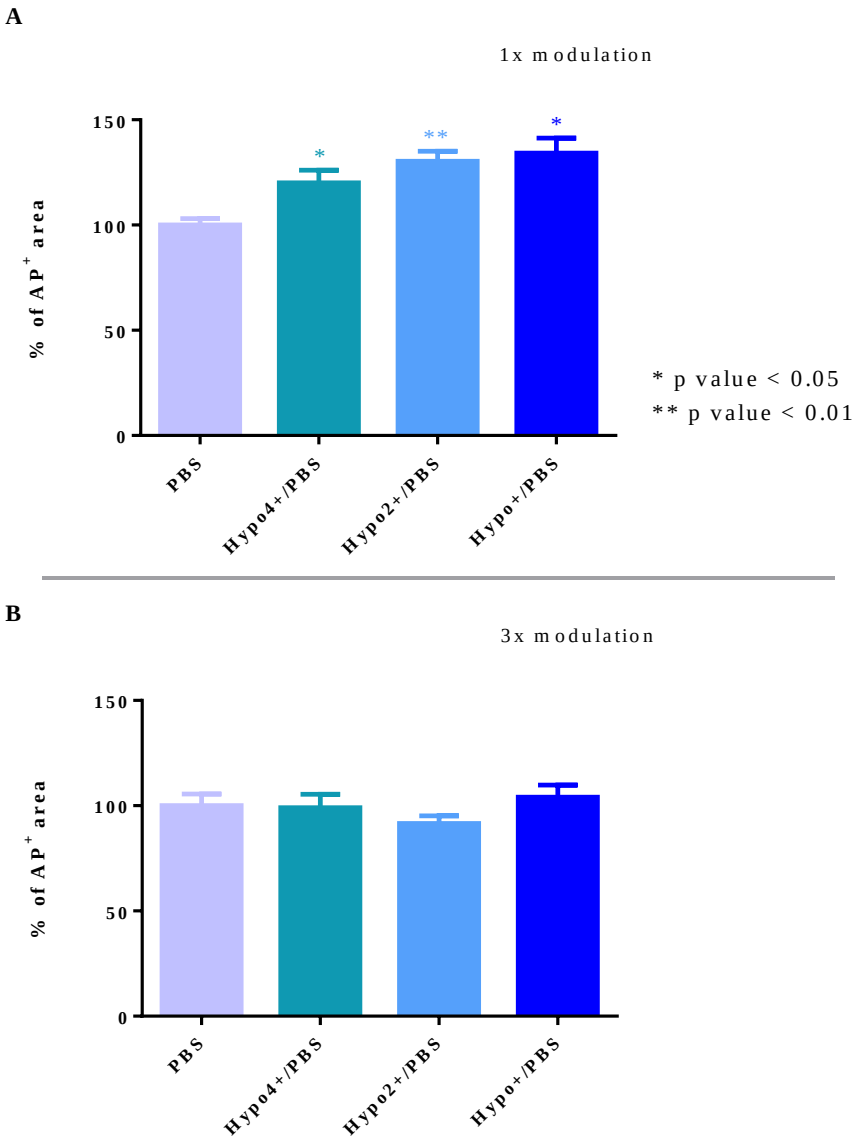

Figure 4.20 – Reprogramming efficiency with different osmotic modulation protocols in NDHFs. The reprogramming efficiency was assessed by alkaline phosphatase staining at day 17. The area for positive staining was calculated with the IN Cell Analyzer 2200. The control condition was considered to be 100% and the other conditions were normalised to this value. In panel A, the effect of a single hyposmotic modulation on NDHF reprogramming is shown (±SEM; n=4). In panel B, the results of three hyposmotic shocks on NDHF reprogramming are shown (±SEM; n=4). These changes are statistically significant when highlighted in the graphs (p value < 0.05; p value < 0.01).

Apart from the reprogramming efficiency and establishment of a new transcriptional network, the production of isoforms characteristic of specific phenotypes was also assessed. It is already described that pluripotency-related factors suffer alternative splicing (Atlasi et al., 2008; Das et al., 2011; Gabut et al., 2011; Gopalakrishna-Pillai and Iverson, 2011; Graveley, 2011), and in the case of Oct4 the splicing

events are associated with the generation of proteins characteristic either from pluripotent cells (Oct4A), cells undergoing differentiation or fully differentiated cells (Oct4-B1 and Oct4-B) (Atlasi et al., 2008). The analysis of the expression of Oct4, Oct4-A and Oct4-B was done on day 11 of reprogramming, where cells were modulated three times with the hyposmotic cocktails. With the hyposmotic modulation, a trend of decreased expression of all genes in the condition hypo4+/PBS and a specific downregulation of Oct4-B in the conditions hypo2+/PBS and hypo+/PBS can be observed (Figure 4.21). Additionally within the condition hypo4+/PBS, although expression of Oct4 and isoforms is downregulated, the ratio of expression between the two isoforms tested is maintained when compared to the reprogramming control (NDHF PBS) as shown in Figure 4.22.

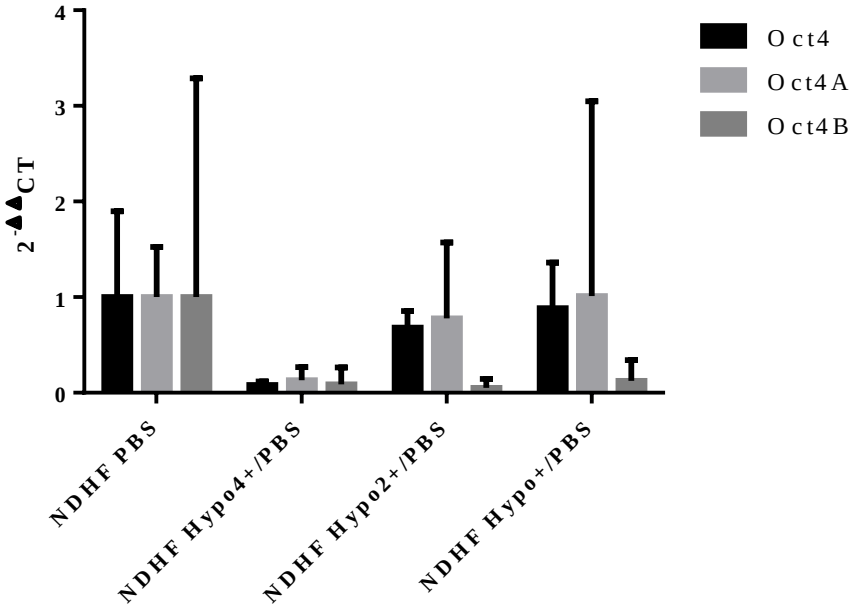

Figure 4.21 – Expression of Oct4 and Oct4 isoforms. Gene expression assessed by quantitative real-time PCR at day 11 of the NDHF reprogramming (±SD; n=1).

The conditions hypo2+/PBS and hypo+/PBS seem to induce a decrease of the expression of Oct4-B, the isoform characteristic of differentiated cells (Atlasi et al., 2008) as shown in Figure 4.21 and Figure 4.22.

This result is very interesting as alternative splicing is correlated with speed of transcription and cellular ATP content (Guantes et al., 2015; das Neves et al., 2010) and stress situations also drive the expression of long-non-coding RNAs (lnc-RNAs) that can also modulate the transcriptional adaptation (Zhao et al., 2016). Therefore, in this system would be very interesting to explore possible correlations

between reprogramming, metabolic and mitochondrial changes with transcription speed and generation of different isoforms and non-coding RNAs.

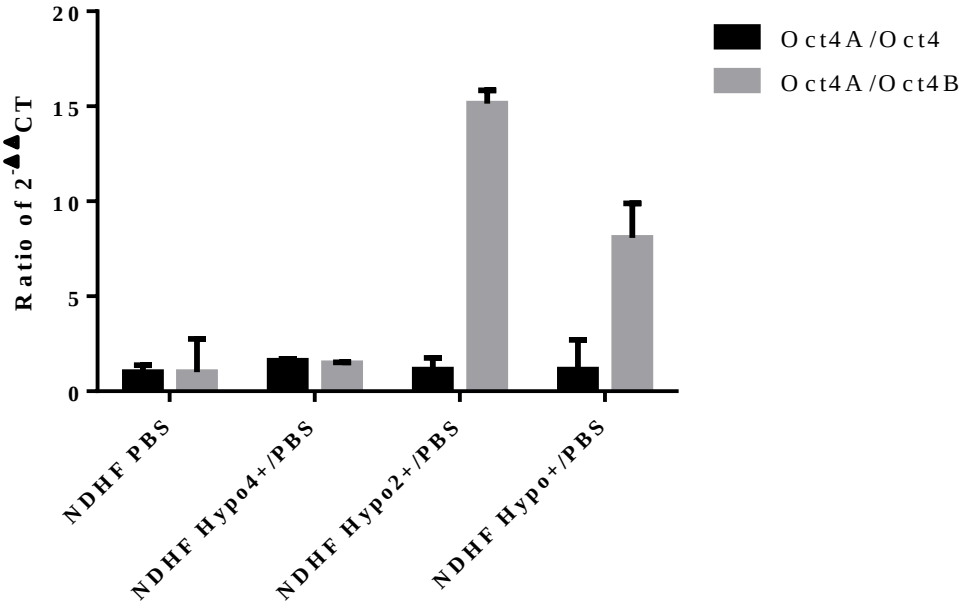

Figure 4.22 – Ratio of expression of Oct4 and Oct4 isoforms. Gene expression assessed by quantitative real-time PCR at day 11 of NDHF reprogramming (±SD; n=1).

These experiments guided our interest into a physiological system where changes in osmolarity can occur. It is difficult to find in the literature reports where osmotic imbalances have causal relationships with pathophysiological conditions. Nevertheless, the relevance of the ionic balance in several diseases such as cancer has been shown during the past years (Lang and Stournaras, 2014; Nriagu et al., 2016; Sontheimer, 2009). The research suggests that certain ion channels, K^+ channels in particular, may be involved in aberrant tumour growth (Sontheimer, 2009). In the particular case of glioma, cell invasion and the formation of brain metastasis has been associated with the activity of K^+ and Cl^- channels (Sontheimer, 2009).

To model *in vitro* the impact that osmolarity can have in pathophysiological scenarios is very complex and would involve many uncontrollable variables. Nevertheless, we believe that simple systems that allow a controllable overexpression of a defined set of TFs are useful tools for proof of concept of the impact that osmolarity may have in cell phenotype and fate. Moreover, reporter cell lines for relevant cellular functions are also very useful and informative tools. Therefore in the next chapter, the impact of environmental changes in cell phenotype, cell fate decisions and alternative splicing will be explored. To

address these issues we used a transdifferentiation system by overexpression of CEBPα (Bussmann et al., 2009) and a neuroblastoma reporter cell line for alternative splicing events (Zheng et al., 2013).

4.2. Concluding observations

This chapter provides evidence of the importance of the osmolarity control and the phenotypic impacts that it can have under specific cellular situations.

Within the scope of this chapter is important to point out that the osmotic control and osmotic imbalances:

- Have a relevant role in the phenotypic characteristics of UCB cells;
- Can be used as a tool to achieve quicker kinetics and better efficiencies of reprogramming;
- Seems to differentially promote the expression of gene isoforms.

Chapter 5 : Osmolarity influence on cell commitment to metabolic and phenotypic fates

Cell fate determination is a very complex process and is not only determined by embryonic development and normal physiology but also by pathological events (Ito and Ito, 2016; Madonna et al., 2013; Morris and Daley, 2013; Pauklin and Vallier, 2013; Sugawara et al., 2012; Symmons and Raj, 2016; Wagers and Christensen, 2002; Wu and Ng, 2011). Maintenance and differentiation of specialised tissues are regulated by coordination between differentiation and proliferation of specific stem or progenitor cells (Cao et al., 2013; Tavakoli et al., 2009). The relevance of these mechanisms has been well documented in early development in different systems and tissues (Fuchs, 2009; Lange and Calegari, 2010; Li and Clevers, 2010) and also in different disease scenarios like cancer (Honeycutt et al., 2004). Very recently, a study hypothesised that stem cell (SC) mutagenesis together with extrinsic factors that promote SC proliferation, create a "perfect storm" which ultimately determines cancer risk for a specific tissue or organ (Zhu et al., 2016).

Nevertheless, experiments by John Gurdon have shown that the adult cell fate and adult cell phenotype is not a static nor an irreversible state (Gurdon, 1962). In this experiment, the transplantation of intestinal epithelial cells nuclei from feeding tadpoles into enucleated eggs gave rise to normal and healthy tadpoles (Gurdon, 1962). Cell fate reversibility was recently challenged by the work of Shinya Yamanaka and colleagues (Takahashi et al., 2007). Where they described a new concept for pluripotency induction, attained by forced expression of embryonic related genes to revert the somatic cell phenotype into a pluripotent state (induce pluripotency stem cells – iPSCs) (Takahashi et al., 2007). In addition, the somatic nuclear transfer was also proven to be able to give rise to pluripotent cells as described by French and colleagues (French et al., 2008). It has also been shown by several groups, that is possible to transdifferentiate a specific somatic cell into another different somatic cell by induction of specific transcription factors (TFs) (Chin, 2014; Graf, 2011; Ladewig et al., 2013; Orkin and Hochedlinger, 2011; Sebban and Buganim, 2016). These breakthroughs challenged the classical view of cell fate and lineage commitment.

Cell fate is determined by a unique combination of gene expression profiles which lead to a protein repertoire in each specialised cell. Although the vast majority of studies tend to give a dominant role to genetics and epigenetics, there has been a recent focus on metabolism and mitochondrial function which seem to be essential for cell function and cell fate decisions (Folmes et al., 2012a; Galloway et al., 2012; Guantes et al., 2015; Ito and Ito, 2016). Mitochondria are essential to lineage commitment and development of organic systems like the heart. It is also a key player in processes like reprogramming and

transdifferentiation (Chen et al., 2012; Prigione et al., 2015; Wanet et al., 2015). Mitochondrial function is greatly influenced by the environmental conditions that surround the cells and enable the cells to adapt to different energy requirements depending on the type of substrate available (Gottlieb and Bernstein, 2016; Picard et al., 2013).

In the next subchapters, we will explore the environmental influence, namely osmolarity and glucose content, in systems where cell commitment and cell phenotype decisions were evaluated.

5.1. Results and Discussion

5.1.1. The influence of osmolarity in transdifferentiation

The transdifferentiation system used in this work is a B-cell line with a β-estradiol-inducible form of C/EBPα, where the original cells can be converted into macrophage-like cells with high efficiency as described in the literature (Bussmann et al., 2009). Chromatin structure remodelling is an essential step to overcome obstacles to the establishment of the new transcriptional profile characteristic of macrophage-like cells. With this in mind, some transdifferentiation systems apply the expression of pluripotency-related factors to enhance chromatin remodelling and then introduce the transdifferentiation specific TFs (Han et al., 2015; Mitchell et al., 2014). This is because, the great majority of the pluripotency-related factors have been shown to have a pioneer activity; which is defined by the ability to bind to DNA in areas where chromatin is tightly packed (Zaret and Carroll, 2011). Therefore, the use of pioneer factors, within transdifferentiation, is a tool for chromatin loosening and facilitates the access of the transdifferentiation factors to the respective DNA binding sites (Han et al., 2015; Mitchell et al., 2014). C/EBPα has been described as a pioneer factor and therefore this transdifferentiation system has a high and robust efficiency which can be related to the ability of this TF to bind to DNA even in packed chromatin areas (Bussmann et al., 2009; van Oevelen et al., 2016). Indeed, the transdifferentiation system that we used in this work is very efficient; 100% efficiency can be achieved in certain conditions. Also, it allows temporal control of the process because it is an inducible system. The detailed description of this experiment is provided in the Material and methods section, but briefly, the experimental layout consisted in the induction of transdifferentiation by the addition of β-estradiol and the transient osmotic modulation started one day after this point.

The transdifferentiation cell line was characterised; the cells display the specific morphology, expression of CD19, a B-cell marker, and absence of expression of CD11b, a macrophage marker, as shown in Figure 5.1. It is also possible to observe in Figure 5.1 that the cell line expresses enhanced green fluorescent protein (EGFP) as a reporter of the construct.

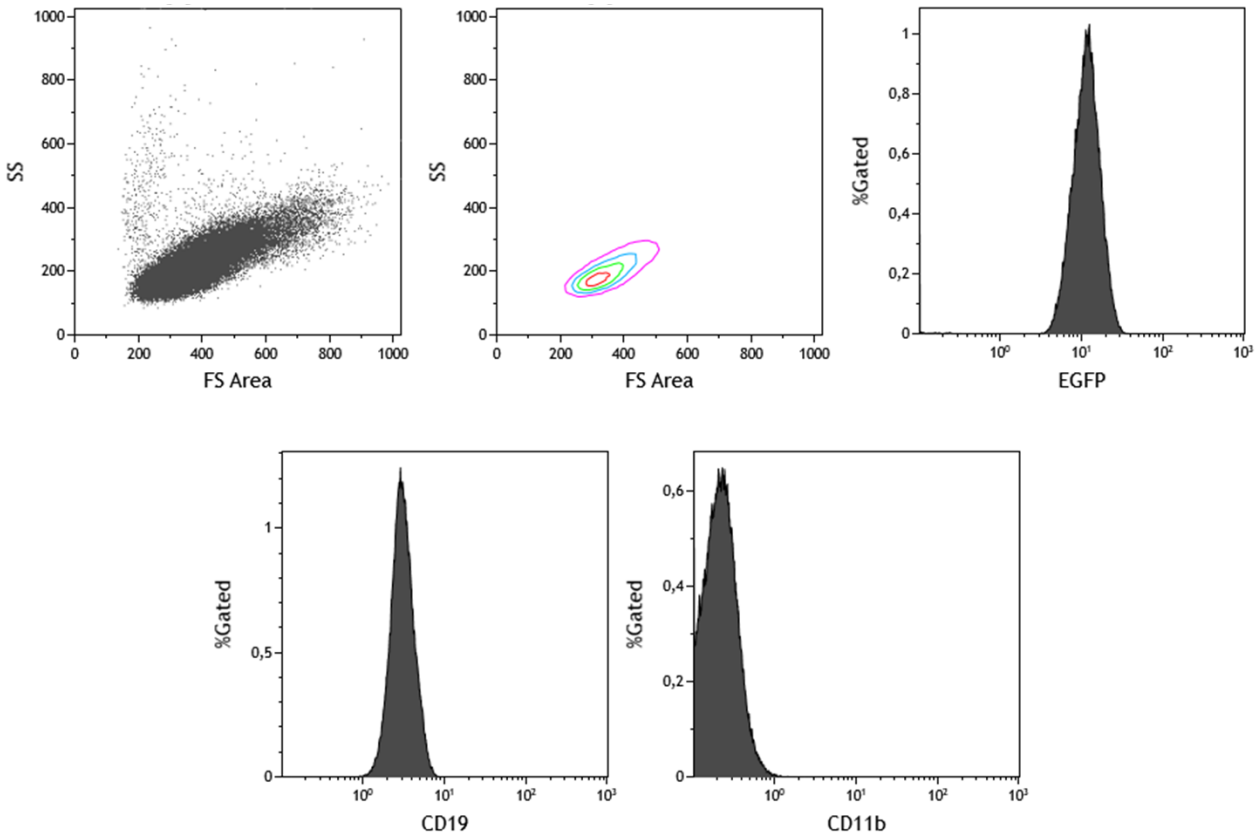

Figure 5.1 – HAFTL C10 cell line phenotypic characterisation. HAFTL C10 cell line flow cytometry analysis for cell morphology, side scatter (SS) and forward side scatter (FS), EGFP expression (cell line reporter protein), labelling with CD19 and CD11b prior to induction of cell transdifferentiation. Although the images provided are from a single experiment, the same experiment was repeated at least three more times with similar results.

Several osmotic modulation schemes were tested, but the osmotic modulation which leads to a difference in expression of CD11b at day 4 of transdifferentiation was the condition where an hyposmotic shock with hypo2+/PBS was done once a day 24 hours after the addition of β-estradiol, during 3 consecutive days. During the transdifferentiation process, the cells were evaluated for cell morphology (Figure 5.2), expression of CD11b and CD19 (Figure 5.3 and Figure 5.4) and sampled for RNA extracts.

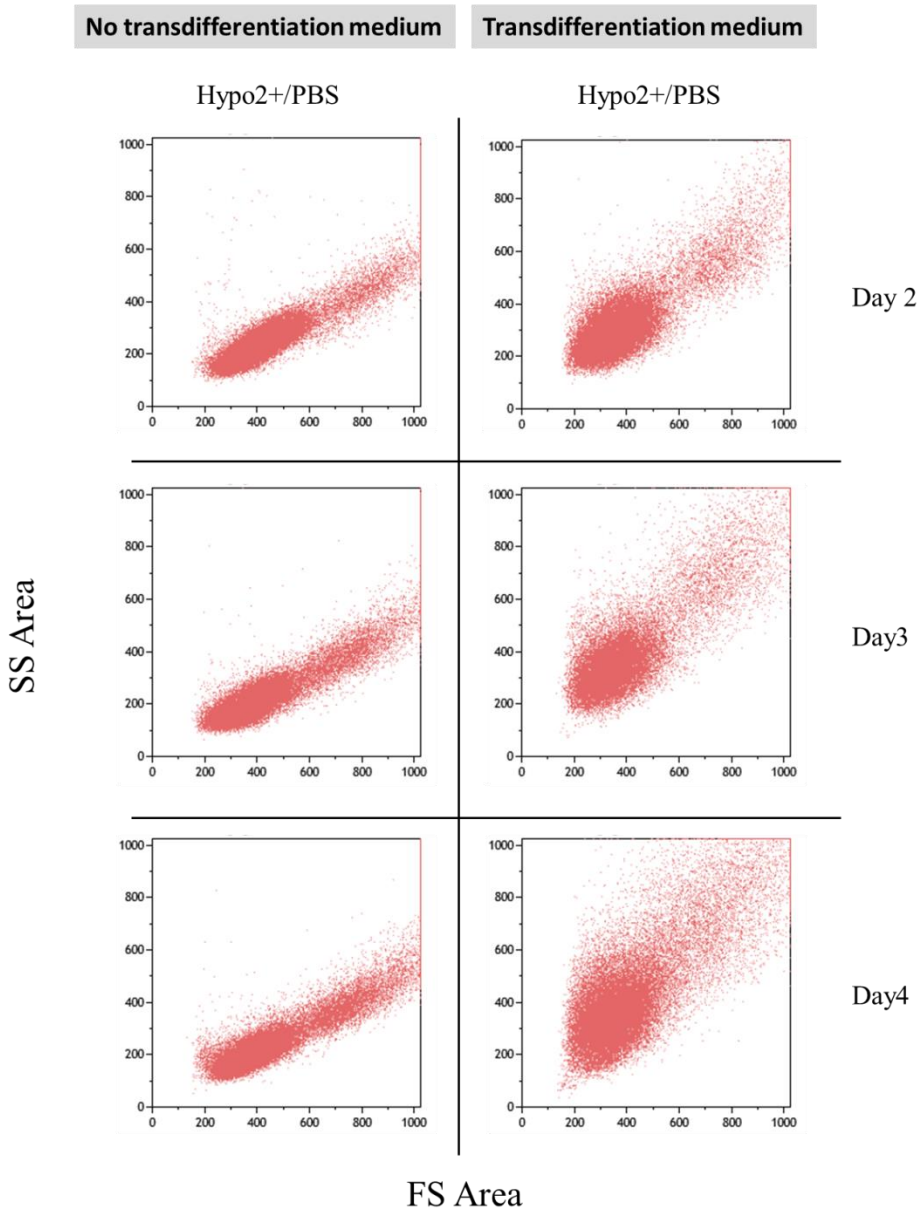

Figure 5.2 – HAFTL C10 cell line morphology assessed during the transdifferentiation process. HAFTL C10 cell line flow cytometry analysis for cell morphology, side scatter (SS) and forward side scatter (FS), during the cell transdifferentiation process. Although the images provided are from a single experiment, the same experiment was done at least two more times with similar results.

The morphology of the cell is a very important parameter in this transdifferentiation setting. During this transdifferentiation protocol, there is a clear increase in the side scatter parameter (SS) which denotes an increase in cell granularity (Figure 5.2). This change is consistent with reports in the literature and denotes the appearance of the macrophage-like phenotype (Bussmann et al., 2009).

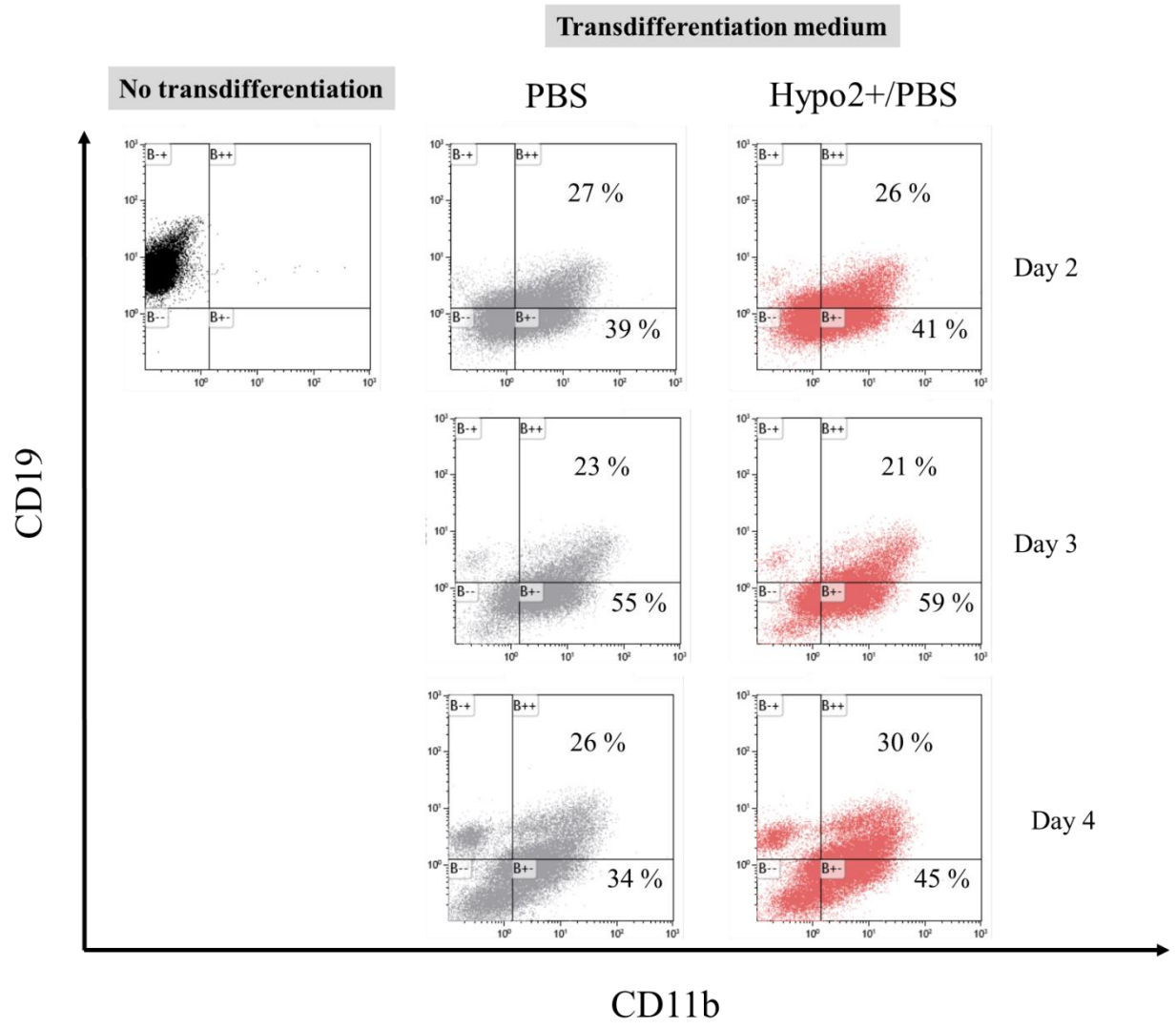

Figure 5.3 – HAFTL C10 cell line phenotypic characterisation assessed during the transdifferentiation process. HAFTL C10 cell line flow cytometry analysis of CD19 and CD11b expression within the control condition (No transdifferentiation) and the transdifferentiation conditions without osmotic modulation (PBS) or with osmotic modulation (hypo2+/PBS). Although the images provided are from a single experiment, the same experiment was done at least two more times with similar results.

The hyposmotic stimulus promotes an increase in the percentage of cells expressing CD11b, a macrophage-specific marker, and a reduction of expression of CD19, a B-cell-specific marker, as shown in Figure 5.1, Figure 5.3 and Figure 5.4. The loss of expression of CD19 at day 3 in the transdifferentiation condition where the hyposmotic modulation was used seems to be more noticeable (Figure 5.4).

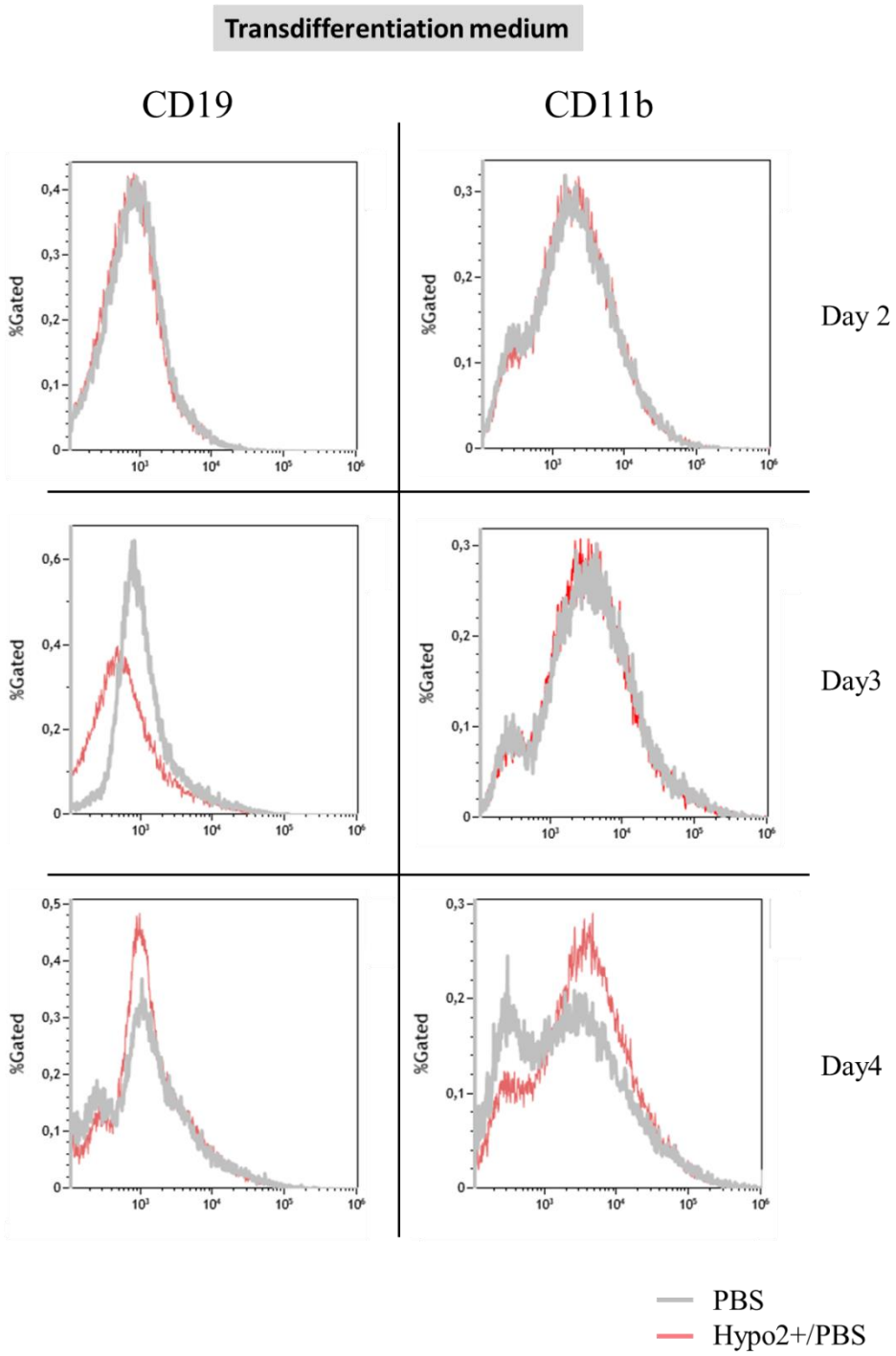

Figure 5.4 – HAFTL C10 cell line phenotypic characterisation assessed during the transdifferentiation process. HAFTL C10 cell line flow cytometry analysis of CD19 and CD11b expression during cell transdifferentiation within the control condition (PBS) and the transdifferentiation condition with osmotic modulation (hypo2+/PBS). Although the images provided are from a single experiment, the same experiment was done at least two more times with similar results.

The average of CD11b positive normalised cell percentage and the intensity levels at day 4 of transdifferentiation can be seen in Figure 5.5 and Figure 5.6, respectively. Within the transdifferentiation process, when β-estradiol is added to the cell culture media, the hyposmotic modulation (hypo2+/PBS) has a significant impact (p value < 0.05) on the percentage of cells expressing the macrophage-related marker CD11b at day 4 when compared to the control (PBS) (Figure 5.5).

As expected, if β-estradiol is not added to the cell culture media (No transdifferentiation conditions), the cells do not express CD11b at day 4 of the transdifferentiation (Figure 5.5). And the hyposmotic stimuli by itself have no effect on the HAFTL C10 cell line CD11b expression without induction of transdifferentiation (No transdifferentiation PBS versus No transdifferentiation hypo2+/PBS in Figure 5.5).

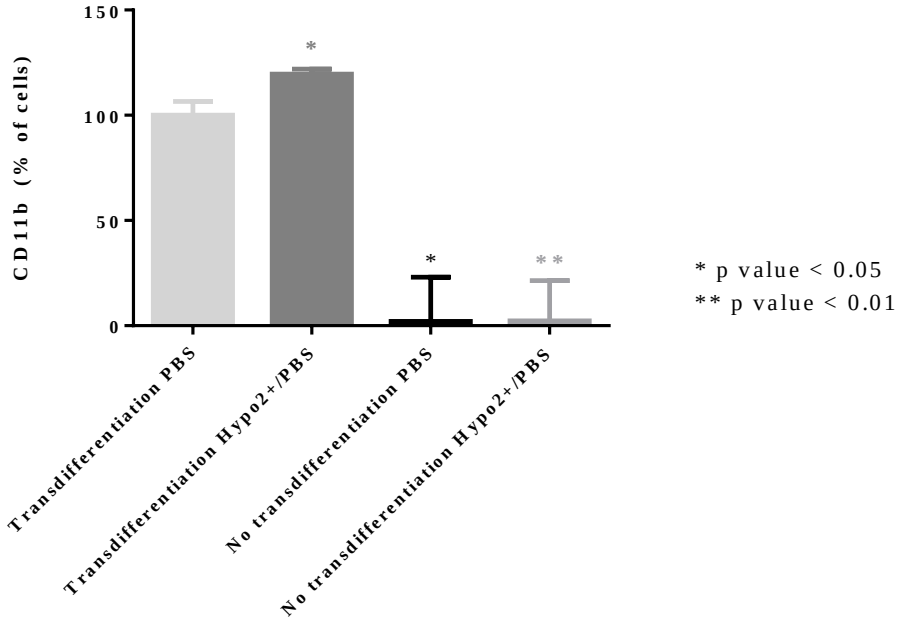

Figure 5.5 – HAFTL C10 cell line phenotypic characterisation assessed at day 4 of transdifferentiation. HAFTL C10 cell line flow cytometry analysis for CD11b expression at day 4. The negative control conditions (No transdifferentiation) without (PBS) and with osmotic modulation (hypo2+/PBS) and the transdifferentiation condition without (PBS) and with osmotic modulation (hypo2+/PBS) percentage of cells expressing CD11b normalised to the transdifferentiation control condition (PBS) (±SEM; n=3). The change is statistically significant when highlighted in the graphs (p value < 0.05; p value < 0.01).

The cells subjected to the hyposmotic modulation express the same intensity level of CD11b (Figure 5.6) as the transdifferentiation control, meaning that there is an increase of the efficiency of the transdifferentiation process in terms of cell number obtained with macrophage-like characteristics. As

CEBPα can act as a pioneer factor in this transdifferentiation system, the hyposmotic stimulus might promote just access to a few DNA areas, and the impact of this modulation may promote bigger differences in systems using non-pioneer TFs or where the epigenetic landscape of the mother cells is really unfavourable to cell fate alterations.

Nevertheless, even using a pioneer factor based system the transcription profile of the cells during transdifferentiation is also shifted towards a macrophage-related profile and with differences when performing the hyposmotic transient stimuli.

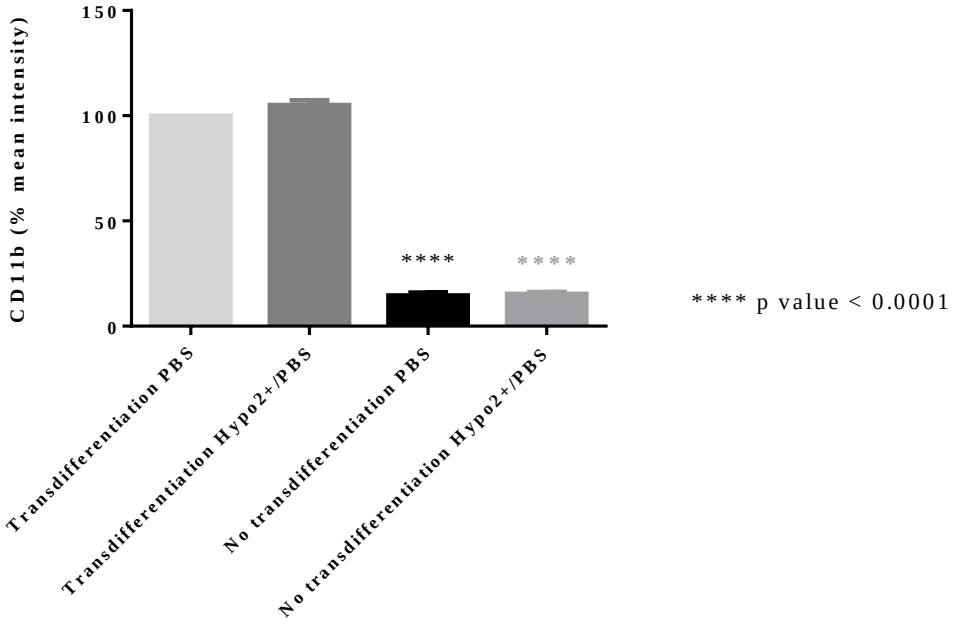

Figure 5.6 – HAFTL C10 cell line phenotypic characterisation assessed at day 4 of transdifferentiation. HAFTL C10 cell line flow cytometry analysis for CD11b expression at day 4. The negative control conditions (No transdifferentiation) without (PBS) and with osmotic modulation (hypo2+/PBS) and the transdifferentiation condition without (PBS) and with osmotic modulation (hypo2+/PBS) mean fluorescence intensity of cells expressing CD11b normalised to the transdifferentiation control condition (PBS) (±SEM; n=3). The change is statistically significant when highlighted in the graphs (p value < 0.0001).

The hyposmotic modulation has a positive effect on the expression of CEBPα during the transdifferentiation (Figure 5.5) but interestingly it also promotes the expression of CEBPβ and CEBPΔ (Figure 5.7). This effect is significant and might denote increased access to chromatin regions within the osmotic modulation condition that favours the expression of these particular genes, which are in excess within the cell nucleus.

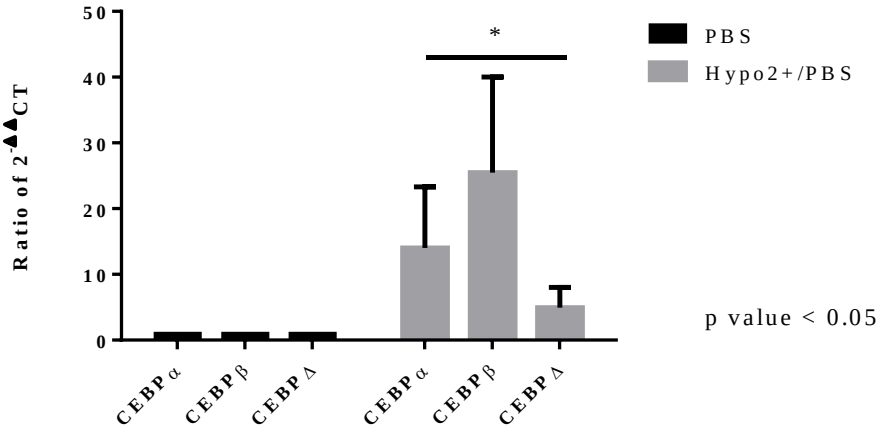

Figure 5.7 – Transcriptional characterisation of CEBP-family genes assessed at day 4 of transdifferentiation in HAFTL C10 cell line. HAFTL C10 cell line characterisation was done by qRT-PCR analysis at day 4. The transdifferentiation without osmotic modulation (PBS) and with osmotic modulation (hypo2+/PBS) conditions were normalised by their respective negative controls (No transdifferentiation PBS and hypo2+/PBS). After calculation of ΔΔCT, a ratio between the expression levels ($2^{-\Delta\Delta CT}$) in the two transdifferentiation conditions was done (±SEM; n=3). The change is statistically significant when highlighted in the graphs (p value < 0.05; two-way ANOVA test).

Moreover, some of the genes, shown to be increased by the microarray analysis done in the publication where this transdifferentiation system was described (Bussmann et al., 2009), were also significantly increased after the transdifferentiation with hyposmotic transient modulation when compared to the control transdifferentiation. These genes included FOS, FOSL2, JUN and NFIL3 (Figure 5.8). Although, these genes are involved in the transdifferentiation they are also involved in other pathways that might be influenced in different ways by the transient hyposmotic stimuli. One of the hits for TF association scores to the different areas where RNA Polymerase II (RNA Pol II) is bound in the chromatin in our results described in Chapter 3 included FOS and JUN. Therefore the osmotic modulation by itself might already favour the binding of these TFs.

Additionally, as these cells are transdifferentiating towards a macrophage-like phenotype there is a decrease of B-cells master regulators, like Pax5, and chromatin-associated factors (Figure 5.9) as seen in the publication where this transdifferentiation system was described (Bussmann et al., 2009).

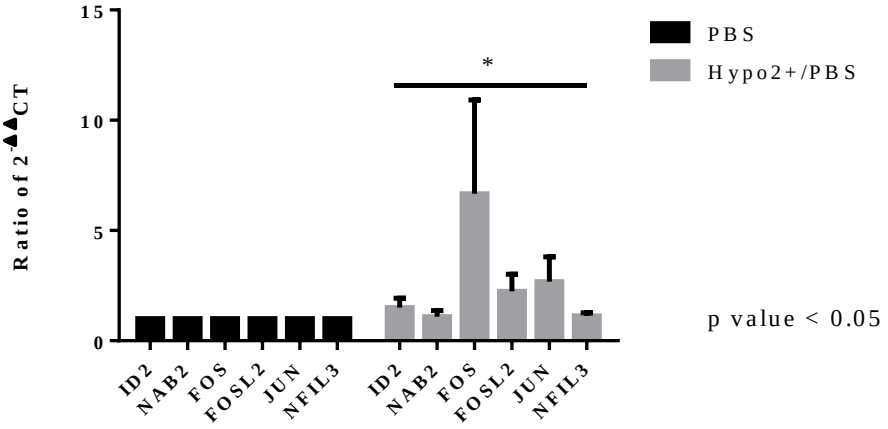

Figure 5.8 – Transcriptional characterisation of transcription factors assessed at day 4 of transdifferentiation in HAFTL C10 cell line. HAFTL C10 cell line characterisation was done by qRT-PCR analysis at day 4. The transdifferentiation without osmotic modulation (PBS) and with osmotic modulation (hypo2+/PBS) conditions were normalised by their respective negative controls (No transdifferentiation PBS and hypo2+/PBS). After calculation of ΔΔCT, a ratio between the expression levels ($2^{-\Delta\Delta CT}$) in the two transdifferentiation conditions was done (±SEM; n=3). The change is statistically significant when highlighted in the graphs (p value < 0.05; two-way ANOVA test).

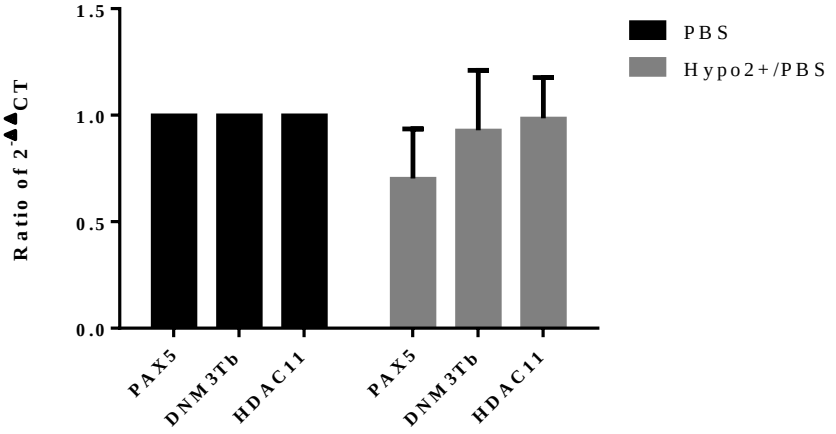

Figure 5.9 – Transcriptional characterisation of transcription factors and chromatin-associated factors assessed at day 4 of transdifferentiation in HAFTL C10 cell line. HAFTL C10 cell line was done by qRT-PCR analysis at day 4. The transdifferentiation without osmotic modulation (PBS) and with osmotic modulation (hypo2+/PBS) conditions were normalised by their respective negative controls (No transdifferentiation PBS and hypo2+/PBS). After calculation of ΔΔCT, a ratio between the expression levels ($2^{-\Delta\Delta CT}$) in the two transdifferentiation conditions was done (±SEM; n=3).

The direct impact of osmotic modulation in cell chromatin and transcription is parallel to an impact in mitochondrial function, as we discussed in the first chapter of this thesis. Therefore, the hyposmotic

modulation has also an impact on cellular metabolism that has a relevant role within cell fate decisions scenarios.

The next subchapters describe the impact of osmotic modulation in mitochondrial morphology and the changes in cell phenotype, more specifically alternative splicing, induced by distinct glucose concentrations in the extracellular medium.

5.1.1.1. Osmolarity influence on mitochondrial morphology

Mitochondria are key organelles that participate in several cellular basic functions, such as cellular energy production, apoptosis, calcium homoeostasis, and redox balance. Additionally, mitochondria are crucial to diverse biological outcomes such as proliferation, differentiation and adaptation to stress (Gottlieb and Bernstein, 2016; Ito and Ito, 2016; Picard et al., 2013). This organelle communicates with the cellular nucleus and cytoplasm by information transfer in a process called retrograde signalling. These pathways are essential tools to promote adaptive responses to cellular stress that ultimately lead to gene expression alterations (Butow and Avadhani, 2004; Hill and Van Remmen, 2014; Liu and Butow, 2006; Picard et al., 2013) .

Interestingly, mitochondrial morphology is a very important aspect that modulates the organelle function. The mitochondrial morphology is linked to susceptibility to permeability transition and apoptotic signalling, mitochondrial respiratory chain function, reactive oxygen species (ROS) production in physiological and stress conditions.

Processes of mitochondrial fusion and fission are known as mitochondrial dynamics. Importantly, abnormal mitochondrial dynamics causes bioenergetics defects (Berman et al., 2008; Chen et al., 2005; Galloway et al., 2012) and is related to several human diseases (Yu-Wai-Man and Chinnery, 2012), attesting its pivotal role for physio and pathological processes. Therefore, in the last years, mitochondrial morphology has become a relevant parameter for evaluating mitochondrial functionality.

To assess the hyposmotic modulation impact on mitochondrial morphology, MitoGreen HeLa cells were used for time-lapse confocal microscopy (LSM 710). The hyposmotic modulation has an immediate impact on mitochondrial morphology as presented in Figure 5.10, Figure 5.11, Figure 5.12 and Figure 5.13. By changing the complete growth medium to PBS there is no clear change in mitochondrial morphology (Figure 5.10). On the other hand, when complete growth medium is substituted by hypo2+/PBS there is a drastic change in mitochondrial morphology that seems to be partially reversed with time as shown in the above-mentioned figures (Figure 5.10 to Figure 5.13).

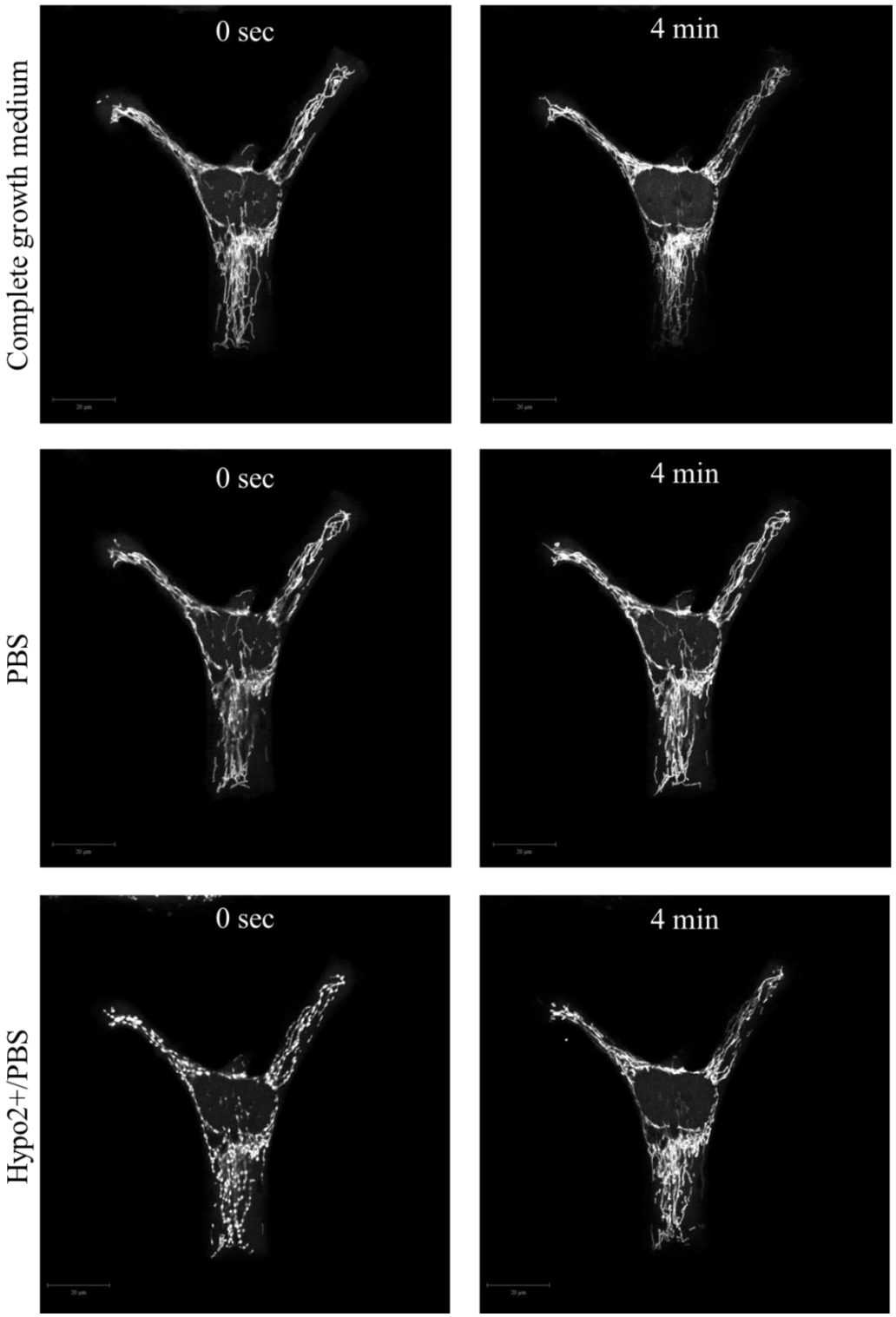

Figure 5.10 – Mitochondrial morphology within different osmolarity environments. MitoGreen HeLa cells were imaged on an LSM 710 (Carl Zeiss) confocal microscope (scale bar 20μm). The acquisition time and osmolarity environment used are shown in the figure.

Although it is not clear what happens to the mitochondria after an hyposmotic shock, morphologically it is a process very similar to mitochondrial fission (Picard et al., 2013). The morphological change observed denotes a spotted mitochondrial phenotype instead of a network enriched structure. This effect seems to be partially reverted after some minutes in hypo2+/PBS where the mitochondria tend to regain some of the network structures over the time (Figure 5.10 to Figure 5.13).

Some cells seem more resilient to the mitochondrial morphological change observed in the presence of the hypo2+/PBS solution like the example presented in Figure 5.11.

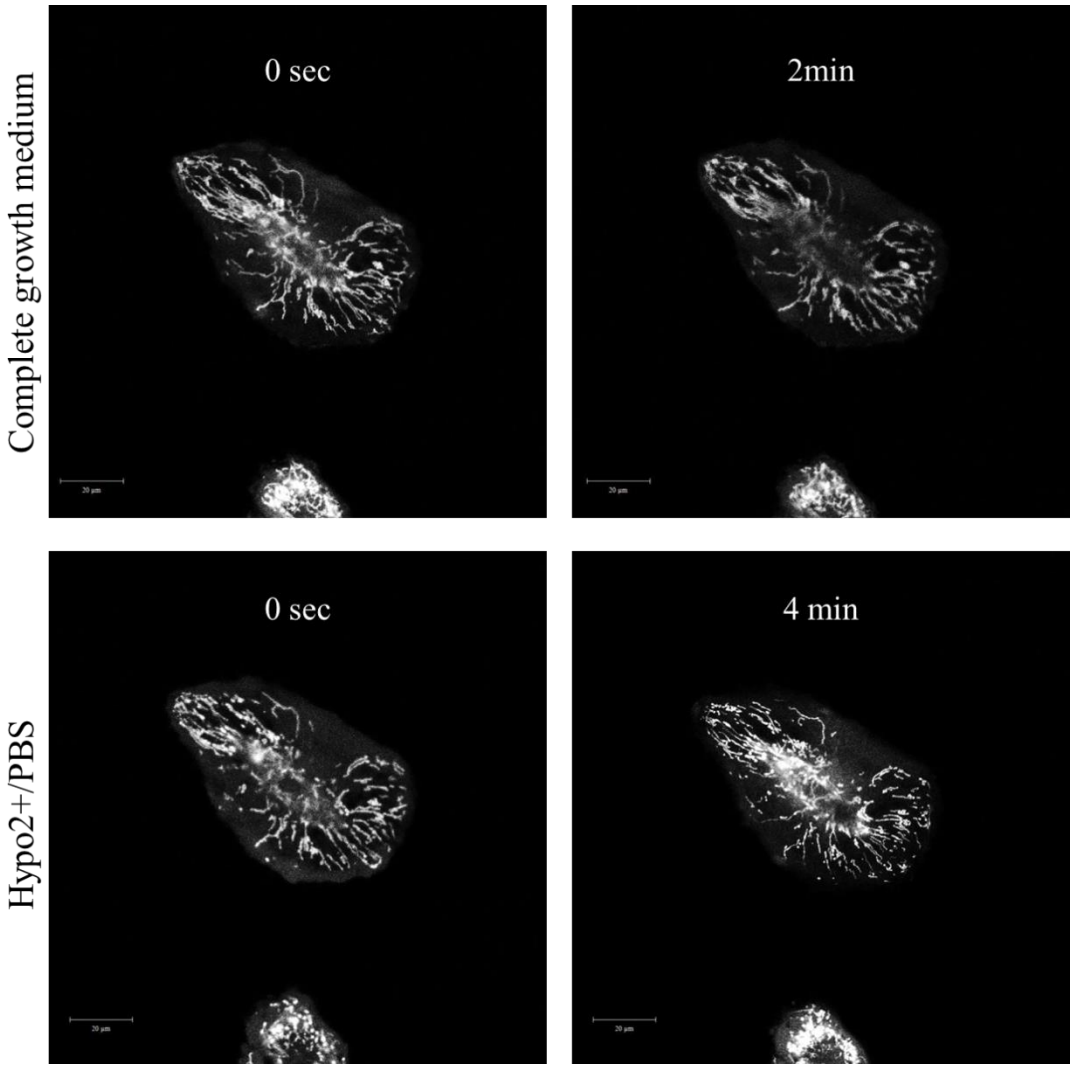

Figure 5.11 – Mitochondrial morphology within different osmolarity environments. MitoGreen HeLa cells were imaged on an LSM 710 (Carl Zeiss) confocal microscope (scale bar 20μm). The acquisition time and osmolarity environment used is shown in the figure.

Nevertheless, the alterations in mitochondrial morphology are especially clear in cells with rich and dense mitochondrial networks, like the cells presented in Figure 5.12. The ionic imbalance and other components affected like the ATP might trigger a quick and partially reversible mitochondrial morphology change. These changes tend to diminish with the time as it can be observed after 8 minutes of having the cells in hypo2+/PBS solution (Figure 5.12).

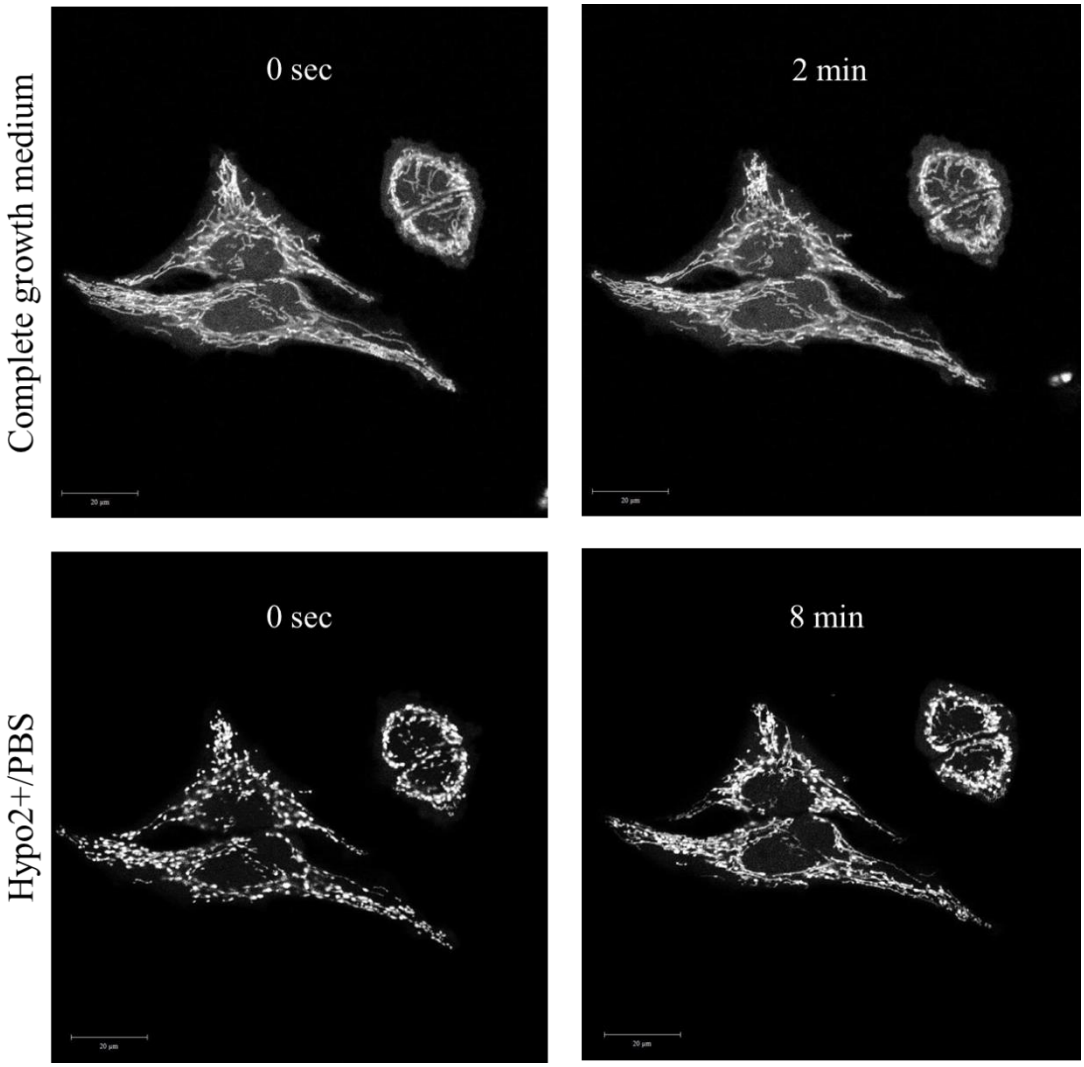

Figure 5.12 – Mitochondrial morphology within different osmolarity environments. MitoGreen HeLa cells were imaged on an LSM 710 (Carl Zeiss) confocal microscope (scale bar 20μm). The acquisition time and osmolarity environment used is shown in the figure.

The same effect is observed if we substitute the hypo2+/PBS solution by distilled water, but a more dramatic morphological change takes place and does not appear to be reverted over time (Figure 5.13). It is difficult to evaluate the mechanisms that are activated to promote this morphological change but is

important to note that the morphology is intrinsically related to mitochondrial function. Therefore, mitochondrial morphological changes can be related to alterations in ionic currents within the mitochondria that lead to a "mitochondrial swelling", as described in the literature (Garlid and Paucek, 2003; Kaasik et al., 2007; Kahlert and Reiser, 2002), but might also be related to a possible effect on mitochondrial fusion and fission machinery.

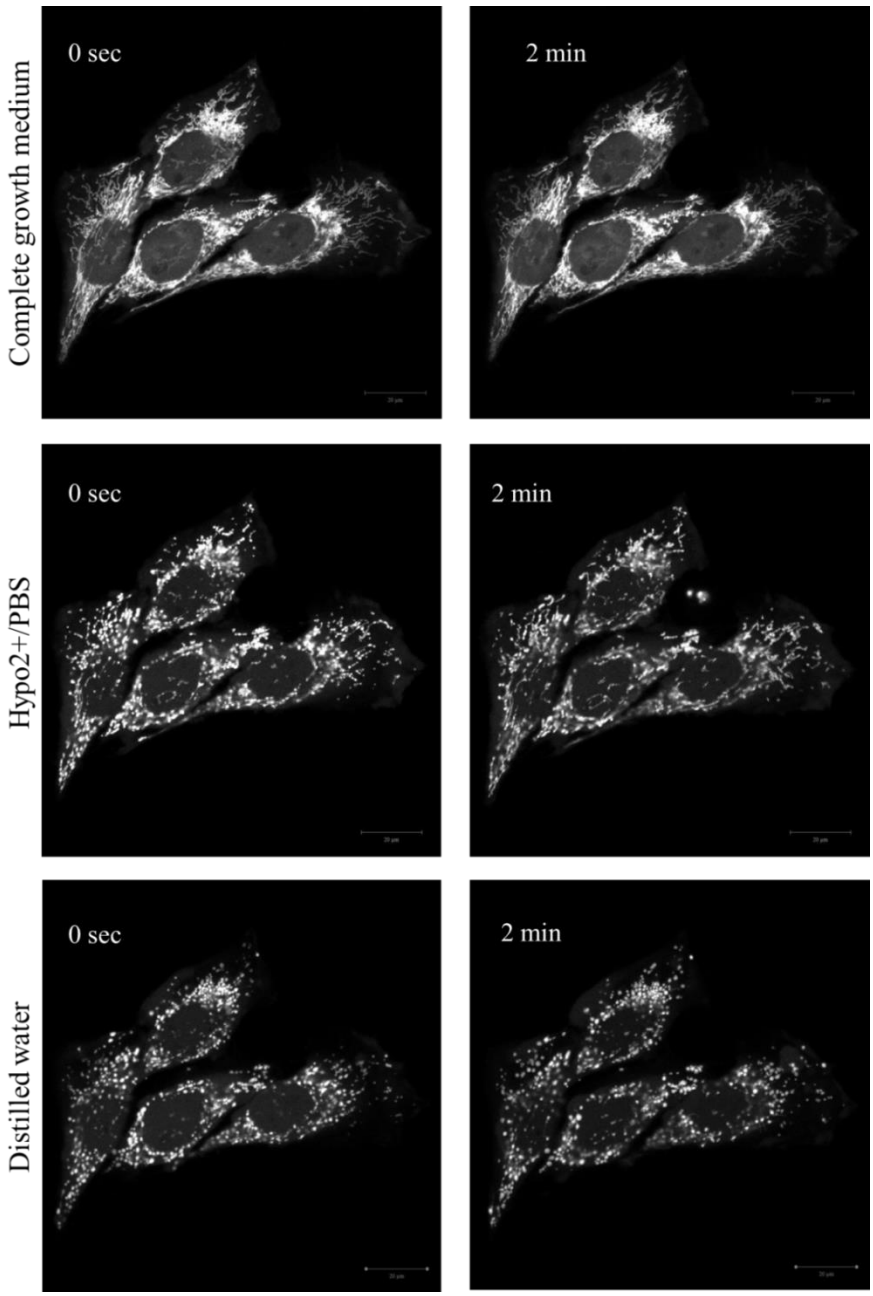

Figure 5.13 – Mitochondrial morphology within different osmolarity environments. MitoGreen HeLa cells were imaged on an LSM 710 (Carl Zeiss) confocal microscope (scale bar 20μm). The acquisition time and osmolarity environment used is shown in the figure.

To gain quantitative knowledge of the hyposmotic modulation-induced mitochondrial morphological changes, an ImageJ plugin validated in the literature (Vowinckel et al., 2015) for analysis of mitochondrial network morphology was used.

The significant decrease (p value < 0.001) in mitochondrial surface area and the significant increase (p value < 0.01) in surface area/volume ratio after exposure to hypo2+/PBS denote increased fragmentation of the mitochondrial network as presented in Figure 5.14 and Figure 5.15.

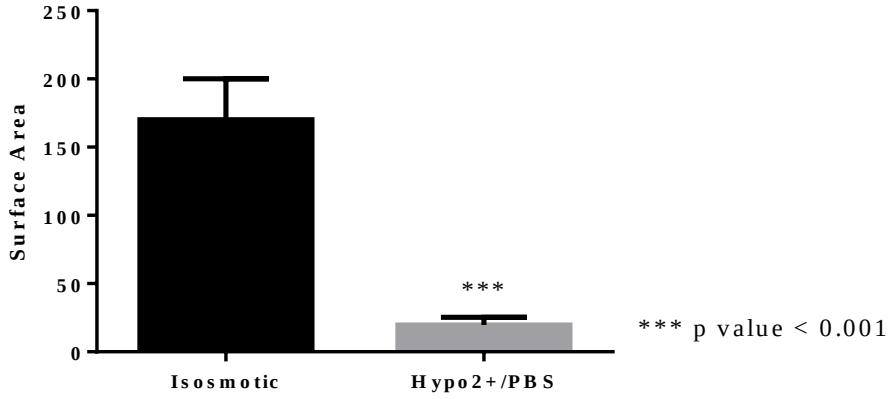

Figure 5.14 – Mitochondrial surface area within different osmolarity environments. MitoGreen HeLa cells were imaged on an LSM 710 (Carl Zeiss) confocal microscope. The analysis of this parameter (±SEM) was done using an ImageJ plugin (Vowinckel et al., 2015). The change is statistically significant when highlighted in the graph (p value < 0.001).

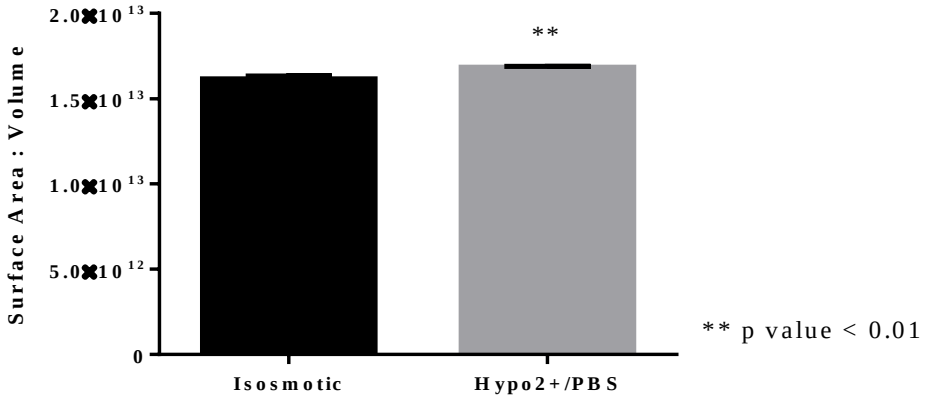

Figure 5.15 – Mitochondrial surface area:volume ratio within different osmolarity environments. MitoGreen HeLa cells were imaged on an LSM 710 (Carl Zeiss) confocal microscope. The analysis of this parameter (±SEM) was done using an ImageJ plugin (Vowinckel et al., 2015). The change is statistically significant when highlighted in the graph (p value < 0.01).

In agreement with these findings is also the significant increase (p value < 0.001) in the mitochondrial fragmentation index (f-index) after exposure to hypo2+/PBS as illustrated in Figure 5.16. This f-index is defined in the literature as the sum of relative fragment volumes that individually constitute less than 20% of total mitochondrial volume (Vowinckel et al., 2015).

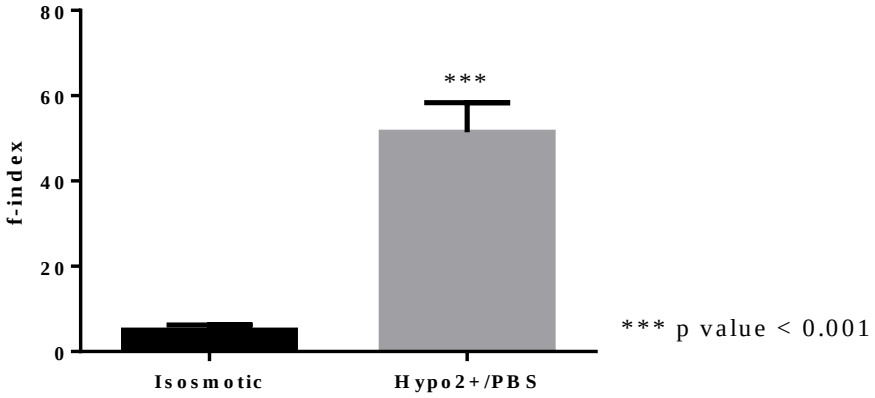

Figure 5.16 – Mitochondrial fragmentation index (f-index) within different osmolarity environments. MitoGreen HeLa cells were imaged on an LSM 710 (Carl Zeiss) confocal microscope. The analysis of the volume of fragments was done using an ImageJ plugin (Vowinckel et al., 2015) and the f-index (±SEM) was calculated afterwards. The change is statistically significant when highlighted in the graph (p value < 0.001).

Additionally, the mitochondrial compactness, as a measure of tubularity (Vowinckel et al., 2015), is significantly decreased (p value < 0.01) after exposure to hypo2+/PBS as shown in Figure 5.17.

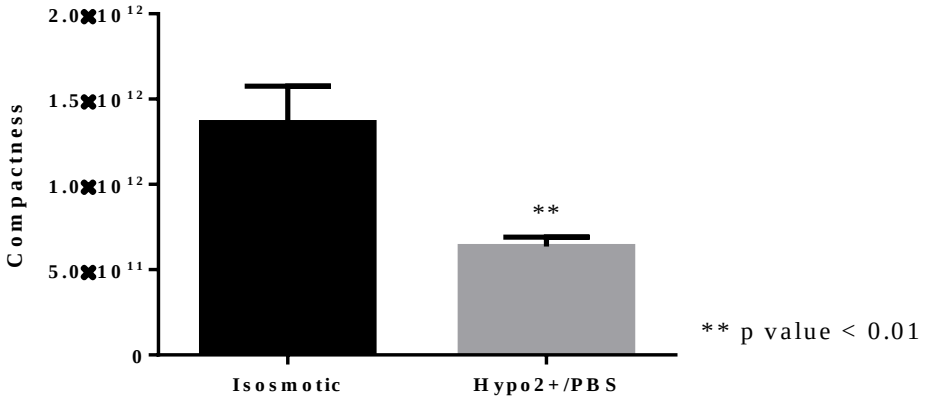

Figure 5.17 – Mitochondrial compactness within different osmolarity environments. MitoGreen HeLa cells were imaged on an LSM 710 (Carl Zeiss) confocal microscope. The analysis of this parameter (±SEM) was done using an ImageJ plugin (Vowinckel et al., 2015). The change is statistically significant when highlighted in the graph (p value < 0.01).

These alterations constitute another route by which the hyposmotic modulation can favour a phenotype change. These changes can support the metabolic changes that can occur in reprogramming and transdifferentiation, promote activation of stress-related pathways and transcriptional alterations by alteration of mitochondrial morphology and function.

Another way to modulate the mitochondrial function is to modulate the metabolic sources available to the cell. Therefore the next subchapter is devoted to explore the impact of glucose availability in the culture media and its repercussions in the production of different gene transcripts.

5.1.2. Influence of glucose concentration within cell phenotype changes

As mention in Chapter 4, the relevance of the osmotic changes within the extracellular environment is illustrated by some physiological and pathophysiological situations where imbalances in the osmolarity are associated with a normal cellular function (Hoffmann and Pedersen, 2011; Hohmann, 2015; Lang et al., 1998) or with certain diseases, such as brain cancer (Sontheimer, 2009; Thompson and Sontheimer, 2016).

Although the main focus of this work is the influence of extracellular osmolarity on cell phenotype and fate decisions, we should emphasise that mitochondrial function and cellular metabolism play a fundamental role in these processes. Indeed, in regular cell culture situations, cells are cultured at high concentrations of glucose and different cellular fates may be obtained if its levels are changed. This might affect the regular cell behaviour and make it distinct from the one observed within a physiological environment (Ferreira et al., 2012; Galloway et al., 2012; Gottlieb and Bernstein, 2016). One should also note that glucose is an osmolyte and variations in its levels may induce osmotic stress and cell size alterations.

Therefore, to study the long-term impact of cellular metabolic changes we used several cell culture media with different concentrations of glucose as presented in Table 5.1. The cell line used (N2A) is described in the literature (Zheng et al., 2013) and is a dual reporter cell line for monitoring of the expression of two different gene isoforms using a fluorescent readout (GFP to one isoform of the gene and RFP to another isoform of the gene). We used three different cell clones (N2A B11, C9 and E11) which were described in the literature (Zheng et al., 2013). In addition to the glucose variable, we have to consider that in the absence of glucose the medium osmolarity is lower and to control this variable, a metabolically inert osmotic stabiliser, galactose, was used.

Table 5.1 – Glucose content in the different media used.

Condition name	Abbreviation	Glucose concentration
High Glucose	HG	25mM
Low Glucose 1	LG1	12.5mM
Low Glucose 2	LG2	7.5mM
No Glucose	NG	0mM
Galactose	Galac	0mM

In a long-term adaptation to the different media conditions, for more than one month, there are significant changes (p value < 0.0001) in the ratio of the gene isoforms produced by the cells in all the three cell clones used (Figure 5.20, Figure 5.18 and Figure 5.19). The evaluation of fluorescence levels for the GFP and RFP reporter proteins was done with the help of IN Cell 2200 Analyzer. The metabolic and energy production changes induced by different media have an impact in the generation of different transcripts. As reported in the literature, the ATP content in the cell is crucial for transcription and alternative splicing events (Guantes et al., 2015; das Neves et al., 2010). Therefore, when restraints in glucose availability are present, the cells will have to adapt their metabolic processes and use other sources of fuel power. These metabolic changes have a clear impact in alternative splicing in the N2A cell clones used as we can see in Figure 5.18, Figure 5.19 and Figure 5.20. Is important to stress out that these cells are generated from a neuroblastoma and therefore as cancer cells their primordial pathway of energy production will be glycolysis (Ganapathy-Kanniappan and Geschwind, 2013; Zheng et al., 2013). Faced with a shortage in glucose these cells need to adapt and reprogram their metabolism. This impacts clearly on their transcriptional repertoire. The GFP isoform which was underexpressed with respect to the RFP isoform in glycolytic conditions is clearly privileged when mitochondrial metabolism and energy production are favoured, in all 3 tested clones of N2A cells.

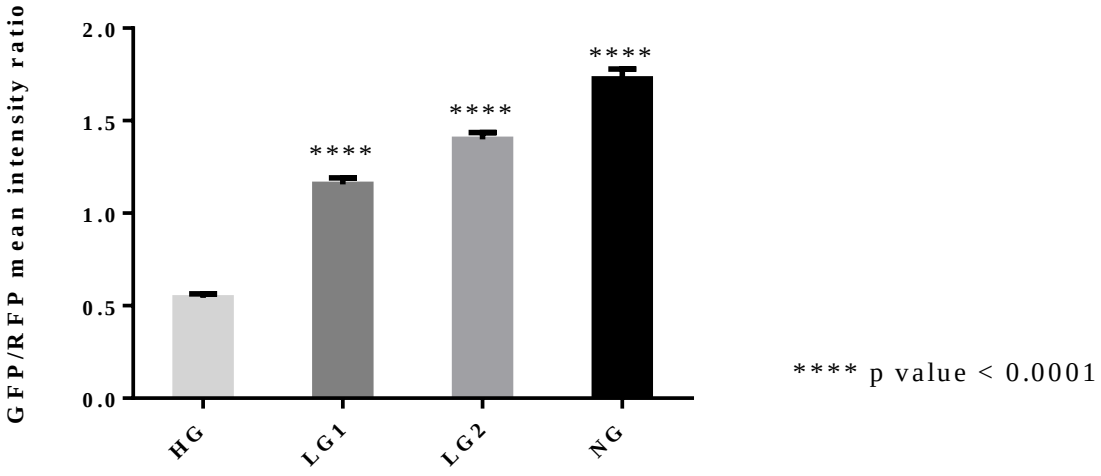

Figure 5.18 - N2A (clone C9) long-term adaptation to different glucose concentrations. N2A cell clone C9 evaluation of the GFP, RFP mean fluorescence intensity ratios. For all the conditions (High Glucose – HG; Low Glucose1 – LG1; Low Glucose2 – LG2 and No Glucose – NG), the mean fluorescence intensity ratios are presented (±SEM; n=15). These changes are statistically significant when highlighted in the graph (p value < 0.0001).

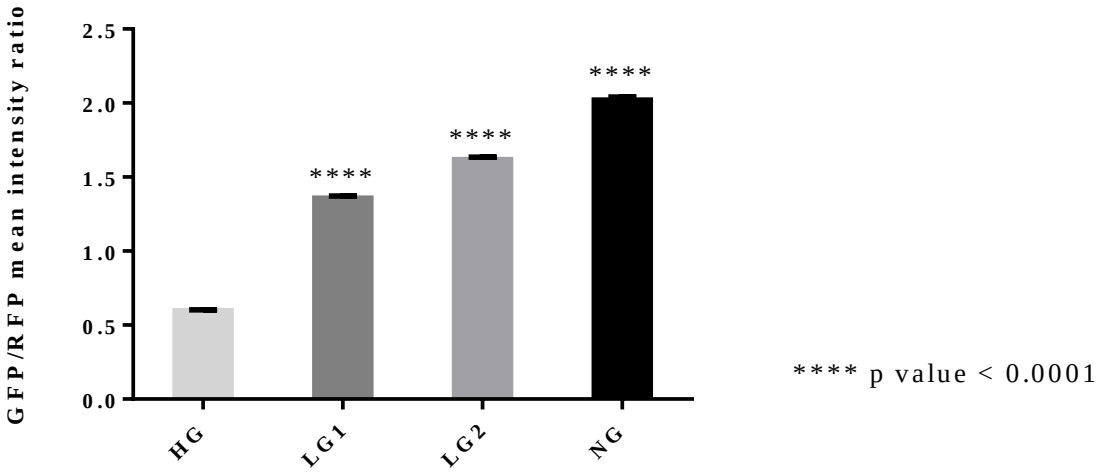

Figure 5.19 – N2A (clone E11) long-term adaptation to different glucose concentrations. N2A cell clone E11 evaluation of the GFP, RFP mean fluorescence intensity ratios. For all the conditions (High Glucose – HG; Low Glucose1 – LG1; Low Glucose2 – LG2 and No Glucose – NG), the mean fluorescence intensity ratios are presented (±SEM; n=15). These changes are statistically significant when highlighted in the graph (p value < 0.0001).

To assess the influence of osmotic changes induced by different glucose concentrations in the media, we used galactose as a metabolically inert osmotic stabiliser control. This long-term adaptation was done only in clone B11 because this clone was reported to have higher stability (Zheng et al., 2013). The

galactose adaptation shows that the lack of glucose is the key element playing a more relevant role in terms of long-term impact in transcription (Figure 5.20). If we compare the ratio of the two reporter fluorescent proteins in the condition NG and Galac they are very similar, and although there are osmotic differences between the two conditions, cells in both transcribe the different isoforms in a similar fashion (Figure 5.20). Taking this into consideration and our previous findings in this thesis, it seems that osmotic modulation may impact transcription immediately (and transiently) but metabolic conditioning has more long lasting effects in gene expression.

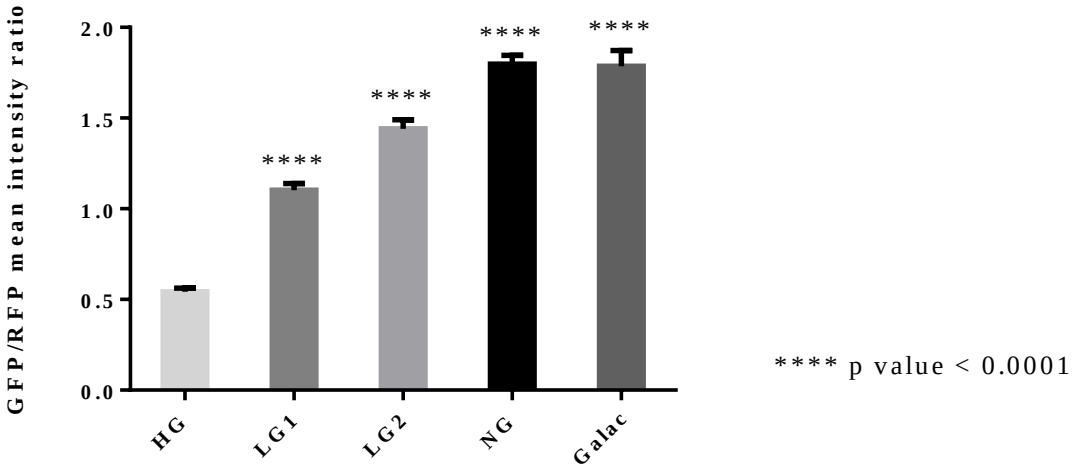

Figure 5.20 – N2A (clone B11) long-term adaptation to different glucose concentrations. N2A cell clone B11 evaluation of the GFP, RFP mean fluorescence intensity ratios. For all the conditions (High Glucose – HG; Low Glucose1 – LG1; Low Glucose2 – LG2; No Glucose – NG and Galactose – Galac), the mean fluorescence intensity ratios are presented (±SEM; n≥12). These changes are statistically significant when highlighted in the graph (p value < 0.0001).

It would have been very interesting to do transient osmotic modulation with these cells and image them afterwards. Actually, this was the first experiment done with these cells in this work but the cells are very sensitive and after 15 minutes in hyposmotic conditions or even in PBS the cells started to detach and therefore the imaging was not possible.

By changing the environmental glucose conditions the N2A cells change their transcriptome profile and this control over the environmental conditions could be used as a tool to change the cells behaviour and cell phenotype.

The tumour microenvironment is an active research area but the osmolarity is not a parameter that is commonly assessed in these studies (Bolouri, 2015; Hui and Chen, 2015). Nevertheless, it is well known that tumourigenesis influences the ability of the cell to balance the electrolytes (Lang and Stournaras, 2014; Pedersen et al., 2013; Voutouri and Stylianopoulos, 2014) and future research in this area will be fruitful and with potential for therapeutic applications.

5.2. Concluding observations

Within this chapter, a group of broad results elucidated some important aspects of the osmotic modulation relevance in cell phenotype and mitochondrial morphology. In addition to the mitochondrial morphology data, the relevance of glucose availability to cell phenotype was also explored.

Therefore the main observations within this chapter can be summarised as:

- The hyposmotic modulation has a relevant impact on transdifferentiation efficiency;
- The hyposmotic modulation promotes a transcriptional change within cells;
- The hyposmotic modulation promotes a clear morphological change on cellular mitochondria;
- The metabolic state of the cells, modulated by the different availability of glucose, alters the isoform transcription profile.

Chapter 6 : Discussion, conclusions and future work.

How can cells react to hyposmotic modulation and how that modulation can alter their phenotype and fate?

The answer to this question will provide crucial knowledge that will allow the use of hyposmotic modulation as a cell modulator tool.

The osmotic regulation is involved in several physiological and pathological events. Although the great majority of the studies have focused on the effect induced by hypertonicity, the hyposmotic modulation provides exciting and underexplored avenues for induction of chromatin and transcriptional changes. The transcriptional profile of a cell defines cellular behaviour and phenotype and it would be relevant to control the transcriptional activity using a simple and easy biophysical stimulus like osmolarity.

In this chapter we will discuss in a general way the results obtained and the main contributes of this work to the osmotic regulation field.

Cellular parameters

The work presented in this thesis shows the numerous changes in cellular parameters that are induced by hyposmotic modulation, such as the increase in cell size, decrease in intracellular levels of adenosine triphosphate (ATP), a decrease in cell membrane potential and increase in intracellular calcium. Several of these alterations were reported in the literature for different cell types (Finan and Guilak, 2010; Kim et al., 2000; Nandigama et al., 2006; Pasantes-Morales et al., 2006).

A very interesting trend is the observed decrease of intracellular ATP and the marked rise in intracellular calcium levels. These molecules share a historical pathway that was critical to define the form of life that emerged and evolved on Earth. Definitely, ATP is a universal substrate for energy storage, whereas calcium is a ubiquitous intracellular signalling molecule. From an evolutionary perspective, the primordial alkaline ocean provided an environment specifically suitable for ATP metabolism, which can proceed only at very low (sub-micromolar) concentrations of ionised calcium. As a result, the cytosol of the most primitive cellular ancestors contained low levels of cytosolic free calcium. With the ocean acidification and washout of calcium from the rocks, the development of a system

controlling calcium movements across the cellular membrane became vital, and was the basis for cellular calcium homeostatic and calcium-based signalling systems (Petersen et al., 2016; Plattner and Verkhratsky, 2016).Therefore calcium that usually is present within the cells at 0.1 μM (and extracellularly at ≥ 1mM) has emerged as one of the most important regulators of different cellular functions. These functions include membrane vesicle interaction, exocytosis, endocytosis, signalling, cell motility, apoptosis and ATP production. The close interaction between ATP and calcium is clearer in the mitochondria where the tight calcium balance is a master regulator for ATP production.

Contrariwise to calcium, cytosolic concentrations of ATP typically amount to approximately 3–5 mM, whereas the extracellular concentration is very low (0.1–1 μM) (Petersen et al., 2016; Plattner and Verkhratsky, 2016). Despite the huge concentration gradient, ATP and other nucleotides cannot permeate cell membranes due to their negative charge, but this nucleotide is released into the extracellular medium and stimulates purinergic receptors in an autocrine and paracrine manner, activating downstream signalling cascades (Nandigama et al., 2006; Schwiebert and Fitz, 2008; Schwiebert and Zsembery, 2003). It has been previously shown that ATP extracellular concentrations as low as 0.1–10 μM are biologically active, which means that the cells need to release less than 1% of their cellular ATP content to achieve full activation of receptor-mediated signalling. The ATP release can occur under basal conditions to maintain physiological "thresholds" for cell signalling and function, but can also be observed under pathophysiological conditions such as hypoxia, mechanical and osmotic stress and cancer.

ATP was shown to stimulate tumour growth (Ganapathy-Kanniappan and Geschwind, 2013; Nandigama et al., 2006) and also functions as a potent mitogen in cells such as vascular and the smooth muscle cells among others (Petersen et al., 2016; Schwiebert and Zsembery, 2003).

The ability of hyposmotic modulation to interfere with cell function is enormous and constitutes a powerful tool to manipulate two of the most powerful molecules in the cell, ATP and calcium. The modulation of the tumour microenvironment with osmotic modulation is an interesting approach to study and model the importance and susceptibility of cancer cells to ATP oscillations, calcium fluxes and biophysical changes of the properties of the cell and the nucleus.

In addition to the signalling activities of ATP upon release to the extracellular environment, the relevance of ATP in transcription rate has been studied (das Neves et al., 2010), and we believe that within the osmotic modulation the decrease of available ATP for transcription is crucial for some of the transcription changes observed.

Chromatin and transcription and cell fate determinations

As mentioned before, the hyposmotic modulation influences major cellular signalling molecules. It also impacts in crucial features that determine cellular fate determination like transcriptional activity, chromatin structure and mitochondrial activity.

Although many of the factors that are responsible for chromatin structural modifications can be induced by the signalling cascades activated by the osmotic cell response, the biophysical impact of the water entrance into the cell might play a crucial role in the nuclear architecture and chromatin arrangement. Technically is difficult to prove such theory but some studies have shown that the physical impairment of chromatin structure plays a role in the overall chromatin structure and transcriptional activity (Ito et al., 2014; Lopez-Atalaya and Barco, 2014; Medrano-Fernández and Barco, 2016). For instance, the increase in H4K16 acetylation is a synonym of transcriptional activity (Canals-Hamann et al., 2013; Iborra et al., 1996, 2001; Johnston et al., 2012; das Neves et al., 2010). It can be argued that the results obtained with hyposmotic modulation could be achieved by the use of drugs and small molecules that promote chromatin remodelling. We propose that our strategy presents the advantage of a broader action and general/unbiased approach (in opposite to what is expected when a specific enzymatic target is modulated). Also, some small molecules can have opposite effects when used in different cellular contexts. The use of one of the more potent histone deacetylase inhibitors, valproic acid (VPA), as a booster for reprogramming processes has been studied and was shown to induce an increase in reprogramming efficiency (Huangfu et al., 2008). It was shown to induce the expression of embryonic related factors in the absence of the reprogramming factors in mouse embryonic fibroblasts (Huangfu et al., 2008). Contrariwise, in a differentiation context, this drug was shown to favour specific lineage fate decisions of $CD34^+$ umbilical cord blood cells (Chaurasia et al., 2011). Showing that virtually all of the $CD34^+$ cells treated with VPA in clonogenic assays were erythroid progenitor cells (Chaurasia et al., 2011).

The search for booster molecules able to increase the efficiency of the reprogramming process has mostly been done in fibroblasts. Therefore, it is difficult to analyse the impact of these drugs depending on the starting cell type in reprogramming processes. Nevertheless, the fact that specific drugs work better than others, that basically work towards the same objective that is the opening of chromatin for active transcription, suggests that there is some cell type constraint. Indeed, several studies focusing on reprogramming have shown that not only deacetylase inhibitors but also DNA methyltransferase inhibitors, MEK and GSK3 pathway inhibitors can interfere with the reprogramming process.

Additionally, a diverse range of small molecules like BIX (an inhibitor of G9a histone methyltransferase), BayK, RG108 and CYT296 have been studied for their effects in the reprogramming process. Studies doing chemical library screenings identified the DNA methyltransferase inhibitor RG108 and an L-calcium channel agonist BayK as small molecules that can significantly enhance the reprogramming of BIX-treated mouse embryonic fibroblasts in the absence of Sox2 and c-Myc. Nonetheless, the mechanism by which BayK acts is still unclear, but is important to have in mind that this drug is an ionic channel regulator and the ionic balance might constitute a major way of action of this drug in reprogramming.

Nevertheless, the use of the above-mentioned drugs is in some cases associated with side effects and toxicity effects reported in the literature (Chateauvieux et al., 2010; Powell et al., 2016).

We believe that in addition to the chromatin state, the profile and stoichiometry of specific transcription factors (TFs) is a crucial factor for the establishment of new transcriptional profiles. Therefore, the use of drugs such as VPA might have different phenotype outputs depending on the repertoire of TFs present in the cell and soluble signalling molecules within the cell´s environment. The use of a biophysical approach has the advantage of avoiding the use of drugs and does not have a bias towards a specific enzyme family to promote chromatin and DNA structural changes (Finan and Guilak, 2010; Finan et al., 2009; Martins et al., 2012).

Strategies with biophysical cues have been used to improve reprogramming of somatic cells into pluripotent stem cells like the use of cell-adhesive substrates with parallel microgrooves. This study claimed that the use of this patterned surface can replace the effects of small-molecule epigenetic modifiers and significantly improve reprogramming efficiency (Downing et al., 2013). This study is a good example of a biophysical stimulus that drives an increase in reprogramming efficiency by having an effect that can replace the use of epigenetic modifiers. Nevertheless, the development of biocompatible material applications, the batch to batch variations and the scale-up methodology can constitute major drawbacks to future application of such technologies when compared with the hyposmotic modulation strategy used throughout the work reported in this thesis.

The transcriptional changes induced by hyposmotic modulation are far from being understood, and we believe that this work provides some clues for the study of specific new targets. The hyposmotic modulation promotes a dilution of the macromolecules and signalling agents inside the cell and also an ATP efflux, as previously mentioned. The fact that ATP is fundamental for the transcription process is a major effect that needs to be taken in consideration when using this type of modulation for cell fate modulation protocols. ATP is a crucial determinant element of the speed of transcription (das Neves et al., 2010). We think that the ATP efflux and/or dilution inside the cells seen after the hyposmotic stimulus

was responsible for the drop in transcription speed observed. This may have a profound effect in the splicing repertoire produced by the cell (Guantes et al., 2015; das Neves et al., 2010) and may impact in stem cell (SC) fate decisions (Johnston et al., 2012; das Neves et al., 2010). This side-effect induced by hyposmotic modulation can be detrimental for specific protocols that need longer/multiple hyposmotic stimuli, but may be rescued or modulated by providing ATP and stabilising agents to the cells after hyposmotic modulation to rescue transcription speed. Nevertheless, the fact that the osmotic modulation enabled the recruitment of more RNA Polymerase II (RNA Pol II) into chromatin is an important result that opens an avenue of new possibilities to modulate transcription and cell fate by introducing high levels of exogenous TFs inside the cell.

To understand the biological meaning of RNA Pol II binding is not a straightforward or easy task, but in this study we show that the hyposmotic modulation promotes a general significant increase of the different forms of RNA Pol II bound to chromatin. We believe that this is a combined effect of chromatin relaxation and recruitment of RNA Pol II by different TFs.

The hydration state of the DNA might condition the methylation state of different genomic areas and also favour the binding of specific TFs. The specific access of TFs to cell's DNA is a crucial step for fate determination and a lot has been learned about the molecular players in this field from the hemato-oncology research (Blobel et al., 2009; Collins et al., 2014; Tao et al., 2015). One example is the highly conserved promyelocytic leukaemia zinc finger TF (PLZF) which is a multifunctional zinc finger TF that has an important role in the maintenance of the balance between self-renewal and differentiation of long-term hematopoietic stem cells (HSCs) and other SCs. De-regulation of this TF as the name indicates is responsible for cases of acute promyelocytic leukaemia and affects cell growth, differentiation, and apoptosis (Liu et al., 2015a).

Zinc fingers (ZFs) are small protein domains in which at least one zinc ion plays a structural role contributing to the stability of the domain and the "finger" refers to the secondary structures (α-helix and β-sheet) held together by the zinc ion. ZFs are structurally diverse and are present in a wide variety of biological functions such as replication and repair, transcription and translation, metabolism and signalling, cell proliferation, cell differentiation and apoptosis. ZFs typically function as interaction modules and bind to a wide variety of compounds, such as DNA, RNA, proteins or small molecules (Brayer and Segal, 2008; Klug, 2010; Laity et al., 2001; Maret, 2013; Vandevenne et al., 2013). Several structurally distinct classes of ZFs are able to act as DNA-binding modules, including GATA-type ZFs (Lowry et al., 2009), steroid hormone receptor ZFs (Schwabe et al., 1993), Gal4-type ZFs (Hansen et al., 1991; Johnston, 1987).

In our study, eight out of the top ten TFs, responsible for the significantly enriched binding of initiating RNA Pol II after hyposmotic modulation, are classified as ZF TFs. We believe this number is too big to be a coincidence and propose that this class of TFs is very important in osmotic regulation. From this list, the presence of ERG-1 was an interesting hit because it is reported in the literature as having activity impairment with increasing amounts of osmolytes (Mikles et al., 2015). One of the first events after the hyposmotic stimulus is the exit of osmolytes from the cell to balance the extracellular hyposmotic environment. Also, under hyposmotic stimulus, osmolytes leave the interaction pockets of proteins; this type of effect renders the ERG-1 TF freedom to interact with the DNA. This control mechanism where the TF is released and quickly binds to the DNA enlists ZF TF binding as one of the first events after this type of stress.

Additionally the hydration state of the DNA has also an influence in the DNA-protein interactions (Franck et al., 2015; Poon, 2012; Schneider et al., 2014; Wang et al., 2014). The importance of this mechanism is already described for preferential hydration as the defining feature in DNA sequence discrimination for the TF PU.1. Therefore the hydration state plays a very important role in driving DNA binding and the formation of high and low-affinity specific DNA sites (Poon, 2012; Wang et al., 2014). The connection between hydration of DNA sequences and the entrance of water inside the cell under hyposmotic modulation has not been described so far in the literature. Nevertheless, one would expect the thermodynamic forces present at the interface between DNA and chromatin and proteins to be different in an over-hydrated intracellular environment. Our results show that more TF binding is induced by hyposmotic modulation and the superclass of TFs that is privileged is the zinc-coordinating DNA binding domain. This relationship deserves more investigation as it suggests that zinc TFs have preferential binding to hydrated DNA-binding sequences.

Zinc is a key element of life involved in numerous cellular functions (Maret, 2013) and ZF proteins have been widely studied due to their highly conserved structures and DNA-binding specificity of ZF domains (Liu et al., 2014). Their involvement in osmotic regulation is transversal from plants to yeast. For example the MSN2 and MSN4 genes encode homologous and functionally redundant ZF proteins essential for activation of stress-response elements. By disrupting MSN2 and MSN4 genes a higher sensitivity to carbon source starvation, heat shock and severe osmotic and oxidative stresses is promoted (Jacquet et al., 2003; Martinez-Pastor1 et al., 1996). The osmotic stress response is also mediated by ZF proteins in *Arabidopsis* (AtRZF protein), *Festuca arundinacea* (FaZF protein) and the rice plant (ZF protein 36) (Martin et al., 2012; Zang et al., 2016). Therefore, although not very explored in humans, the osmotic modulation response might be also mediated by ZF proteins and thus is relevant to develop further studies within this context.

Another DNA modification that might depend on hydration is methylation, and the hydrophobicity of the methylated DNA might be a crucial player for explaining gene silencing upon DNA methylation(Kaur et al., 2012). This DNA modification is characteristic on methylated cytosine residues on the bulk of DNA while the unmethylated ones are mainly located within particular regions termed CpG islands. The majority of cytosine and guanine (CpG) pairs are modified by the covalent modification of the cytosine ring with a methyl group in the C5 position. This modified residue is distributed throughout the genome in gene bodies, endogenous repeats and transposable elements that function to repress transcription (Caiafa and Zampieri, 2005; Deaton and Bird, 2011; Illingworth and Bird, 2009).The methylcytosine can spontaneously deaminate to thymine resulting in the under-representation of CpG pairs (21% of that expected in the human genome) (International Human Genome Sequencing, 2001). The non-methylated DNA sequences called CpG islands have an elevated guanine and cytosine (GC) content and little CpG suppression (Bird et al., 1985; Cooper et al., 1983; Larsen et al., 1992). CpG islands represent about 1% of the genomic DNA and are generally found in the promoter region of housekeeping genes. Consistently with promoter association, CpG islands are generally characterised by a transcriptionally permissive chromatin state (Guenther et al., 2007; Tazi and Bird, 1990; Weber et al., 2007).

Not all CpG islands are found in transcription starting sites and approximately half of these islands are either within or between characterised transcription units and are termed as "orphan" CpG islands. Some examples of CpG "orphan" islands turn up to be actually in intragenic promoters that at the time of CpG island characterisation were unknown. The mechanism by which CpG islands stay hypomethylated during *de novo* methylation during early development remains unclear (Antequera, 2003; Antequera and Bird, 1999). And the methylation of CpG islands is seen in some physiological processes like in X chromosome inactivation, genomic imprinting and potentially during cell specification (Edwards and Ferguson-Smith, 2007; Reik, 2007). The disruption of CpG island methylation pattern is also a well-known hallmark of cancer (Esteller, 2007). The CpG island general distribution pattern may serve as instructive clues for TF binding and the absence of methylation in this regions is an essential condition for the correct expression of related genes (Bird, 1995; Illingworth and Bird, 2009; Prestridge and Burks, 1993).

It is a complex task to determine the effect of DNA methylation at CpG islands. Although the extensive evidence supporting a functional role for CpG islands and methylation in transcriptional repression (Futscher et al., 2002; Song et al., 2005; Weber et al., 2007) supports the hypothesis that the major function of CpG island methylation is to repress transcription, there are many genes that display a relatively poor correlation between hypermethylation and the transcriptional status of associated genes (Illingworth et al., 2008; Oakes et al., 2007; Rauch et al., 2009). Some of these inconsistencies might

come from the difficulty of defining straightforward parameters to define CpG islands, usually defined by sequence length, the ratio of the observed and expected CpG pairs and GC composition.

The DNA specific methylation pattern results from the balance between maintenance, *de novo* methylation and demethylation processes. DNA methyltransferase 1 is considered the primary responsible for methylation maintenance due to its preference for hemimethylated DNA. Nonetheless, a complex set of machinery is necessary to attain a coordinated and balanced DNA methylation pattern.

Regarding CpG island role in this study, our results show that the DNA-binding profile induced after the hyposmotic modulation is assisted by a set of specific TFs that bind more pronouncedly to CpG enriched regions and possible CpG islands. These are very interesting results that need further complementation with ribonucleic acid-sequencing (RNA-Seq) data and methylation profile of these osmotic induced new binding sites. It would be very interesting to complement these results with further methylation studies at global and specific genome areas where our study shows to occur an altered preference to CpG enriched areas.

It will be very important to clarify if the altered binding profile of RNA Pol II and the new binding sites are transduced into distinctive patterns of RNA molecules. The validation of some of the transcriptional targets identified in this work and RNA-Sequencing data would complement the data presented in this work. Due to time and funding constraints, we have chosen to proceed to the evaluation of the biological impact of this type of modulation in cell fate determination protocols.

We have managed to show that hyposmotic stimuli are able to impact three specific cell fate protocols: two reprogramming and one transdifferentiation assay have proven the point that this type of modulation of chromatin and transcription can be used in this context. The changes in efficiency are moderate but we believe that in these scenarios this would be the expected output. This may be related with the fact that reprogramming is mainly dependent on pioneer factors which don't need chromatin to be accessible. Therefore, the full power of the impact of hyposmotic modulation on chromatin structure and transcriptional changes might be shadowed by the action of the pioneer factors, which are present in a stoichiometric advantage within the cell nucleus. Nevertheless, there was a significant impact in the reprogramming efficiency in fibroblasts and we believe that the kinetic changes seen in UCB cell reprogramming also show the ability of the osmotic stimulus to modulate the speed of the process.

In the case of the transdifferentiation experiment, CEBPα can also have a pioneer activity (Bussmann et al., 2009; van Oevelen et al., 2016) and mask the full potential of hyposmotic modulation. This knowledge opens other possibilities for the hyposmotic modulation as a tool for discovery of new pioneer TFs. That in theory would not have their binding ability impaired by chromatin relaxation. Additionally it could be an interesting tool to unveil characteristics of pioneer (such as PU.1) and non-pioneer TFs that are affected by the hydration state of the DNA molecule. For that, it would be important to have a

measure of the hydration of DNA at a global level. What has been done so far has been *in vitro* in very simple systems using specific DNA sequences and TFs and nuclear magnetic resonance (NMR) to access the hydration and binding rates (De et al., 2014; Desjardins et al., 2016; Sam and Clubb, 2012; Wang et al., 2014). One possibility would be to use tritium-doped water in the osmotic cocktails to try to have a measure of this global hydration.

To unveil the full potential of the hyposmotic modulation would be very interesting to use models where cell fate changes are especially hard. For instance, the reprogramming of non-terminally differentiated B-cells to pluripotency was possible using the four Yamanaka-TFs (Oct4, Sox2, Klf4, and c-Myc) but it was impossible to do the same with mature B-cells. To improve the reprogramming efficiency of mature B cells CEBPα has also been used to enhance the reprogramming efficiency when co-expressed with Yamanaka factors (Hanna et al., 2008), although the mechanism remains unknown and the final efficiency only reaches 1–3%. A recent study found that an 18 h pulse of CEBPα expression in mature B-cells followed by induction of Yamanaka factors expression induces a high fold increase (>100) in the iPSC reprogramming efficiency (Di Stefano et al., 2014). The study reports an epithelial to mesenchymal transition, upregulation of pluripotency genes to levels comparable to embryonic stem and iPSCs and downregulation of B-cell commitment master regulators. We believe that this system would be an interesting way to understand if the CEBPα pulse has a role in chromatin opening to allow the access of the pluripotency-related transcription factors and if this effect could be mimicked by hyposmotic modulation.

In both reprogramming and transdifferentiation it would also be very informative to complement our data with the temporal binding sites and profile of the TFs involved in both processes as done in the K562 Chip-Seq of RNA Pol II in Chapter 3.

In addition, mitochondrial changes induced by hyposmotic modulation are another important route of impact in cellular fate determination. This work shows that the hyposmotic modulation favours a fragmented mitochondrial phenotype. This phenotype in the literature is associated with a pluripotent cell phenotype, where mitochondria are globular, with poorly developed cristae and perinuclear localisation (Chen et al., 2012; Folmes et al., 2012b; Prigione et al., 2015; Wanet et al., 2015). In pluripotent stem cells the glycolysis is favoured as a metabolic source of energy. The glycolytic metabolism is also correlated with global chromatin changes as shown in the literature (Etchegaray and Mostoslavsky, 2016; Liu et al., 2015b; Schneider and Grosschedl, 2007; Thurman et al., 2012).

The reprogramming process, depending on the cell type, comprises morphological and functional changes within the mitochondria. In our experiments, the osmotic-induced mitochondrial functional and morphological changes might be beneficial for the metabolic shift in the reprogramming process from

fibroblasts into pluripotent stem cells. The cross-talk between mitochondria and the cell nucleus is also a subject that we believe that is very important and should be further explored within the hyposmotic modulation scenario.

The mitochondrial cell content and activity was already correlated with alterations in the alternative splicing pattern (Guantes et al., 2015). Therefore, the alteration of alternative splicing in the N2A model under hyposmotic environment and glucose-deprived conditions, presented in this work, is complementary evidence that the alterations in transcription can have phenotypic changes and an important role in cellular function. These preliminary studies would provide interesting results if we could culture these N2A cells in hyposmotic solutions and image in real time the changes in the expression of different isoforms.

The general conceptual idea behind this work is represented in Figure 6.1. This work revealed the potential of controlled hyposmotic modulation to alter cell phenotype and fate determination. The elements underlying this complex response are an intricate network between signalling, transcription, metabolism and chromatin remodelling. This work provides knowledge that opens new avenues of research in this underexplored field.

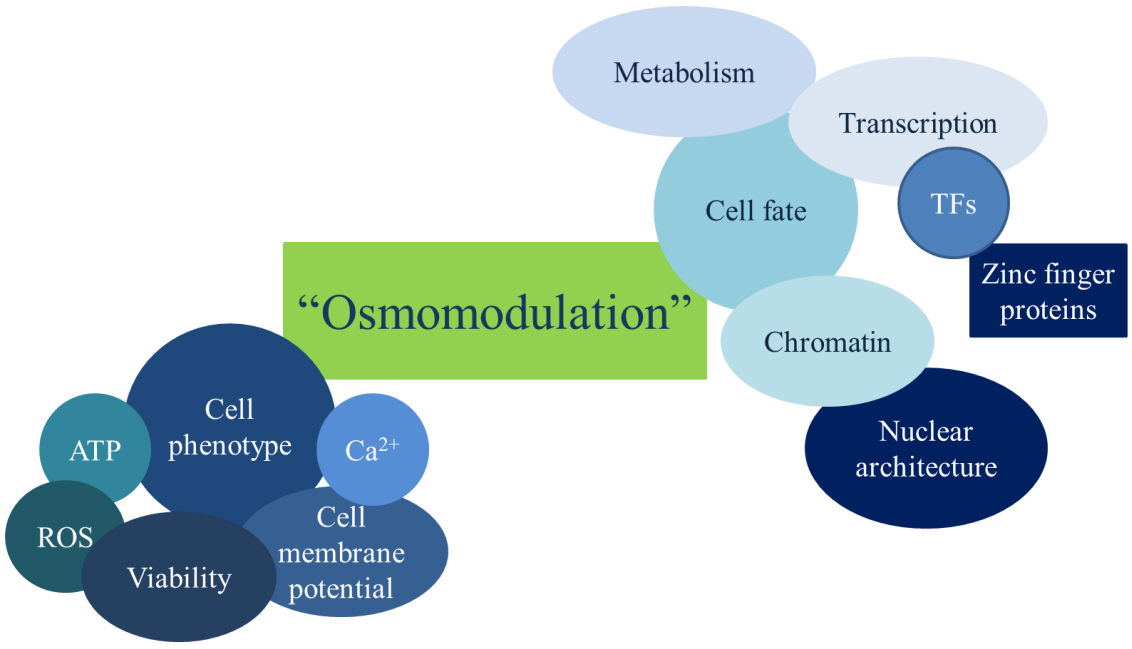

Figure 6.1 – Work hypothesis scheme.

In the cellular therapy field the use of environmental cues to serve as triggers for delivering strategies is a very relevant area. The advent of smart polymers that respond to environmental cues is one example of these strategies (Bhat and Kumar, 2013; Pribenszky et al., 2010; Stace et al., 2016). In this line of thought, the use of osmolyte-sensitive triggers for therapeutic release is an interesting approach that can take advantage of specific microenvironments. Also, environment modulation for a targeted and temporally controlled release of therapeutic agents can be envisioned. Such strategy could include the use of engineered ZF proteins and ZF nucleases that are very relevant for targeted transcriptional control and also for tailored genome editing, respectively (Klug, 2010; van Rensburg et al., 2012; Vandevenne et al., 2013).

As is already described in the literature, some ZF proteins show osmolyte sensitivity that impairs its TF activity (like ERG1). The *in vitro* engineering of ZF proteins to be activated under the effect of osmolyte concentration would be a relevant approach for local transcriptional control *in vivo*.

The area of cancer is also, in our opinion, an important area where the altered ionic and water balance might have a crucial role.

In silico work could provide clues for future targeted approaches in this vast field for tailored therapeutic approaches. A simplistic and general scheme of how the osmotic modulation could be used as a therapeutic agent is schematised in Figure 6.2. The main idea behind the therapeutic potential of osmotic modulation is that by modulating the osmolarity of the environment we can attain a non-toxic stimulus that can have a direct effect on macromolecules and signalling agents that ultimately promote a transcriptional control tool and a biophysical modulator of the nuclear structure.

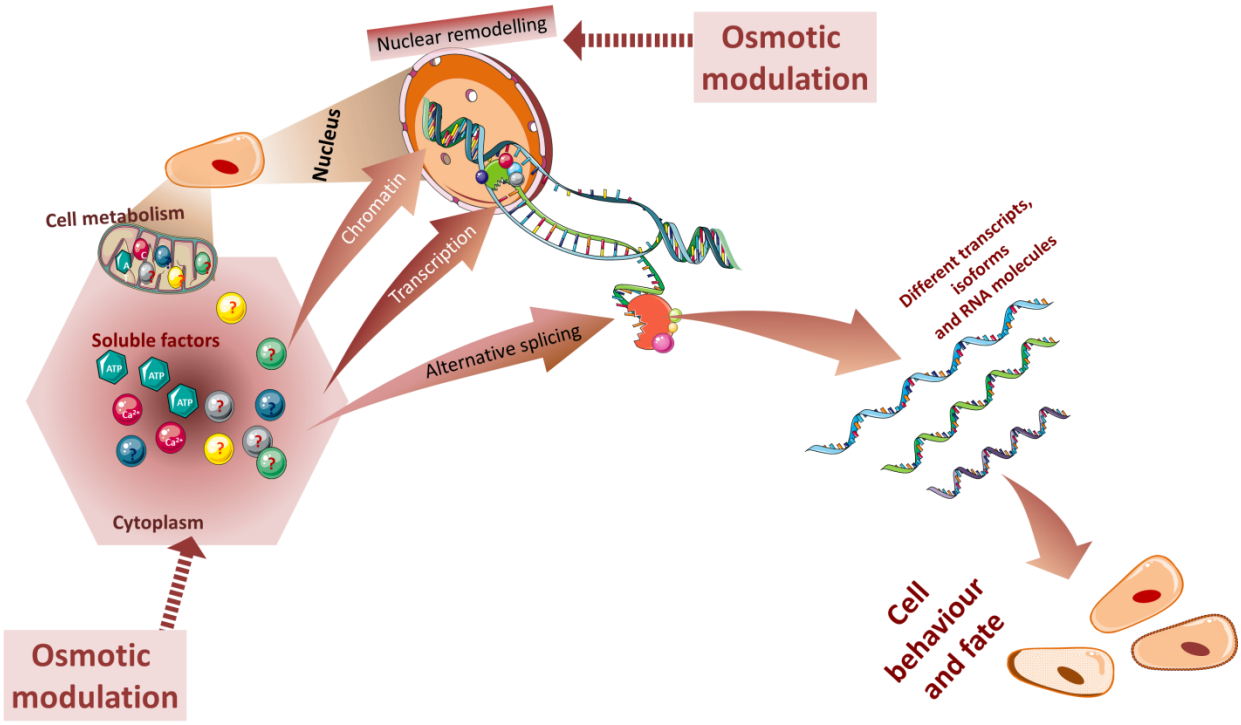

Figure 6.2 – Translational application schematic representation.

The ionic channels are already recognised in the cancer field as interesting targets with clinical potential. This interest is denoted by the increasing number of publications in the area as depicted in Figure 6.3. On the other hand the water homoeostasis and cancer relations are less explored.

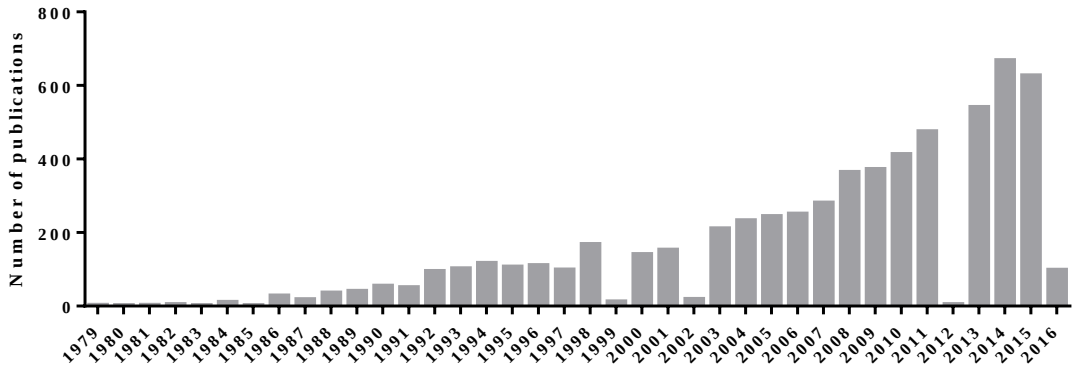

Figure 6.3 – Ionic channel and cancer-related publications over time. Results for the search did on https://www.ncbi.nlm.nih.gov/pubmed/ with the keywords “ionic channels” and “cancer”.

By performing a simple and quick search of genes described as ionic channels and involved in human cancer the result is a hit list of 165 genes as illustrated in Figure 6.4. Further modelling studies can be very valuable to understand the role of the ionic and water homoeostasis mechanisms in specific types of cancer and cancer development.

Search results

Items: 1 to 20 of 165 << First

Showing Current items.

Name/Gene ID	Description	Location	Aliases
CHRNA3 ID: 1136	cholinergic receptor nicotinic alpha 3 subunit [*Homo sapiens* (human)]	Chromosome 15, NC_000015.10 (78593052..78621295, complement)	LNCR2, NACHRA3, PAOD2
CHRNA5 ID: 1138	cholinergic receptor nicotinic alpha 5 subunit [*Homo sapiens* (human)]	Chromosome 15, NC_000015.10 (78565520..78595269)	LNCR2
HTR3B ID: 9177	5-hydroxytryptamine receptor 3B [*Homo sapiens* (human)]	Chromosome 11, NC_000011.10 (113904796..113949682)	5-HT3B
CHRNB4 ID: 1143	cholinergic receptor nicotinic beta 4 subunit [*Homo sapiens* (human)]	Chromosome 15, NC_000015.10 (78623282..78655586, complement)	
P2RX7 ID: 5027	purinergic receptor P2X 7 [*Homo sapiens* (human)]	Chromosome 12, NC_000012.12 (121132819..121189478)	P2X7
CLIC1 ID: 1192	chloride intracellular channel 1 [*Homo sapiens* (human)]	Chromosome 6, NC_000006.12 (31730581..31737318, complement)	G6, NCC27

Figure 6.4 - Ionic channel and cancer-related gene list. Results for the search did on https://www.ncbi.nlm.nih.gov/pubmed/gene/ with the keywords "ionic channels", "cancer" and "*Homo sapiens*".

We believe that future work with water homoeostasis and the ionic balance will provide fruitful knowledge for understanding the normal and pathological behaviour of cells in specific contexts. In our opinion, osmotic modulation withholds a huge potential for future development of targeted therapeutic approaches either by the impact on cellular function and metabolism but especially by its ability to influence transcription.

Final concluding remarks

Generically, the results in this work show that a hyposmotic modulation promotes:

- Increased cell size, that activates a regulatory volume decrease mechanism;
- Decreased ATP levels;
- Decreased cell membrane resting potential;

- Unchanged reactive oxygen species and mitochondrial superoxide levels;
- Decreased mitochondrial membrane potential;
- Alterations in phenotypic characteristics of umbilical cord blood cells;
- Morphological changes in cellular mitochondria and furthermore, the metabolic state of the cells, modulated by the different availability of glucose, alters the isoform transcription profile;
- Increased intracellular calcium levels;
- Cellular fate determination changes;
- Differentially alternative splicing events;
- Relaxed chromatin;
- Increased RNA polymerase II binding to chromatin;
- Increased RNA polymerase II fully engaged in transcription bound to chromatin;
- Increased RNA polymerase II initiation;
- Decreased RNA polymerase II in its free form;
- Decreased transcription speed;
- Altered binding profile of transcription factors;
- Changed transcriptional profile.

The work presented in this thesis contributes to the understanding of the functional consequences of the hyposmotic modulation with a special emphasis on cell fate determination. The osmotic regulation field is underexplored in what concerns to transient hyposmotic modulation strategies, therefore this work provides some evidence of the mechanisms involved in hyposmotic modulation and also opens new avenues for further studies of the hyposmotic modulation potential.

Chapter 7 : References

Abbasalizadeh, S., and Baharvand, H. (2013). Technological progress and challenges towards cGMP manufacturing of human pluripotent stem cells based therapeutic products for allogeneic and autologous cell therapies. Biotechnology Advances *31*, 1600–1623.

Adams, D.S., and Levin, M. (2014). Measuring Resting Membrane Potential Using the Fluorescent Voltage Reporters DiBAC4 (3) and CC2-DMPE. Cold Spring Harb Protoc. *2012*, 459–464.

Amit, M., Carpenter, M.K., Inokuma, M.S., Chiu, C.P., Harris, C.P., Waknitz, M. a, Itskovitz-Eldor, J., and Thomson, J. a (2000). Clonally derived human embryonic stem cell lines maintain pluripotency and proliferative potential for prolonged periods of culture. Developmental Biology *227*, 271–278.

Andronic, J., Shirakashi, R., Pickel, S.U., Westerling, K.M., Klein, T., Holm, T., Sauer, M., and Sukhorukov, V.L. (2015). Hypotonic activation of the myo-inositol transporter SLC5A3 in HEK293 cells probed by cell volumetry, confocal and super-resolution microscopy. PLoS ONE *10*, 1–22.

Anjamrooz, S.H. (2013). The Cellular Memory Disc of Reprogrammed Cells. Stem Cell Reviews and Reports *9*, 190–209.

Antequera, F. (2003). Structure, function and evolution of CpG island promoters. Cellular and Molecular Life Sciences : CMLS *60*, 1647–1658.

Antequera, F., and Bird, A. (1999). CpG islands as genomic footprints of promoters that are associated with replication origins. Current Biology : CB *9*, R661-7.

Atlasi, Y., Mowla, S.J., Ziaee, S.A.M.M., Gokhale, P.J., and Andrews, P.W. (2008). OCT4 Spliced Variants Are Differentially Expressed in Human Pluripotent and Nonpluripotent Cells. Stem Cells *26*, 3068–3074.

Avior, Y., Sagi, I., and Benvenisty, N. (2016). Pluripotent stem cells in disease modelling and drug discovery. Nature Reviews Molecular Cell Biology *17*, 170–182.

Baltz, J.M. (2001). Osmoregulation and cell volume regulation in the preimplantation embryo. Current Topics in Developmental Biology *52*, 55–106.

Baltz, J.M., and Tartia, A.P. (2009). Cell volume regulation in oocytes and early embryos: Connecting physiology to successful culture media. Human Reproduction Update *16*, 166–176.

Belmont, A.S. (2014). Large-scale chromatin organization: The good, the surprising, and the still perplexing. Current Opinion in Cell Biology *26*, 69–78.

Belsey, M.J., Davies, A.R.L., Witchel, H.J., and Kozlowski, R.Z. (2007). Inhibition of ERK and JNK decreases both osmosensitive taurine release and cell proliferation in glioma cells. Neurochemical Research *32*, 1940–1949.

Berger, S.L. (2002). Histone modifications in transcriptional regulation. Current Opinion in Genetics & Development *12*, 142–148.

Berman, S.B., Pineda, F.J., and Hardwick, J.M. (2008). Mitochondrial fission and fusion dynamics: the long and short of it. Cell Death & Differentiation *15*, 1147–1152.

Bernardi, R., and Pandolfi, P.P. (2007). Structure, dynamics and functions of promyelocytic leukaemia nuclear bodies. Nat Rev Mol Cell Biol *8*, 1006–1016.

Berridge, M.J., Lipp, P., and Bootman, M.D. (2000). The versatility and universality of calcium signalling. Nat Rev Mol Cell Biol *1*, 11–21.

Bersten, A.D., and Soni, N. (2009). Diabetes insipidus and other polyuric syndromes. In Oh's Intensive Care Manual, (Elsevier), pp. 621–628.

Bhat, S., and Kumar, A. (2013). Biomaterials and bioengineering tomorrow ' s healthcare. Landes Bioscience *3*, 1–12.

Bhatia, M. (2007). Hematopoietic development from human embryonic stem cells. Hematology / the Education Program of the American Society of Hematology. American Society of Hematology. Education Program 11–16.

Bianco, P. (2015). Stem cells and bone: A historical perspective. Bone *70*, 2–9.

Bilic, J., and Izpisua Belmonte, J.C. (2012). Concise review: Induced pluripotent stem cells versus embryonic stem cells: Close enough or yet too far apart? Stem Cells *30*, 33–41.

Bird, A.P. (1995). Gene number, noise reduction and biological complexity. Trends in Genetics : TIG *11*, 94–100.

Bird, A., Taggart, M., Frommer, M., Miller, O.J., and Macleod, D. (1985). A fraction of the mouse genome that is derived from islands of nonmethylated, CpG-rich DNA. Cell *40*, 91–99.

Blobel, G. a., Kadauke, S., Wang, E., Lau, A.W., Zuber, J., Chou, M.M., and Vakoc, C.R. (2009). A Reconfigured Pattern of MLL Occupancy within Mitotic Chromatin Promotes Rapid Transcriptional Reactivation Following Mitotic Exit. Molecular Cell *36*, 970–983.

Bolouri, H. (2015). Network dynamics in the tumor microenvironment. Seminars in Cancer Biology *30*, 52–59.

Brayer, K.J., and Segal, D.J. (2008). Keep your fingers off my DNA: Protein-protein interactions mediated by C2H2 zinc finger domains. Cell Biochemistry and Biophysics *50*, 111–131.

Brix, J., Zhou, Y., and Luo, Y. (2015). The Epigenetic Reprogramming Roadmap in Generation of iPSCs from Somatic Cells. Journal of Genetics and Genomics *42*, 661–670.

Broxmeyer, H.E. (2016). Enhancing the efficacy of engraftment of cord blood for hematopoietic cell transplantation. Transfusion and Apheresis Science *54*, 364–372.

Brunt, K.R., Weisel, R.D., and Li, R.-K. (2012). Stem cells and regenerative medicine — future perspectives. Can. J. Physiol. Pharmacol. 327–335.

Buschbeck, M., and Ullrich, A. (2005). The unique C-terminal tail of the mitogen-activated protein kinase ERK5 regulates its activation and nuclear shuttling. Journal of Biological Chemistry *280*, 2659–2667.

Bussmann, L.H., Schubert, A., Vu Manh, T.P., De Andres, L., Desbordes, S.C., Parra, M., Zimmermann, T., Rapino, F., Rodriguez-Ubreva, J., Ballestar, E., et al. (2009). A Robust and Highly Efficient Immune Cell Reprogramming System. Cell Stem Cell *5*, 554–566.

Butow, R.A., and Avadhani, N.G. (2004). Mitochondrial signaling: The retrograde response. Molecular

Cell *14*, 1–15.

Cagnone, G., and Sirard, M.-A. (2016). The embryonic stress response to in vitro culture: insight from genomic analysis. Reproduction *152*, R247–R261.

Caiafa, P., and Zampieri, M. (2005). DNA methylation and chromatin structure: The puzzling CpG islands. Journal of Cellular Biochemistry *94*, 257–265.

Calo, E., and Wysocka, J. (2013). Modification of Enhancer Chromatin: What, How, and Why? Molecular Cell *49*, 825–837.

Canals-Hamann, A.Z., das Neves, R.P., Reittie, J.E., Iñiguez, C., Soneji, S., Enver, T., Buckle, V.J., and Iborra, F.J. (2013). A biophysical model for transcription factories. BMC Biophysics *6*, 2.

Cao, N., Liang, H., Huang, J., Wang, J., Chen, Y., Chen, Z., and Yang, H.-T. (2013). Highly efficient induction and long-term maintenance of multipotent cardiovascular progenitors from human pluripotent stem cells under defined conditions. Cell Research *23*, 1119–1132.

Cargnello, M., and Roux, P.P. (2011). Activation and function of the MAPKs and their substrates, the MAPK-activated protein kinases. Microbiology and Molecular Biology Reviews : MMBR *75*, 50–83.

Ceci, M., Ross Jr, J., and Condorelli, G. (2016). Molecular determinants of the physiological adaptation to stress in the cardiomyocyte: a focus on AKT. Journal of Molecular and Cellular Cardiology *37*, 905–912.

Chang, L., and Karin, M. (2001). Mammalian MAP kinase signalling cascades. Nature *410*, 37–40.

Chateauvieux, S., Morceau, F., Dicato, M., and Diederich, M. (2010). Molecular and Therapeutic Potential and Toxicity of Valproic Acid. Journal of Biomedicine and Biotechnology *2010*.

Chaurasia, P., Berenzon, D., and Hoffman, R. (2011). Chromatin-modifying agents promote the ex vivo production of functional human erythroid progenitor cells. Blood *117*, 4632–4641.

Chen, C.T., Hsu, S.H., and Wei, Y.H. (2012). Mitochondrial bioenergetic function and metabolic plasticity in stem cell differentiation and cellular reprogramming. Biochimica et Biophysica Acta - General Subjects *1820*, 571–576.

Chen, H., Chomyn, A., and Chan, D.C. (2005). Disruption of fusion results in mitochondrial heterogeneity and dysfunction. Journal of Biological Chemistry *280*, 26185–26192.

Chin, M.T. (2014). Reprogramming cell fate: a changing story. Frontiers in Cell and Developmental Biology *2*, 46.

Chiri, S., Bogliolo, S., Ehrenfeld, J., and Ciapa, B. (2004). Activation of extracellular signal-regulated kinase ERK after hypo-osmotic stress in renal epithelial A6 cells. Biochimica et Biophysica Acta - Biomembranes *1664*, 224–229.

Choi, K., Kennedy, M., Kazarov, a, Papadimitriou, J.C., and Keller, G. (1998). A common precursor for hematopoietic and endothelial cells. Development (Cambridge, England) *125*, 725–732.

Choi, K.D., Vodyanik, M. a., Togarrati, P.P., Suknuntha, K., Kumar, A., Samarjeet, F., Probasco, M.D., Tian, S., Stewart, R., Thomson, J. a., et al. (2012). Identification of the Hemogenic Endothelial Progenitor and Its Direct Precursor in Human Pluripotent Stem Cell Differentiation Cultures. Cell Reports *2*, 553–567.

Di Ciano-Oliveira, C., Thirone, a. C.P., Szászi, K., and Kapus, a. (2006). Osmotic stress and the cytoskeleton: The R(h)ole of Rho GTPases. Acta Physiologica *187*, 257–272.

Cirillo, L.A., Lin, F.R., Cuesta, I., Friedman, D., Jarnik, M., and Zaret, K.S. (2002). Opening of compacted chromatin by early developmental transcription factors HNF3 (FoxA) and GATA-4. Molecular Cell *9*, 279–289.

Cláudio, N., Dalet, A., Gatti, E., and Pierre, P. (2013). Mapping the crossroads of immune activation and cellular stress response pathways. The EMBO Journal *32*, 1214–1224.

Cobb, M.H. (1999). MAP kinase pathways. Progress in Biophysics and Molecular Biology *71*, 479–500.

Cockerill, P.N. (2011). Structure and function of active chromatin and DNase i hypersensitive sites. FEBS Journal *278*, 2182–2210.

Coelho, P.M.P., Rosado-de-Castro, P.H., Gubert, F., and Mendez-Otero, R. (2016). Transplantation of Umbilical Cord Blood Cells for Patients with Neonatal Hypoxic-Ischemic Encephalopathy and Cerebral Palsy: From Preclinical Studies to Ongoing Clinical Trials. Frontiers in Stem Cell and Regenerative Medicine *2*, 225–254.

Collins, C., Wang, J., Miao, H., Bronstein, J., Nawer, H., Xu, T., Figueroa, M., Muntean, A.G., and Hess, J.L. (2014). C/EBPalpha is an essential collaborator in Hoxa9/Meis1-mediated leukemogenesis. Proceedings of the National Academy of Sciences of the United States of America *111*, 9899–9904.

Cooper, M.D. (2003). Robert A. Good May 21, 1922–June 13, 2003. The Journal of Immunology *171*, 6318–6319.

Cooper, D.N., Taggart, M.H., and Bird, A.P. (1983). Unmethylated domains in vertebrate DNA. Nucleic Acids Research *11*, 647–658.

Crepel, V., Panenka, W., Kelly, M.E., and MacVicar, B.A. (1998). Mitogen-activated protein and tyrosine kinases in the activation of astrocyte volume-activated chloride current. The Journal of Neuroscience : The Official Journal of the Society for Neuroscience *18*, 1196–1206.

Cuadrado, A., and Nebreda, A.R. (2010). Mechanisms and functions of p38 MAPK signalling. The Biochemical Journal *429*, 403–417.

Cyert, M.S. (2001). Regulation of Nuclear Localization during Signaling. Journal of Biological Chemistry *276*, 20805–20808.

Cyranoski, D. (2012). Stem-cell pioneer banks on future therapies. Nature *488*, 139–139.

Dahl, S.C., Handler, J.S., and Kwon, H.M. (2001). Hypertonicity-induced phosphorylation and nuclear localization of the transcription factor TonEBP. American Journal of Physiology - Cell Physiology *280*, C248 LP-C253.

vom Dahl, S., Schliess, F., Graf, D., and Häussinger, D. (2001). Role of $p38^{MAPK}$ in Cell Volume Regulation of Perfused Rat Liver. Cellular Physiology and Biochemistry *11*, 285–294.

Dai, D.-F., Chiao, Y.A., Marcinek, D.J., Szeto, H.H., and Rabinovitch, P.S. (2014). Mitochondrial oxidative stress in aging and healthspan. Longevity & Healthspan *3*, 6.

Darzacq, X., Shav-Tal, Y., de Turris, V., Brody, Y., Shenoy, S.M., Phair, R.D., and Singer, R.H. (2007). In vivo dynamics of RNA polymerase II transcription. Nat Struct Mol Biol *14*, 796–806.

Das, S., Jena, S., and Levasseur, D.N. (2011). Alternative splicing produces nanog protein variants with different capacities for self-renewal and pluripotency in embryonic stem cells. Journal of Biological Chemistry *286*, 42690–42703.

Davies, K.J.A. (2016). Adaptive homeostasis. Molecular Aspects of Medicine *49*, 1–7.

De, S., Chan, A.C.K., Coyne III, H.J., Bhachech, N., Hermsdorf, U., Okon, M., Murphy, M.E.P., Graves, B.J., and McIntosh, L.P. (2014). Steric Mechanism of Auto-Inhibitory Regulation of Specific and Non-Specific DNA Binding by the ETS Transcriptional Repressor ETV6. Journal of Molecular Biology *426*, 1390–1406.

Deaton, A., and Bird, A. (2011). CpG islands and the regulation of transcription. Genes & Development *25*, 1010–1022.

Delgado-Olguín, P., and Recillas-Targa, F. (2011). Chromatin structure of pluripotent stem cells and induced pluripotent stem cells. Briefings in Functional Genomics *10*, 37–49.

Demaurex, N., Poburko, D., and Frieden, M. (2009). Regulation of plasma membrane calcium fluxes by mitochondria. Biochim Biophys Acta *1787*, 1383–1394.

Demirovic, D., and Rattan, S.I.S. (2013). Establishing cellular stress response profiles as biomarkers of homeodynamics, health and hormesis. Experimental Gerontology *48*, 94–98.

Desjardins, G., Okon, M., Graves, B.J., and McIntosh, L.P. (2016). Conformational Dynamics and the Binding of Specific and Nonspecific DNA by the Autoinhibited Transcription Factor Ets-1. Biochemistry *55*, 4105–4118.

Dhawan, V. (2014). Reactive Oxygen and Nitrogen Species: General Considerations. In Studies on Respiratory Disorders, N.K. Ganguly, S.K. Jindal, S. Biswal, P.J. Barnes, and R. Pawankar, eds. (New York, NY: Springer New York), pp. 27–47.

Dhillon, A.S., Hagan, S., Rath, O., and Kolch, W. (2007). MAP kinase signalling pathways in cancer. Oncogene *26*, 3279–3290.

Diaz-Rodriguez, E., and Pandiella, A. (2010). Multisite phosphorylation of Erk5 in mitosis. Journal of Cell Science *123*, 3146–3156.

Downing, T.L., Soto, J., Morez, C., Houssin, T., Fritz, A., Yuan, F., Chu, J., Patel, S., Schaffer, D. V, and Li, S. (2013). Biophysical regulation of epigenetic state and cell reprogramming. Nature Materials *12*, 1154–1162.

Du, X.Y., and Sorota, S. (2000). Cardiac swelling-induced chloride current is enhanced by endothelin. Journal of Cardiovascular Pharmacology *35*, 769–776.

Dudek, R.M., Chuang, Y., and Leonard, J.N. (2014). Engineered Cell-Based Therapies:AVanguard of Design-Driven Medicine. *844*, 117–129.

Edwards, C.A., and Ferguson-Smith, A.C. (2007). Mechanisms regulating imprinted genes in clusters. Current Opinion in Cell Biology *19*, 281–289.

Eguizabal, C., Montserrat, N., Veiga, A., and Belmonte, J.I. (2013). Dedifferentiation, transdifferentiation, and reprogramming: Future directions in regenerative medicine. Seminars in Reproductive Medicine.

Ehrensberger, A.H., and Svejstrup, J.Q. (2012). Reprogramming chromatin. Critical Reviews in Biochemistry and Molecular Biology *47*, 464–482.

Esteller, M. (2007). Cancer epigenomics: DNA methylomes and histone-modification maps. Nature Reviews. Genetics *8*, 286–298.

Etchegaray, J.P., and Mostoslavsky, R. (2016). Interplay between Metabolism and Epigenetics: A Nuclear Adaptation to Environmental Changes. Molecular Cell *62*, 695–711.

Evans, M.J., and Kaufman, M.H. (1981). Establishment in culture of pluripotential cells from mouse embryos. Nature *292*, 154–156.

Faivre, L., Parietti, V., Sineriz, F., Chantepie, S., Gilbert-Sirieix, M., Albanese, P., Larghero, J., and Vanneaux, V. (2016). In vitro and in vivo evaluation of cord blood hematopoietic stem and progenitor cells amplified with glycosaminoglycan mimetic. Stem Cell Research & Therapy *7*, 3.

Feng, B., Ng, J.-H., Heng, J.-C.D., and Ng, H.-H. (2009). Molecules that promote or enhance reprogramming of somatic cells to induced pluripotent stem cells. Cell Stem Cell *4*, 301–312.

Ferreira, M.S.V., Schneider, R.K., Wagner, W., Jahnen-Dechent, W., Labude, N., Bovi, M., Piroth, D., Knüchel, R., Hieronymus, T., Müller, A.M., et al. (2012). Two-Dimensional Polymer-Based Cultures Expand Cord Blood-Derived Hematopoietic Stem Cells and Support Engraftment of NSG Mice. Tissue Engineering Part C: Methods *19*, 120823093401006.

Ferreiro, I., Joaquin, M., Islam, A., Gomez-Lopez, G., Barragan, M., Lombardía, L., Domínguez, O., Pisano, D.G., Lopez-Bigas, N., Nebreda, A.R., et al. (2010a). Whole genome analysis of p38 SAPK-mediated gene expression upon stress. BMC Genomics *11*, 144.

Ferreiro, I., Barragan, M., Gubern, A., Ballestar, E., Joaquin, M., and Posas, F. (2010b). The p38 SAPK is recruited to chromatin via its interaction with transcription factors. Journal of Biological Chemistry *285*, 31819–31828.

Fiedler, K., and Brunner, C. (2012). The role of transcription factors in the guidance of granulopoiesis. American Journal of Blood Research *2*, 57–65.

Finan, J.D., and Guilak, F. (2010). The effects of osmotic stress on the structure and function of the cell nucleus. Journal of Cellular Biochemistry *109*, 460–467.

Finan, J.D., Chalut, K.J., Wax, A., and Guilak, F. (2009). Nonlinear osmotic properties of the cell nucleus. Annals of Biomedical Engineering *37*, 477–491.

Finan, J.D., Leddy, H. a., and Guilak, F. (2011). Osmotic stress alters chromatin condensation and nucleocytoplasmic transport. Biochemical and Biophysical Research Communications *408*, 230–235.

Fischle, W., Wang, Y., and Allis, C.D. (2003). Histone and chromatin cross-talk. Current Opinion in Cell Biology *15*, 172–183.

Folmes, C.D.L., Dzeja, P.P., Nelson, T.J., and Terzic, A. (2012a). Mitochondria in control of cell fate. Circulation Research *110*, 526–529.

Folmes, C.D.L., Nelson, T.J., Dzeja, P.P., and Terzic, A. (2012b). Energy metabolism plasticity enables stemness programs. Annals of the New York Academy of Sciences *1254*, 82–89.

Franck, J.M., Ding, Y., Stone, K., Qin, P.Z., and Han, S. (2015). Anomalously Rapid Hydration Water

Diffusion Dynamics Near DNA Surfaces. Journal of the American Chemical Society *137*, 12013–12023.

Franco, R., Rodríguez, R., and Pasantes-Morales, H. (2004). Mechanisms of the ATP potentiation of hyposmotic taurine release in Swiss 3T3 fibroblasts. Pflugers Archiv European Journal of Physiology *449*, 159–169.

French, A.J., Adams, C.A., Anderson, L.S., Kitchen, J.R., Hughes, M.R., and Wood, S.H. (2008). Development of human cloned blastocysts following somatic cell nuclear transfer with adult fibroblasts. Stem Cells (Dayton, Ohio) *26*, 485–493.

Fuchs, E. (2009). The Tortoise and the Hair: Slow-Cycling Cells in the Stem Cell Race. Cell *137*, 811–819.

Futscher, B.W., Oshiro, M.M., Wozniak, R.J., Holtan, N., Hanigan, C.L., Duan, H., and Domann, F.E. (2002). Role for DNA methylation in the control of cell type specific maspin expression. Nature Genetics *31*, 175–179.

Gabut, M., Samavarchi-Tehrani, P., Wang, X., Slobodeniuc, V., O'Hanlon, D., Sung, H.K., Alvarez, M., Talukder, S., Pan, Q., Mazzoni, E.O., et al. (2011). An alternative splicing switch regulates embryonic stem cell pluripotency and reprogramming. Cell *147*, 132–146.

Galizia, L., Flamenco, M.P., Rivarola, V., Capurro, C., and Ford, P. (2008). Role of AQP2 in activation of calcium entry by hypotonicity: implications in cell volume regulation. American Journal of Physiology. Renal Physiology *294*, F582-90.

Galloway, C. a, Lee, H., and Yoon, Y. (2012). Mitochondrial morphology - Emerging role in bioenergetics. Free Radical Biology & Medicine *53*, 1–11.

Gan, Q., Yoshida, T., McDonald, O.G., and Owens, G.K. (2007). Concise review: epigenetic mechanisms contribute to pluripotency and cell lineage determination of embryonic stem cells. Stem Cells *25*, 2–9.

Ganapathy-Kanniappan, S., and Geschwind, J.-F.H. (2013). Tumor glycolysis as a target for cancer therapy: progress and prospects. Molecular Cancer *12*, 152.

Gao, W., Pu, Y., Luo, K.Q., and Chang, D.C. (2001). Temporal relationship between cytochrome c release and mitochondrial swelling during UV-induced apoptosis in living HeLa cells. Journal of Cell Science *114*, 2855–2862.

Garg, S., Madkaikar, M., and Ghosh, K. (2013). Investigating cell surface markers on normal hematopoietic stem cells in three different niche conditions. International Journal of Stem Cells *6*, 129–133.

Garigan, D., Hsu, A.L., Fraser, A.G., Kamath, R.S., Abringet, J., and Kenyon, C. (2002). Genetic analysis of tissue aging in Caenorhabditis elegans: A role for heat-shock factor and bacterial proliferation. Genetics *161*, 1101–1112.

Garlid, K.D., and Paucek, P. (2003). Mitochondrial potassium transport: The K+ cycle. Biochimica et Biophysica Acta - Bioenergetics *1606*, 23–41.

Gasiorowski, J.Z., Murphy, C.J., and Nealey, P.F. (2013). Biophysical cues and cell behavior: the big impact of little things. Annual Review of Biomedical Engineering *15*, 155–176.

Gehart, H., Kumpf, S., Ittner, A., and Ricci, R. (2010). MAPK signalling in cellular metabolism: stress or wellness? EMBO Reports *11*, 834–840.

Gems, D., and Partridge, L. (2008). Stress-Response Hormesis and Aging: "That which Does Not Kill Us Makes Us Stronger." Cell Metabolism *7*, 200–203.

Gill, G. (2003). Post-translational modification by the small ubiquitin-related modifier SUMO has big effects on transcription factor activity. Current Opinion in Genetics & Development *13*, 108–113.

Giorgetti, A., Montserrat, N., Rodriguez-Piza, I., Azqueta, C., Veiga, A., and Izpisúa Belmonte, J.C. (2010). Generation of induced pluripotent stem cells from human cord blood cells with only two factors: Oct4 and Sox2. Nature Protocols *5*, 811–820.

Gomez, N., Erazo, T., and Lizcano, J.M. (2016). ERK5 and Cell Proliferation: Nuclear Localization Is What Matters. Frontiers in Cell and Developmental Biology Front. Cell Dev. Biol *4*, 1–7.

Gopalakrishna-Pillai, S., and Iverson, L.E. (2011). A DNMT3B alternatively spliced exon and encoded peptide are novel biomarkers of human pluripotent stem cells. PLoS ONE *6*.

Gori, J.L., Chandrasekaran, D., Kowalski, J.P., Adair, J.E., Beard, B.C., D'Souza, S.L., and Kiem, H.P. (2012). Efficient generation, purification, and expansion of CD34+ hematopoietic progenitor cells from nonhuman primate-induced pluripotent stem cells. Blood *120*, 34–44.

Gottlieb, R.A., and Bernstein, D. (2016). Mitochondrial remodeling: Rearranging, recycling, and reprogramming. Cell Calcium *60*, 88–101.

Graf, T. (2011). Historical origins of transdifferentiation and reprogramming. Cell Stem Cell *9*, 504–516.

Graveley, B.R. (2011). Splicing up pluripotency. Cell *147*, 22–24.

Guantes, R., Rastrojo, A., Neves, R., Lima, A., Aguado, B., and Iborra, F.J. (2015). Global variability in gene expression and alternative splicing is modulated by mitochondrial content. Genome Research *125*, 633–644.

Guenther, M.G., Levine, S.S., Boyer, L.A., Jaenisch, R., and Young, R.A. (2007). A chromatin landmark and transcription initiation at most promoters in human cells. Cell *130*, 77–88.

Guo, T., and Fang, Y. (2014). Functional organization and dynamics of the cell nucleus. Frontiers in Plant Science *5*, 378.

Guo, C., Sun, L., Chen, X., and Zhang, D. (2012). Oxidative stress, mitochondrial damage and neurodegenerative diseases. Neural Regeneration Research *7*, 440–444.

Gurdon, J.B. (1962). The Developmental Capacity of Nuclei taken from Intestinal Epithelium Cells of Feeding Tadpoles. Journal of Embryology and Experimental Morphology *10*, 622 LP-640.

Haase, A., Olmer, R., Schwanke, K., Wunderlich, S., Merkert, S., Hess, C., Zweigerdt, R., Gruh, I., Meyer, J., Wagner, S., et al. (2009). Generation of Induced Pluripotent Stem Cells from Human Cord Blood. Cell Stem Cell *5*, 434–441.

Halterman, J. a., Kwon, H.M., and Wamhoff, B.R. (2012). Tonicity-independent regulation of the osmosensitive transcription factor TonEBP (NFAT5). American Journal of Physiology. Cell Physiology *302*, C1–C8.

Hämäläinen, R.H. (2016). Mitochondria and mtDNA integrity in stem cell function and differentiation. Current Opinion in Genetics & Development *38*, 83–89.

Han, S.-M., Coh, Y.-R., Ahn, J.-O., Jang, G., Yum, S.Y., Kang, S.-K., Lee, H.-W., and Youn, H.-Y. (2015). Enhanced hepatogenic transdifferentiation of human adipose tissue mesenchymal stem cells by gene engineering with Oct4 and Sox2. PloS One *10*, e0108874.

Hanna, E., Rémuzat, C., Auquier, P., and Toumi, M. (2016). Advanced therapy medicinal products: current and future perspectives. Journal of Market Access & Health Policy *4*, 1–10.

Hanna, J., Markoulaki, S., Schorderet, P., Carey, B.W., Beard, C., Wernig, M., Creyghton, M.P., Steine, E.J., Cassady, J.P., Foreman, R., et al. (2008). Direct reprogramming of terminally differentiated mature B lymphocytes to pluripotency. Cell *133*, 250–264.

Hansen, A., Van Hoy, M., and Kodadek, T. (1991). Spectroscopic studies of the DNA binding site of the GAL4 "zinc finger" protein. Biochemical and Biophysical Research Communications *175*, 492–499.

Hao, Q.L., Shah, a J., Thiemann, F.T., Smogorzewska, E.M., and Crooks, G.M. (1995). A functional comparison of CD34 + CD38- cells in cord blood and bone marrow. Blood *86*, 3745–3753.

Heslop, J.A., Hammond, T.G., Santeramo, I., Tort Piella, A., Hopp, I., Zhou, J., Baty, R., Graziano, E.I., Proto Marco, B., Caron, A., et al. (2015). Concise review: workshop review: understanding and assessing the risks of stem cell-based therapies. Stem Cells Translational Medicine *4*, 389–400.

Hill, S., and Van Remmen, H. (2014). Mitochondrial stress signaling in longevity: A new role for mitochondrial function in aging. Redox Biology *2*, 936–944.

Hirose, Y., and Ohkuma, Y. (2007). Phosphorylation of the C-terminal domain of RNA polymerase II plays central roles in the integrated events of eucaryotic gene expression. Journal of Biochemistry *141*, 601–608.

Ho, S.N. (2006). Intracellular water homeostasis and the mammalian cellular osmotic stress response. Journal of Cellular Physiology *206*, 9–15.

Hoffmann, E.K., and Pedersen, S.F. (2011). Cell volume homeostatic mechanisms: effectors and signalling pathways. Acta Physiologica (Oxford, England) *202*, 465–485.

Hoffmann, E.K., Lambert, I.H., and Pedersen, S.F. (2009). Physiology of cell volume regulation in vertebrates. Physiological Reviews *89*, 193–277.

Hohmann, S. (2002). Osmotic stress signaling and osmoadaptation in yeasts. Microbiology and Molecular Biology Reviews : MMBR *66*, 300–372.

Hohmann, S. (2015). An integrated view on a eukaryotic osmoregulation system. Current Genetics *61*, 373–382.

Honeycutt, K.A., Koster, M.I., and Roop, D.R. (2004). Genes involved in stem cell fate decisions and commitment to differentiation play a role in skin disease. J Investig Dermatol Symp Proc *9*, 261–268.

Huang, P., Zhang, L., Gao, Y., He, Z., Yao, D., Wu, Z., Cen, J., Chen, X., Liu, C., Hu, Y., et al. (2014). Direct reprogramming of human fibroblasts to functional and expandable hepatocytes. Cell Stem Cell *14*, 370–384.

Huang, W., Liu, H., Wang, T., Zhang, T., Kuang, J., Luo, Y., Chung, S.S.M., Yuan, L., and Yang, J.Y. (2011). Tonicity-responsive microRNAs contribute to the maximal induction of osmoregulatory transcription factor OREBP in response to high-NaCl hypertonicity. Nucleic Acids Research *39*, 475–485.

Huangfu, D., Maehr, R.R., Guo, W., Eijkelenboom, A., Snitow, M., Chen, A.E., and Melton, D.A. (2008). Induction of pluripotent stem cells by defined factors is greatly improved by small-molecule compounds. Nature Biotechnology *26*, 795–797.

Hui, L., and Chen, Y. (2015). Tumor microenvironment: Sanctuary of the devil. Cancer Letters *368*, 7–13.

Hunt, C.J., Armitage, S.E., and Pegg, D.E. (2003a). Cryopreservation of umbilical cord blood: 1. Osmotically inactive volume, hydraulic conductivity and permeability of CD34+ cells to dimethyl sulphoxide. Cryobiology *46*, 61–75.

Hunt, C.J., Armitage, S.E., and Pegg, D.E. (2003b). Cryopreservation of umbilical cord blood: 2. Tolerance of CD34+ cells to multimolar dimethyl sulphoxide and the effect of cooling rate on recovery after freezing and thawing. Cryobiology *46*, 76–87.

Iborra, F.J., Pombo, a, Jackson, D. a, and Cook, P.R. (1996). Active RNA polymerases are localized within discrete transcription "factories' in human nuclei. Journal of Cell Science *109 (Pt 6*, 1427–1436.

Iborra, F.J., Jackson, D.A., and Cook, P.R.. R. (1998). The path of transcripts from extra-nucleolar synthetic sites to nuclear pores:transcripts in transit are concentrated in discrete structures containing SRproteins. Journal of Cell Science *111*, 2269–2282.

Iborra, F.J., Jackson, D.A., and Cook, P.R. (2001). Coupled Transcription and Translation Within Nuclei of Mammalian Cells. Science *293*, 1139 LP-1142.

Iborra, F.J., Escargueil, A.E., Kwek, K.Y., Akoulitchev, A., and Cook, P.R. (2004). Molecular cross-talk between the transcription, translation, and nonsense-mediated decay machineries. Journal of Cell Science *117*, 899–906.

Illingworth, R.S., and Bird, A.P. (2009). CpG islands - "A rough guide." FEBS Letters *583*, 1713–1720.

Illingworth, R., Kerr, A., Desousa, D., Jorgensen, H., Ellis, P., Stalker, J., Jackson, D., Clee, C., Plumb, R., Rogers, J., et al. (2008). A novel CpG island set identifies tissue-specific methylation at developmental gene loci. PLoS Biology *6*, e22.

Indumathi, S., Harikrishnan, R., Rajkumar, J.S., and Dhanasekaran, M. (2013). Immunophenotypic comparison of heterogenous non-sorted versus sorted mononuclear cells from human umbilical cord blood: a novel cell enrichment approach. Cytotechnology 1–8.

Inesta-Vaquera, F.A., Campbell, D.G., Tournier, C., Gomez, N., Lizcano, J.M., and Cuenda, A. (2010). Alternative ERK5 regulation by phosphorylation during the cell cycle. Cellular Signalling *22*, 1829–1837.

International Human Genome Sequencing, C. (2001). Initial sequencing and analysis of the human genome. Nature *409*, 860–921.

Irarrazabal, C.E., Liu, J.C., Burg, M.B., and Ferraris, J.D. (2004). ATM, a DNA damage-inducible kinase, contributes to activation by high NaCl of the transcription factor TonEBP/OREBP. Proceedings of the National Academy of Sciences of the United States of America *101*, 8809–8814.

Irianto, J., Swift, J., Martins, R.P., McPhail, G.D., Knight, M.M., Discher, D.E., and Lee, D.A. (2013). Osmotic challenge drives rapid and reversible chromatin condensation in chondrocytes. Biophysical Journal *104*, 759–769.

Ito, K., and Ito, K. (2016). Metabolism and the Control of Cell Fate Decisions and Stem Cell Renewal.

Annual Review of Cell and Developmental Biology *32*, annurev-cellbio-111315-125134.

Ito, S., Magalska, A., Alcaraz-Iborra, M., Lopez-Atalaya, J.P., Rovira, V., Contreras-Moreira, B., Lipinski, M., Olivares, R., Martinez-Hernandez, J., Ruszczycki, B., et al. (2014). Loss of neuronal 3D chromatin organization causes transcriptional and behavioural deficits related to serotonergic dysfunction. Nature Communications *5*, 4450.

Iwafuchi-Doi, M., and Zaret, K.S. (2014). Pioneer transcription factors in cell reprogramming. 1–11.

Jackson, D.A., Iborra, F.J., Manders, E.M., and Cook, P.R. (1998). Numbers and organization of RNA polymerases, nascent transcripts, andtranscription units in HeLa nuclei. Molecular Biology of the Cell *9*, 1523–1536.

Jackson, D.A., Pombo, A., and Iborra, F. (2000). The balance sheet for transcription: an analysis of nuclear RNA metabolism in mammalian cells. The FASEB Journal *14*, 242–254.

Jacquet, M., Renault, G., Lallet, S., De Mey, J., and Goldbeter, A. (2003). Oscillatory behavior of the nuclear localization of the transcription factors Msn2 and Msn4 in response to stress in yeast. TheScientificWorldJournal *3*, 609–612.

Jaenisch, R. (2009). Stem cells, pluripotency and nuclear reprogramming. Journal of Thrombosis and Haemostasis *7*, 21–23.

Jaenisch, R., and Young, R. (2008). Stem Cells, the Molecular Circuitry of Pluripotency and Nuclear Reprogramming. Cell *132*, 567–582.

Jang, J.-H., Kim, S.-K., Choi, J.-E., Kim, Y.-J., Lee, H.-W., Kang, S.-Y., Park, J.-S., Choi, J.-H., Lim, H.-Y., and Kim, H.C. (2007). Endothelial progenitor cell differentiation using cryopreserved, umbilical cord blood-derived mononuclear cells. Acta Pharmacologica Sinica *28*, 367–374.

Jasnovidova, O., and Stefl, R. (2013). The CTD code of RNA polymerase II: A structural view. Wiley Interdisciplinary Reviews: RNA.

Jenkins, M.J., and Farid, S.S. (2015). Human pluripotent stem cell-derived products: Advances towards robust, scalable and cost-effective manufacturing strategies. Biotechnology Journal *10*, 83–95.

Jhun, B.S., Mishra, J., Monaco, S., Fu, D., Jiang, W., Sheu, S.-S., and O-Uchi, J. (2016). The mitochondrial Ca^{2+} uniporter: Regulation by auxiliary subunits and signal transduction pathways. American Journal of Physiology - Cell Physiology ajpcell.00319.2015.

Jiang, F., Zhang, Y., and Dusting, G.J. (2011). NADPH oxidase-mediated redox signaling: roles in cellular stress response, stress tolerance, and tissue repair. Pharmacological Reviews *63*, 218–242.

Johnston, M. (1987). Genetic evidence that zinc is an essential co-factor in the DNA binding domain of GAL4 protein. Nature *328*, 353–355.

Johnston, I.G., Gaal, B., das Neves, R.P., Enver, T., Iborra, F.J., and Jones, N.S. (2012). Mitochondrial variability as a source of extrinsic cellular noise. PLoS Computational Biology *8*, 35–37.

Juhaszova, M., Zorov, D.B., Kim, S., Pepe, S., Fu, Q., Fishbein, K.W., Ziman, B.D., Wang, S., Ytrehus, K., Antos, C.L., et al. (2004). Glycogen synthase kinase-3beta mediates convergence of protection signaling to inhibit the mitochondrial permeability transition pore. The Journal of Clinical Investigation *113*, 1535–1549.

Kaasik, A., Safiulina, D., Zharkovsky, A., and Veksler, V. (2007). Regulation of mitochondrial matrix volume. American Journal of … *292*, 157–163.

Kahlert, S., and Reiser, G. (2002). Swelling of mitochondria in cultured rat hippocampal astrocytes is induced by high cytosolic Ca2+ load, but not by mitochondrial depolarization. FEBS Letters *529*, 351–355.

Kassahn, K.S., Crozier, R.H., Pörtner, H.O., and Caley, M.J. (2009). Animal performance and stress: Responses and tolerance limits at different levels of biological organisation. Biological Reviews *84*, 277–292.

Kato, Y., Chao, T.H., Hayashi, M., Tapping, R.I., and Lee, J.D. (2000). Role of BMK1 in regulation of growth factor-induced cellular responses. Immunol Res *21*, 233–237.

Kaufman, R.J., and Malhotra, J.D. (2014). Calcium trafficking integrates endoplasmic reticulum function with mitochondrial bioenergetics. Biochimica et Biophysica Acta - Molecular Cell Research *1843*, 2233–2239.

Kaur, P., Plochberger, B., Costa, P., Cope, S.M., Vaiana, S.M., and Lindsay, S. (2012). Hydrophobicity of Methylated DNA as a Possible Mechanism for Gene Silencing. Physical Biology *9*, 65001.

Kim, C.H., Rhee, P.L., Rhee, J.C., Kim, Y.I., So, I., Kim, K.W., Park, M.K., Uhm, D.Y., and Kang, T.M. (2000). Hypotonic swelling increases L-type calcium current in smooth muscle cells of the human stomach. Experimental Physiology *85*, 497–504.

Kim, Y., Phan, D., van Rooij, E., Wang, D.-Z., McAnally, J., Qi, X., Richardson, J.A., Hill, J.A., Bassel-Duby, R., and Olson, E.N. (2008). The MEF2D transcription factor mediates stress-dependent cardiac remodeling in mice. The Journal of Clinical Investigation *118*, 124–132.

Kimura, H., Sugaya, K., and Cook, P.R. (2002). The transcription cycle of RNA polymerase II in living cells. The Journal of Cell Biology *159*, 777–782.

Kimura, T., Mills, F.C., Allan, J., and Gould, H. (1983). Selective unfolding of erythroid chromatin in the region of the active beta-globin gene. Nature *306*, 709–712.

Klapperstück, T., Glanz, D., Klapperstück, M., and Wohlrab, J. (2009). Methodological aspects of measuring absolute values of membrane potential in human cells by flow cytometry. Cytometry Part A *75*, 593–608.

Klug, A. (2010). The discovery of zinc fingers and their development for practical applications in gene regulation and genome manipulation. Annual Review of Biochemistry *79*, 213.

Knoepfler, P.S., Zhang, X., Cheng, P.F., Gafken, P.R., McMahon, S.B., and Eisenman, R.N. (2006). Myc influences global chromatin structure. The EMBO Journal *25*, 2723–2734.

Ko, B.C.B., Lam, A.K.M., Kapus, A., Fan, L., Chung, S.K., and Chung, S.S.M. (2002). Fyn and p38 signaling are both required for maximal hypertonic activation of the osmotic response element-binding protein/tonicity-responsive enhancer-binding protein (OREBP/TonEBP). Journal of Biological Chemistry *277*, 46085–46092.

Koblas, T., Leontovyc, I., Loukotova, S., Kosinova, L., and Saudek, F. (2016). Reprogramming of Pancreatic Exocrine Cells AR42J Into Insulin-producing Cells Using mRNAs for Pdx1, Ngn3, and MafA Transcription Factors. Molecular Therapy. Nucleic Acids *5*, e320.

Koivusalo, M., Kapus, A., and Grinstein, S. (2009). Sensors, transducers, and effectors that regulate cell size and shape. Journal of Biological Chemistry.

Kölbel, B., Wienert, S., Dimitriadis, J., Kendoff, D., Gehrke, T., Huber, M., Frommelt, L., Tiemann, A., Saeger, K., and Krenn, V. (2015). CD15 focus score for diagnostics of periprosthetic joint infections. Zeitschrift F{ü}r Rheumatologie *74*, 622–630.

Krause, M.N., Sancho-Martinez, I., and Izpisua Belmonte, J.C. (2015). Understanding the molecular mechanisms of reprogramming.

Krieger, T., and Simons, B.D. (2015). Dynamic stem cell heterogeneity. Development *142*, 1396–1406.

Kshitiz, Park, J., Kim, P., Helen, W., Engler, A.J., Levchenko, A., and Kim, D.-H. (2012). Control of stem cell fate and function by engineering physical microenvironments. Integrative Biology : Quantitative Biosciences from Nano to Macro *4*, 1008–1018.

Kültz, D. (2001). Cellular osmoregulation: beyond ion transport and cell volume. Zoology (Jena, Germany) *104*, 198–208.

Kültz, D. (2005). Molecular and Evolutionary Basis of the Cellular Stress Response. Annual Review of Physiology *67*, 225–257.

Kurup, P. a., Arun, P., Gayathri, N.S., Dhanya, C.R., and Indu, a. R. (2003). Modified formulation of CPDA for storage of whole blood, and of SAGM for storage of red blood cells, to maintain the concentration of 2,3-diphosphoglycerate. Vox Sanguinis *85*, 253–261.

Kyriakis, J.M., and Avruch, J. (2012). Mammalian MAPK signal transduction pathways activated by stress and inflammation: a 10-year update. Physiological Reviews *92*, 689–737.

Ladewig, J., Koch, P., and Brüstle, O. (2013). Leveling Waddington: the emergence of direct programming and the loss of cell fate hierarchies. Nature Reviews. Molecular Cell Biology *14*, 225–236.

Laity, J.H., Lee, B.M., and Wright, P.E. (2001). Zinc finger proteins: new insights into structural and functional diversity. Current Opinion in Structural Biology *11*, 39–46.

Lang, F., and Stournaras, C. (2014). Ion channels in cancer: future perspectives and clinical potential. Philosophical Transactions of the Royal Society of London. Series B, Biological Sciences *369*, 20130108.

Lang, F., Busch, G.L., Ritter, M., Völkl, H., Waldegger, S., Gulbins, E., and Häussinger, D. (1998). Functional significance of cell volume regulatory mechanisms. Physiological Reviews *78*, 247–306.

Lange, C., and Calegari, F. (2010). Cdks and cyclins link G1 length and differentiation of embryonic, neural and hematopoietic stem cells. Cell Cycle (Georgetown, Tex.) *9*, 1893–1900.

Langmead, B., Trapnell, C., Pop, M., and Salzberg, S. (2009). Ultrafast and memory-efficient alignment of short DNA sequences to the human genome. Genome Biol. *10*, R25.

Larsen, F., Gundersen, G., Lopez, R., and Prydz, H. (1992). CpG islands as gene markers in the human genome. Genomics *13*, 1095–1107.

Lavelle, C. (2014). Pack, unpack, bend, twist, pull, push: The physical side of gene expression. Current Opinion in Genetics and Development *25*, 74–84.

De Lázaro, I., Yilmazer, A., and Kostarelos, K. (2014). Induced pluripotent stem (iPS) cells: A new

source for cell-based therapeutics? Journal of Controlled Release *185*, 37–44.

Lee, Y.H., and Peng, C.A. (2009). Effect of hypotonic stress on retroviral transduction. Biochemical and Biophysical Research Communications *390*, 1367–1371.

Lee, J.-S., Lee, J.-J., and Seo, J.-S. (2005). HSP70 deficiency results in activation of c-Jun N-terminal Kinase, extracellular signal-regulated kinase, and caspase-3 in hyperosmolarity-induced apoptosis. The Journal of Biological Chemistry *280*, 6634–6641.

Lee, J.D., Ulevitch, R.J., and Han, J. (1995). Primary structure of BMK1: a new mammalian map kinase. Biochemical and Biophysical Research Communications *213*, 715–724.

Lee, K., Yu, P., Lingampalli, N., Kim, H.J., Tang, R., and Murthy, N. (2015a). Peptide-enhanced mRNA transfection in cultured mouse cardiac fibroblasts and direct reprogramming towards cardiomyocyte-like cells. International Journal of Nanomedicine *10*, 1841–1854.

Lee, M.D., Bingham, K.N., Mitchell, T.Y., Meredith, J.L., and Rawlings, J.S. (2015b). Calcium mobilization is both required and sufficient for initiating chromatin decondensation during activation of peripheral T-cells. Molecular Immunology *63*, 540–549.

Lee, M.W., Jang, I.K., Yoo, K.H., Sung, K.W., and Koo, H.H. (2010). Stem and progenitor cells in human umbilical cord blood. International Journal of Hematology *92*, 45–51.

Li, L., and Clevers, H. (2010). Coexistence of quiescent and active adult stem cells in mammals. Science (New York, N.Y.) *327*, 542–545.

Li, M.A., and He, L. (2012). microRNAs as novel regulators of stem cell pluripotency and somatic cell reprogramming. BioEssays *34*, 670–680.

Li, J., Song, W., Pan, G., and Zhou, J. (2014). Advances in understanding the cell types and approaches used for generating induced pluripotent stem cells. 1–18.

Lim, W.F., Inoue-Yokoo, T., Tan, K.S., Lai, M., and Sugiyama, D. (2013). Hematopoietic cell differentiation from embryonic and induced pluripotent stem cells. Stem Cell Research & Therapy *4*, 71.

Ling, G., and Waxman, D.J. (2013). DNase I digestion of isolated nulcei for genome-wide mapping of DNase hypersensitivity sites in chromatin. Methods in Molecular Biology (Clifton, N.J.) *977*, 21–33.

Liu, Z., and Butow, R. a (2006). Mitochondrial retrograde signaling. Annual Review of Genetics *40*, 159–185.

Liu, J., Xu, W., Sun, T., Wang, F., Puscheck, E., Brigstock, D., Wang, Q.T., Davis, R., and Rappolee, D.A. (2009). Hyperosmolar Stress Induces Global mRNA Responses in Placental Trophoblast Stem Cells that Emulate Early Post-implantation Differentiation. Placenta *30*, 66–73.

Liu, T.M., Lee, E.H., Lim, B., and Shyh-Chang, N. (2015a). Balancing Stem Cell Self-renewal and Differentiation with PLZF. Stem Cells (Dayton, Ohio) 277–287.

Liu, X., Bandyopadhyay, B., Nakamoto, T., Singh, B., Liedtke, W., Melvin, J.E., and Ambudkar, I. (2006). A role for AQP5 in activation of TRPV4 by hypotonicity: Concerted involvement of AQP5 and TRPV4 in regulation of cell volume recovery. Journal of Biological Chemistry *281*, 15485–15495.

Liu, X., Little, J.B., and Yuan, Z. (2015b). Glycolytic metabolism influences global chromatin structure. Oncotarget *6*, 4214–4225.

Liu, Z., Zhang, F., Zhao, X., and Bai, F. (2014). [Effects of zinc-finger proteins and artificial zinc-finger proteins on microbial metabolisms--a review]. Sheng wu gong cheng xue bao = Chinese journal of biotechnology *30*, 331–340.

Lopez-Atalaya, J.P., and Barco, A. (2014). Can changes in histone acetylation contribute to memory formation? Trends in Genetics *30*, 529–539.

Lowry, J.A., Gamsjaeger, R., Thong, S.Y., Hung, W., Kwan, A.H., Broitman-Maduro, G., Matthews, J.M., Maduro, M., and Mackay, J.P. (2009). Structural analysis of MED-1 reveals unexpected diversity in the mechanism of DNA recognition by GATA-type zinc finger domains. The Journal of Biological Chemistry *284*, 5827–5835.

Lund, J., Tedesco, P., Duke, K., Wang, J., Kim, S.K., and Johnson, T.E. (2002). Transcriptional profile of aging in C. elegans. Current Biology *12*, 1566–1573.

Lyamzaev, K.G., Izyumov, D.S., Avetisyan, A. V, Yang, F., Pletjushkina, O.Y., and Chernyak, B. V (2004). Inhibition of mitochondrial bioenergetics : the effects on struc- ture of mitochondria in the cell and on apoptosis *. Cell *51*, 553–562.

Madonna, R., Görbe, A., Ferdinandy, P., and De Caterina, R. (2013). Glucose metabolism, hyperosmotic stress, and reprogramming of somatic cells. Molecular Biotechnology *55*, 169–178.

Mahmud, N., Petro, B., Baluchamy, S., Li, X., Taioli, S., Lavelle, D., Quigley, J.G., Suphangul, M., and Araki, H. (2014). Differential effects of epigenetic modifiers on the expansion and maintenance of human cord blood stem/progenitor cells. Biology of Blood and Marrow Transplantation *20*, 480–489.

Malhas, A.N., and Vaux, D.J. (2011). The nuclear envelope and its involvement in cellular stress responses. Biochemical Society Transactions *39*, 1795–1798.

Mancinelli, F., Tamburini, A., Spagnoli, A., Malerba, C., Suppo, G., Lasorella, R., de Fabritiis, P., and Calugi, A. (2006). Optimizing umbilical cord blood collection: impact of obstetric factors versus quality of cord blood units. Transplantation Proceedings *38*, 1174–1176.

Marchenko, S.M., and Sage, S.O. (2000). Hyperosmotic but not hyposmotic stress evokes a rise in cytosolic Ca2+ concentration in endothelium of intact rat aorta. Experimental Physiology *85*, 151–157.

Maret, W. (2013). Zinc biochemistry: from a single zinc enzyme to a key element of life. Advances in Nutrition (Bethesda, Md.) *4*, 82–91.

Markstein, M., and Levine, M. (2002). Decoding cis-regulatory DNAs in the Drosophila genome. Current Opinion in Genetics & Development *12*, 601–606.

Martin, G.R. (1981). Isolation of a pluripotent cell line from early mouse embryos cultured in medium conditioned by teratocarcinoma stem cells. Proceedings of the National Academy of Sciences of the United States of America *78*, 7634–7638.

Martin, R.C., Glover-Cutter, K., Baldwin, J.C., and Dombrowski, J.E. (2012). Identification and characterization of a salt stress-inducible zinc finger protein from Festuca arundinacea. BMC Research Notes *5*, 66.

Martinez-Pastor1, M.T., Marchler2, G., Schuller2, C., Marchler-Bauer3, A., Ruis2, H., and Estruch1a4, F. (1996). The Saccharomyces cerevisiae zinc finger proteins Msn2p and Msn4p are required for transcriptional induction through the stress-response element (STRE). The EMBO Journal *15*, 2227–2235.

Martins, R., Finan, J., Guilak, F., and Lee, D. (2012). Mechanical regulation of nuclear structure and function. Annual Review of Biomedical Engineering *14*, 431–455.

Mattson, M.P. (2008). Hormesis defined. Ageing Research Reviews *7*, 1–7.

McCulloch, E.A., and Till, J.E. (1960). The Radiation Sensitivity of Normal Mouse Bone Marrow Cells, Determined by Quantitative Marrow Transplantation into Irradiated Mice. Radiation Research *13*, 115–125.

McKenna, D.H., and Brunstein, C.G. (2011). Umbilical cord blood: Current status and future directions. Vox Sanguinis *100*, 150–162.

Medrano-Fernández, A., and Barco, A. (2016). Nuclear organization and 3D chromatin architecture in cognition and neuropsychiatric disorders. Molecular Brain *9*, 83.

Meinhart, A., Kamenski, T., Hoeppner, S., Baumli, S., and Cramer, P. (2005). A structural perspective of CTD function A structural perspective of CTD function. Genes & Developments 1401–1415.

Mendenhall, E.M., and Bernstein, B.E. (2008). Chromatin state maps: new technologies, new insights. Current Opinion in Genetics and Development *18*, 109–115.

Mikles, D.C., Bhat, V., Schuchardt, B.J., McDonald, C.B., and Farooq, A. (2015). Effect of osmolytes on the binding of EGR1 transcription factor to DNA. Biopolymers *103*, 74–87.

Minamikawa, T., Williams, D.A., Bowser, D.N., and Nagley, P. (1999). Mitochondrial Permeability Transition and Swelling Can Occur Reversibly without Inducing Cell Death in Intact Human Cells. Experimental Cell Research *246*, 26–37.

Mitchell, R., Szabo, E., Shapovalova, Z., Aslostovar, L., Makondo, K., and Bhatia, M. (2014). Molecular evidence for OCT4-induced plasticity in adult human fibroblasts required for direct cell fate conversion to lineage specific progenitors. Stem Cells (Dayton, Ohio) *32*, 2178–2187.

Morris, S. a, and Daley, G.Q. (2013). A blueprint for engineering cell fate: current technologies to reprogram cell identity. Cell Research *23*, 33–48.

Mount, N.M., Ward, S.J., Kefalas, P., and Hyllner, J. (2015). Cell-based therapy technology classifications and translational challenges. Philosophical Transactions of the Royal Society of London. Series B, Biological Sciences *370*, 20150017-.

Mountford, J.C. (2008). Human embryonic stem cells: Origins, characteristics and potential for regenerative therapy. Transfusion Medicine.

Mullen, S.F., Agca, Y., Broermann, D.C., Jenkins, C.L., Johnson, C.A., and Critser, J.K. (2004). The effect of osmotic stress on the metaphase II spindle of human oocytes, and the relevance to cryopreservation. Human Reproduction *19*, 1148–1154.

Muralidharan, S., and Mandrekar, P. (2013). Cellular stress response and innate immune signaling: integrating pathways in host defense and inflammation. Journal of Leukocyte Biology *94*, 1167–1184.

de Nadal, E., Ammerer, G., and Posas, F. (2011). Controlling gene expression in response to stress. Nature Reviews Genetics *12*, 833–845.

De Nadal, E., and Posas, F. (2015). Osmostress-induced gene expression - A model to understand how stress-activated protein kinases (SAPKs) regulate transcription. FEBS Journal *282*, 3275–3285.

Nagy, A., Rossant, J., Nagy, R., Abramow-Newerly, W., and Roder, J.C. (1993). Derivation of completely cell culture-derived mice from early-passage embryonic stem cells. Proceedings of the National Academy of Sciences of the United States of America *90*, 8424–8428.

Nandigama, R., Padmasekar, M., Wartenberg, M., and Sauer, H. (2006). Feed forward cycle of hypotonic stress-induced ATP release, purinergic receptor activation, and growth stimulation of prostate cancer cells. Journal of Biological Chemistry *281*, 5686–5693.

Neuhofer, W., Muller, E., Grunbein, R., Thurau, K., and Beck, F.X. (1999). Influence of NaCl, urea, potassium and pH on HSP72 expression in MDCK cells. Pflugers Archiv : European Journal of Physiology *439*, 195–200.

das Neves, R.P., Jones, N.S., Andreu, L., Gupta, R., Enver, T., and Iborra, F.J. (2010). Connecting variability in global transcription rate to mitochondrial variability. PLoS Biology *8*.

Nicoud, I.B., Clarke, D.M., Taber, G., Stolowski, K.M., Roberge, S.E., Song, M.K., Mathew, A.J., and Reems, J.A. (2012). Cryopreservation of umbilical cord blood with a novel freezing solution that mimics intracellular ionic composition. Transfusion *52*, 2055–2062.

Niisato, N., Taruno, A., and Marunaka, Y. (2007). Involvement of p38 MAPK in hypotonic stress-induced stimulation of b- and g-ENaC expression in renal epithelium. Biochemical and Biophysical Research Communications *358*, 819–824.

Nriagu, J., Darroudi, F., and Shomar, B. (2016). Health effects of desalinated water: Role of electrolyte disturbance in cancer development. Environmental Research *150*, 191–204.

Oakes, C.C., La Salle, S., Smiraglia, D.J., Robaire, B., and Trasler, J.M. (2007). A unique configuration of genome-wide DNA methylation patterns in the testis. Proceedings of the National Academy of Sciences of the United States of America *104*, 228–233.

van Oevelen, C., Collombet, S., Vicent, G., Hoogenkamp, M., Lepoivre, C., Badeaux, A., Bussmann, L., Sardina, J.L., Thieffry, D., Beato, M., et al. (2016). C/EBPa; Activates Pre-existing and De Novo Macrophage Enhancers during Induced Pre-B Cell Transdifferentiation and Myelopoiesis. Stem Cell Reports *5*, 232–247.

Okada, Y. (2004). Ion channels and transporters involved in cell volume regulation and sensor mechanisms. Cell Biochemistry and Biophysics *41*, 233–258.

Orkin, S.H., and Hochedlinger, K. (2011). Chromatin connections to pluripotency and cellular reprogramming. Cell *145*, 835–850.

Orkin, S.H., and Zon, L.I. (2008). Hematopoiesis: An Evolving Paradigm for Stem Cell Biology. Cell *132*, 631–644.

Oyadomari, S., Koizumi, A., Takeda, K., Gotoh, T., Akira, S., Araki, E., and Mori, M. (2002). Targeted disruption of the Chop gene delays endoplasmic reticulum stress-mediated diabetes. Journal of Clinical Investigation *109*, 525–532.

Ozcelik, H., Hindie, M., Hasan, A., Engin, N., Cell, V., Barthes, J., Özçelik, H., Hindié, M., Ndreu-halili, A., and Vrana, N.E. (2014). Cell Microenvironment Engineering and Monitoring for Tissue Engineering and Regenerative Medicine : The Citation Accessed Citable Link Cell Microenvironment Engineering and Monitoring for Tissue Engineering and Regenerative Medicine : The Recent Advances. *2014*.

Pakos-Zebrucka, K., Koryga, I., Mnich, K., Ljujic, M., Samali, A., and Gorman, A.M. (2016). The

integrated stress response. EMBO Reports *17*, 1374 LP-1395.

Pan, Z., Capó-Aponte, J.E., Zhang, F., Wang, Z., Pokorny, K.S., and Reinach, P.S. (2007). Differential dependence of regulatory volume decrease behavior in rabbit corneal epithelial cells on MAPK superfamily activation. Experimental Eye Research *84*, 978–990.

Park, S.K., and Won, J.H. (2009). Usefulness of umbilical cord blood cells in era of hematopoiesis research. International Journal of Stem Cells *2*, 90–96.

Park, H., Lee, S., Ji, M., Kim, K., Son, Y., Jang, S., and Park, Y. (2016). Measuring cell surface area and deformability of individual human red blood cells over blood storage using quantitative phase imaging. Scientific Reports *6*, 34257.

Park, S.-K., Xiang, Y., Feng, X., and Garrard, W.T. (2014). Pronounced cohabitation of active immunoglobulin genes from three different chromosomes in transcription factories during maximal antibody synthesis. Genes & Development *28*, 1159–1164.

Pasantes-Morales, H., Lezama, R.A., Ramos-Mandujano, G., and Tuz, K.L. (2006). Mechanisms of cell volume regulation in hypo-osmolality. Am J Med *119*, S4-11.

Patergnani, S., Suski, J.M., Agnoletto, C., Bononi, A., Bonora, M., De Marchi, E., Giorgi, C., Marchi, S., Missiroli, S., Poletti, F., et al. (2011). Calcium signaling around Mitochondria Associated Membranes (MAMs). Cell Communication and Signaling *9*, 19.

Pauklin, S., and Vallier, L. (2013). The cell cycle state of stem cells determines cell fate propensity. Cell *155*, 135–147.

Pearce, K.F., Hildebrandt, M., Greinix, H., Scheding, S., Koehl, U., Worel, N., Apperley, J., Edinger, M., Hauser, A., Mischak-Weissinger, E., et al. (2014). Regulation of advanced therapy medicinal products in Europe and the role of academia. Cytotherapy *16*, 289–297.

Pedersen, S.F., Hoffmann, E.K., and Novak, I. (2013). Cell volume regulation in epithelial physiology and cancer. Frontiers in Physiology *4*, 233.

Pessina, A., Bonomi, A., Sisto, F., Baglio, C., Cavicchini, L., Ciusani, E., Coccé, V., and Gribaldo, L. (2010). CD45+/CD133+ positive cells expanded from umbilical cord blood expressing PDX-1 and markers of pluripotency. Cell Biology International *34*, 783–790.

Petersen, O.H., Verkhratsky, A., and Petersen, O.H. (2016). Calcium and ATP control multiple vital functions.

Picard, M., Shirihai, O.S., Gentil, B.J., and Burelle, Y. (2013). Mitochondrial morphology transitions and functions: implications for retrograde signaling? American Journal of Physiology. Regulatory, Integrative and Comparative Physiology *304*, R393-406.

Picker, S.M., Schneider, V., Oustianskaia, L., and Gathof, B.S. (2009). Sickle Hb polymerization in RBC components from donors with sickle cell trait prevents effective WBC reduction by filtration. Blood Components *49*, 2311–2318.

Plattner, H., and Verkhratsky, A. (2016). Inseparable tandem: evolution chooses ATP and Ca2+ to control life, death and cellular signalling. Philosophical Transactions of the Royal Society of London. Series B, Biological Sciences *371*, 20150419.

Pockley, A.G. (2002). Heat shock proteins, inflammation, and cardiovascular disease. Circulation *105*,

1012–1017.

Pombo, A., and Dillon, N. (2015). Three-dimensional genome architecture: players and mechanisms. Nature Reviews. Molecular Cell Biology *16*, 245–257.

Pombo, a, Jackson, D. a, Hollinshead, M., Wang, Z., Roeder, R.G., and Cook, P.R. (1999). Regional specialization in human nuclei: visualization of discrete sites of transcription by RNA polymerase III. The EMBO Journal *18*, 2241–2253.

Pong, K. (2004). Ischaemic preconditioning: therapeutic implications for stroke? Expert Opinion on Therapeutic Targets *8*, 125–139.

Poon, G.M.K. (2012). Sequence discrimination by DNA-binding domain of ETS family transcription factor PU.1 is linked to specific hydration of protein-DNA interface. The Journal of Biological Chemistry *287*, 18297–18307.

Poppe, M., Reimertz, C., Düssmann, H., Krohn, a J., Luetjens, C.M., Böckelmann, D., Nieminen, a L., Kögel, D., and Prehn, J.H. (2001). Dissipation of potassium and proton gradients inhibits mitochondrial hyperpolarization and cytochrome c release during neural apoptosis. The Journal of Neuroscience : The Official Journal of the Society for Neuroscience *21*, 4551–4563.

Porada, C.D., Atala, A.J., and Almeida-Porada, G. (2016). The hematopoietic system in the context of regenerative medicine. Methods *99*, 44–61.

Potthoff, M.J., and Olson, E.N. (2007). MEF2: a central regulator of diverse developmental programs. Development *134*, 4131–4140.

Powell, A.B., Williams, K., Conrad, &, and Cruz, R.Y. (2016). Gene-modified, cell-based therapies—an overview. Cytotherapy *18*, 1351–1359.

Prestridge, D.S., and Burks, C. (1993). The density of transcriptional elements in promoter and non-promoter sequences. Human Molecular Genetics *2*, 1449–1453.

Pribenszky, C., Vajta, G., Molnar, M., Du, Y., Lin, L., Bolund, L., and Yovich, J. (2010). Stress for stress tolerance? A fundamentally new approach in mammalian embryology. Biology of Reproduction *83*, 690–697.

Pribenszky, C., Lin, L., Du, Y., Losonczi, E., Dinnyes, A., and Vajta, G. (2012). Controlled stress improves oocyte performance - cell preconditioning in assisted reproduction. Reproduction in Domestic Animals *47*, 197–206.

Prigione, A., Ruiz-P??rez, M.V., Bukowiecki, R., and Adjaye, J. (2015). Metabolic restructuring and cell fate conversion. Cellular and Molecular Life Sciences 1759–1777.

Qin, H., Zhao, A., Zhang, C., and Fu, X. (2016). Epigenetic Control of Reprogramming and Transdifferentiation by Histone Modifications. Stem Cell Reviews and Reports 708–720.

Radtke, S., Görgens, A., Kordelas, L., Schmidt, M., Kimmig, K.R., Köninger, A., Horn, P.A., and Giebel, B. (2015). CD133 allows elaborated discrimination and quantification of haematopoietic progenitor subsets in human haematopoietic stem cell transplants. British Journal of Haematology *169*, 868–878.

Ragoonanan, V., Less, R., and Aksan, A. (2013). Response of the cell membrane-cytoskeleton complex to osmotic and freeze/thaw stresses. Part 2: The link between the state of the membrane-cytoskeleton complex and the cellular damage. Cryobiology *66*, 96–104.

Rando, O.J. (2007). Chromatin structure in the genomics era. Trends in Genetics *23*, 67–73.

Rasouli, M. (2016). Basic concepts and practical equations on osmolality: Biochemical approach. Clinical Biochemistry 6–11.

Rauch, T.A., Wu, X., Zhong, X., Riggs, A.D., and Pfeifer, G.P. (2009). A human B cell methylome at 100-base pair resolution. Proceedings of the National Academy of Sciences of the United States of America *106*, 671–678.

Reik, W. (2007). Stability and flexibility of epigenetic gene regulation in mammalian development. Nature *447*, 425–432.

van Rensburg, R., Beyer, I., Yao, X.-Y., Wang, H., Denisenko, O., Li, Z.-Y., Russell, D.W., Miller, D.G., Gregory, P., Holmes, M., et al. (2012). Chromatin structure of two genomic sites for targeted transgene integration in induced pluripotent stem cells and hematopoietic stem cells. Gene Therapy 1–14.

Rizzuto, R., De Stefani, D., Raffaello, A., and Mammucari, C. (2012). Mitochondria as sensors and regulators of calcium signalling. Nature Reviews Molecular Cell Biology *13*, 566–578.

Roider, H.G., Manke, T., O'keeffe, S., Vingron, M., and Haas, S.A. (2009). PASTAA: Identifying transcription factors associated with sets of co-regulated genes. Bioinformatics *25*, 435–442.

Ronai, Z. (1999). Deciphering the mammalian stress response - a stressful task. Oncogene *18*, 6084–6086.

Rosa, A., and Ballarino, M. (2016). Long Noncoding RNA Regulation of Pluripotency. Stem Cells International.

Roura, S., Pujal, J.-M., Gálvez-Montón, C., and Bayes-Genis, A. (2015). The role and potential of umbilical cord blood in an era of new therapies: a review. Stem Cell Research & Therapy *6*, 123.

Sabapathy, K., Hochedlinger, K., Nam, S.Y., Bauer, A., Karin, M., and Wagner, E.F. (2004). Distinct roles for JNK1 and JNK2 in regulating JNK activity and c-Jun-dependent cell proliferation. Molecular Cell *15*, 713–725.

Safiulina, D., Veksler, V., Zharkovsky, A., and Kaasik, A. (2006). Loss of mitochondrial membrane potential is associated with increase in mitochondrial volume: physiological role in neurones. Journal of Cellular Physiology *206*, 347–353.

Sam, M.D., and Clubb, R.T. (2012). Preparation and Optimization of Protein–DNA Complexes Suitable for Detailed NMR Studies. Methods in Molecular Biology (Clifton, N.J.) *831*, 219–232.

Saudemont, A., and Madrigal, J.A. (2016). Immunotherapy after hematopoietic stem cell transplantation using umbilical cord blood-derived products. Cancer Immunology, Immunotherapy.

Schneider, R., and Grosschedl, R. (2007). Dynamics and interplay of nuclear architecture, genome organization, and gene expression. Genes & Development *21*, 3027–3043.

Schneider, B., Černý, J., Svozil, D., Čech, P., Gelly, J.C., and De Brevern, A.G. (2014). Bioinformatic analysis of the protein/DNA interface. Nucleic Acids Research *42*, 3381–3394.

Schwabe, J.W., Chapman, L., Finch, J.T., and Rhodes, D. (1993). The crystal structure of the estrogen receptor DNA-binding domain bound to DNA: how receptors discriminate between their response elements. Cell *75*, 567–578.

Schwiebert, E.M., and Fitz, J.G. (2008). Purinergic signaling microenvironments: An introduction. Purinergic Signalling *4*, 89–92.

Schwiebert, E.M., and Zsembery, A. (2003). Extracellular ATP as a signaling molecule for epithelial cells. Biochimica et Biophysica Acta (BBA) - Biomembranes *1615*, 7–32.

Sebban, S., and Buganim, Y. (2016). Nuclear Reprogramming by Defined Factors: Quantity Versus Quality.

Serrano, L., Vazquez, B.N., and Tischfield, J. (2013). Chromatin structure, pluripotency and differentiation. Experimental Biology and Medicine (Maywood, N.J.) *238*, 259–270.

Shamblott, M.J., Axelman, J., Wang, S., Bugg, E.M., Littlefield, J.W., Donovan, P.J., Blumenthal, P.D., Huggins, G.R., and Gearhart, J.D. (1998). Derivation of pluripotent stem cells from cultured human primordial germ cells. Proceedings of the National Academy of Sciences *95*, 13726–13731.

Shapiro, H.M. (2003). Practical Flow Cytometry (NJ: Wiley-Liss).

Shaughnessy, D.T., McAllister, K., Worth, L., Haugen, A.C., Meyer, J.N., Domann, F.E., Van Houten, B., Mostoslavsky, R., Bultman, S.J., Baccarelli, A.A., et al. (2015). Mitochondria, energetics, epigenetics, and cellular responses to stress. Environmental Health Perspectives *122*, 1271–1278.

Shen, M.R., Chou, C.Y., Browning, J.A., Wilkins, R.J., and Ellory, J.C. (2001). Human cervical cancer cells use Ca2+ signalling, protein tyrosine phosphorylation and MAP kinase in regulatory volume decrease. J Physiol *537*, 347–362.

Shim, E.-H., Kim, J.-I., Bang, E.-S., Heo, J.-S., Lee, J.-S., Kim, E.-Y., Lee, J.-E., Park, W.-Y., Kim, S.-H., Kim, H.-S., et al. (2002). Targeted disruption of hsp70.1 sensitizes to osmotic stress. EMBO Reports *3*, 857–861.

Shogren-Knaak, M. (2006). Histone H4-K16 Acetylation Controls Chromatin Structure and Protein Interactions. Science *311*, 844–847.

Simmons, S.O., Fan, C.Y., and Ramabhadran, R. (2009). Cellular stress response pathway system as a sentinel ensemble in toxicological screening. Toxicological Sciences *111*, 202–225.

Solaini, G., Baracca, A., Lenaz, G., and Sgarbi, G. (2010). Hypoxia and mitochondrial oxidative metabolism. Biochimica et Biophysica Acta (BBA) - Bioenergetics *1797*, 1171–1177.

Song, L., and Crawford, G.E. (2013). NIH Public Access. *2010*, 1–13.

Song, F., Smith, J.F., Kimura, M.T., Morrow, A.D., Matsuyama, T., Nagase, H., and Held, W.A. (2005). Association of tissue-specific differentially methylated regions (TDMs) with differential gene expression. Proceedings of the National Academy of Sciences of the United States of America *102*, 3336–3341.

Song, L., Zhang, Z., Grasfeder, L.L., Boyle, A.P., Giresi, P.G., Lee, B., Sheffield, N.C., Gra, S., Huss, M., Keefe, D., et al. (2011). Open chromatin defined by DNaseI and FAIRE identifies regulatory elements that shape cell-type identity. 1757–1767.

Sontheimer, H. (2009). An unexpected role for ion channels in brain tumour metastasis. Exp Biol Med *233*, 779–791.

Stace, E.T., Dakin, S.G., Mouthuy, P.A., and Carr, A.J. (2016). Translating Regenerative Biomaterials Into Clinical Practice. Journal of Cellular Physiology *231*, 36–49.

Di Stefano, B., Sardina, J.L., van Oevelen, C., Collombet, S., Kallin, E.M., Vicent, G.P., Lu, J., Thieffry, D., Beato, M., and Graf, T. (2014). C/EBPalpha poises B cells for rapid reprogramming into induced pluripotent stem cells. Nature *506*, 235–239.

Stein, G.S., Van Wijnen, A.J., Stein, J.L., Lian, J.B., Bidwell, J.P., and Montecino, M. (1994). Nuclear architecture supports integration of physiological regulatory signals for transcription of cell growth and tissue-specific genes during osteoblast differentiation. Journal of Cellular Biochemistry *55*, 4–15.

Stojkovic, M., Lako, M., Strachan, T., and Murdoch, A. (2004). Derivation, growth and applications of human embryonic stem cells. Reproduction *128*, 259–267.

Su, J., Pei, D., and Qin, B. (2013a). Roles of small molecules in somatic cell reprogramming. Acta Pharmacologica Sinica *34*, 719–724.

Su, R.J., Baylink, D.J., Neises, A., Kiroyan, J.B., Meng, X., Payne, K.J., Tschudy-Seney, B., Duan, Y., Appleby, N., Kearns-Jonker, M., et al. (2013b). Efficient Generation of Integration-Free iPS Cells from Human Adult Peripheral Blood Using BCL-XL Together with Yamanaka Factors. PLoS ONE *8*.

Sugawara, T., Nishino, K., Umezawa, A., and Akutsu, H. (2012). Investigating cellular identity and manipulating cell fate using induced pluripotent stem cells. Stem Cell Research & Therapy *3*, 8.

Sugaya, K., Vigneron, M., and Cook, P.R. (2000). Mammalian cell lines expressing functional RNA polymerase II tagged with the green fluorescent protein. Journal of Cell Science *113 (Pt 1*, 2679–2683.

Sugimura, R. (2016). Bioengineering Hematopoietic Stem Cell Niche toward Regenerative Medicine. Advanced Drug Delivery Reviews *99*, 212–220.

Swygert, S.G., and Peterson, C.L. (2014). Chromatin dynamics: Interplay between remodeling enzymes and histone modifications. Biochimica et Biophysica Acta - Gene Regulatory Mechanisms *1839*, 728–736.

Symmons, O., and Raj, A. (2016). What's Luck Got to Do with It: Single Cells, Multiple Fates, and Biological Nondeterminism. Molecular Cell *62*, 788–802.

Takahashi, K. (2012). Cellular reprogramming - lowering gravity on Waddington's epigenetic landscape. Journal of Cell Science *125*, 2553–2560.

Takahashi, K., and Ohnuki, M. (2015). Present and future challenges of induced pluripotent stem cells. Royal Society.

Takahashi, K., and Yamanaka, S. (2016). A decade of transcription factor-mediated reprogramming to pluripotency. Nature Reviews. Molecular Cell Biology *17*, 183–193.

Takahashi, K., Tanabe, K., Ohnuki, M., Narita, M., Ichisaka, T., Tomoda, K., and Yamanaka, S. (2007). Induction of Pluripotent Stem Cells from Adult Human Fibroblasts by Defined Factors. Cell *131*, 861–872.

Takahashi, K., Yan, I.K., Haga, H., and Patel, T. (2014). Modulation of hypoxia-signaling pathways by extracellular linc-RoR. Journal of Cell Science *127*, 1585–1594.

Talwar, S., Kumar, A., Rao, M., Menon, G.I., and Shivashankar, G. V. (2013). Correlated spatio-temporal fluctuations in chromatin compaction states characterize stem cells. Biophysical Journal *104*, 553–564.

Tao, Y.-F., Fang, F., Hu, S.-Y., Lu, J., Cao, L., Zhao, W.-L., Xiao, P.-F., Li, Z.-H., Wang, N.-N., Xu, L.-

X., et al. (2015). Hypermethylation of the GATA binding protein 4 (GATA4) promoter in Chinese pediatric acute myeloid leukemia. BMC Cancer *15*, 756.

Taruno, A., Niisato, N., and Marunaka, Y. (2007). Hypotonicity stimulates renal epithelial sodium transport by activating JNK via receptor tyrosine kinases. American Journal of Physiology. Renal Physiology *293*, F128-38.

Tavakoli, T., Xu, X., Derby, E., Serebryakova, Y., Reid, Y., Rao, M.S., Mattson, M.P., and Ma, W. (2009). Self-renewal and differentiation capabilities are variable between human embryonic stem cell lines I3, I6 and BG01V. BMC Cell Biology *10*, 44.

Tazi, J., and Bird, A. (1990). Alternative chromatin structure at CpG islands. Cell *60*, 909–920.

Terro, F., Czech, C., Esclaire, F., Elyaman, W., Yardin, C., Baclet, M.C., Touchet, N., Tremp, G., Pradier, L., and Hugon, J. (2002). Neurons overexpressing mutant presenilin-1 are more sensitive to apoptosis induced by endoplasmic reticulum-golgi stress. Journal of Neuroscience Research *69*, 530–539.

Tewari, A.K., Yardimci, G.G., Shibata, Y., Sheffield, N.C., Song, L., Taylor, B.S., Georgiev, S.G., Coetzee, G.A., Ohler, U., Furey, T.S., et al. (2012). Chromatin accessibility reveals insights into androgen receptor activation and transcriptional specificity. Genome Biology *13*, R88.

Thiel, G., Lesch, A., and Keim, A. (2012). Transcriptional response to calcium-sensing receptor stimulation. Endocrinology *153*, 4716–4728.

Thompson, E.G., and Sontheimer, H. (2016). A role for ion channels in perivascular glioma invasion. European Biophysics Journal 1–14.

Thomson, J.A., Itskovitz-Eldor, J., Shapiro, S.S., Waknitz, M.A., Swiergiel, J.J., Marshall, V.S., and Jones, J.M. (1998). Embryonic stem cell lines derived from human blastocysts. Science (New York, N.Y.) *282*, 1145–1147.

Thurman, R.E., Rynes, E., Humbert, R., Vierstra, J., Maurano, M.T., Haugen, E., Sheffield, N.C., Stergachis, A.B., Wang, H., Vernot, B., et al. (2012). The accessible chromatin landscape of the human genome. Nature *489*, 75–82.

Thurman-Newell, J.A., Petzing, J.N., and Williams, D.J. (2015). Quantification of biological variation in blood-based therapy - a summary of a meta-analysis to inform manufacturing in the clinic. Vox Sanguinis *109*, 394–402.

Tsompana, M., and Buck, M.J. (2014). Chromatin accessibility: a window into the genome. Epigenetics & Chromatin *7*, 33.

Tsuji, H., Matsudo, Y., Tsuji, S., Hanaoka, F., Hyodo, M., and Hori, T. aki (1990). Isolation of temperature-sensitive CHO-K1 cell mutants exhibiting chromosomal instability and reduced DNA synthesis at nonpermissive temperature. Somatic Cell and Molecular Genetics *16*, 461–476.

Vadodaria, K.C., Mertens, J., Paquola, A., Bardy, C., Li, X., Jappelli, R., Fung, L., Marchetto, M.C., Hamm, M., Gorris, M., et al. (2016). Generation of functional human serotonergic neurons from fibroblasts. Molecular Psychiatry *21*, 49–61.

Valadkhan, S., and Valencia-Hipólito, A. (2016). lncRNAs in Stress Response. In Long Non-Coding RNAs in Human Disease, K. V Morris, ed. (Cham: Springer International Publishing), pp. 203–236.

Valgardsdottir, R., Chiodi, I., Giordano, M., Rossi, A., Bazzini, S., Ghigna, C., Riva, S., and Biamonti, G.

(2008). Transcription of Satellite III non-coding RNAs is a general stress response in human cells. Nucleic Acids Research *36*, 423–434.

Vandevenne, M., Jacques, D.A., Artuz, C., Nguyen, C.D., Kwan, A.H.Y., Segal, D.J., Matthews, J.M., Crossley, M., Guss, J.M., and MacKay, J.P. (2013). New insights into DNA recognition by zinc fingers revealed by structural analysis of the oncoprotein ZNF217. Journal of Biological Chemistry *288*, 10616–10627.

Verbalis, J.G. (2003). Disorders of body water homeostasis. Best Practice and Research: Clinical Endocrinology and Metabolism *17*, 471–503.

Voutouri, C., and Stylianopoulos, T. (2014). Evolution of osmotic pressure in solid tumors. Journal of Biomechanics *47*, 3441–3447.

Vowinckel, J., Hartl, J., Butler, R., and Ralser, M. (2015). MitoLoc: A method for the simultaneous quantification of mitochondrial network morphology and membrane potential in single cells. Mitochondrion *24*, 77–86.

Wagers, A.J. (2012). The stem cell niche in regenerative medicine. Cell Stem Cell.

Wagers, A.J., and Christensen, J.L. (2002). Cell fate determination from stem cells. Gene Therapy *9*, 606–612.

Waldegger, S., Steuer, S., Risler, T., Heidland, A., Capasso, G., Massry, S., and Lang, F. (1998). Mechanisms and clinical significance of cell volume regulation. Nephrology Dialysis Transplantation *13*, 867–874.

Wanet, A., Arnould, T., Najimi, M., and Renard, P. (2015). Connecting Mitochondria, Metabolism, and Stem Cell Fate. Stem Cells and Development *24*, 1957–1971.

Wang, P., Li, Y., Wang, X., Guo, L., Su, X., and Liu, Q. (2012). Membrane damage effect of continuous wave ultrasound on K562 human leukemia cells. Journal of Ultrasound in Medicine *31*, 1977–1986.

Wang, S., Linde, M.H., Munde, M., Carvalho, V.D., Wilson, W.D., and Poon, G.M.K. (2014). Mechanistic heterogeneity in site recognition by the structurally homologous DNA-binding domains of the ETS family transcription factors Ets-1 and PU.1. The Journal of Biological Chemistry *289*, 21605–21616.

Warlich, E., Kuehle, J., Cantz, T., Brugman, M.H., Maetzig, T., Galla, M., Filipczyk, A. a, Halle, S., Klump, H., Schöler, H.R., et al. (2011). Lentiviral vector design and imaging approaches to visualize the early stages of cellular reprogramming. Molecular Therapy : The Journal of the American Society of Gene Therapy *19*, 782–789.

Weber, M., Hellmann, I., Stadler, M.B., Ramos, L., Paabo, S., Rebhan, M., and Schubeler, D. (2007). Distribution, silencing potential and evolutionary impact of promoter DNA methylation in the human genome. Nature Genetics *39*, 457–466.

Wehner, F., Olsen, H., Tinel, H., Kinne-Saffran, E., and Kinne, R.K. (2003). Cell volume regulation: osmolytes, osmolyte transport, and signal transduction. Reviews of Physiology Biochemistry and Pharmacology *148*, 1–80.

Wei, X., Chen, Y., Xu, Y., Zhan, Y., Zhang, R., Wang, M., Hua, Q., Gu, H., Nan, F., and Xie, X. (2014). Small molecule compound induces chromatin de-condensation and facilitates induced pluripotent stem

cell generation. Journal of Molecular Cell Biology mju024-.

Weipoltshammer, K., and Schofer, C. (2016). Morphology of nuclear transcription. Histochemistry and Cell Biology *145*, 343–358.

Welstead, G.G., Schorderet, P., and Boyer, L. a. (2008). The reprogramming language of pluripotency. Current Opinion in Genetics and Development *18*, 123–129.

Whiting, P., Kerby, J., Coffey, P., Da Cruz, L., and Mckernan, R. (2015). Progressing a human embryonic stem- cell-based regenerative medicine therapy towards the clinic. The Royal Society.

Wu, Q., and Ng, H.-H. (2011). Mark the transition: chromatin modifications and cell fate decision. Cell Research *21*, 1388–1390.

Xiao, X., Zuo, X., Davis, A.A., McMillan, D.R., Curry, B.B., Richardson, J.A., and Benjamin, I.J. (1999). HSF1 is required for extra-embryonic development, postnatal growth and protection during inflammatory responses in mice. EMBO Journal *18*, 5943–5952.

Xu, Y., Liu, L., Zhang, L., Fu, S., Hu, Y., Wang, Y., Fu, H., Wu, K., Xiao, H., Liu, S., et al. (2012). Efficient commitment to functional cd34+ progenitor cells from human bone marrow mesenchymal stem-cell-derived induced pluripotent stem cells. PLoS ONE *7*, 1–10.

Yang, S.H., Sharrocks, A.D., and Whitmarsh, A.J. (2013). MAP kinase signalling cascades and transcriptional regulation. Gene *513*, 1–13.

Ye, Z., Zhan, H., Mali, P., Dowey, S., Williams, D.M., Jang, Y.Y., Dang, C. V., Spivak, J.L., Moliterno, A.R., and Cheng, L. (2009). Human-induced pluripotent stem cells from blood cells of healthy donors and patients with acquired blood disorders. Blood *114*, 5473–5480.

Ye, Z., Liu, C.F., and Jang, Y.Y. (2011). Hematopoietic cells as sources for patient-specific iPSCs and disease modeling. Cell Cycle *10*, 2840–2844.

Yellon, D.M., and Downey, J.M. (2003). Preconditioning the myocardium: from cellular physiology to clinical cardiology. Physiological Reviews *83*, 1113–1151.

Yu-Wai-Man, P., and Chinnery, P.F. (2012). Dysfunctional mitochondrial maintenance: What breaks the circle of life? Brain *135*, 9–11.

Yuzuru, I., Mariko, S., and Ryosuke, T. (2000). Parkin suppresses unfolded protein stress-induced cell death through its E3 ubiquitin- protein ligase activity Yuzuru. The American Society for Biochemistry and Molecular Biology.

Zang, D., Li, H., Xu, H., Zhang, W., Zhang, Y., Shi, X., and Wang, Y. (2016). An Arabidopsis Zinc Finger Protein Increases Abiotic Stress Tolerance by Regulating Sodium and Potassium Homeostasis, Reactive Oxygen Species Scavenging and Osmotic Potential. Frontiers in Plant Science *7*, 1–14.

Zaret, K. (2005). Micrococcal Nuclease Analysis of Chromatin Structure. In Current Protocols in Molecular Biology, (Hoboken, NJ, USA: John Wiley & Sons, Inc.), p.

Zaret, K.S., and Carroll, J.S. (2011). Pioneer transcription factors: Establishing competence for gene expression. Genes and Development *25*, 2227–2241.

Zaret, K.S., Lerner, J., and Iwafuchi-Doi, M. (2016). Chromatin Scanning by Dynamic Binding of Pioneer Factors. Molecular Cell *62*, 665–667.

Zhang, H., Davies, K.J.A., and Forman, H.J. (2015a). Oxidative stress response and Nrf2 signaling in aging. Free Radical Biology and Medicine *88*, *Part B*, 314–336.

Zhang, T., Cooper, S., and Brockdorff, N. (2015b). The interplay of histone modifications - writers that read. EMBO Rep *16*, 1467–1481.

Zhang, Y., Liu, T., Meyer, C.A., Eeckhoute, J., Johnson, D.S., Bernstein, B.E., Nussbaum, C., Myers, R.M., Brown, M., Li, W., et al. (2008). Model-based Analysis of ChIP-Seq (MACS). Genome Biology *9*, R137.

Zhang, Y., Li, W., Laurent, T., and Ding, S. (2012). Small molecules, big roles - the chemical manipulation of stem cell fate and somatic cell reprogramming. Journal of Cell Science *125*, 5609–5620.

Zhang, Z., Ferraris, J.D., Irarrazabal, C.E., Dmitrieva, N.I., Park, J.-H., and Burg, M.B. (2005). Ataxia telangiectasia-mutated, a DNA damage-inducible kinase, contributes to high NaCl-induced nuclear localization of transcription factor TonEBP/OREBP. American Journal of Physiology - Renal Physiology *289*, F506 LP-F511.

Zhao, Z., Dammert, M.A., Grummt, I., and Bierhoff, H. (2016). LncRNA-Induced Nucleosome Repositioning Reinforces Transcriptional Repression of rRNA Genes upon Hypotonic Stress. Cell Reports *14*, 1876–1882.

Zheng, S., Damoiseaux, R., Chen, L., and Black, D.L. (2013). A broadly applicable high-throughput screening strategy identifies new regulators of Dlg4 (Psd-95) alternative splicing. Genome Research *23*, 998–1007.

Zhou, X., Naguro, I., Ichijo, H., and Watanabe, K. (2016). Mitogen-activated protein kinases as key players in osmotic stress signaling. Biochimica et Biophysica Acta (BBA) - General Subjects *1860*, 2037–2052.

Zhu, L., Finkelstein, D., Gao, C., Shi, L., Wang, Y., López-Terrada, D., Wang, K., Utley, S., Pounds, S., Neale, G., et al. (2016). Multi-organ Mapping of Cancer Risk. Cell *166*, 1132–1146.e7.

Zou, G., Zhao Quin, B., and Jack E., D. (1995). Components of a New Human Protein Kinase Signal Transduction Pathway. The Journal of Biological Chemistry *270*, 12665–12669.